REACTION MECHANISMS ON THE WAY FROM CHF3 TO ARCF3. THE NATURE OF THE ORTHO-EFFECT AND ELECTRONIC PROPERTIES OF THE CF3 GROUP.

Andrey I. Konovalov

Dipòsit Legal: T 1587-2015

Reaction Mechanisms on the Way from CHF_3 to $ArCF_3$. The Nature of the Ortho-Effect and Electronic Properties of the CF_3 Group

Andrey I. Konovalov

Doctoral Thesis

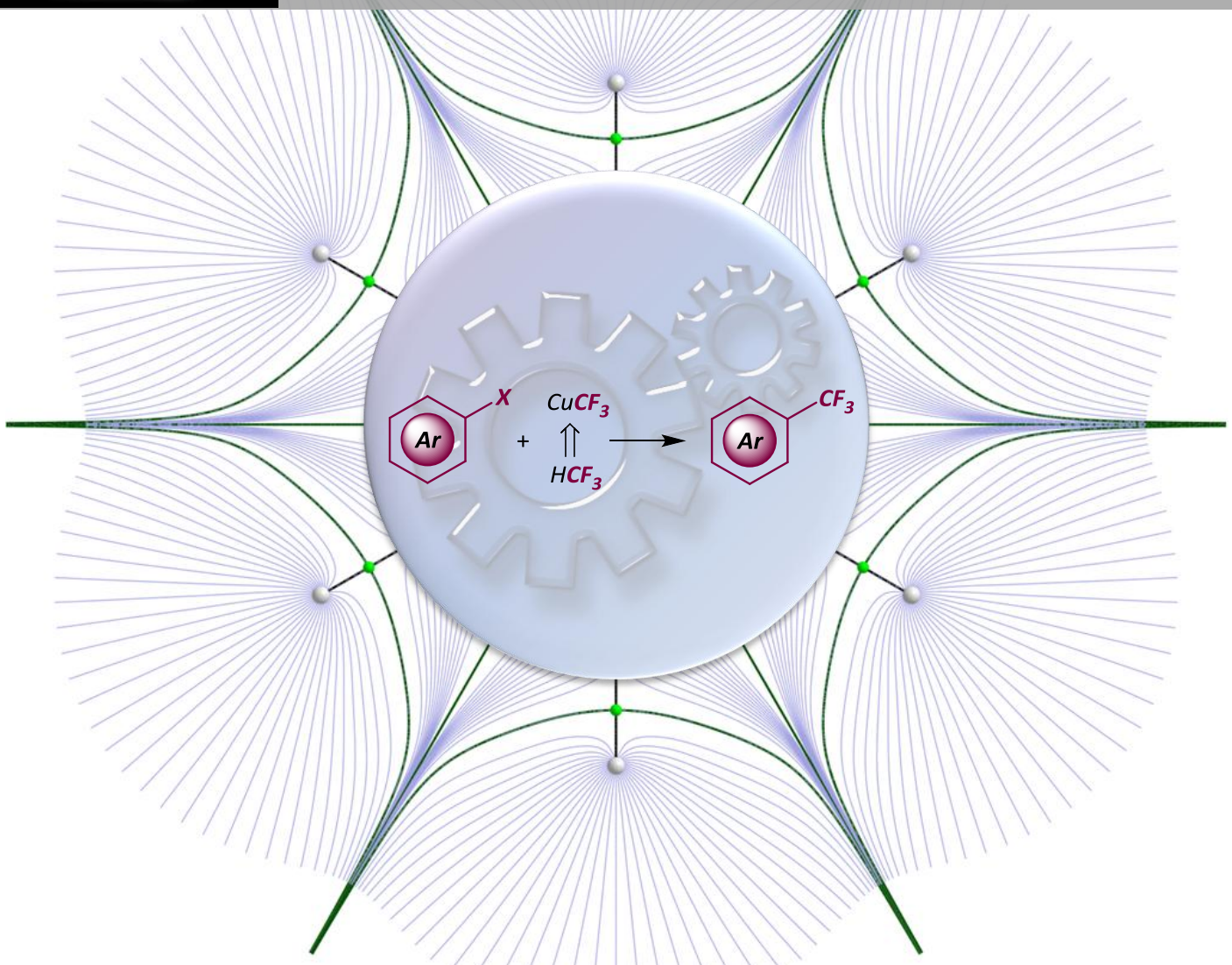

Institute of Chemical Research of Catalonia

Rovira i Virgili University

REACTION MECHANISMS ON THE WAY FROM CHF3 TO ARCF3. THE NATURE OF THE ORTHO-EFFECT AND ELECTRONIC PROPERTIES OF THE CF3 GROUP.
Andrey I. Konovalov
Dipòsit Legal: T 1587-2015

REACTION MECHANISMS ON THE WAY FROM CHF3 TO ARCF3. THE NATURE OF THE ORTHO-EFFECT AND ELECTRONIC PROPERTIES OF THE CF3 GROUP.
Andrey I. Konovalov
Dipòsit Legal: T 1587-2015

REACTION MECHANISMS ON THE WAY FROM CHF3 TO ARCF3. THE NATURE OF THE ORTHO-EFFECT AND ELECTRONIC PROPERTIES OF THE CF3 GROUP.
Andrey I. Konovalov
Dipòsit Legal: T 1587-2015

Andrey I. Konovalov

Reaction Mechanisms on the Way from CHF_3 to $ArCF_3$. The Nature of the Ortho-Effect and Electronic Properties of the CF_3 Group

DOCTORAL THESIS

Supervised by Vladimir V. Grushin and Feliu Maseras

Institut Català d'Investigació Química (ICIQ)

UNIVERSITAT ROVIRA I VIRGILI

Tarragona

2015

REACTION MECHANISMS ON THE WAY FROM CHF3 TO ARCF3. THE NATURE OF THE ORTHO-EFFECT AND ELECTRONIC PROPERTIES OF THE CF3 GROUP.
Andrey I. Konovalov
Dipòsit Legal: T 1587-2015

UNIVERSITAT ROVIRA I VIRGILI
DEPARTAMENT DE QUIMICA ANALITICA I QUIMICA ORGANICA
C/ Marcel.lí Domingo s/n
Campus Sescelades
43007 Tarragona
Tel. 34 977 55 97 69
Fax 34 977 55 84 46
e-mail: secqaqo@urv.net

INSTITUT CATALÀ D'INVESTIGACIÓ QUÍMICA (ICIQ)
Av Països Catalans 16
43007 Tarragona
Tel. 34 977 92 08 24
Fax 34 977 92 08 25
e-mail: iciq@iciq.es.

We STATE that the present study, entitled "Reaction Mechanisms on the Way from CHF_3 to $ArCF_3$. The Nature of the Ortho-Effect and Electronic Properties of the CF_3 Group", presented by Andrey I. Konovalov for the award of the degree of Doctor, has been carried out under our supervision at the Institute of Chemical Research of Catalonia (ICIQ).

Tarragona, 07 July 2015

Vladimir V. Grushin

Feliu Maseras Cuní

Doctoral Thesis Supervisors

First and foremost I am extremely thankful and indebted to Prof. Vladimir V. Grushin for sharing his experience and sincere and valuable guidance. Without his professional supervision, constant help, and patience this dissertation would have never been accomplished.

I express my deepest gratitude to Prof. Feliu Maseras for sharing his pearls of wisdom with me and for the great opportunity to learn advanced computational tools from him.

It is a pleasure to thank Ms. Noemí Panadès Muñoz and Ms. Núria Vendrell for their friendly, professional administrative support and for navigating me through the bureaucratic maze.

I am immensely grateful to the ICIQ research and administrative staff for providing me with all necessary facilities for my research projects. My sincerest thanks go to Drs. Jordi Benet-Buchholz, Eddy Martin, and Eduardo C. Escudero-Adán for numerous superb X-ray crystallographic studies. I also thank Germán Gómez and Israel Macho for their assistance with NMR experiments. A special thanks to Martin Gumbau, System Manager of the ICIQ Computational Laboratory, who was very patient with my knowledge gaps in IT technologies.

I would like to take this opportunity to thank all my former and present lab mates and colleagues for numerous fruitful discussions and for their direct or indirect assistance in my research work. I am particularly indebted to Drs. Fedor M. Miloserdov and Anton Lishchynskyi for collaboration and for sharing their illuminating insights on a number of issues related to my projects.

Prof. Stuart A. Macgregor of Heriot-Watt University is gratefully acknowledged for his preliminary computational studies on the mechanism of trifluoromethylation of

aryl halides described in Chapters 2 and 3 of this Thesis and for many thought-provoking discussions.

In addition, I would like to extend my thanks and appreciation to my school teachers Vera A. Mihalitsyna and Natalia A. Letunova who instilled in me a deep sense of scientific curiosity.

I wish to express my deepest gratitude to my former supervisors Dr. Eduard E. Karslyan, Dr. Dmitry S. Perekalin, and Prof. Alexander R. Kudinov of the Nesmeyanov Institute of Organoelement Compounds, who introduced me to organometallic chemistry and taught me the basics of laboratory techniques in the field.

The ICIQ Foundation and the Spanish Government are gratefully acknowledged for their financial support (Grant CTQ2011-25418).

Last but not least, I owe my most important acknowledgements to my family, whose moral support and encouragement I felt constantly during all these years, despite the thousands of kilometers separating us.

At the printing of this manuscript, the results presented herein have been published in:

- The Critical Effect of the Countercation in the Direct Cupration of Fluoroform with $[Cu(OR)_2]^-$
  A. I. Konovalov, J. Benet-Buchholz, E. Martin, V. V. Grushin, *Angew. Chem., Int. Ed.* **2013**, *52*, 11637.

- Mechanism of Trifluoromethylation of Aryl Halides with $CuCF_3$ and the Ortho Effect
  A. I. Konovalov, A. Lishchynskyi, V. V. Grushin, *J. Am. Chem. Soc.* **2014**, *136*, 13410.

Other publications (during the graduate studies) not directly related to the topics covered in this manuscript:

- Easy Access to the Copper(III) Anion $[Cu(CF_3)_4]^-$
  A. M. Romine, N. Nebra, A. I. Konovalov, E. Martin, J. Benet-Buchholz, V. V. Grushin, *Angew. Chem., Int. Ed.* **2015**, *54*, 2745.

- Ruthenium-Catalyzed Nucleophilic Fluorination of Halobenzenes
  A. I. Konovalov, E. O. Gorbacheva, F. M. Miloserdov, V. V. Grushin, *Chem. Commun.* **2015**, *51*, 13527.

- The Trifluoromethyl Anion
  A. Lishchynskyi, F. M. Miloserdov, E. Martin, J. Benet-Buchholz, E. C. Escudero-Adán, A. I. Konovalov, V. V. Grushin, submitted for publication.

Table of Contents

Abbreviations and Acronyms

AIM:	Atoms in Molecules Analysis
AMLA:	Ambiphilic Metal-Ligand Activation
BCP:	Bond Critical Point
BDE:	Bond Dissociation Energy
BSSE:	Basis Set Superposition Error
bpy:	2,2'-Bipyridine
CEL:	Chan-Evans-Lam Reaction
CNDO/2:	Complete Neglect of Differential Overlap Method
dcypf:	1,1′-Bis(Dicyclohexylphosphino)Ferrocene
DFT:	Density Functional Theory
DMAC:	*N*,*N*-Dimethylacetamide
DMF:	*N*,*N*-Dimethylformamide
DMPU:	*N*,*N'*-Dimethylpropyleneurea
DMSO:	Dimethyl Sulfoxide
dppp:	1,3-Bis(Diphenylphosphino)Propane
ECP:	Effective Core Potential
EDA:	Energy Decomposition Analysis
EPR:	Electron Paramagnetic Resonance Spectroscopy
ETS:	Extended Transition State Method
ESCA:	Electron Spectroscopy for Chemical Analysis
HAT:	Halogen Atom Transfer
HFC:	Hydrofluorocarbons
HMPA:	Hexamethylphosphoramide
HOMO:	Highest Occupied Molecular Orbital
HSAB:	Hard and Soft Acids and Bases Principle
IAT:	Iodine Atom Transfer
IPr:	1,3-Bis(2,6-Diisopropylphenyl)Imidazol-2-ylidene
IRC:	Intrinsic Reaction Coordinate Analysis
GAPT:	Generalized Atomic Polar Tensor
GS-MS:	Gas Chromatography – Mass Spectrometry
LUMO:	Lowest Occupied Molecular Orbital

MBS:	Minimal Basis Set Mulliken Population Analysis
MESP:	Molecular Electrostatic Potential
MM:	Molecular Mechanics
NBBP:	Natural Bond-Bond Polarizability Index
NBO:	Natural Bond Orbital Analysis
NCE:	Natural Coulomb Electrostatics Analysis
NHC:	*N*-Heterocyclic Carbene
NMP:	*N*-Methyl-2-Pyrrolidone
NMR:	Nuclear Magnetic Resonance
NOCV:	Natural Orbitals for Chemical Valence
NPA:	Natural Population Analysis
NST:	Natural Steric Analysis
OA-RE:	Oxidative Addition – Reductive Elimination
ORTEP:	Oac Ridge Thermal Ellipsoid Plot
PBN:	*N*-*tert*-Butyl-α-Phenylnitrone
phen:	1,10-Phenanthroline
Py:	Pyridine
R_f:	Perfluoroalkyl Group
S_EAr:	Electrophilic Aromatic Substitution
S_NAr:	Nucleophilic Aromatic Substitution
$S_{RN}1$:	Radical Nucleophilic Aromatic Substitution
SET:	Single Electron Transfer
SI*i*Pr:	1,3-Di-Isopropylimidazolin-2-ylidene
SMB:	σ-Bond Metathesis
TEMPO:	(2,2,6,6-Tetramethyl-Piperidin-1-yl)Oxyl
THF:	Tetrahydrofuran
TMEDA:	*N,N,N′,N′*-Tetramethylethane-1,2-Diamine
TMS:	Trimethylsilyl Group
UFF:	Universal Force Field
ZORA:	Zeroth-Order Regular Approximation

REACTION MECHANISMS ON THE WAY FROM CHF3 TO ARCF3. THE NATURE OF THE ORTHO-EFFECT AND ELECTRONIC PROPERTIES OF THE CF3 GROUP.
Andrey I. Konovalov
Dipòsit Legal: T 1587-2015

General Introduction.

Mechanisms of Cu-Mediated Aromatic Trifluoromethylation

Selectively fluorinated organic compounds play an exceptionally important role in the development of biologically active compounds, specialty materials, and polymers possessing unique properties.[1] Approximately 20-30% of all pharmaceuticals and 30-40% of all agrochemicals on the current market are based on fluorine-containing active ingredients.[2] Aromatic and heteroaromatic derivatives bearing a trifluoromethyl group (CF_3) on the ring represent a particularly important and widely used class of fluorine-containing biologically active materials.[3] Selected examples of active ingredients of both pharmaceuticals and agrochemicals of this type are presented in Figure 1.

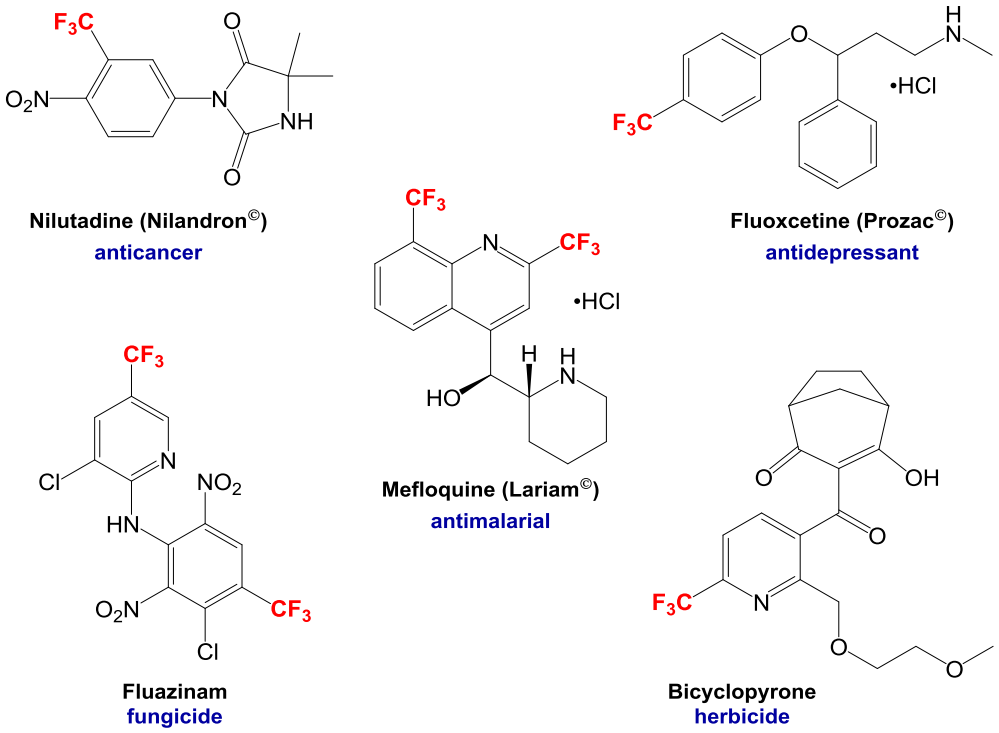

Figure 1. *Examples of CF_3-containing biologically active compounds*

[1] (a) Hudlicky, M. *Chemistry of Organic Fluorine Compounds*; Ellis Horwood: New York, 1976. (b) Banks, R. E. *Organofluorine Chemicals and Their Industrial Applications*; Ellis Horwood: West Sussex, U. K., 1979. (c) Filler, R.; Kobayashi, Y. *Biomedicinal Aspects of Fluorine Chemistry*; Kodansha-Elsevier: New York, 1982. (d) Clark, J. H.; Wails, D.; Bastock, T. W. *Aromatic Fluorination*; CRC Press: Boca Raton, FL, 1996. (e) Kirsch, P. *Modern Fluoroorganic Chemistry*; Wiley-VCH: Weinheim, 2004. (f) Uneyama, K. *Organofluorine Chemistry*; Blackwell: Oxford, U. K., 2006. (g) Ojima, I. *Fluorine in Medicinal Chemistry and Chemical Biology*; Wiley-Blackwell: Chichester, U. K., 2009. (h) Petrov, V. A. *Fluorinated Heterocyclic Compounds. Synthesis, Chemistry and Applications*; Wiley: Hoboken, New Jersey, 2009.

[2] Xu, J.; Liu, X.; Fu, Y. *Tetrahedron Lett.* **2014**, 585.

[3] Tomashenko, O. A.; Grushin, V. V. *Chem. Rev.* **2011**, *111*, 4475.

Trifluoromethylated aromatic compounds are currently manufactured by a Swarts-type process that involves exhaustive radical chlorination of the CH_3 group on the ring with subsequent Cl/F-exchange with HF (Scheme 1).[4]

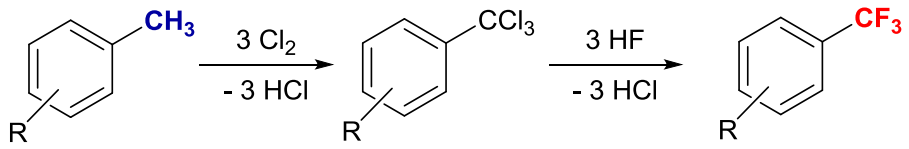

Scheme 1. *Industrial synthesis of trifluoromethylated aromatic compounds*

As follows from the stoichiometry of this two-step synthesis, in order to make 1 equiv of benzotrifluoride, at least 3 equiv of each Cl_2 and HF are required and 6 equiv of HCl are by-produced, making the overall process environmentally malevolent. Another drawback of this transformation is an extremely limited number of functional groups and aromatic cores that can survive the reaction conditions.

In spite of the great demand for trifluoromethylated aromatic compounds, there have been no reports of industrially feasible methods that could possibly replace the currently employed technology. A potentially useful alternative to the industrial process shown in Scheme 1 would be selective trifluoromethylation of pre-functionalized aromatic substrates (Scheme 2).

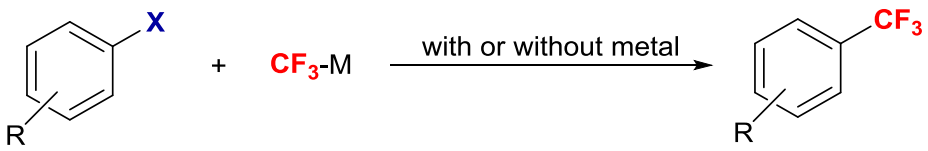

Scheme 2. *Selective aromatic trifluoromethylation*

[4] Filler, R. *Adv. Fluorine Chem.* **1970**, *6*, 1.

Since the first transformation of this type was discovered by McLoughlin and Thrower in the 1960s,[5] tremendous effort has been made by numerous research groups toward the development of metal-mediated aromatic trifluoromethylation reactions. Most of the methods reported to date use copper as a promoter or catalyst with various CF_3 sources, such as polyfluorinated methanes (CF_3I, CF_3Br, CF_3H), trifluoroacetic acid derivatives, Ruppert's reagent CF_3SiMe_3 or its ethyl analogue CF_3SiEt_3, and pre-isolated well-defined or generated *in situ* $CuCF_3$ compounds.3

Depending on the nature of the aromatic substrate used, all existing trifluoromethylation methods can be divided into four general types (Scheme 3): a) nucleophilic trifluoromethylation of aryl halides, b) oxidative Ar-CF_3 coupling reactions of aryl boronic acids and their derivatives, c) Sandmeyer-type trifluoromethylation of arenediazonium salts, and d) direct C-H functionalization of arenes with or without a directing group.3,[6]

While considerable progress has been made in the development of new trifluoromethylation methodologies, very little is known about mechanisms of copper-promoted Ar-CF_3 bond-forming reactions. Establishing reaction mechanisms is paramount not only for the generation of new basic knowledge, but also for targeted research aimed at practicable synthesis. The goal of this Introduction is to review all available mechanistic information on copper-mediated/catalyzed aromatic trifluoromethylation. The main focus will be on the reactions of aryl halides (Scheme 3, a), the most economical, readily available, safe, and widely used aromatic electrophiles.

[5] (a) McLoughlin, V. C. R.; Thrower, J. U. S. Patent 3408411, **1968**. (b) McLoughlin, V. C. R.; Thrower, J. *Tetrahedron* **1969**, *25*, 5921.
[6] For selected reviews, see: (a) Alonso, C.; Marigorta, E. M.; Rubiales, G.; Palacios F. *Chem. Rev*. **2015**, *115*, 1847. (b) McClinton, M. A.; McClinton, D. A. *Tetrahedron* **1992**, *32*, 6555. (c) Burton, D. J.; Yang, Z. Y. *Tetrahedron* **1992**, *48*, 189.

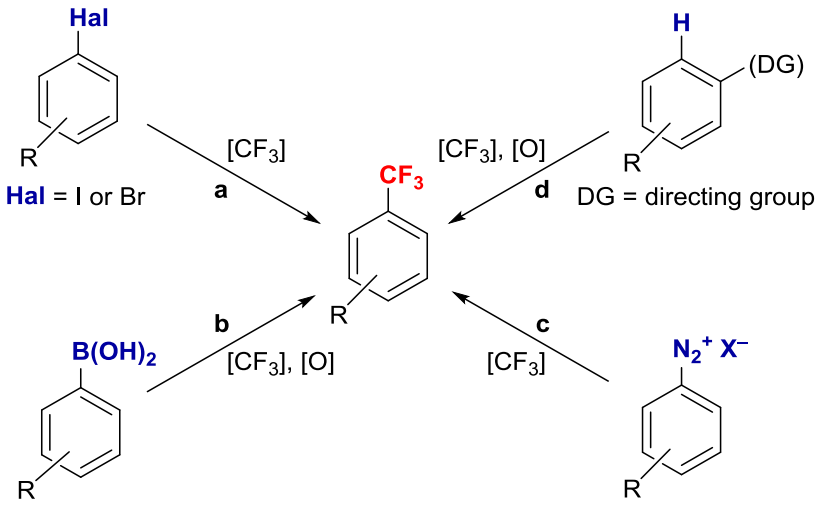

***Scheme 3**. General strategies for Cu-mediated aromatic trifluoromethylation*

Trifluoromethylation of Aryl Halides. As mentioned above, the first copper-mediated perfluoroalkylation of haloarenes was reported by McLoughlin and Thrower over 45 years ago.5 They discovered that aryl halides reductively couple with perfluoroalkyl iodides in the presence of stoichiometric or super-stoichiometric amounts of Cu metal powder (Scheme 4).

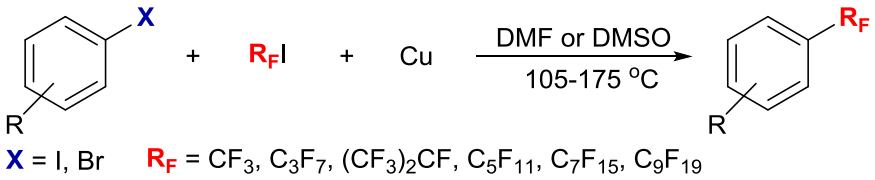

***Scheme 4**. The McLoughlin-Thrower reaction*5

In most instances, the McLoughlin-Thrower reaction is chemo- and regioselective: the substitution occurs only at the halogen atom site, the perfluoroalkyl group does not rearrange during the coupling, and biaryls from the Ullmann reaction[7]

[7] For selected reviews: (a) Sambiagio, C.; Marsden, S. P.; Blackera, A. J.; McGowan, P. C. *Chem. Soc. Rev.* **2014**, *43*, 3525. (b) Hassan, J.; Sévignon, M.; Gozzi, C.; Schulz, E.; Lemaire, M. *Chem. Rev.* **2002**, *102*, 1359.

are seldom side-produced. Furthermore, this reaction tolerates a variety of substituents, including protic ones, such as CO_2H, OH, and NH_2. The order of reactivity of aryl halides in the coupling with R_fI is ArI >> ArBr >> ArCl. Aryl fluorides and chlorides, except for *o*-$NO_2C_6H_4Cl$, do not undergo this transformation. In general, electron-deficient substrates are more reactive, although under the enforcing conditions used (105-175 °C), the difference in reactivity is pronounced only weakly. In most cases, DMSO is the best medium for the reaction. However, other dipolar aprotic solvents, such as DMF, pyridine, DMAC, and HMPA can be used as well. Interestingly, even stoichiometric quantities of coordinating amide solvents can promote the reaction in an inert medium such as hexafluorobenzene. In contrast with perfluoroalkyl iodides, their non-fluorinated analogues do not cross-couple with ArX under similar conditions.

The Ar-R_f coupling (Scheme 4) can be carried out in a one-pot or two-step fashion with pre-generated R_fCu. On the basis of experimental observations, a mechanism has been proposed5[b] that is shown in Scheme 5.

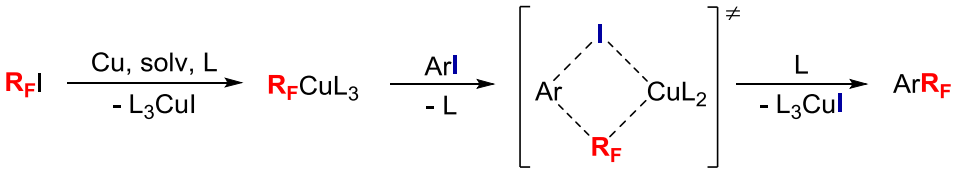

Scheme 5. *Proposed mechanism for the McLoughlin-Thrower reaction*5[b]

In the first step, an R_fCu species is formed as a solvated complex. Subsequent coupling with ArI may occur *via* a four-center transition state, although no evidence has ever been provided that such concerted mechanism, *i.e.* σ-bond metathesis (SBM), indeed operates in the reaction. These two steps might have opposite solvent requirements. The Cu-R_f bond formation is promoted by solvents that can act as

stabilizing ligands to copper. On the other hand, such solvents inhibit the perfluoroalkyl transfer to the aryl halide substrate. In certain systems, the formation of R_fCu from R_fI and Cu can be the rate-determining step of the entire coupling process.

Immediately after the original patent5[a] by McLoughlin and Thrower was published, their discovery turned into a point of growth, with Kobayashi and Kumadaki[8] being the first to join the field as early as the very late 1960s. In the 1970-1980s, evidence was obtained for the trifluoromethylation reactions of aryl halides being effected by pre-formed or generated *in situ* $CuCF_3$.[9] This species was detected, for the first time, in a ^{19}F NMR study by Wiemers and Burton[10] who generated $CuCF_3$ upon addition of CuBr to a mixture of $M(CF_3)_2$ and CF_3MX (M = Zn or Cd; X = Br or Cl). However, the mechanism of these trifluoromethylation reactions of aryl halides still remained unclear due to, at least in part, the lack of structural information on $CuCF_3$, "*an elusive and complex species*."[10] It was not until 2008, that the first structurally characterized $CF_3Cu(I)$ compounds were reported by Vicic *et al*.[11] Since then, a handful more examples of $CF_3Cu(I)$ complexes have been synthesized and characterized by single-crystal X-ray diffraction (Figure 2).[12]

[8] Kobayashi, Y.; Kumadaki, I. *Tetrahedron Lett.* **1969**, 4095.
[9] (a) Kobayashi, Y.; Kumadaki, I.; Sato, S.; Hara, N.; Chikami, E. *Chem. Pharm. Bull*. **1970**, *18*, 2334. (b) Kobayashi, Y.; Yamamoto, K.; Asai, T.; Nakano, M.; Kumadaki, I. *J. Chem. Soc., Perkin Trans. 1* **1980**, 2755. (c) Kondratenko, N. V.; Vechirko, E. P.; Yagupolskii, L. M. *Synthesis* **1980**, 932. (d) Matsui, K.; Tobita, E.; Ando, M.; Kondo, K. *Chem. Lett.* **1981**, 1719. (e) Suzuki, H.; Yoshida, Y.; Osuka, A. *Chem. Lett*. **1982**, 135. (f) LeRoy, J.; Rubinstein, M.; Wakselman, C. *J. Fluorine Chem.* **1985**, *27*, 291.
[10] (a) Wiemers, D. M.; Burton, D. J. *J. Am. Chem. Soc.* **1986**, *108*, 832. (b) MacNeil, J. G.; Burton, D. J. *J. Fluorine Chem.* **1991**, *55*, 225.
[11] (a) Dubinina, G. G.; Furutachi, H.; Vicic, D. A. *J. Am. Chem. Soc.* **2008**, *130*, 8600. (b) Dubinina, G. G.; Ogikubo, J.; Vicic, D. A. *Organometallics* **2008**, *27*, 6233.
[12] (a) Zanardi, A.; Novikov, M. A.; Martin, E.; Benet-Buchholz, J.; Grushin, V. V. *J. Am. Chem. Soc.* **2011**, *133*, 20901. (b) Tomashenko, O. A.; Escudero-Adán E. C.; Martínez Belmonte, M.; Grushin, V. V. *Angew. Chem., Int. Ed.* **2011**, *50*, 7655. (c) Weng, Z.; Lee, R.; Jia, W.; Yuan, Y.; Wang, W.; Feng, X.; Huang, K.-W. *Organometallics* **2011**, *30*, 3229. (d) Konovalov, A. I.; Benet-Buchholz, J.; Martin, E.; Grushin, V. V. *Angew. Chem., Int. Ed.* **2013**, *52*, 11637. (e) Jover, J.; Miloserdov, F. M.; Benet-Buchholz, J.; Grushin, V. V.; Maseras, F. *Organometallics* **2014**, *33*, 6531.

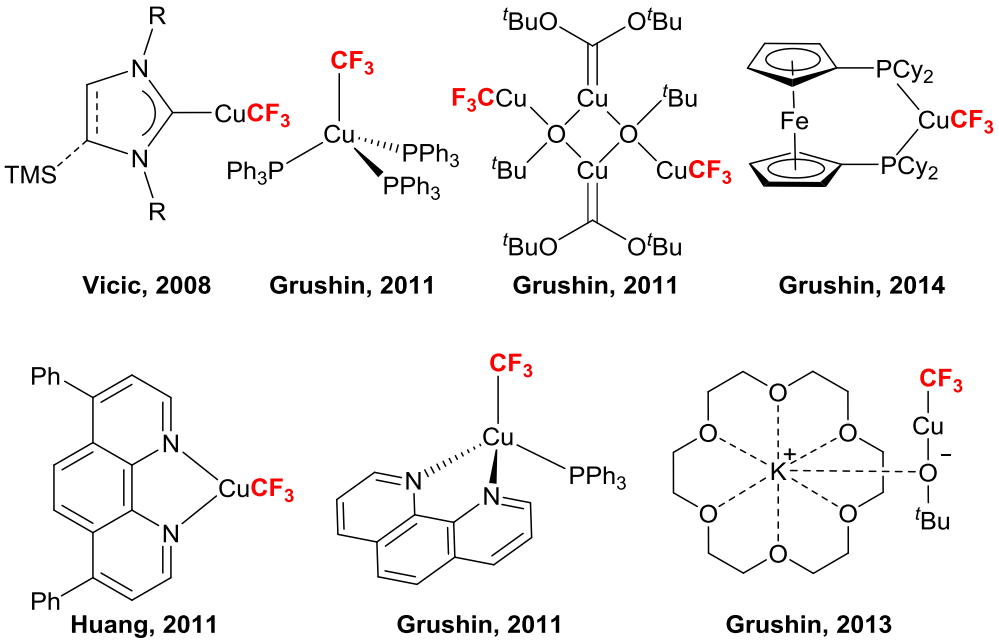

***Figure 2**. Structurally characterized Cu(I)CF_3 compounds*

Auxiliary ligands on the metal in a $CuCF_3$ species can have a dramatic effect on its ability to trifluoromethylate aryl halides. For instance, the addition of phen to $CuCF_3$ can both speed up and slow down the trifluoromethylation of iodoarenes.[13] In general, however, ligands that bind tightly to Cu impede the trifluoromethylation. For instance, [(NHC)$CuCF_3$] (Figure 2) has been reported[11a] to react only sluggishly with neat iodobenzene at room temperature, furnishing benzotrifluoride in only 33% yield after 44 h. Apparently, availability of an accessible vacant coordination site on Cu plays an important role in the Ar-CF_3 coupling.

In spite of the recent progress toward the synthesis and characterization of well-defined Cu(I) trifluoromethylating agents, there still remains a severe shortage of conclusive mechanistic studies of trifluoromethylation reactions of haloarenes. Moreover, the available scarce and scattered mechanistic data on such transformations are not without controversy, as signs of both radical and non-radical mechanisms have

[13] Nakamura, Y.; Fujiu, M.; Murase, T.; Itoh, Y.; Serizawa, H.; Aikawa, K.; Mikami, K. *Beilstein J. Org. Chem.* **2013**, *9*, 2404.

been observed. Single electron transfer (SET) has been proposed for the reaction of FSO_2CF_2I/Cu with aryl halides,[14] which was partially suppressed in the presence of a radical scavenger (*p*-dinitrobenzene) or inhibitor (hydroquinone). These observations prompted Chen[14] to propose a mechanism involving two SET processes from Cu to FSO_2CF_2I, followed by the fragmentation of the $[FSO_2CF_2]^-$ anion to dufluorocarbene CF_2 and fluoride F^- (Scheme 6). To prove this hypothesis, the reaction was performed in the presence of tetramethylethylene as a trapping agent. In addition to the expected *gem*-difluorocyclopropane, a product of $[FSO_2CF_2]^\bullet$ addition-elimination to $Me_2C{=}CMe_2$ was observed. Interestingly, however, a similar trifluoromethylation reaction with $FSO_2CF_2CO_2Me$/CuI in the presence of tetramethylethylene did not give rise to detectable cyclopropanation or radical addition byproducts.[15]

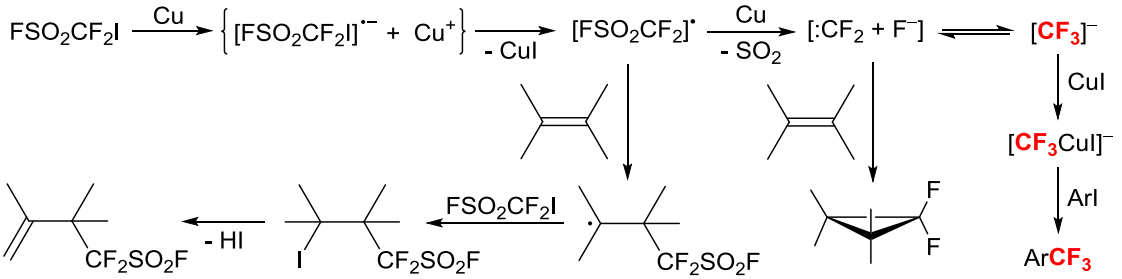

***Scheme 6**. Proposed mechanism of trifluoromethylation of ArI with FSO_2CF_2I/Cu*[14]

Two radical clock experiments have been conducted to probe the mechanism of trifluoromethylation of aryl iodides. No cyclized products were observed in the reactions of $[(phen)CuCF_3]$ with 1-(allyloxy)-2-iodobenzene (Scheme 7) [16] or CF_3SnBu_3/CuI with a similar radical clock iodoaromatic substrate (Scheme 8).[17] These data lend support to a non-radical mechanism governing the trifluoromethylation.

[14] Chen, Q.-Y.; Wu, S-W. *J. Chem. Soc., Perkin Trans. 1* **1989**, 2385.
[15] Chen, Q.-Y.; Wu, S-W. *J. Chem. Soc., Chem. Commun.* **1989**, 705.
[16] Morimoto, H.; Tsubogo, T.; Litvinas, N. D.; Hartwig, J. F. *Angew. Chem., Int. Ed.* **2011**, *50*, 3793.
[17] Sanhueza, I. A.; Nielsen, M. C.; Ottiger, M.; Schoenebeck, F. *Helv. Chim. Acta* **2012**, *95*, 2231.

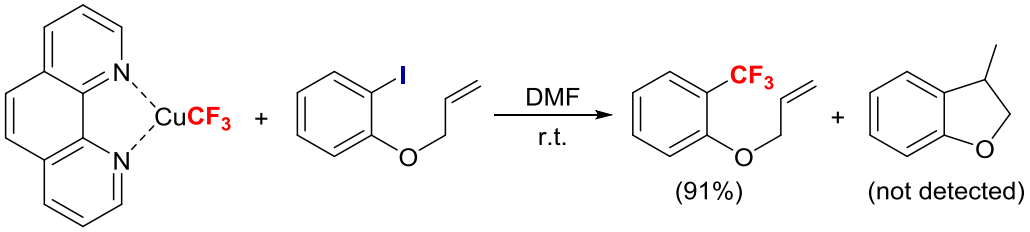

Scheme 7. *Hartwig's radical clock experiment*[16]

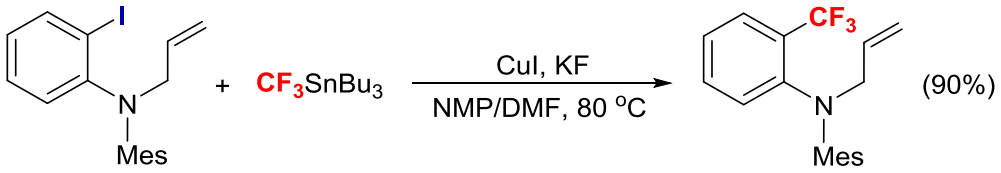

Scheme 8. *Schoenebeck's radical clock test*[17]

In 1988, Chambers and co-workers reported a Hammett correlation study of the decarboxylative trifluoromethylation reaction of a series of *para*-substituted aryl iodides (Scheme 9).[18] The plot of $\lg(k_R/k_H)$ against σ-constants produced a small positive ρ value (+0.46), which is characteristic of copper-mediated nucleophilic aromatic substitution reactions.[19] (In general, a low positive ρ value is an indication of a transition state with poor interaction between the reaction center and a -M substituent on the benzene ring.[20]) It was therefore concluded[18] that the reactive species involved in the trifluoromethylation (Scheme 9) are of nucleophilic nature. Various reaction pathways that were considered by Chambers are shown in Scheme 10.

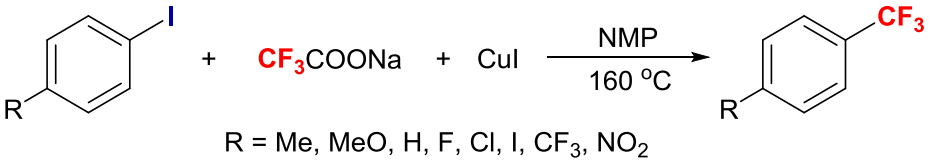

Scheme 9. *Decarboxylative trifluoromethylation reaction used in the Hammett study*[18]

[18] Carr, G. E.; Chambers, R. D.; Holmes, T. F. *J. Chem. Soc., Perkin Trans. 1* **1988**, 921.
[19] Lindley, J. *Tetrahedron* **1984**, *40*, 1433.
[20] Litvak, V. V.; Shein, S. M. *Zh. Org. Khim.* **1974**, *10*, 550.

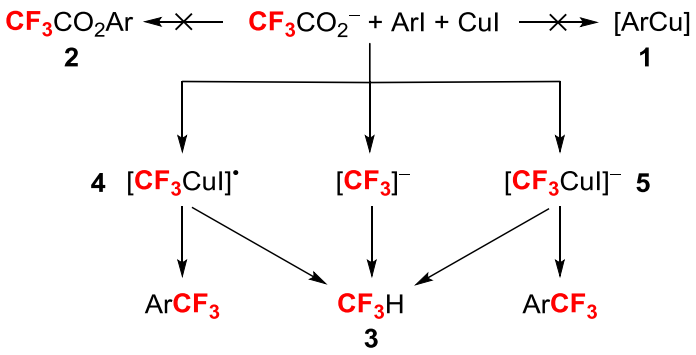

***Scheme 10**. Proposed reaction pathways for the decarboxylative trifluoromethylation*[18]

The formation of [ArCu] species (**1** in Scheme 10) was ruled out since biaryls, characteristic products of decomposition of copper aryls, were usually absent among the reaction products. Copper-mediated nucleophilic iodine/trifluoroacetate exchange leading to **2** in Scheme 10 was also discounted because the corresponding esters CF_3CO_2Ar were found unreactive toward decarboxylation under the reaction conditions used. The accelerating effect of CuI on decomposition of trifluoroacetate in water producing CHF_3 (**3**, Scheme 10) suggested copper-assisted decarboxylation of trifluoroacetate *via* $[CF_3CuI]^{\bullet}$ (**4**) or $[CF_3CuI]^{-}$ (**5**). As the authors perceived the former and the latter as an electrophile and a nucleophile, respectively, the positive ρ value (see above) was consistent with the intermediacy of **5** rather than **4**. This trifluoromethylation reaction requires the initial formation of Cu(I) trifluoroacetate, as follows from the observed inhibition of the decarboxylation in the presence of deliberately added ligands.[18] A recent similar study under flow conditions and at a higher temperature produced virtually the same ρ value of +0.52 (Scheme 11 and Figure 3).[21] A nucleophilic $CuCF_3$ species was proposed as a key intermediate,[21] like in the original Chambers report.[18]

[21] Chen, M.; Buchwald, S. L. *Angew. Chem., Int. Ed.* **2013**, *52*, 11628.

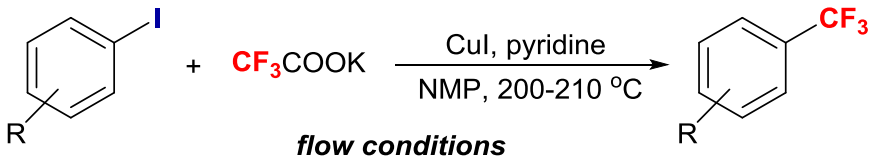

Scheme 11. *Decarboxylative trifluoromethylation in a flow process*[21]

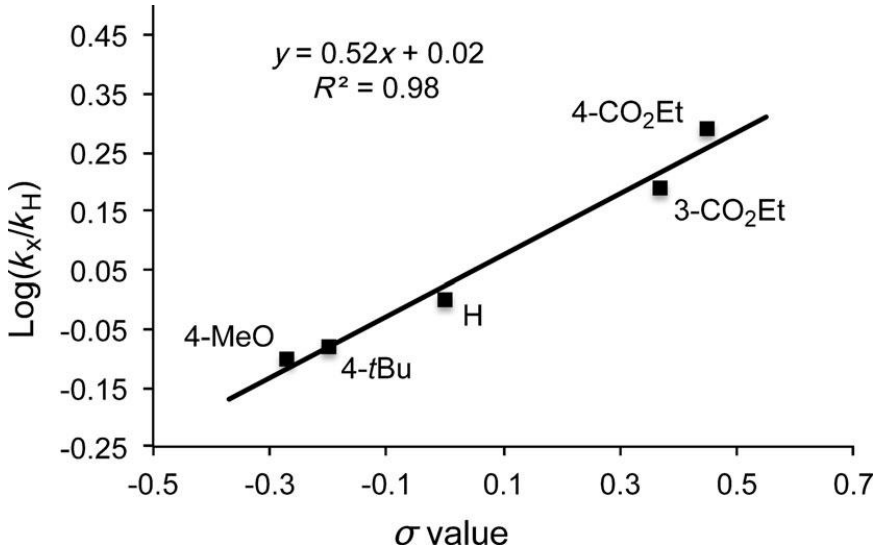

Figure 3. *The Hammett plot for the continuous flow process reported in ref. 21*

The lowest-cost and arguably most efficient method for trifluoromethylation of aryl halides with fluoroform-derived $CuCF_3$ has been recently developed in our group (Scheme 12).[22] The process is highly chemoselective, not giving rise to arene, biaryl, or C_2F_5-derivative side products. This and the stepwise trifluoromethylation of 1,4-dihalobenzene substrates suggested that SET and $S_{RN}1$ are not operational in the reaction. Added ligands do not benefit the process but rather make it less efficient in many instances. Like many other Cu-mediated coupling reactions of aryl halides, the trifluoromethylation occurs at higher rates with *ortho*-substituted substrates, the so-called "ortho-effect" (see Chapter 3 for details).

[22] Lishchynskyi, A.; Novikov, M. A.; Martin, E.; Escudero-Adán, E. C.; Novák, P.; Grushin, V. V. *J. Org. Chem.* **2013**, *78*, 11126.

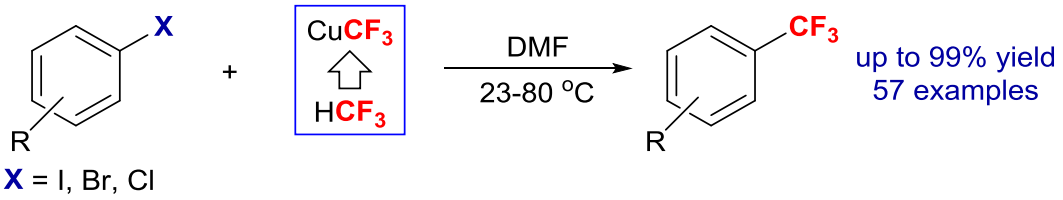

Scheme 12. *Trifluoromethylation of aryl halides with fluoroform-derived $CuCF_3$*[22]

The reaction shown in Scheme 12 seemed to be an ideal candidate for a detailed mechanistic investigation by experimental and computational means. We have recently carried out such a study.[23] Although this work is described in full detail in Chapters 2 and 3, its brief overview is worth presenting in this Introduction. Note that our paper[23] is the first report of a targeted mechanistic investigation of an aromatic trifluoromethylation reaction.

The previously proposed[22] non-radical character of the reaction has been confirmed[23] in a radical clock experiment with 1-(allyloxy)-2-iodobenzene (k_c = 5.3 × 10^9 s^{-1} at 25 °C),[24] as shown in Scheme 13. The lack of formation of the cyclized product is consistent with the absence of side-produced arenes and biaryls in the reactions of fluoroform-derived $CuCF_3$ with a broad variety of aryl halides.

Kinetic studies by the method of initial rates showed that the trifluoromethylation is a bimolecular process, first order with respect to each reactant, and also provided an estimated $\Delta G^{\neq}$ value of 24 kcal/mol at 298 K for the reaction with iodobenzene.

[23] Konovalov A. I.; Lishchynskyi, A.; Grushin, *J. Am. Chem. Soc.* **2014**, *136*, 13410.
[24] (a) Giese, B.; Kopping, B.; Göbel, T.; Dickhaut, J.; Thoma, G.; Kulicke, K. J.; Trach, F. *Org. React.* **1996**, *48*, 301. (b) Johnston, L. J.; Lusztyk, J.; Wayner, D. D. M.; Abeywickreyma, A. N.; Beckwith, A. L. J.; Scaiano, J. C.; Ingold, K. U. *J. Am. Chem. Soc.* **1985**, *107*, 4594. (c) Abeywickrema, A. N.; Beckwith, A. L. J. *Chem. Commun*. **1986**, 464. (d) Abeywickrema, A. N.; Beckwith, A. L. J.; Gerba, S. *J. Org. Chem.* **1987**, *52*, 4072. (e) Annunziata, A.; Galli, C.; Marinelli, M.; Pau, T. *Eur. J. Org. Chem.* **2001**, 1323.

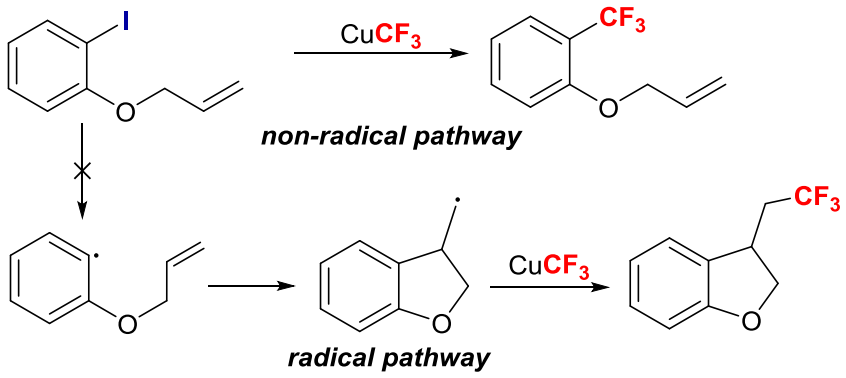

Scheme 13. *Radical clock reaction of fluoroform-derived* $CuCF_3$[23]

An interesting observation was made in the Hammett correlation studies.[23] Plotting $\lg(k_R/k_H)$ against σ_p constants produced two linear correlations ($\rho_1 = 0.69$; $\rho_2 = 1.83$), suggesting two different mechanisms. However, using the resonance parameter σ_p^- for the plot gave an excellent single linear correlation ($\rho_3 = 0.91$), suggesting only one mechanism with significant -M interaction between the reaction center and the substituent. Subsequent DFT calculations confirmed that indeed only one mechanism was operational, involving Ar-X oxidative addition to the Cu(I) center as the rate-determining step. A single linear correlation with σ_p^- obtained using the DFT data ($\rho = 0.92$) is in excellent agreement with the experimental value of 0.91 (see above). Other mechanisms previously proposed in the literature[25] such as SET, S_NAr, SBM, and halogen atom transfer (HAT) were also studied and ruled out on the basis of prohibitively high computed barriers and experimental data.

The long-known yet poorly understood accelerating effect of *ortho*-substituents on many Cu-mediated reactions of aryl halides ("ortho-effect") was quantified for the first time for the trifluoromethylation of a series of *o*-RC_6H_4Br substrates with $CuCF_3$. A competition kinetics study produced the following order of reactivity: R(k_R/k_H) = H

[25] (a) Jones, G. O.; Liu, P.; Houk, K. N.; Buchwald, S. L. *J. Am. Chem. Soc.* **2010**, *132*, 6205. (b) Yu, H.-Z.; Jiang, Y.-Y.; Fu, Y.; Liu, L. *J. Am. Chem. Soc.* **2010**, *132*, 18078.

(1) < Me (3.5) < MeO (4) < CN (20) < CHO (250) < CO_2Me (850) < NO_2 (4300) < Ac (7300) < CO_2H (150000). DFT calculations revealed that electronic factors are a minor contributor to the ortho-effect that is chiefly determined by chelation of the *ortho*-substituent to Cu in the transition state and by the steric bulk of the substituent, which raises the ground state free energy of the substrate by increasing molecular tension and consequently weakening the Ar-X bond (see Chapter 3 for details).

Very soon after publication of our paper,[23] two articles came out,[26,27] reporting mechanistic studies of trifluoromethylation reactions of haloarenes. Unlike our combined experimental-computational work, however, both were purely DFT investigations. One of the two papers, by Li and co-workers,[26] describes calculations on the trifluoromethylation of iodobenzene with Vicic's NHC complexes [(IPr)$CuCF_3$] and [(SI*i*Pr)$CuCF_3$].[11] Four widely proposed mechanisms were probed: a) oxidative addition-reduction elimination (OA-RE), b) iodine atom transfer (IAT), c) SET, and d) SBM (Scheme 14).

The computed activation energies for the SBM pathway and for the key SET Ph-I activation step are prohibitively high and almost isoenergetic (Scheme 14, c and d). Although the OA activation barrier and the energy required for IAT were close (Scheme 14, a and b), the latter was excluded from further considerations on the basis of the unreasonably high activation energy estimated by the Marcus-Hush theory,[28] 42.7 and 71.7 kcal/mol for [(IPr)$CuCF_3$] and [(SI*i*Pr)$CuCF_3$], respectively. In addition, the frontier orbital analysis derived the energy values of -0.62 eV for the LUMO on PhI and -6.30 and -6.26 eV for the HOMO on [(IPr)$CuCF_3$] and [(SI*i*Pr)$CuCF_3$], respectively, indicate that electron transfer between these reactants is unlikely.[26]

[26] Yu, D.-H.; Shao, J.-N.; He, R.-X.; Li, M. *Chin. Chem. Lett*. **2015**, *26*, 564.
[27] Jover, J. *ACS Catal*. **2014**, *4*, 4389.
[28] (a) Houmam, A. *Chem. Rev.* **2008**, *108*, 2180. (b) Lin, C. Y.; Coote, M. L.; Gennaro, A.; Matyjaszewski, K. *J. Am. Chem. Soc.* **2008**, *130*, 12762.

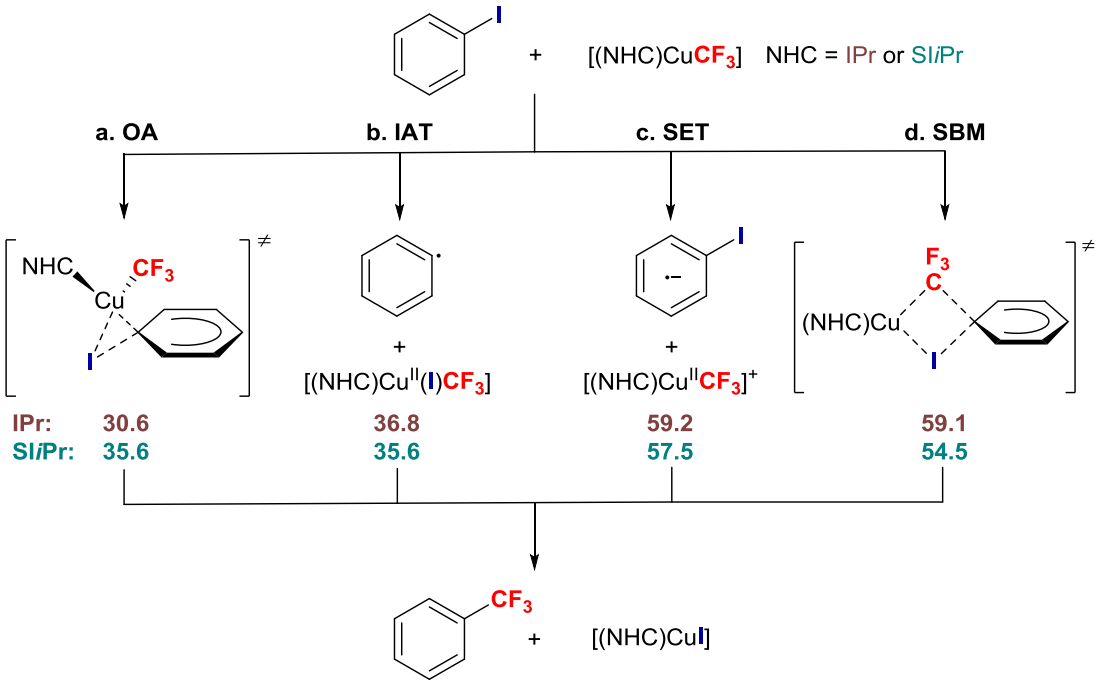

***Scheme 14**. Key stationary points for the mechanisms studied by Li[26] (free energies in kcal/mol)*

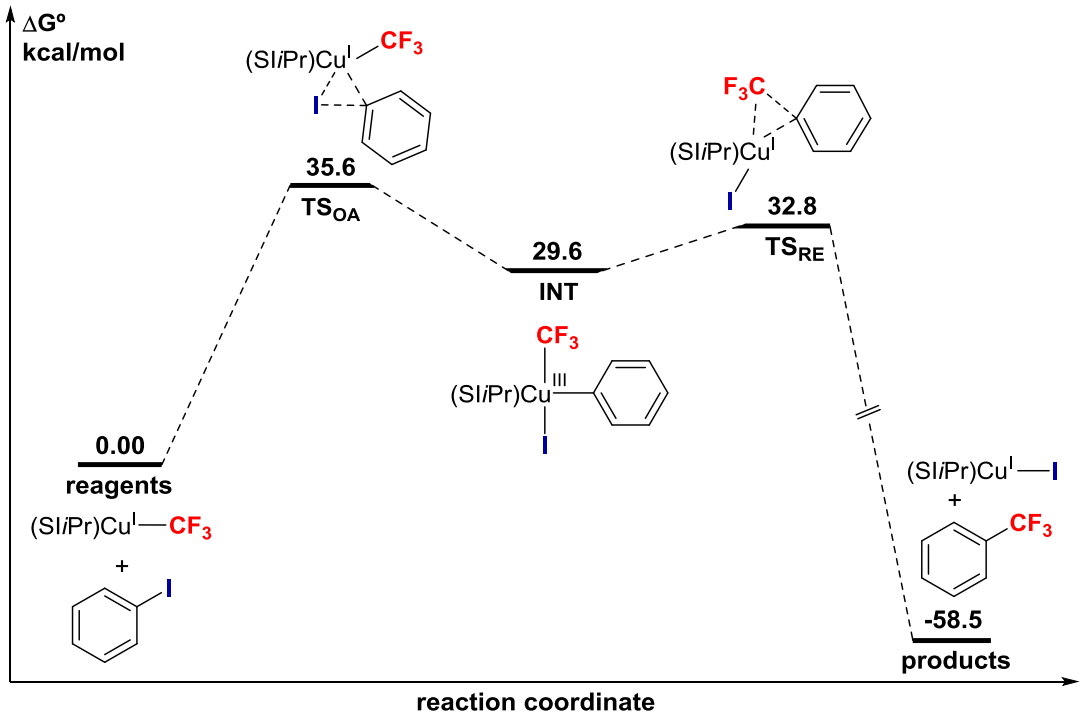

***Scheme 15**. Energy profile of OA-RE pathway for the reaction of [(SIiPr)CuCF3] with PhI[26] (free energies in kcal/mol)*

As follows from the energy profile (Scheme 15), the reaction is highly exergonic with OA as the rate-determining step and overall free energy effect of -58.5 kcal/mol.

The computed barriers to the oxidative addition (Scheme 15) are considerably higher than those in our report.[23] As the NHC-stabilized $CuCF_3$ compounds were computed to lie 22.1 kcal/mol lower in energy than their DMF-ligated analogues, it was concluded[26] that the reactivity of $CuCF_3$ derivatives varies inversely with the binding ability of the ligand on the metal center. This conclusion is consistent with previously reported experimental observations and computational results described above. Although of the four reaction pathways computed by Li[26] the concerted OA-RE mechanism is most favorable, the calculated barriers are inconsistent with the experimentally observed reaction rates.[11]

In the other paper, Jover[27] reports a DFT study of the first Cu-*catalyzed* trifluoromethylation of iodoarenes originally developed by Amii *et al.*[29] The method employs 10 mol % of [(phen)CuI] generated *in situ*, which catalyzes the trifluoromethylation of aryl iodides with CF_3SiEt_3 in the presence of KF (Scheme 16).

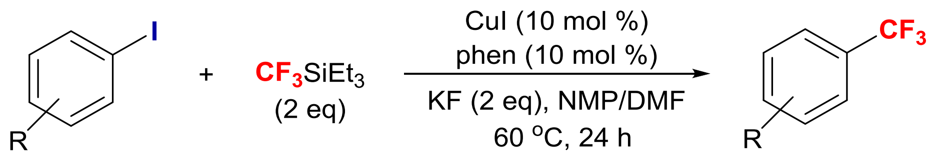

Scheme 16. *The Amii Cu-catalyzed trifluoromethylation of aryl iodides*[29]

First, Jover studied the mechanism of the reaction of CF_3SiEt_3 with KF to give KCF_3 (Scheme 17) because the latter was previously proposed[30] to bring about the Cu-CF_3 bond formation upon transmetalation with [(phen)CuI].

[29] Oishi, M.; Kondo, H.; Amii, H. *Chem. Commun.* **2009**, 1909.
[30] Jover, J.; Maseras, F. *Chem. Commun.* **2013**, *49*, 10486.

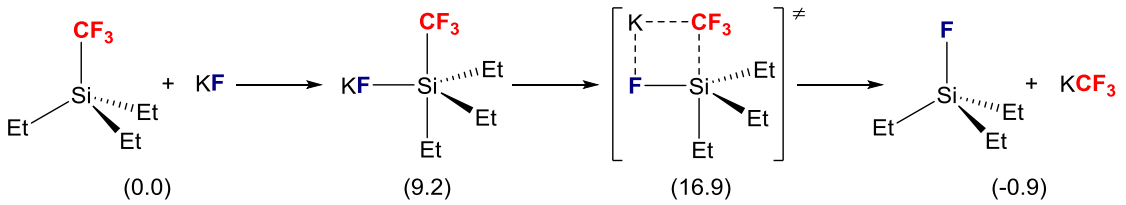

***Scheme 17**. Generation of KCF_3 from CF_3SiEt_3 and KF[27] (free energies in kcal/mol)*

As follows from the data in Scheme 17, the reaction has a very small exergonic effect of -0.9 kcal/mol. The easily accessible transition state (16.9 kcal/mol) for the CF_3 transfer from Si to K brings about fast equilibrium between CF_3SiEt_3 and KCF_3. Although the extremely low stability of KCF_3 1[e] raises doubts about the possibility of its transmetalation with Cu(I), alternative computed reaction pathways from [(phen)CuI] and CF_3SiEt_3 to [(phen)$CuCF_3$] (**I4**) were found to be uncompetitive (Scheme 18).

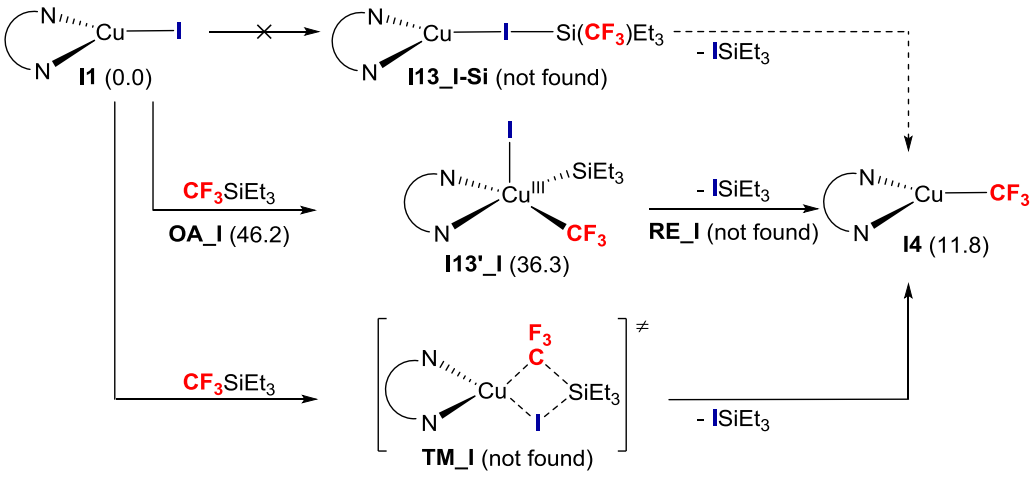

***Scheme 18**. Pathways leading to [(phen)$CuCF_3$] (**I4**) from [(phen)CuI] and CF_3SiEt_3[27] (free energies in kcal/mol)*

The key intermediate **I4** lies higher in energy than the reactants (11.8 kcal/mol), apparently because the energy of the Si-I bond formation is insufficient to provide the driving force for this transformation. Furthermore, the barrier to the direct oxidative

addition of CF_3SiEt_3 to Cu(I) **OA_I** is prohibitively high (46.2 kcal/mol). Other pathways such as IAT (**I13_I-Si**) and SBM (**TM_I**) were also found improbable.

A number of conceivable catalytic cycles were computationally explored in order to identify the most plausible mechanism for the Amii trifluoromethylation of iodobenzene. The detailed reaction network is very complex and includes a large number of reactive species involved in several alternative catalytic loops. Only two mutually related pathways were found plausible (Scheme 19).

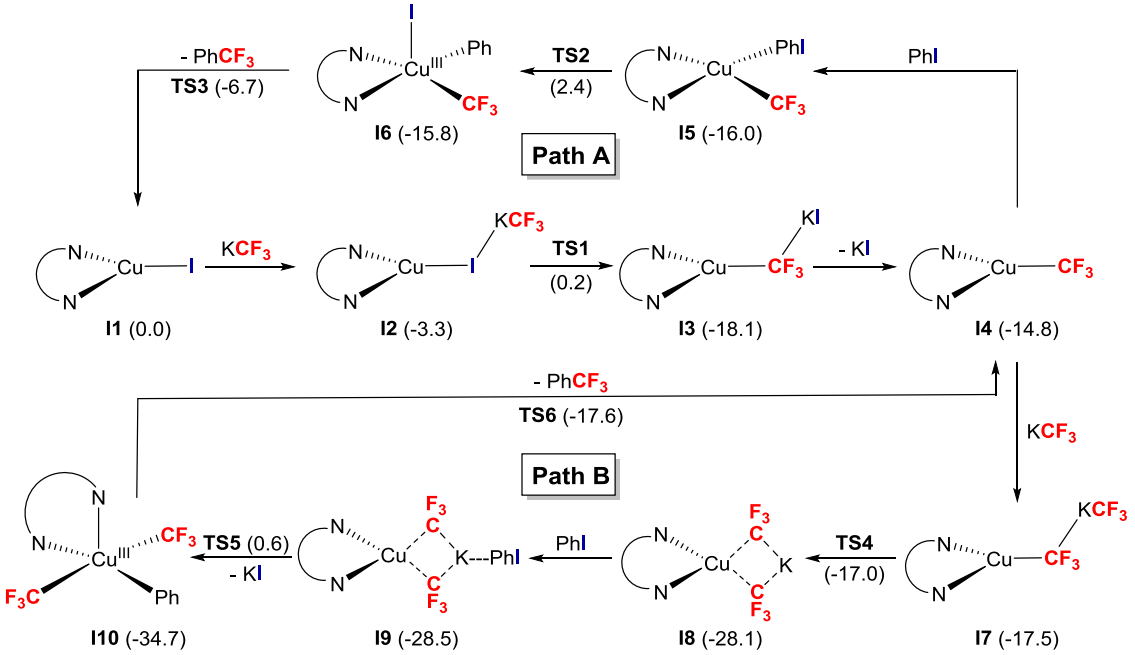

***Scheme 19**. Plausible computed catalytic cycles for the Amii catalytic reaction[27] (free energies in kcal/mol)*

Path A starts by the reaction of [(phen)CuI] **I1** with KCF_3 generated *in situ* as shown in Scheme 17. Their interaction leads to the formation of the adduct **I2** (-3.3 kcal/mol) where the potassium is weakly bound to the iodine atom. **I2** then undergoes CF_3-transfer to the Cu center *via* a low-lying transition state **TS1** (0.2 kcal/mol) to produce **I3** (-18.1 kcal/mol), with KI and CF_3 remaining connected. Elimination of KI

provides the catalytically active $CuCF_3$ complex **I4** (-14.8 kcal/mol). The latter interacts with PhI to give **I5** (-16.0 kcal/mol), which undergoes facile Ph-I oxidative addition *via* **TS2** (2.4 kcal/mol), the rate-determining step of the process ($\Delta G^{\neq}$ = 20.5 kcal/mol). After the C-I bond cleavage (**I6**, -15.8 kcal/mol), Ph-CF_3 reductive elimination occurs *via* **TS3** (-6.7 kcal/mol). The release of the final product, $PhCF_3$, recovers **I1**, the starting point of the catalytic loop.

Path B is invoked by the addition of the second molecule of KCF_3 to **I4** to give rise to **I7** (-17.5 kcal/mol) that is 2.7 and 1.5 kcal/mol lower in energy than **I4** and **I5**, respectively. The easily accessible transition state **TS4** (-17.0 kcal/mol) mediates another transmetalation to deliver **I8** (-28.1 kcal/mol) with two CF_3 groups on Cu and K^+ electrostatically attached to both. This potassium cation plays an important role in the subsequent catching of PhI (**I9**, -28.5 kcal/mol). The interaction of the K^+ with the π-system of PhI strongly influences the Ph-I oxidative addition *via* **TS5** (0.6 kcal/mol). The overcrowded coordination sphere of copper prompts iodide transfer to the potassium after the C-I bond cleavage. A considerable molecular reorganization required for this transformation results in a significantly higher barrier of 29.1 kcal/mol. The release of the KI molecule into the reaction medium leads to square-pyramidal **I10** (-34.7 kcal/mol) with two CF_3 groups mutually trans. Interestingly, **I10** is the lowest point among all of the computed structures. Consequently, the reductive elimination of $PhCF_3$ occurs with a higher barrier of 17.1 kcal/mol *via* **TS6** (-17.6 kcal/mol) to bring the catalytic cycle back to **I4**.

The overall Gibbs free energy of -56.9 kcal/mol for both cycles indicates that the reaction is highly exergonic. Although Path A has a much lower activation energy than Path B (20.5 *vs*. 29.1 kcal/mol), it was concluded[27] that it is Path B that governs the process. This conclusion was arrived at on the basis of the following considerations.

First, **I4** is shared by both routes, suggesting that the reaction direction is determined by the energy stabilization effect of the next step. In this case, the trapping of KCF_3 rather than PhI is favored by 1.5 kcal/mol. Second, the reagent ratio in Amii's experiments (Scheme 16) is 2 equiv of CF_3SiEt_3/KF per 1 equiv of PhI. As a consequence, the probability for **I4** to meet KCF_3 is believed[27] to be higher. Finally, a reaction with $\Delta G^{\neq}$ = 20.5 kcal/mol should be instantaneous at 60 ºC, which is clearly not the case for the Amii reaction that takes 24 h to go to completion.[29] Therefore, it was reasoned that Path B is more probable, although its alternative, Path A, should not be ruled out completely as it could be operating in parallel or under stoichiometric conditions. We cannot agree with this argumentation. Importantly, the Amii catalytic process occurs under heterogeneous, not homogeneous conditions. The extremely low solubility of KF in the reaction medium suggests that the reactive CF_3^- synthetic equivalent ("KCF_3") is slowly generated from CF_3SiEt_3 on the surface of the solid KF promoter rather than in the bulk of the liquid phase. Therefore, the concentration of the substrate (PhI) in the reaction solution is not two times lower than that of "KCF_3", but orders of magnitude higher at the beginning of the reaction and remains higher until nearly full conversion of PhI is reached. Hence, Path B might compete with Path A only after almost all of the iodobenzene substrate is consumed, *i.e.* [PhI] is lower than ["KCF_3"] that is still continuously and slowly generated at the KF/solvent interface.

Jover[27] then probed computationally the Ph-I activation step (Scheme 20) to show that concerted OA-RE (**TS2**, $\Delta G^{\neq}$ = 18.4 kcal/mol) is more plausible than alternative mechanisms such as SBM, IAT, and SET. The SBM pathway could be discounted on the basis of the prohibitively high barrier of 52.4 kcal/mol. Although outer-sphere SET and IAT were found to be less energetically demanding (34.6 and 24.0 kcal/mol, respectively), the activation barriers derived from the Marcus-Hush

theory[28] would be even higher. It was therefore concluded that the transformation of **I4** to **I6** is governed exclusively by the Ph-I OA-RE mechanism. This conclusion was substantiated by showing computationally that, in accordance with experimental data, the order of reactivity is PhI > PhBr > PhCl and that electron-withdrawing substituents on the ring facilitate the reaction.

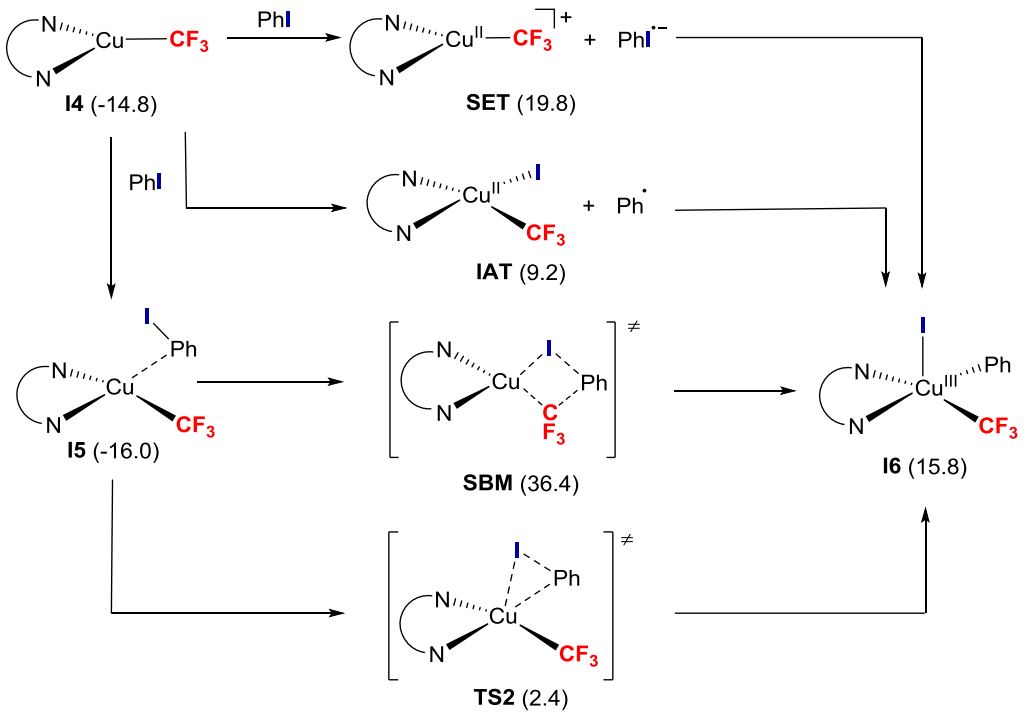

***Scheme 20**. Possible reaction pathways from **I4** to **I6**[27] (free energies in kcal/mol)*

On the basis of the computational results, two general strategies were proposed[27] for improvement of the catalytic system. First, it was suggested that stronger electron-donating ligands should lower the barrier to the Ph-I oxidative addition, the rate-determining step of the entire process. However, replacing phen with more basic TMEDA ligand in the calculations produced noticeably higher barriers of 20.2 and 30.4 kcal/mol for Paths A and B, respectively.

The other strategy would be employing a "CF_3^-" source that does not easily produce KCF_3, which should suppress the formation of K[(phen)Cu$(CF_3)_2$] (**I8**). We will review this idea even though we do not believe that Path B contributes significantly under the experimental conditions (see above). Among various nucleophilic CF_3 agents, at least two were considered[27] promising, trifluoroacetates CF_3COOM[3,18,21,31] and K[$CF_3B(OMe)_3$], [32] which both have been used for copper-promoted/catalyzed trifluoromethylation reactions of haloarenes. Preliminary calculations[27] suggested that neither CF_3COOK nor K[$CF_3B(OMe)_3$] can give rise to KCF_3 because both processes, by-producing CO_2 and $B(OMe)_3$, respectively, are thermodynamically forbidden. However, alternative mechanisms for CF_3 transfer from K[$CF_3B(OMe)_3$] and from CF_3COOK leading to **I1** were found (Scheme 21). The reaction of **I1** with K[$CF_3B(OMe)_3$] gives **I2_B** (-3.7 kcal/mol) that loses KI upon rearrangement to **I3_B** (13.0 kcal/mol). This intermediate is 16.7 kcal/mol higher in energy than the preceding one, yet accessible. More importantly, **I3_B** is a dead end as the computed barrier of 39.5 kcal/mol for CF_3 transfer to the Cu *via* a four-membered transition state **TS_B1** (35.8 kcal/mol) is prohibitively high. Alternatively, extrusion of $B(OMe)_3$ molecule from **I2_B** leads to **I2** (6.8 kcal/mol) *via* an easily accessible transition state **TS2_B2** (12.3 kcal/mol) constitutes a viable pathway with $\Delta G^{\neq}$ = 16.0 kcal/mol. Similarly, with CF_3COOK in place of K[$CF_3B(OMe)_3$], one pathway (*via* **I3_C**) had a prohibitively high barrier, whereas decarboxylation of **I2_C** was computed to proceed with $\Delta G^{\neq}$ = 19.3 kcal/mol to give **I2** (Scheme 21). Once **I2** at 10.8 kcal/mol is formed, the reaction will evolve through Path A, as shown in Scheme 19 and described above. It is worth to note that, while not questioning the technical quality of these calculations, we find the

[31] (a) Langlois, B. R.; Roques, N. *J. Fluorine Chem*. **2007**, *128*, 1318. (b) Schareina, T.; Wu, X.-F.; Zapf, A.; Cotté, A.; Gotta, M.; Beller, M. *Top Catal.* **2012**, *55*, 426.
[32] (a) Knauber, T.; Arikan, F.; Röschenthaler, G.-V.; Gooβen, L. J. *Chem. Eur. J.* **2011**, *17*, 2689. (b) Gonda, Z.; Kovács, S.; Wéber, C.; Gáti, T.; Mészáros, A.; Kotschy, A.; Novák Z. *Org. Lett.* **2014**, *16*, 4268.

barrier of 19.3 kcal/mol to the decarboxylation inconsistent with the experimentally established need to perform the decarboxylative trifluoromethylation reactions of aryl iodides at 150-160 °C and above.[18,21]

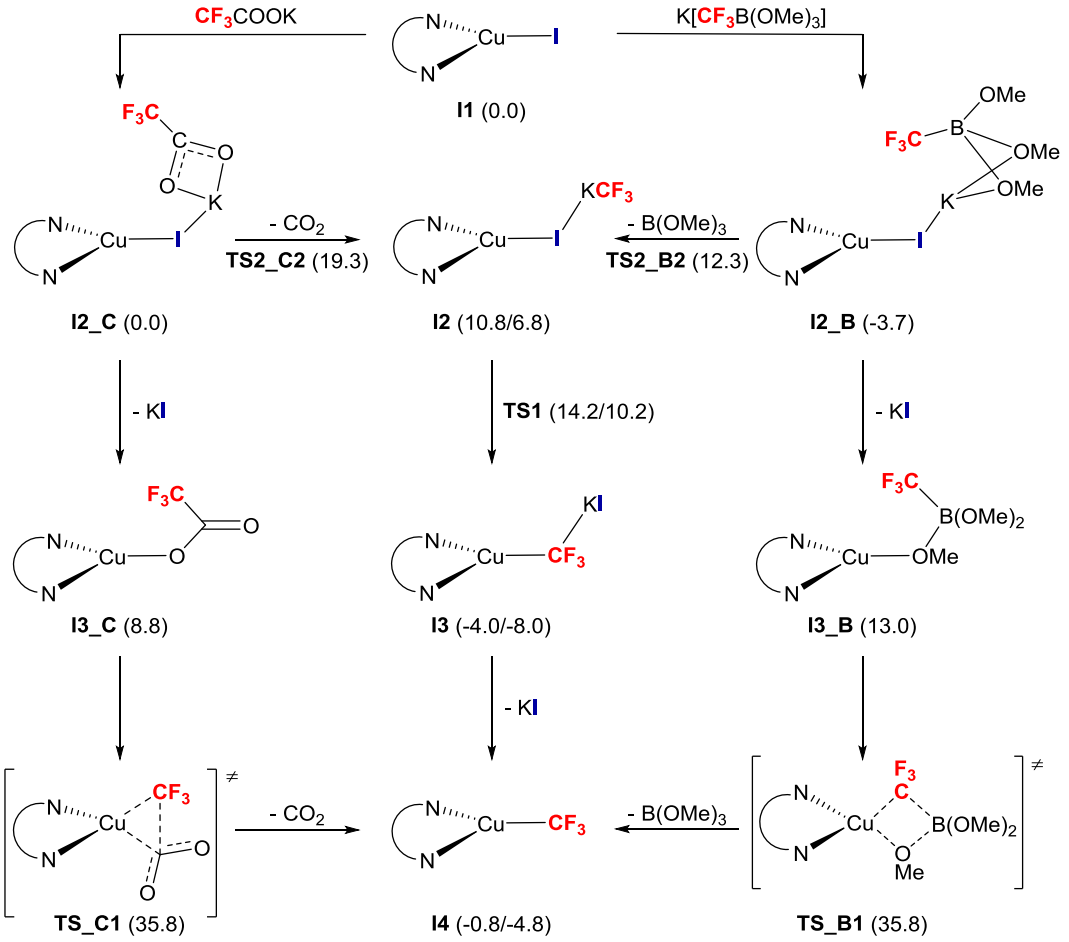

Scheme 21. *Generation of **I4** from CF_3 sources[27] (free energies in kcal/mol)*

Trifluoromethylation of Arylboronic Acids and Their Derivatives. The copper-mediated oxidative trifluoromethylation of arylboronic acids was discovered by Chu and Qing [33] in 2010. They found that $CuCF_3$ generated *in situ* can easily trifluoromethylate a broad range of substrates under mild reaction conditions in the presence of several additives and Ag_2CO_3 as an oxidant. In contrast to aryl halides,

[33] (a) Chu, L.; Qing, F.-L. *Org. Lett.* **2010**, *12*, 5060. (b) Jiang, X.; Chu, L.; Qing, F.-L. *J. Org. Chem.* **2012**, *77*, 1251 (c) Chu, L.; Qing, F.-L. *Acc. Chem. Res.* **2014**, *47*, 1513.

arylboronic acids with electron-donating groups were found to promote the reaction to higher yields. Soon after the original Chu-Qing report,[33a] an alternative procedure using O_2 in place of costly Ag_2CO_3 was reported[34] as well as similar methodologies using other arylboronic derivatives such as fluoroborates[35] and pinacol esters.[35a,b,36] Among the considerable number of known protocols for trifluoromethylation of arylboronic acids, one holds promise for larger scale operations owing to its simplicity, high efficiency, low-cost, and safety (air is used as the oxidant).[37]

Both aryl boronic acids and $CF_3Cu(I)$ are nucleophiles and therefore do not react with one another. An oxidant is needed to produce a higher oxidation state, *electrophilic* $CuCF_3$ species that can be reactive toward $ArB(OH)_2$. Therefore, mechanistically, the oxidative trifluoromethylation of aryl boronic acids might seem to be akin to the Chan-Evans-Lam (CEL) reaction.[38] It has been shown[39] that CEL can be effected by Cu(II) to 50% conversion in the absence of an oxidant (O_2) due to the spontaneous disproportionation to inactive Cu(I) and active Cu(III) (Scheme 22, A). When oxygen is added, the inactive Cu(I) is oxidized to active Cu(III), which brings the conversion to quantitative. This is not the case, however, with the recently studied[40] oxidative trifluoromethylation of aryl boronic acids. *Both* the Cu(I) and Cu(III) CF_3-ligated complexes produced from a Cu(II) precursor are unreactive toward $PhB(OH)_2$. Only on exposure to air does the reaction occur due to the formation of an active species by oxidation of the Cu(I) with O_2 (Scheme 22, B). This was established in a mechanistic

[34] Senecal, T. D.; Parsons, A. T.; Buchwald, S. L. *J. Org. Chem*. **2011**, *76*, 1174.
[35] (a) Liu, T.; Shao, X.; Wu, Y.; Shen, Q. *Angew. Chem., Int. Ed*. **2012**, *51*, 540. (b) Huang, Y.; Fang, X.; Lin, X.; Li, H.; He, W.; Huang, K.-W.; Yuan, Y.; Weng, Z. *Tetrahedron* **2012**, *68*, 9949. (c) Presset, M.; Oehlrich, D.; Rombouts, F.; Molander, G. A. *J. Org. Chem.* **2013**, *78*, 12837.
[36] (a) Litvinas, N. D.; Fier, P. S.; Hartwig, J. F. *Angew. Chem., Int. Ed.* **2012**, *51*, 536. (b) Khan, B. A.; Buba, A. E.; Gooßen, L. J. *Chem. Eur. J.* **2012**, *18*, 1577.
[37] Novák, P.; Lishchynskyi, A.; Grushin, V. V. *Angew. Chem., Int. Ed.* **2012**, *51*, 7767.
[38] (a) Chan, D. M. T.; Monaco, K. L.; Wang, R. P.; Winters, M. P. *Tetrahedron Lett.* **1998**, *39*, 2933. (b) Evans, D. A.; Katz, J. L.; West, T. R. *Tetrahedron Lett.* **1998**, *39*, 2937. (c) Lam, P. Y. S.; Clark, C. G.; Saubern, S.; Adams, J.; Winters, M. P.; Chan, D. M. T.; Combs, A. *Tetrahedron Lett*. **1998**, *39*, 2941.
[39] King, A. E.; Brunold, T. C.; Stahl, S. S. *J. Am. Chem. Soc*. **2009**, *131*, 5044.
[40] Nebra, N.; Grushin, V. V. *J. Am. Chem. Soc*. **2014**, *136*, 16998.

study[40] where the formation of two Cu(III) ([(bpy)$CuCF_3)_3$], [$Cu(CF_3)_4]^-$) and two Cu(I) ([(bpy)$CuCF_3$], [$Cu(CF_3)_2]^-$) complexes was observed from clean disproportionation of [(bpy)$Cu(CF_3)_2$] generated *in situ* from [(bpy)$CuF_2(H_2O)_3$] and excess $TMSCF_3$ under rigorously O_2-free conditions (Scheme 23). In the absence of an oxidant, none of the resultant species is reactive toward $PhB(OH)_2$, including the Cu(III) complexes that are remarkably robust and can be isolated and structurally characterized.[41] Both of these Cu(III) complexes stay unchanged throughout the process. Opening the reaction mixture to air triggers immediate oxidation of the Cu(I) to Cu(III) in the form of [(bpy)$Cu(CF_3)_2$(OTMS)] that undergoes transmetalation with $PhB(OH)_2$, followed by Ph-CF_3 reductive elimination. The Cu(I) coproduced then commences another turnover (Scheme 23). Therefore, this trifluoromethylation is catalytic in Cu even if the starting fluoro complex is used in stoichiometric quantities for the reaction. The key oxidation step likely[30] occurs as shown in Scheme 24.

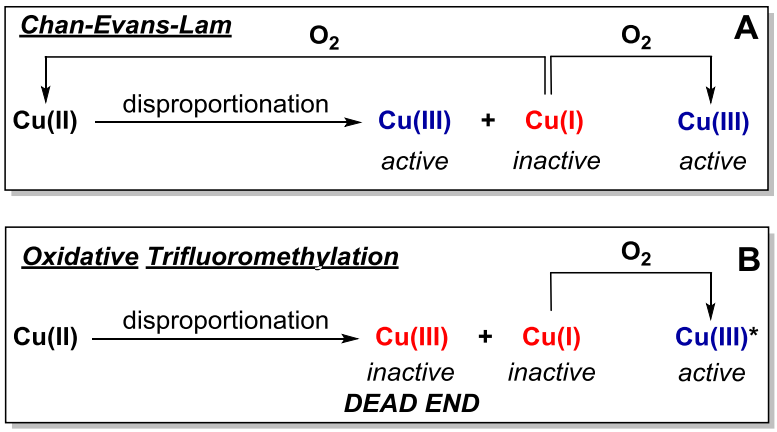

Scheme 22. *Different pathways to active Cu(III) species in the CEL (A) and oxidative trifluoromethylation (B) reactions*[40]

[41] (a) Naumann, D.; Roy, T.; Tebbe, K.-F.; Crump, W. *Angew. Chem., Int. Ed.* **1993**, *32*, 1482. (b) Romine, A. M.; Nebra, N.; Konovalov, A. I.; Martin, E.; Benet-Buchholz, J.; Grushin, V. V. *Angew. Chem., Int. Ed.* **2015**, *54*, 2745.

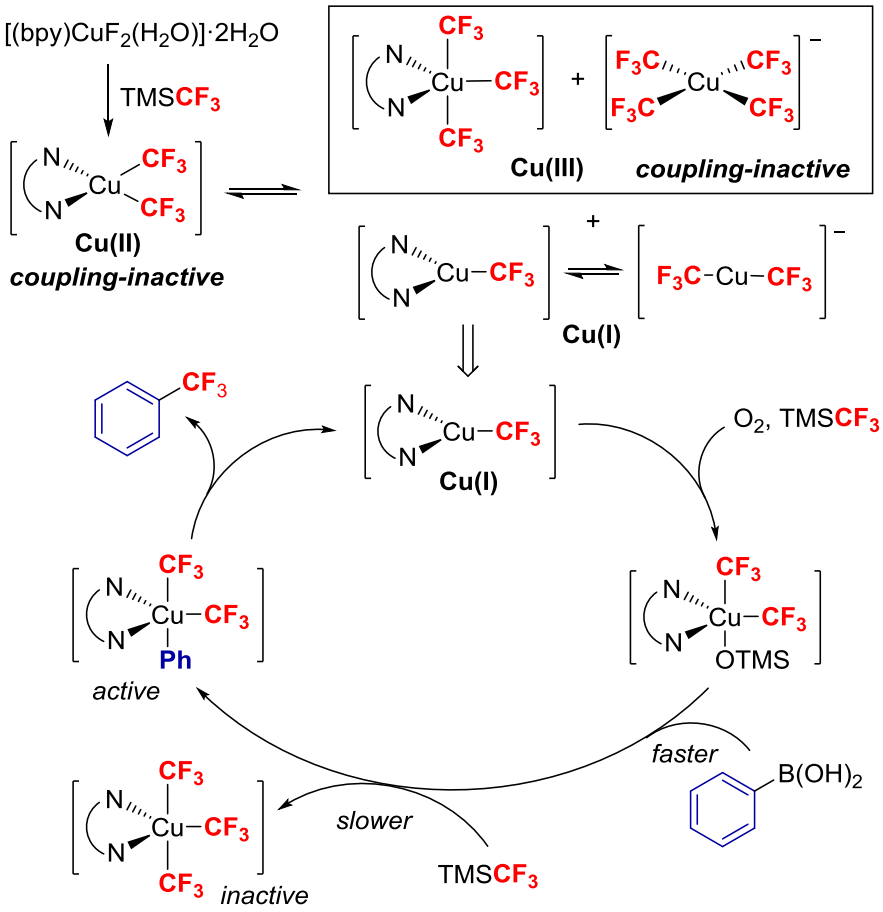

***Scheme 23**. Mechanism of oxidative trifluoromethylation of PhB(OH)$_2$*[40]

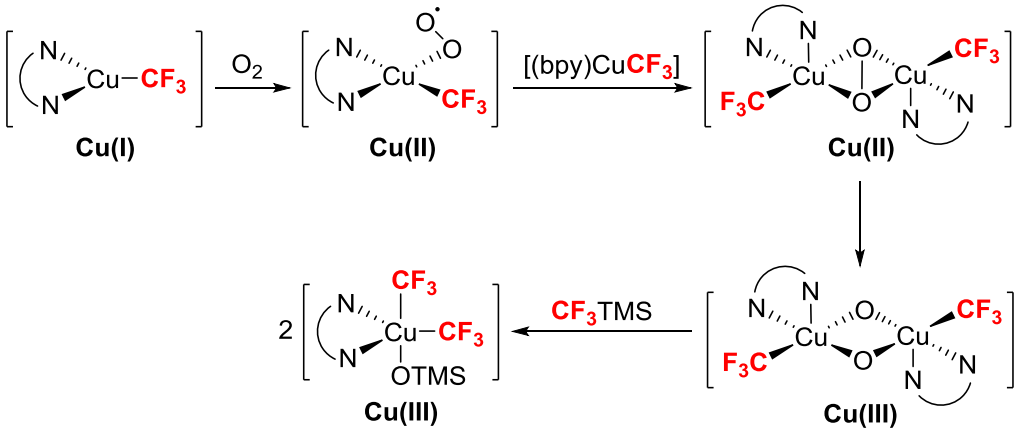

***Scheme 24**. Proposed mechanism of air-oxidation of [(bpy)Cu(CF$_3$)]*[30]

Trifluoromethylation of Arenediazonium Salts. The Sandmeyer-type [42] trifluoromethylation of arenediazonium salts (Scheme 3) is a very recent development.[43] Like the classical Sandmeyer reaction,[42] the trifluoromethylation of diazonium compounds is a radical process, as has been established beyond any doubt in radical clock experiments reported by two groups[43a,d] (Scheme 25). Acetonitrile as a solvent or co-solvent has a critical beneficial effect on the reaction selectivity and yield of the desired product.

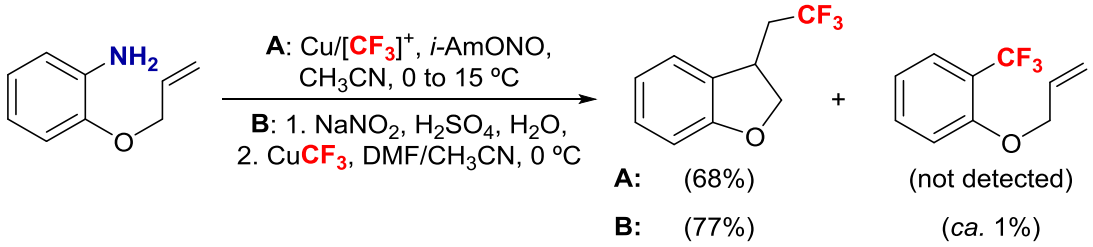

***Scheme 25**. Radical clock experiments reported in refs. 43a (A) and 43d (B)*

Interestingly, Fu *et al.*[43a] have claimed detection of an adduct of $CF_3^{\cdot}$ with TEMPO, a radical scavenger, by GC-MS, whereas in our group it has been found[43d] that such radical traps as 1,1-diphenylethylene and 2,6-bis(1,1-dimethylethyl)-4-methylphenol do not affect the reaction. This observation, along with the detection of small quantities of protodiazotization products, suggests that like various Sandmeyer-type transformations, the trifluoromethylation of diazonium salts occurs in a solvent cage. The ~100% selectivity of the radical clock reaction (Scheme 25) indicates that the Ar-CF_3 coupling is at least ca. two orders of magnitude slower than the cyclization yet

[42] For reviews, see: (a) Hodgson, H. H. *Chem. Rev*. **1947**, *40*, 251. (b) Galli, C. *Chem. Rev*. **1988**, *88*, 765.
[43] (a) Dai, J.-J.; Fang, C.; Xiao, B.; Yi, J.; Xu, J.; Liu, Z.-J.; Lu, X.; Liu, L.; Fu, Y. *J. Am. Chem. Soc*. **2013**, *135*, 8436. (b) Danoun, G.; Bayarmagnai, B.; Grünberg, M. F.; Gooßen, L. J. *Angew. Chem., Int. Ed*. **2013**, *52*, 7972. (c) Bayarmagnai, B.; Matheis, C.; Risto, E.; Gooßen, L. J. *Adv. Synth. Catal*. **2014**, *356*, 2343. (d) Lishchynskyi, A.; Berthon, G.; Grushin, V. V. *Chem. Commun.* **2014**, *50*, 10237. (e) Danoun, G.; Bayarmagnai, B.; Grünberg, M. F.; Matheis, C.; Risto, E.; Gooßen, L. J. *Synthesis* **2014**, *46*, 2283.

considerably faster than the escape of the aryl radical from the solvent cage. Given these considerations and the k_c value of 5.3×10^9 s^{-1} (25 ºC) for the 2-(allyloxy)-aniline-derived radical clock,[24e] the solvent cage lifetime in the trifluoromethylation reaction may be estimated at $>10^{-7}$ s, much longer than the typical value of ca. 10^{-11} s.[44] It is believed that the high affinity of CH_3CN as a ligand for Cu results in a vastly enhanced stability of the solvent cage. In addition, being a poor H atom donor for radicals,[45] acetonitrile diminishes the undesired protodiazotization. Interestingly, a non-radical mechanism has been proposed for the trifluoromethylation of arenediazonium salts with $AgCF_3$.[46]

Direct C-H Aromatic Trifluoromethylation. Transition metal-free trifluoromethylation of aromatic C-H bonds with CF_3 radicals has been known since the early 1960s.[47,48] It was quickly recognized back then that this method has virtually no synthetic value because of the lack of positional selectivity. Indeed, isomers of aromatic compounds bearing a CF_3 group in various positions are widely known to conventionally possess nearly identical physicochemical properties and, as a result, cannot be separated from their mixtures. Nonetheless, a few years ago, radical trifluoromethylation of (hetero)aromatic C-H bonds was "reinvented" and successfully oversold as a superior, atom-economical general method to prepare trifluoromethylated aromatics. The expert verdict,[49] however, provides a sober view on the real synthetic utility of radical aromatic C-H trifluoromethylation reactions.

[44] Reichard, C.; Welton, T. *Solvents and Solvent Effects in Organic Chemistry*; Wiley-VCH: Weinheim, 2011.
[45] Doyle, M. P.; Dellaria, J. F., Jr.; Siegfried, B.; Bishop, S. W. *J. Org. Chem*. **1977**, *42*, 3494.
[46] Wang, X.; Xu, Y.; Mo, F.; Ji, G.; Qiu, D.; Feng, J.; Ye, Y.; Zhang, S.; Zhang, Y.; Wang, J. *J. Am. Chem. Soc*. **2013**, *135*, 10330.
[47] (a) Tiers, G. V. D. *J. Am. Chem. Soc*. **1960**, *82*, 5513. (b) Drysdale, J. J.; Coffman, D. D. *J. Am. Chem. Soc*. **1960**, *82*, 5111.
[48] Dolbier, W. R., Jr. *Chem. Rev*. **1996**, *96*, 1557.
[49] Studer, A. *Angew. Chem., Int. Ed*. **2012**, *51*, 8950.

Examples of Cu-promoted trifluoromethylation of aromatic C-H bonds are rare. The first transformation of this type was reported by Chu and Qing [50] for some heterocycles and pentafluorobenzene under oxidizing conditions. They proposed a mechanism involving metalation of the C-H bond with Cu(I). For substrates bearing a directing group such as amide, good *ortho*-selectivity is naturally observed.6[a] For instance, pivalamido arenes have been trifluoromethylated at the *ortho*-position with Togni's reagent in the presence of CuCl as a catalyst.[51] This transformation might occur *via* a radical pathway as TEMPO completely suppresses the reaction. The EPR-detected $CF_3^{\cdot}$ radical adduct with *N-tert*-butyl-α-phenylnitrone (PBN, Scheme 26) provides additional support for a radical mechanism, whose intimate details, nevertheless, remain unknown.

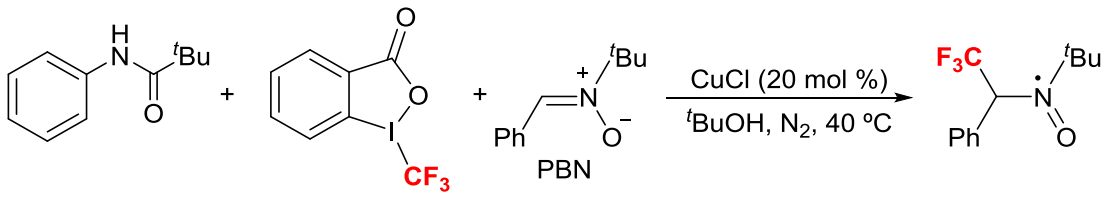

***Scheme 26**. Radical trap experiment*[51]

Concluding Remarks. The above survey presents the current state of affairs in our understanding of mechanisms of Cu-mediated aromatic trifluoromethylation reactions. The very few mechanistic studies of these transformations contrast sharply with the flood of many hundreds of papers reporting further methodology development work in the area. It is not until very recently that this scientifically unhealthy imbalance has begun to be addressed. The targeted mechanistic studies reported to date, however, are almost exclusively computational. Although reports of trifluoromethylation

[50] Chu, L.; Qing, F.-L. *J. Am. Chem. Soc.* **2012**, *134*, 1298.
[51] Cai, S.; Chen, C.; Sun, Z.; Xi, C. *Chem. Commun*. **2013**, *49*, 4552.

methodology development contain sporadic data on mechanisms of the reactions, this information is limited and most often not fully conclusive.

In this Thesis, we report the first combined experimental and computational studies aimed specifically at elucidation of the mechanism of trifluoromethylation of aryl halides with $CuCF_3$. These results are presented in Chapters 2 and 3 below. The $CuCF_3$ reagent used in our work was prepared by the new reaction of direct cupration of fluoroform, recently discovered[12] in our group. As this remarkable transformation is unprecedented, we have carried out a telic investigation of its mechanism, also by experimental and computational means. This work is reported in Chapter 1. Finally, Chapter 4 describes our theoretical studies of the intriguing3 electronic properties of the CF_3 group as a substituent and ligand in organic and organometallic chemistry. It is needless to say that this subject matter is highly relevant to metal-mediated trifluoromethylation reactions and their mechanisms.

REACTION MECHANISMS ON THE WAY FROM CHF3 TO ARCF3. THE NATURE OF THE ORTHO-EFFECT AND ELECTRONIC PROPERTIES OF THE CF3 GROUP.
Andrey I. Konovalov
Dipòsit Legal: T 1587-2015

Chapter 1.

Mechanism of the Direct Cupration of Fluoroform

Introduction

Trifluoromethane (CHF_3, fluoroform, HFC-23) is a gas (bp = -82 ^oC) that is by-produced (ca. 25000 t/a) by the fluoropolymer and fluorochemicals industries.[1] Fluoroform lacks industrial applications on a scale commensurate with its side production. Being neither toxic nor ozone-depleting, the side-generated CHF_3 must nonetheless be treated because of its high global warming potential (> 10^4 that of CO_2) and > 250-year atmospheric lifetime. Incineration of CHF_3, a flame retardant, is, however, a costly and environmentally unfriendly process.

A vastly preferred alternative to the destruction of CHF_3 would be its utilization as a feedstock for production of fluorochemicals. Fluoroform has long been viewed[2] as by far the best CF_3 source for the synthesis of trifluoromethylated building blocks and intermediates that are in great demand for the synthesis of modern agrochemicals, pharmaceuticals, and specialty materials2,[3] (see General Introduction above). However, selective and efficient activation of CHF_3, a rather inert molecule, represents a considerable challenge. Fluoroform is highly thermodynamically stable, as can be seen from the reported C-H and C-F bond dissociation energies of 106 and 127 kcal/mol, respectively.[4] Until very recently, deprotonation of weakly acidic fluoroform (pK_a = 27 in H_2O),[5] with strong bases remained the only methodology to employ CHF_3 in

[1] (a) Grushin, V. V. *Chim. Oggi* **2014**, *32*, 81. (b) Han, W.; Li, Y; Tang, H.; Liu, H. *J. Fluorine Chem*. **2012**, *140*, 7.
[2] Tomashenko, O. A.; Grushin, V. V. *Chem. Rev.* **2011**, *111*, 4475.
[3] (a) Burton, D. J.; Yang, Z. Y. *Tetrahedron* **1992**, *48*, 189. (b) McClinton, M. A.; McClinton, D. A. *Tetrahedron* **1992**, *48*, 6555. (c) Schlosser, M. *Angew. Chem., Int. Ed.* **2006**, *45*, 5432. (d) Roy, S.; Gregg, B. T.; Gribble, G. W.; Le, V.-D.; Roy, S. *Tetrahedron* **2011**, *67*, 2161. (e) Qing, F.-L.; Zheng, F. *Synlett* **2011**, 1052. (f) Jin, Z.; Hammond, G. B.; Xu, B. *Aldrichim. Acta* **2012**, 45, 67. (g) Chen, P.; Liu, G. *Synthesis* **2013**, *45*, 2919. (h) Landelle, G.; Panossian, A.; Pazenok, S.; Vors, J.-P.; Leroux, F. R. *Beilstein J. Org. Chem*. **2013**, *9*, 2476.
[4] (a) Amphlett J. C.; Coomber J. W.; Whittle E. *J. Phys. Chem.* **1966**, *70*, 593. (b) Shia J.; Hea J.; Wang H.-J. *J. Phys. Org. Chem*. **2011**, *24*, 65.
[5] Symons, E. A.; Clermont, M. J. *J. Am. Chem. Soc*. **1981**, *103*, 3127.

synthesis (Scheme 1).[6] This deprotonation approach is not feasible for large scale applications for a number of reasons, including the necessity to use low temperatures in order to avoid the exceedingly facile decomposition of the CF_3^- carbanionic intermediate to difluorocarbene CF_2.

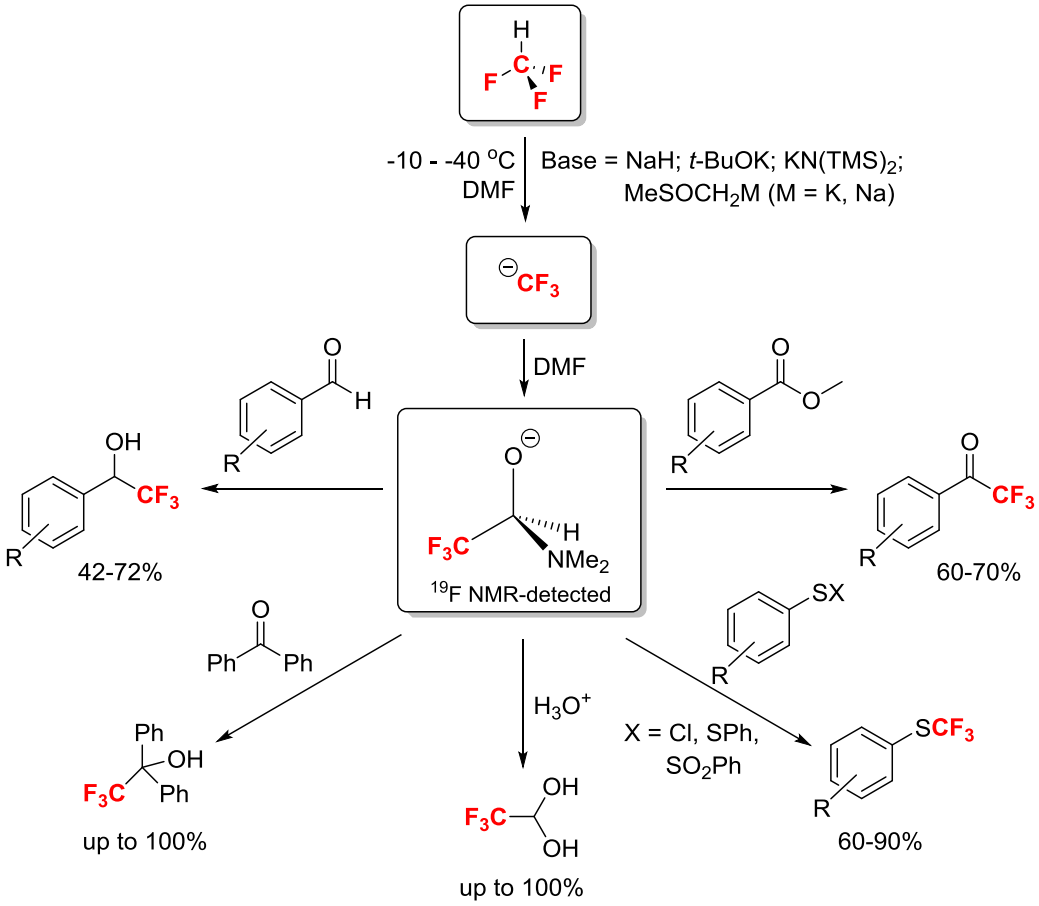

Scheme 1. *Trifluoromethylation of carbonyl and sulfur electrophiles with CHF_3/base*

[6] (a) Shono, T.; Ishifune, M.; Okada, T.; Kashimura, S. *J. Org. Chem.* **1991**, *56*, 2. (b) Roques, N.; Russell, J. PCT Int. Appl. WO 97/19038, 1997. (c) Roques, N.; Russell, J. U. S. Patent 6355849, 2002. (d) Russell, J.; Roques, N. *Tetrahedron* **1998**, *54*, 13771. (e) Barhdadi, R.; Troupel, M.; Perichon, M. *Chem. Commun*. **1998**, 1251. (f) Folleas, B.; Marek, I.; Normant, J.-F.; Saint-Jalmes, L. *Tetrahedron Lett.* **1998**, *39*, 2973. (g) Folleas, B.; Marek, I.; Normant, J.-F.; Saint-Jalmes, L. *Tetrahedron* **2000**, *56*, 275. (h) Billard, T.; Bruns, S.; Langlois, B. R. *Org. Lett*. **2000**, *2*, 2101. (i) Large, S.; Roques, N.; Langlois, B. R. *J. Org. Chem*. **2000**, *65*, 8848. (j) Langlois, B. R.; Billard, T. *ACS Symp. Ser*. **2005**, *911*, 57. (k) Prakash, G. K. S.; Jog, P. V.; Batamack, P. T. D.; Olah, G. A. *Science* **2012**, *338*, 1324. (l) Kawai, H.; Yuan, Z.; Tokunaga, E.; Shibata, N. *Org. Biomol. Chem*. **2013**, *11*, 1446. (m) Zhang Y.; Fujiu M.; Serizawa H.; Mikami K. *J. Fluorine Chem*. **2013**, *156*, 367.

A much more recent, distinctly different approach1 to CHF_3 activation is based on the previously proposed6[g] idea of direct metalation leading to a stable M-CF_3 derivative in one step. In 2011, the first reactions of direct zincation and cupration of fluoroform were reported by Daugulis *et al.* (Scheme 2)[7] and our group (Scheme 3),[2,8] respectively. In the same year, Goldman and co-workers[9] demonstrated H-CF_3 oxidative addition to an iridium pincer complex (Scheme 4). More recently, Takemoto and Grushin[10] reported the highly selective palladation of CHF_3 (Scheme 5).

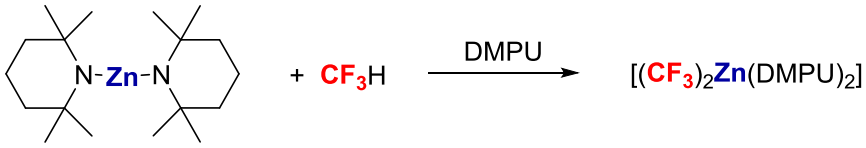

Scheme 2. *Zincation of fluoroform*7

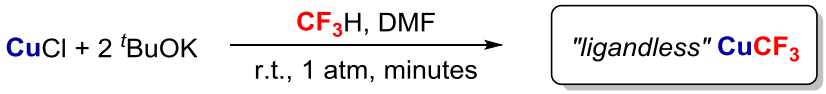

Scheme 3. *Cupration of fluoroform*8

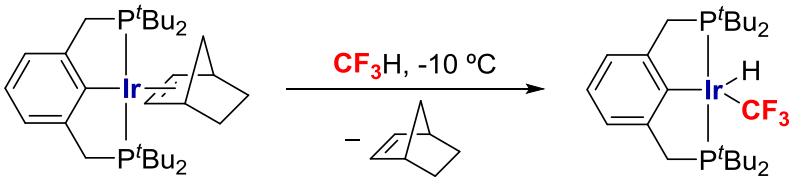

Scheme 4. *Oxidative addition of fluoroform to Ir(I)*9

[7] Popov, I.; Lindeman, S.; Daugulis, O. *J. Am. Chem. Soc.* **2011**, *133*, 9286.
[8] Zanardi, A.; Novikov, M. A.; Martin E.; Benet-Buchholz, J.; Grushin. V. V. *J. Am. Chem. Soc*. **2011**, *133*, 20901.
[9] Choi, J.; Wang, D. Y.; Kundu, S.; Choliy, Y.; Emge, T. J.; Krogh-Jespersen, K.; Goldman, A. S. *Science* **2011**, *332*, 1545.
[10] Takemoto, S.; Grushin, V. V. *J. Am. Chem. Soc.* **2013**, *135*, 16837.

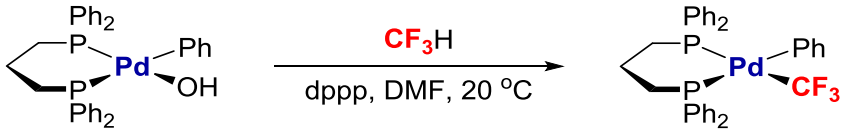

***Scheme 5**. Palladation of fluoroform*[10]

Of the four C-H activation reactions of fluoroform with transition metals shown in Schemes 2-5, the direct cupration (Scheme 3)8 holds particular promise. The cupration reaction employs only low-cost materials and smoothly occurs at room temperature and atmospheric pressure to furnish "ligandless" $CuCF_3$ in >90% yield. Furthermore, a flow process has been recently developed for the production of fluoroform-derived $CuCF_3$ in a continuous manner in up to 94% yield.[11] Most importantly, however, the $CuCF_3$ reagent has been shown[12] to trifluoromethylate a broad variety of substrates in high yield and with excellent selectivity (Scheme 6). Indeed, "*The fluoroform-derived $CuCF_3$ reagent and its reactions with haloarenes provide an unmatched combination of reactivity, selectivity, and low cost*".[12c]

[11] Mazloomi, Z.; Bansode, A.; Benavente, P.; Lishchynskyi, A.; Urakawa, A.; Grushin, V. V. *Org. Proc. Res. Dev.* **2014**, *18*, 1020.
[12] (a) Novák, P.; Lishchynskyi, A.; Grushin, V. V. *Angew. Chem., Int. Ed.* **2012**, *51*, 7767. (b) Novák, P.; Lishchynskyi, A.; Grushin, V. V. *J. Am. Chem. Soc*. **2012**, *134*, 16167. (c) Lishchynskyi, A.; Novikov, M. A.; Martin, E.; Escudero-Adán, E. C.; Novák, P.; Grushin, V. V. *J. Org. Chem*. **2013**, *78*, 11126. (d) Lishchynskyi, A.; Berthon, G.; Grushin, V. V. *Chem. Commun.* **2014**, *50*, 10237. (e) Lishchynskyi, A.; Mazloomi, Z.; Grushin, V. V. *Synlett* **2015**, *26*, 45.

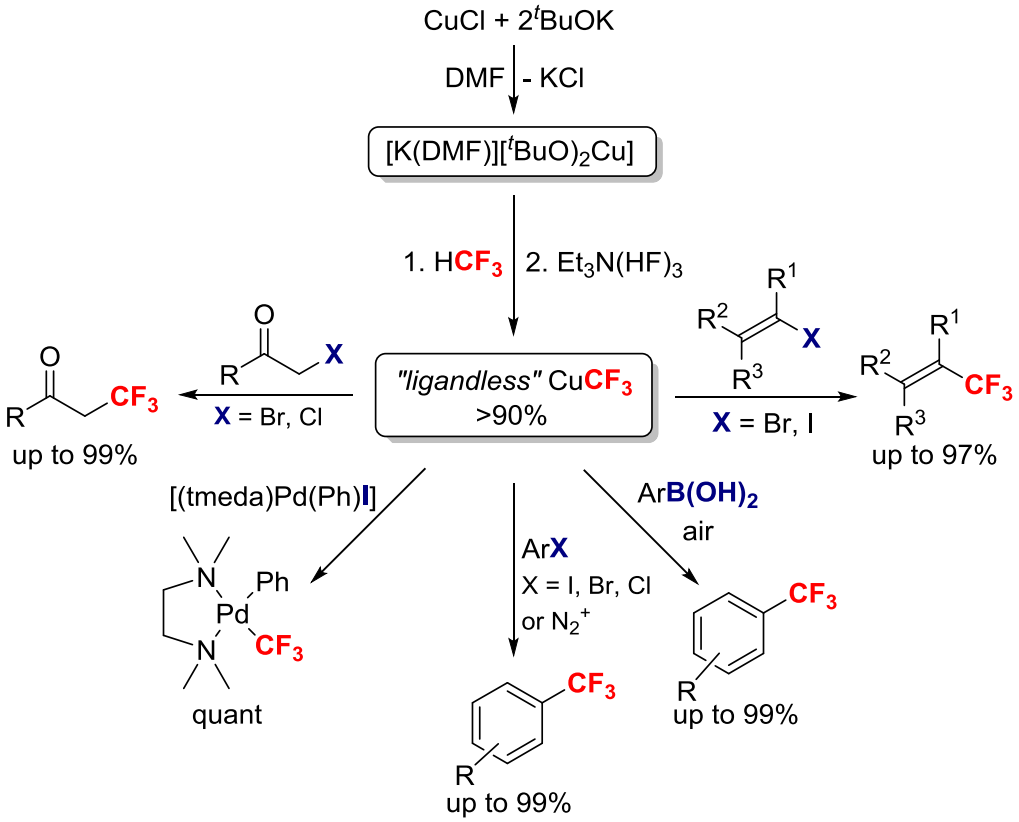

Scheme 6. *Trifluoromethylation reactions with fluoroform-derived $CuCF_3$*[8,12]

Objectives

Considering the importance of the reaction of direct cupration of fluoroform[8,11] for the trifluoromethylation methodology[12] (Schemes 3 and 6), it was of great interest to study and, hopefully, establish the mechanism of this previously unknown transformation. At the beginning of our work, very little mechanistic information was available regarding the CHF_3 cupration. It had been demonstrated[8] that the active cuprating species is the novel dialkoxycuprate [K(DMF)][(*t*-BuO)$_2$Cu] (**1**) that is made quantitatively from CuCl and 2 equiv of *t*-BuOK in DMF (Scheme 6). The structure of **1** had been determined by single crystal X-ray diffraction.[8] The fact that the cupration cleanly occurs at room temperature was a strong indication that "CF_3^-" or its equivalent do not mediate the process. Furthermore, no cyclopropanation took place when the cupration reaction was performed in the presence of deliberately added α-methylstyrene. The latter is known[13] to undergo cycloaddition of CF_2 that is easily produced from the CF_3^- anion.[6] Although evidence had been provided[8] that neither CF_3^- nor CF_2 mediate the H-CF_3 bond activation and Cu-CF_3 bond formation, the mechanism of this process remained unknown.

The objective of the work described in this Chapter was to investigate the mechanism of the cupration reaction of fluoroform in as much detail as possible. We therefore employed the most fruitful modern approach to elucidation of reaction mechanisms, which involves both experimental and computational studies. The results of our work are described in the next section, showing that the mechanism of H-CF_3 activation with **1** is as striking and unprecedented as the reaction itself.

[13] Dolbier, W. R., Jr.; Wojtowicz, H.; Burkholder, C. R. *J. Org. Chem*. **1990**, *55*, 5420.

Results

The reactive species that is produced upon treatment of CuCl and *t*-BuOK in a 1:2 molar ratio and that cuprates fluoroform is [K(DMF)][(*t*-BuO)$_2$Cu] (**1**), as established previously by single-crystal X-ray diffraction (Figure 1).8

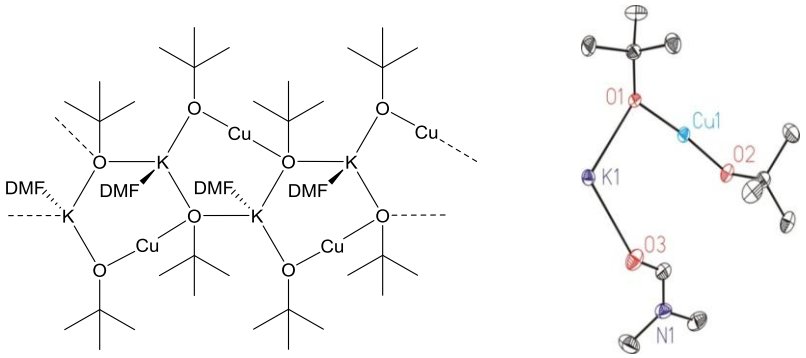

Figure 1. *Solid state structure (left) and ORTEP drawing (right) of* ***1*** *with H atoms omitted for clarity and thermal ellipsoids drawn to the 50% probability level*8

The $CuCF_3$ species directly produced in the reaction of **1** with CHF_3 decays in the course of hours and is too unstable for isolation. This decomposition is caused by the potassium cation that abstracts fluoride from the CF_3 ligand on Cu (α-fluoride elimination)[2,14] to give KF and a Cu(I) carbene (Scheme 7). Freshly prepared solutions of fluoroform-derived $CuCF_3$ can be efficiently stabilized against this decomposition by treatment with a source of HF such as $Et_3N{\cdot}3HF$ or $Py(HF)_n$.8 The mechanism of this stabilization is the sequestering of the reactive potassium cations in the form of highly thermodynamically favored KF that precipitates out. The $CuCF_3$ species in the resultant solution is much more stable (days at room temperature), yet insufficiently robust for

[14] (a) Hughes, R. P. *Adv. Organomet. Chem*. **1990**, *31*, 183. (b) Morrison, J. A. *Adv. Organomet. Chem.* **1993**, *35*, 211. (c) Hughes, R. P. *Eur. J. Inorg. Chem*. **2009**, 4591. (d) García-Monforte, M. A.; Martínez-Salvador, S.; Menjón, B. *Eur. J. Inorg. Chem*. **2012**, 4945.

isolation and structural studies.

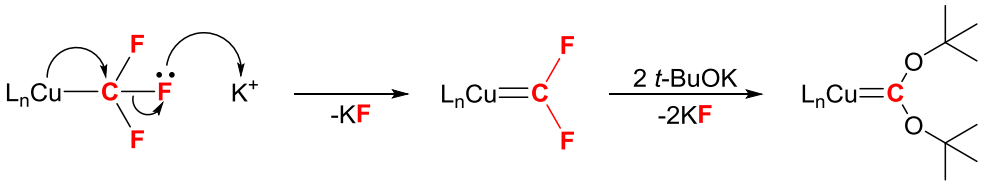

***Scheme 7**. Decomposition of CHF_3-derived $CuCF_3$ via K^+-induced α-F-elimination*8

We reasoned that adding a ligand with a strong affinity for K^+ after the cupration reaction would diminish its electrophilicity, thereby suppressing the decomposition of the just-produced $CuCF_3$. Unlike the treatment with the HF sources, this method was expected to provide a milder, more "noninvasive" technique to stabilize the originally formed $CuCF_3$ species for isolation and further studies. We were delighted to find that the addition of one equivalent of 18-crown-6 to the reaction mixture immediately after the cupration produced quantitatively a stable complex that was amenable to isolation and structure determination.[15] As shown in Figure 2, the product of this complexation is [K(18-crown-6)][(*t*-BuO)Cu(CF_3)] (**2**), a mixed ate species that bears one *t*-BuO and one CF_3 on the Cu(I) center.

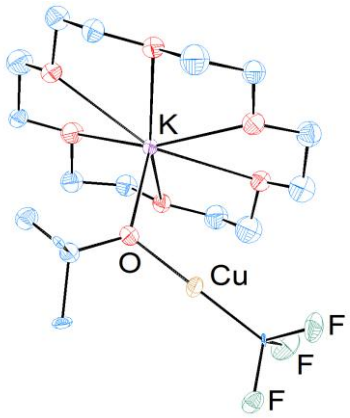

[15] Konovalov, A. I.; Benet-Buchholz, J.; Martin, E.; Grushin, V. V. *Angew. Chem., Int. Ed.* **2013**, *52*, 11637.

***Figure 2**. ORTEP drawing of **2** with H atoms omitted for clarity and thermal ellipsoids drawn to the 50% probability level*[15]

The O atom of the *t*-BuO ligand on Cu is coordinated to K^+ in the crown ether. The O-Cu-CF_3 fragments in the four independent molecules found in the crystal of **2** are nearly linear (174.5(5)-179.7(5)°) and the Cu-CF_3 bond distances (1.81(2), 1.868(14), 1.914(15), and 1.927(13) Å) are, on average, noticeably shorter than in the handful of previously reported structurally characterized Cu-CF_3 complexes.[16]

Under rigorously O_2- and H_2O-free conditions, **2** is stable in the solid state and decomposes only slowly in solution (DMF, THF, benzene). The isolation and structural characterization of **2** provides evidence for the reaction of CHF_3 with **1**, leading to [(*t*-BuO)Cu(CF_3)]$^-$ along with one equivalent of *t*-BuOH (Scheme 8). These two undergo fast exchange, as follows from the observation of only one singlet resonance from the *t*-BuO groups in the room temperature ^{1}H NMR spectrum of a freshly prepared cupration reaction mixture in DMF-d_7. A possible mechanism for this exchange is shown in Scheme 8. In solutions of [(*t*-BuO)Cu(CF_3)]$^-$ prepared from **1** and CHF_3, the lack of strongly stabilizing ligands for the potassium cations accounts for their enhanced electrophilicity toward the F atoms and, as a consequence, facile α-fluoride elimination.

[16] (a) Reported Cu-CF_3 bond lengths: [(TMS*i*Pr)Cu(CF_3)] (1.967(6) Å),[16b] [(SI*i*Pr)Cu(CF_3)] (2.022(4) Å),[16b] [(SIMes)$_2$Cu][(CF_3)$_2$Cu] (1.970(6) Å),[16c] [(phen)Cu(PPh_3)(CF_3)] (1.985(1) Å),[16d] [(bathophen)Cu(CF_3)] (1.907(9) Å),[16e] [(Ph_3P)$_3$Cu(CF_3)] (2.018(7), 2.025(7), and 2.031(10) Å),[16d] [$Cu_4(CF_3)_2$(C(Ot-Bu)$_2$)$_2$(μ^3-Ot-Bu)$_2$] (1.8908(16) Å),8 and [(dcypf)Cu(CF_3)] (1.948(12) and 1.974(7) Å).[16f] (b) Dubinina, G. G.; Furutachi, H.; Vicic, D. A. *J. Am. Chem. Soc*. **2008**, *130*, 8600. (c) Dubinina, G. G.; Ogikubo, J.; Vicic, D. A. *Organometallics* **2008**, *27*, 6233. (d) Tomashenko, O. A.; Escudero-Adan, E. C.; Martinez Belmonte, M.; Grushin, V. V. *Angew. Chem., Int. Ed*. **2011**, *50*, 7655. (e) Weng, Z.; Lee, R.; Jia, W.; Yuan, Y.; Wang, W.; Feng, X.; Huang, K.-W. *Organometallics* **2011**, *30*, 3229. (f) Jover, J.; Miloserdov, F. M.; Benet-Buchholz, J.; Grushin, V. V.; Maseras F. *Organometallics* **2014**, *33*, 6531.

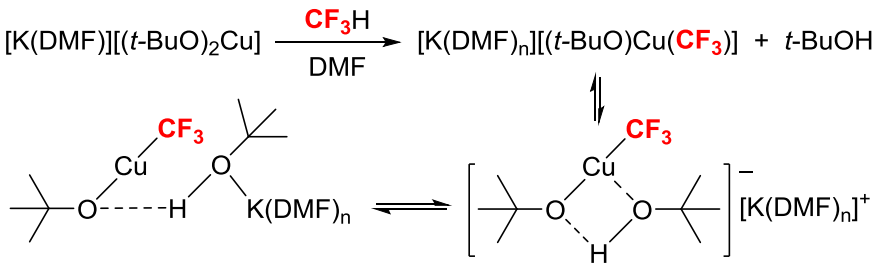

Scheme 8. *Cupration of CHF_3 and t-BuOCu/t-BuOH exchange*

A striking observation was made when the synthesis of **2** was attempted by adding one equivalent of 18-crown-6 to a solution of **1** in DMF *before* rather than after the introduction of fluoroform. In the presence of 18-crown-6, the reaction was sluggish, producing **2** in only 15, 30, and 35% yield after 10, 40, and 60 min, respectively. The cupration was further slowed down in the presence of five equivalents of 18-crown-6 and even more so when the latter was replaced with one equivalent of [2.2.2]cryptand (crypt-222). No detectable change in the reaction rate occurred, however, when the amount of crypt-222 was doubled.

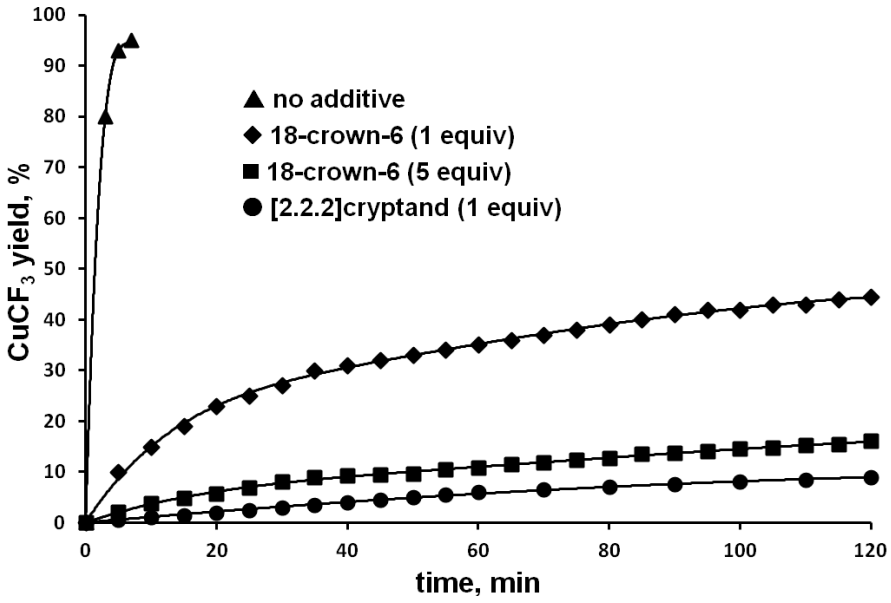

Figure 3. *Kinetics of the cupration reaction of CHF_3 with **1** in DMF ([Cu] = 0.1M) in the absence and in the presence of 18-crown-6 or [2.2.2]cryptand at 25 ^oC*

The kinetic data for these reactions were obtained by ^{19}F NMR with an internal standard under pseudo-first-order conditions in CHF_3. The non-exponential curves (Figure 3) suggested autoinhibition, regardless of the presence or absence of the additives. In the latter case, this effect was difficult to recognize because the reaction was fast, reaching >90% conversion within ca. 5 min. It was confirmed by an independent experiment, however, that the *t*-BuOH by-product (Scheme 8) does slow down the cupration. In the presence of 1.1 equivalents of *t*-BuOH deliberately added to **1** in DMF prior to the introduction of CHF_3, the yield of $CuCF_3$ was only about 65% after 20 min. Although a detailed study of this autoinhibition was beyond the scope of this project, we were able to isolate and structurally characterize a *t*-BuOH – K[(*t*-BuO)$_2$Cu] complex (Figure 4), featuring the K^+ ligated with four molecules of *t*-BuOH that are also H-bonded to [(*t*-BuO)$_2$Cu]$^-$. Herein, we focus on the more mechanistically significant, totally unexpected inhibiting effect of 18-crown-6 and crypt-222, which points to a crucial role of the alkali-metal counter-cation in the CHF_3 activation with **1**.

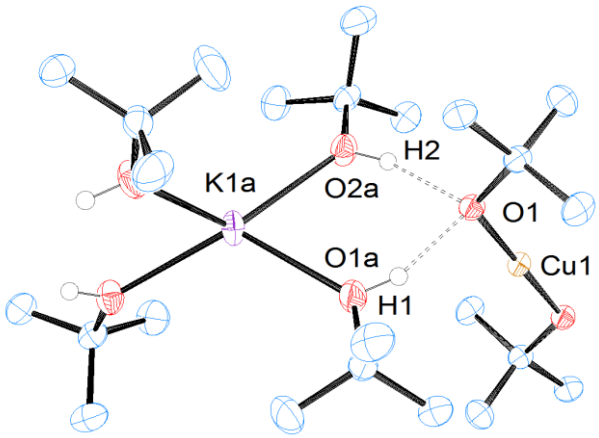

Figure 4. *ORTEP drawing of [K(t-BuOH)$_4$][(t-BuO)$_2$Cu] with H atoms except for OH omitted for clarity and thermal ellipsoids drawn to the 50% probability level*

Upon addition of 18-crown-6 (1 equiv) to **1** in DMF, THF, or benzene, [K(18-crown-6)][(*t*-BuO)$_2$Cu] (**3**) was cleanly formed with concomitant loss of the coordinated DMF molecule. The structure of isolated **3** (Figure 5) shows that the crowned K^+ is coordinated to one of the two O atoms of the dialkoxycuprate anion, with the K-O bond length of 2.668(2) Å being within the range found in the structures of **1** (2.629(2), 2.699(2), and 2.747(2) Å)[8] and **2** (2.652(11), 2.575(10), 2.600(10), and 2.625(10) Å).[15] The Cu-O bond distances (1.804(2) and 1.829(2) Å) and the O-Cu-O angle (169.66(8)°) in **3** are similar to those determined8 for **1** (1.815(2) and 1.825(2) Å and 173.10(10)°, respectively). In spite of these similarities, however, **3** appeared to be much less reactive toward fluoroform (Figure 3).

Likewise, adding one equivalent of crypt-222 to a solution of **1** in DMF-d_7 led to the instantaneous complexation of the potassium cation, as was manifested by the characteristic changes in the ^{1}H NMR spectrum. The resultant salt [K(crypt-222)]$^+$ [(*t*-BuO)$_2$Cu]$^-$ (**4**) was also isolated and structurally characterized (Figure 6). Unlike **3**, **4** does not display coordination of the dialkoxycuprate anion to the K^+ that is confined in the cryptand cage: the two K···O(Cu) distances exceed 6.1 and 8.2 Å.

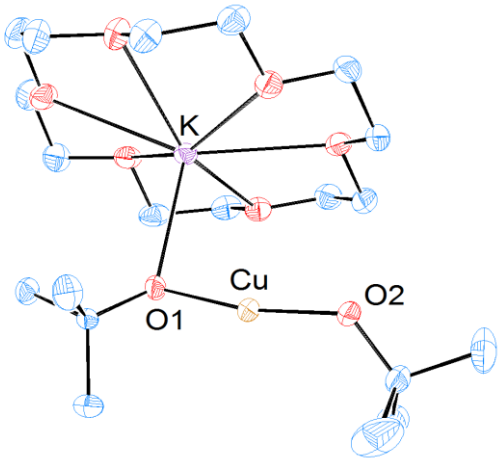

Figure 5. *ORTEP drawing of* ***3*** *with H atoms omitted for clarity and thermal ellipsoids drawn to the 50% probability level*[15]

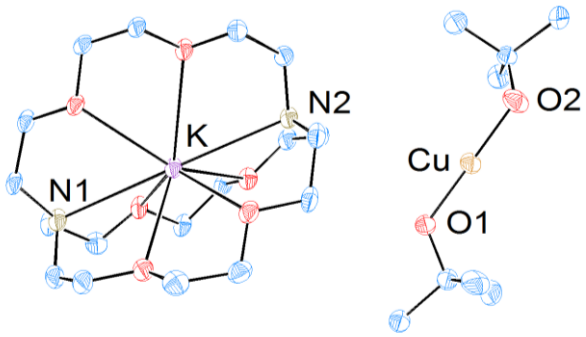

Figure 6*. ORTEP drawing of* ***4*** *with H atoms omitted for clarity and thermal ellipsoids drawn to the 50% probability level*[15]

The observed order of reactivity toward fluoroform (**1** >> **3** > [**3** + 18-crown-6 (4 equiv)] > **4** ≈ [**4** + crypt-222 (1 equiv)] (see above and Figure 3) correlates with the concentration of "free" K^+ in these systems: 0.1 >> 2.4×10^{-3} > 1.2×10^{-3} > 3.5×10^{-5} ≈ 2.5×10^{-5} M, respectively. These [K^+] values were calculated given [**1**] = 0.1 M used in the experiments and the reported lgK_S data for $[K(18\text{-crown-6})]^+$ (4.2-4.3) [17] and $[K(crypt\text{-}222)]^+$ (7.9)[18] in the same solvent (DMF).[19] The observed correlation indicated that the potassium cation provides critical electrophilic assistance to the activation and cleavage of the H-CF_3 bond with the dialkoxycuprate. To understand the key role of the K^+ in the cupration reaction, we studied its mechanism by theoretical calculations.

[17] (a) Takeda, I. *Bull. Chem. Soc. Jpn.* **1981**, *54*, 3133. (b) Ozutsumi, K.; Ohtsu, K.; Kawashima, T. *J. Chem. Soc., Faraday Trans.* **1994**, *90*, 127.
[18] Gutknecht, J.; Schneider, H.; Stroka, J. *Inorg. Chem*. **1978**, *17*, 3326.
[19] The reported[17,18] lgK_S values were obtained for $KClO_4$. As $[(t\text{-}BuO)_2Cu]^-$ is a stronger coordinating anion than ClO_4^-, the calculations might somewhat underestimate the actual concentrations of 18-crown-6- and crypt-222-free K^+. The overall trend in [K^+] and its correlation with the reactivity toward CHF_3, however, remain unaffected.

Analysis of mechanisms of C-H activation with metals[20] suggested that the cupration might proceed, as shown in Scheme 9, *via* (A) oxidative addition of CHF_3 to the Cu(I) center, followed by reductive elimination of *t*-BuOH (OA-RE) or (B) proton transfer from CHF_3 to the O atom of the *t*-BuO ligand on Cu with the simultaneous formation of the Cu-CF_3 bond. This proton-transfer mechanism is similar to ambiphilic metal-ligand activation (AMLA),[21] in which the cooperative effect of the F_3C-H···OCu hydrogen bond and the Lewis acidity of the 14e Cu(I) center provides a low-energy route to fluoroform C-H bond cleavage and Cu-CF_3 bond formation. Each of these two mechanisms was probed with two sets of calculations, one for K^+-free, "naked" $[Cu(OR)_2]^-$ and one for $[K(DMF)][Cu(OR)_2]$, where R = Me (small model).

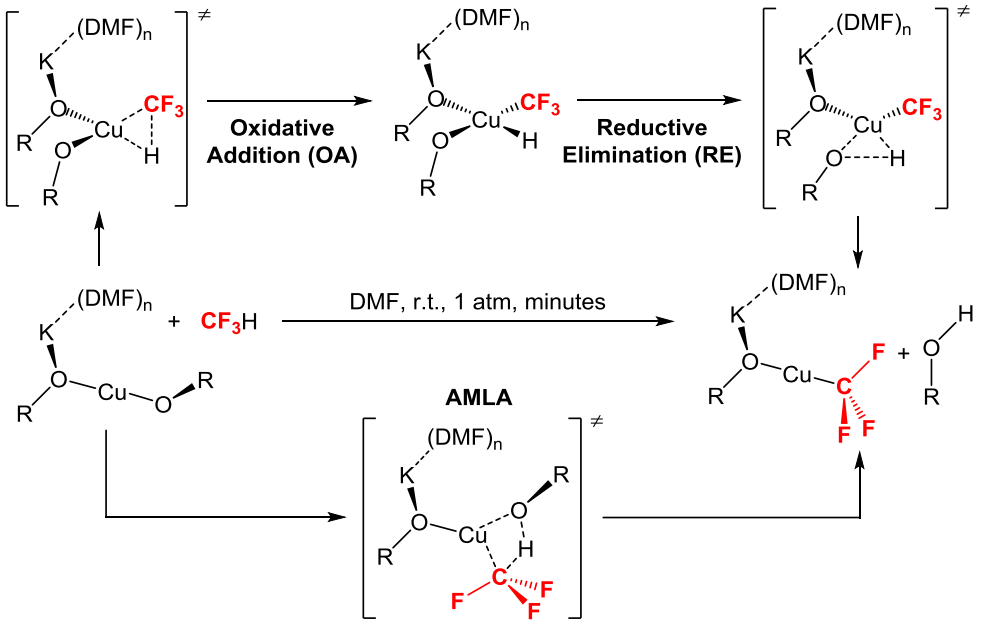

Scheme 9. *OA-RE and AMLA mechanisms for F_3C-H activation with $[K(DMF)_n][Cu(OR)_2]$ (R = alkyl)*

[20] Balcells, D.; Clot, E.; Eisenstein, O. *Chem. Rev.* **2010**, *110*, 749.
[21] Boutadla, Y.; Davies, D. L.; Macgregor, S. A.; Poblador-Bahamonde, A. I. *Dalton Trans*. **2009**, 5820.

The ability of CHF_3 to form hydrogen bonds with O-donors has long been established. [22] Although such H-bonds are largely of electrostatic nature, the contribution of dispersion interactions needed to be taken into account in order to obtain accurate binding energies of CHF_3 to the dialkoxycuprate. Therefore, all calculations were performed at the DFT/B97D[23] level of theory with the Gaussian09 package.

In order to elucidate the experimentally established effect of K^+ on the reaction, two models were considered. In one, the potassium cation was omitted. In the other, $[K(DMF)]^+$ was included. The computed reaction profiles for these two models are shown in Figures 7 and 8, respectively.

In the study of the OA-RE pathway (Scheme 9), no agostic intermediates were located and the molecule always relaxed to the initial compound with a strong hydrogen bond between CHF_3 and $[Cu(OMe)_2]^-$ (r(O···H) = 1.76 Å). With K^+ omitted (Figure 7), a prohibitively high barrier of 47.3 kcal/mol was computed. Inclusion of $[K(DMF)]^+$ in the model resulted in electrostatic interactions between the K^+ and F atoms of CHF_3, which only raised the barrier to 49.6 kcal/mol (Figure 8). We therefore concluded that the OA-RE mechanism is unlikely to operate in the reaction.

An AMLA-type four-center transition state was found for H-CF_3 activation with $[Cu(OMe)_2]^-$ alone. The computed activation barrier $\Delta G^{\neq}_{298K}$ = 27.7 kcal/mol (Figure 7) is fairly consistent with the experimentally observed (Figure 3) slow reaction rate of CHF_3 with **4**, in which the K^+ cation is separated from the reactive centers by encapsulation inside the cryptand host (Figure 6).[24]

[22] (a) Creswell, C. J.; Allred, A. L. *J. Am. Chem. Soc*. **1963**, *85*, 1723. (b) Andreades, S. *J. Am. Chem. Soc*. **1964**, *86*, 2003. (c) Alkorta, I.; Maluendes, S. *J. Phys. Chem*. **1995**, *99*, 6457. (d) Chabinyc, M. L.; Brauman, J. I. *J. Am. Chem. Soc*. **1998**, *120*, 10863. (e) Mukhopadhyay, A.; Pandey, P.; Chakraborty, T. *J. Phys. Chem. A* **2010**, *114*, 5026. (f) Grabowski, S. J. *J. Phys. Chem. A* **2011**, *115*, 12789. (g) Ramasami, P.; Ford, T. A. *J. Mol. Struct*. **2012**, *1023*, 163.
[23] Grimme, S. *J. Comput. Chem*. **2006**, *27*, 1787.
[24] Replacing the MeO ligands in the small model with *t*-BuO raised the barrier by 2.5 kcal/mol.

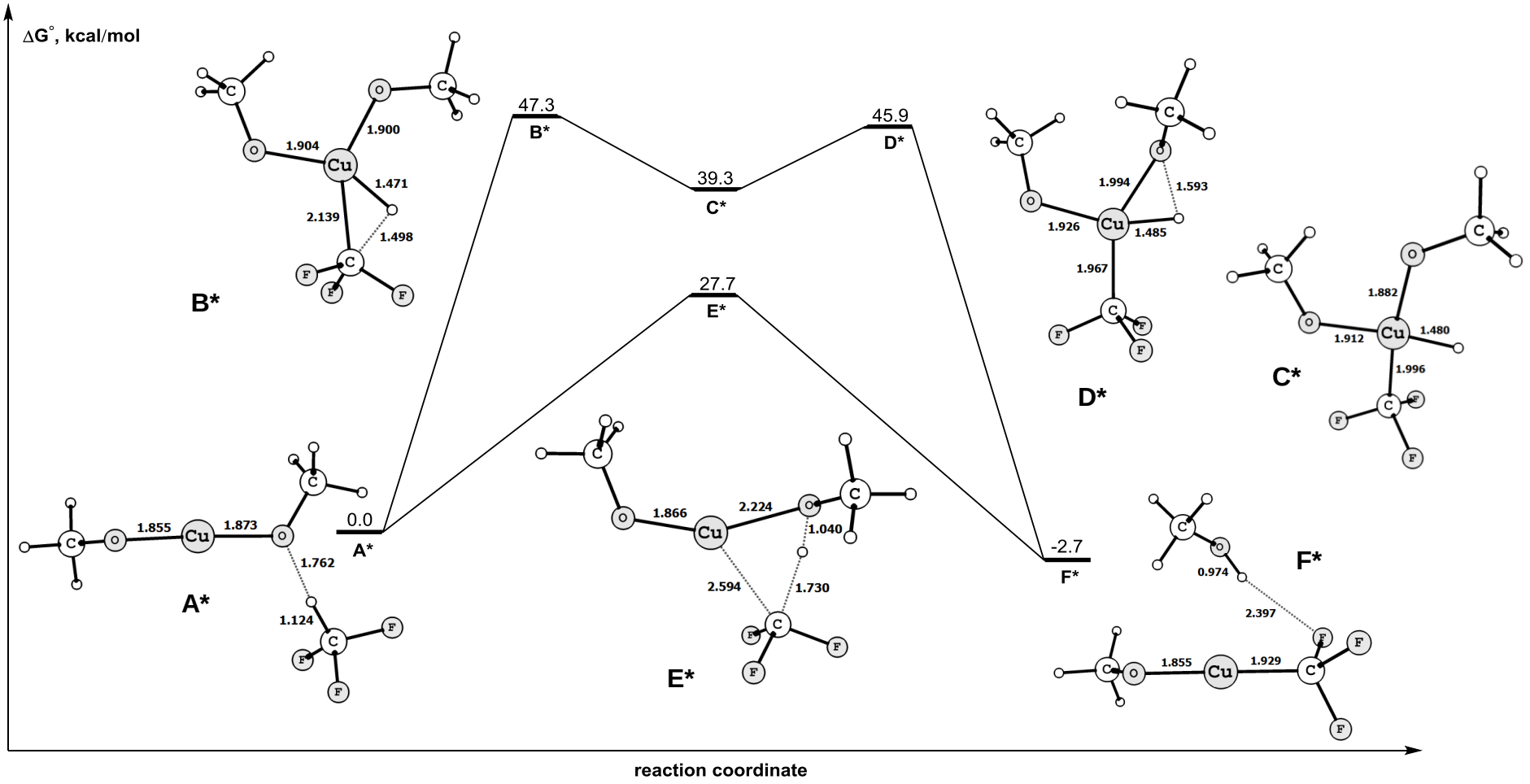

***Figure 7**. Computed reaction profile in the absence of $[K(DMF)]^+$; A* – Reactant, B* – TS_{OA}, C* – Intermediate, D* – TS_{RE}, E* – TS_{AMLA}, F* – Product*

UNIVERSITAT ROVIRA I VIRGILI
REACTION MECHANISMS ON THE WAY FROM CHF3 TO ARCF3. THE NATURE OF THE ORTHO-EFFECT AND ELECTRONIC PROPERTIES
OF THE CF3 GROUP.
Andrey I. Konovalov
Dipòsit Legal: T 1587-2015

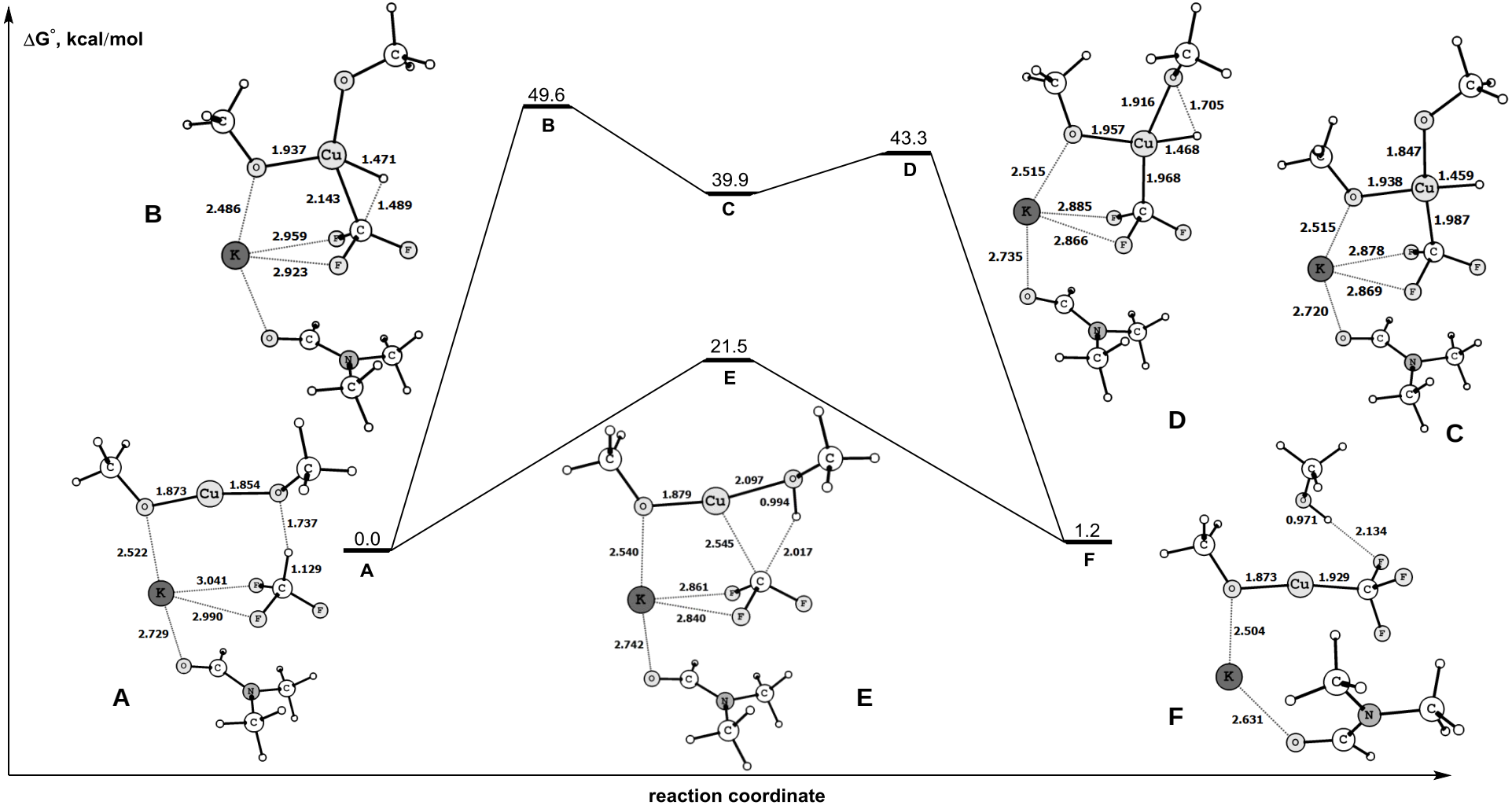

Figure 8. *Computed reaction profile in the presence of* $[K(DMF)]^+$*; A – Reactant, B –* TS_{OA}*, C – Intermediate, D –* TS_{RE}*, E –* TS_{AMLA}*, F – Product*

Placing a CHF_3 molecule in the [K(DMF)][$Cu(OMe)_2$] environment produced a much more stable transition state with $\Delta G^{\neq}_{298K}$ = 21.5 kcal/mol.[25] In addition to the expected pattern involving the H, O, Cu, and C centers, this striking transition state (structure **E** in Figure 8 and Scheme 10) displays interactions of the potassium ion not only with the other O atom on Cu, but also with two of the three F atoms of the fluoroform molecule. These additional K···O and K···F contacts provide extra stabilization to the transition state, thereby lowering considerably the activation barrier. As shown in Figure 9, the presence of the potassium cation creates a remarkable template, in which a total of three Lewis acid centers (H, Cu, K) and five basic centers (O, O, C, F, F) are neatly pre-organized for the C-H bond breakage and Cu-CF_3 bond formation. Apart from the template effect, this assembly facilitates the process by altering electronic properties of the reactive centers. Thus, the K···F contacts increase the acidity of the H-CF_3 bond and the K-O interaction enhances the electrophilicity of the Cu center, as confirmed by NBO charge distribution analysis.[15]

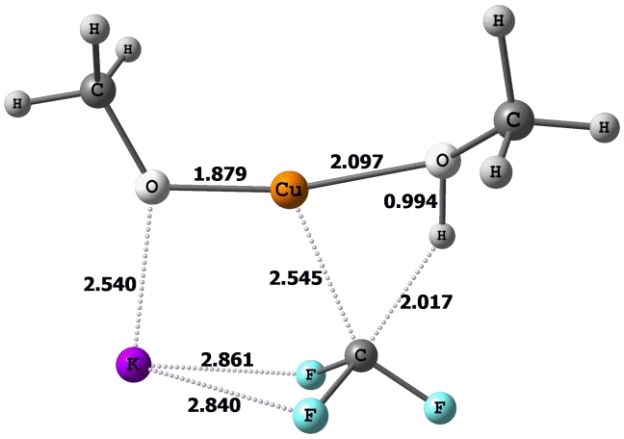

***Figure 9**. Computed AMLA transition state for F_3C-H activation with $[Cu(OR)_2]^-$ involving electrophilic assistance from K^+ (DMF ligand is omitted)*

[25] Recomputing this transition state at the DFT/B3LYP and the DFT/PBE levels produced higher activation barriers of 25.7 and 23.7 kcal/mol, respectively, thus indicating that the contribution from the London dispersion forces is not negligible.

The established Lewis acid effect of K^+ on the cupration reaction prompted us to synthesize a salt of $[(t\text{-BuO})_2Cu]^-$ with a metal-free countercation in order to explore its reactivity toward CHF_3. The organic cation of choice was $[Me_4N]^+$ that is devoid of β-H atoms and hence cannot undergo Hofmann elimination. Attempts to prepare $[Me_4N]^+$ $[(t\text{-BuO})_2Cu]^-$ (**5**) by metathesis between $[Me_4N]^+$ X^- (X = Cl, BF_4) and **1** or $[Na(DMF)_2][(t\text{-BuO})_2Cu]$8 in various solvents were unsuccessful. The reaction of $[Me_4N]^+$ F^- with $[Na(DMF)_2][(t\text{-BuO})_2Cu]$ in THF, however, cleanly produced **5**, which was isolated and structurally characterized (Figure 10).

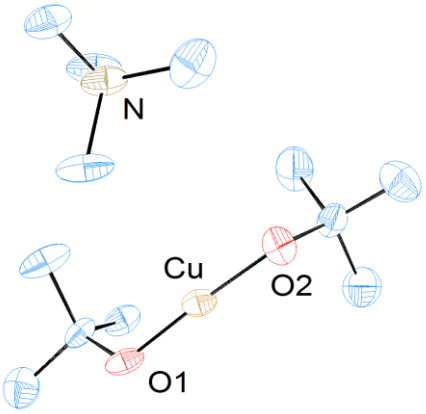

Figure 10. *ORTEP drawing of* ***5*** *with H atoms omitted and thermal ellipsoids drawn to the 50% probability level*[15]

As anticipated, **5** appeared poorly reactive toward fluoroform in DMF, the reaction rate being roughly one half of that with **3**. Somewhat unexpectedly, however, the cupration with **5** proceeded slightly faster than with **1** in the presence of five equivalents of 18-crown-6 and with **4**. We suspected that trace residual amounts of Na^+ in the sample of **5** after the synthesis might have catalyzed the cupration. Therefore, the reaction of CHF_3 with **5** was repeated in the presence of crypt-222 (1 equiv), which would efficiently sequester residual sodium ions in the form of inactive [Na(crypt-

222)]$^+$. However, no change in the reaction rate was observed in this experiment, indicating that the sample of **5** was Na-free and that the measured rate of the reaction of **5** reflected its intrinsic reactivity toward fluoroform. A computational study was then performed and a transition state found where the $[Me_4N]^+$ plays essentially the same role as the potassium cation (Figure 9), providing electrophilic assistance by means of NCH···O and NCH···F interactions (Figure 11). These interactions, however, are considerably weaker than those with K^+. As a consequence, the computed barrier ($\Delta G^{\neq}_{298K}$ = 26.9 kcal/mol) in this case is intermediate between those for the reactions in the presence of more Lewis acidic K^+ (21.5 kcal/mol; **1**) and in the absence of electrophilic assistance (27.7 kcal/mol; **4**). All three $\Delta G^{\neq}$ values are in excellent agreement with the experimentally observed reaction rates for **1**, **4**, and **5** (Figure 3).

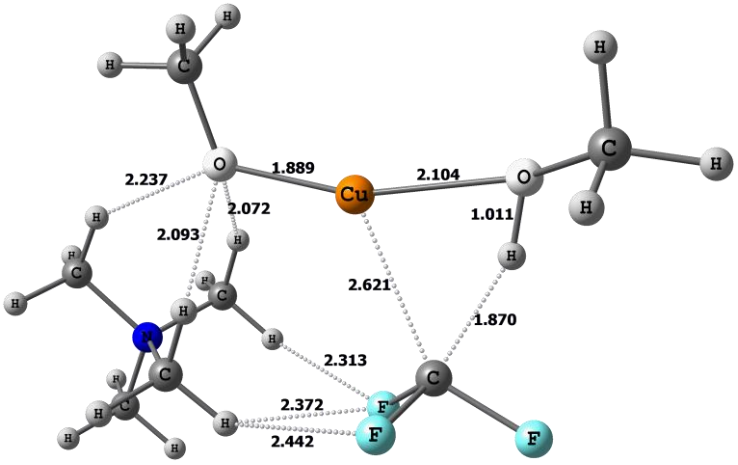

Figure 11. *Computed AMLA transition state for F_3C-H activation with $[Cu(OR)_2]^-$ involving electrophilic assistance from NMe_4^+*

Conclusions

The objectives of this work have been met. We have uncovered the critical role of the countercation in the cupration of fluoroform with dialkoxy Cu(I) ate complexes such as **1**. In accordance with the previous observations,[8] this reaction is not mediated by free CF_3^- and/or difluorocarbene. Both experimental and computational studies indicate that the cupration process is governed by a unique mechanism that involves synchronous C-H bond cleavage and Cu-CF_3 bond formation with electrophilic assistance from the alkali-metal counterion. A total of eight Lewis acid and Lewis base centers interacting with one another are cleverly arranged in the computed stable transition state that provides a low-energy pathway for the transformation. Therefore, the alkali-metal counterion M^+ (*e.g.* M = K or Na) to the dialkoxycuprate is highly important, as it plays a dual role in the overall cupration process. As was shown previously,[8] the cation slowly decomposes the $CuCF_3$ product through α-fluoride elimination. As we demonstrate in the current study, the electrophilic assistance of M^+ is paramount to the occurrence of the CHF_3 cupration reaction in a highly efficient manner.

Experimental Section

All chemicals were purchased from Aldrich (CuCl, *t*-BuONa, KF, crypt-222), Alfa Aesar (*t*-BuOK, 18-crown-6), TCI ($[Me_4N]BF_4$), and Apollo Scientific (CHF_3). All manipulations were performed under argon in a glovebox, unless noted otherwise. Anhydrous DMF (Alfa Aesar or from an MBraun SPS) was used without additional purification. Benzene, hexane, ether, and THF were distilled from Na/benzophenone. All solvents and internal standarts for quantitative ^{19}F analysis were stored over activated 4 Å molecular sieves in a glovebox. Known compounds [K(DMF)][(*t*-BuO)$_2$Cu] (**1**),8 [Na(DMF)$_2$][(*t*-BuO)$_2$Cu],8 and anhydrous $[Me_4N]F$[26] were prepared following the literature procedures. ^1H, ^{13}C, and ^{19}F NMR spectra were recorded on a Brucker Avance 400 Ultrashield NMR spectrometer. Quantitative ^{19}F NMR analyses were carried out with D1 = 5 s. ^{19}F NMR yields (± 5%) are the average of at least two runs. Elemental analyses could not be performed due to extreme air- and moisture-sensitivity of the new compounds.

[K(18-crown-6)][(*t*-BuO)Cu(CF$_3$)] (2). Inside a glove-box, a 10-mL Schlenk tube equipped with a Teflon-coated magnetic stir-bar was charged with **1** (161 mg; 0.5 mmol) and DMF (2.5 mL). The tube was sealed, brought out, evacuated on a vacuum line to ~0.1 mmHg, and back-filled with fluoroform (excess) at vigorous stirring. After 5 min, the tube was brought back to the glove-box and the reaction mixture was treated with 18-crown-6 (145 mg; 0.55 mmol) that quickly dissolved. The resultant solution was diluted with ether (5 mL) and kept at -40 °C for 20 h. The precipitated white needle-shaped crystals were separated by filtration, washed with

[26] Kolomeitsev, A. A.; Kadyrov, A. A.; Szczepkowska-Sztolcman, J.; Milewska, M.; Koroniak, H.; Bissky, G.; Barten, J. A.; Röschenthaler, G.-V. *Tetrahedron Lett.* **2003**, *44*, 8273.

ether (2 × 1 mL), and dried under vacuum. The yield was 320 mg (63%). ^{1}H NMR (C_6D_6, 25 °C), δ: 3.18 (s, 24H, 18-crown-6), 1.57 (s, 9H, *t*-Bu). ^{19}F (DMF, 25 °C), δ: -23.7 (s, minor), -24.7 (s, $CuCF_3$). The minor peak observed in the ^{19}F NMR spectrum is assigned to the product of 18-crown-6 dissociation from **1**.

[K(18-crown-6)][(*t*-BuO)$_2$Cu] (3). A mixture of **1** (32 mg; 0.1 mmol) and 18-crown-6 (29 mg; 0.11 mmol) in benzene (1 mL) was gently heated to 50-55 °C until a solid-free solution was obtained. Hexane (ca. 2 mL) was added and the mixture was kept at -40 °C for 1 h. The white needle-shaped crystals were separated by filtration, washed with cold ether (2 × 0.5 mL), and dried under vacuum. The yield of 3 was 43 mg (84%). ^{1}H NMR (C_6D_6, 25 °C), δ: 3.26 (s, 24H, 18-crown-6), 1.77 (s, 18H, *t*-Bu). ^{13}C (C_6D_6, 25 °C), δ: 70.22 (s, CH_2, 18-crown-6), 68.84 (s, C, *t*-Bu), 37.74 (s, CH_3, *t*-Bu).

Compexation of K$^+$ in 1 by Crypt-222. ^{1}H and ^{13}C NMR spectra were recorded for a freshly prepared solution of **1** (17 mg; 0.05 mmol) and crypt-222 (22 mg; 0.05 mmol) in 0.6 ml of DMF-d_7. ^{1}H NMR (DMF-d_7, 25 °C), δ: 8.03 (s, 1H, DMF-H), 3.61 (s, 12H, OCH_2CH_2O, crypt-222), 3.58 (t, 12H, J = 4 Hz, $NCH_2C\underline{H}_2O$, crypt-222), 2.95 (s, 3H, DMF-CH_3), 2.78 (s, 3H, DMF-CH_3), 2.57 (t, 12H, J = 4 Hz, $NC\underline{H}_2CH_2O$, crypt-222), 1.10 (s, 18H, *t*-Bu). ^{13}C NMR (DMF-d_7, 25 °C), δ: 71.37 (s, OCH_2CH_2O, crypt-222), 68.87 (s, C, *t*-Bu), 68.60 (s, $NCH_2\underline{C}H_2O$, crypt-222), 54.92 (s, $N\underline{C}H_2CH_2O$, crypt-222), 37.78 (s, CH_3, *t*-Bu).

NMR data for free crypt-222: ^{1}H NMR (DMF-d_7, 25 °C), δ: 3.62 (s, 12H, OCH_2CH_2O, crypt-222), 3.56 (t, 12H, J = 4 Hz, $NCH_2C\underline{H}_2O$, crypt-222), 2.59 (t, 12H, J = 4 Hz, $NC\underline{H}_2CH_2O$, crypt-222). ^{13}C NMR (DMF-d_7, 25 °C), δ: 71.27 (s, OCH_2CH_2O,

crypt-222), 70.49 (s, $NCH_2\underline{C}H_2O$, crypt-222), 56.99 (s, $N\underline{C}H_2CH_2O$, crypt-222). These data are consistent with those reported in the literature.[27]

[K(crypt-222)][(*t*-BuO)$_2$Cu] (4). A mixture of **1** (32 mg; 0.1 mmol) and crypt-222 (41 mg; 0.11 mmol) in benzene (1 mL) was gently heated to 50-55 °C until a solid-free solution was obtained. Hexane (ca. 2 mL) was added and the mixture was then kept at -40 °C for 1 h. The white needle-shaped crystals were separated by filtration, washed with cold ether (2 × 0.5 mL), and dried under vacuum. The yield of 4 was 47 mg (75%). ^{1}H NMR (C_6D_6, 25 °C), δ: 3.44 (s, 12H, OCH_2CH_2O, crypt-222), 3.32 (t, 12H, J = 4 Hz, $NCH_2C\underline{H}_2O$, crypt-222), 2.30 (t, 12H, J = 4 Hz, $N\underline{C}H_2CH_2O$, crypt-222), 1.87 (s, 18H, *t*-Bu). ^{13}C (C_6D_6, 25 °C), δ: 70.66 (s, OCH_2CH_2O, crypt-222), 69.07 (s, C, *t*-Bu), 68.02 (s, $NCH_2\underline{C}H_2O$, crypt-222), 54.61 (s, $N\underline{C}H_2CH_2O$, crypt-222), 38.00 (s, CH_3, *t*-Bu).

[Me$_4$N][(*t*-BuO)$_2$Cu] (5). In a glove-box, a mixture of [Na(DMF)$_2$][(*t*-BuO)$_2$Cu] (379 mg; 1 mmol) and [Me$_4$N]F (93 mg; 1.1 mmol) in THF (3 mL) was vigorously stirred at room temperature for 12 h and filtered. The solid NaF was washed on filter with THF (2 × 1 mL). The combined filtrate and the washings were transferred to a 10-mL Schlenk tube equipped with a Teflon-coated magnetic stir-bar, which was then sealed and brought out of the glove-box. After evaporation of the solvent on a vacuum line, the tube was brought back to the glove-box. The residue was washed with cold ether (2 × 1 mL) and dried under vacuum. The yield was 181 mg (64%). ^{1}H NMR (C_6D_6, 25 °C), δ: 2.97 (s, 12H, NMe_4), 1.59 (s, 18H, *t*-Bu). ^{13}C (C_6D_6, 25 °C), δ: 69.20 (s, C, *t*-Bu), 55.04 (s, CH_3, NMe_4), 37.43 (s, CH_3, *t*-Bu).

[27] Adam, K. R.; Atkinson, I. M.; Kim, J.; Lindoy, L. F.; Matthews, O. A.; Meehan, G. V.; Raciti, F.; Skelton, B. W.; Svenstrup, N.; White, A. H. *J. Chem. Soc., Dalton Trans.* **2001**, 2388.

[K(*t*-BuOH)$_4$][(*t*-BuO)$_2$Cu]. A mixture of **1** (161 mg; 0.5 mmol) and *t*-BuOH (48 μL; 0.5 mmol) in toluene (1 mL) was kept at -40 °C in a glove-box for 24 h. The white needle-shaped crystals were separated from the cold mixture and immediately used for crystallographic studies.

Kinetics Experiments. Inside a glove-box, a 5-mm NMR tube was charged with **1** (26 mg; 0.08 mmol), $PhCF_3$ (10 μl; 0.08 mmol; internal standart), and DMF (0.8 mL). The tube was sealed with a rubber septum and brought out. Fluoroform (10 mL, 0.45 mmol) was bubbled through the solution *via* a syringe needle and ^{19}F NMR measurements on the sample were started immediately. The run was repeated (a) in the presence of 1 equiv of 18-crown-6 (21 mg; 0.08 mmol); (b) in the presence of 5 equiv of 18-crown-6 (106 mg; 0.4 mmol); (c) in the presence of 1 equiv of crypt-222 (30 mg; 0.08 mmol); (d) in the presence of 2 equiv of crypt-222 (60 mg; 0.16 mmol); (e) in the presence of 1.1 equiv of *t*-BuOH (0.444 ml of 0.2 M solution of *t*-BuOH in DMF; 0.088 mmol; 1.1 equiv); and (f) with **5** (29 mg; 0.08 mmol).

Computational Studies. All calculations were performed with the Gaussian09 suite of programs[28] at the B97D[23] level of density function theory that produces more accurate results for systems involving weak interactions such as hydrogen bonds and

[28] Gaussian09, Revision A.02, Frisch, M. J.; Trucks, G. W.; Schlegel, H. B.; Scuseria, G. E.; Robb, M. A.; Cheeseman, J. R.; Scalmani, G.; Barone, V.; Mennucci, B.; Petersson, G. A.; Nakatsuji, H.; Caricato, M.; Li, X.; Hratchian, H. P.; Izmaylov, A. F.; Bloino, J.; Zheng, G.; Sonnenberg, J. L.; Hada, M.; Ehara, M.; Toyota, K.; Fukuda, R.; Hasegawa, J.; Ishida, M.; Nakajima, T.; Honda, Y.; Kitao, O.; Nakai, H.; Vreven, T.; Montgomery, Jr., J. A.; Peralta, J. E.; Ogliaro, F.; Bearpark, M.; Heyd, J. J.; Brothers, E.; Kudin, K. N.; Staroverov, V. N.; Kobayashi, R.; Normand, J.; Raghavachari, K.; Rendell, A.; Burant, J. C.; Iyengar, S. S.; Tomasi, J.; Cossi, M.; Rega, N.; Millam, J. M.; Klene, M.; Knox, J. E.; Cross, J. B.; Bakken, V.; Adamo, C.; Jaramillo, J.; Gomperts, R.; Stratmann, R. E.; Yazyev, O.; Austin, A. J.; Cammi, R.; Pomelli, C.; Ochterski, J. W.; Martin, R. L.; Morokuma, K.; Zakrzewski, V. G.; Voth, G. A.; Salvador, P.; Dannenberg, J. J.; Dapprich, S.; Daniels, A. D.; Farkas, Ö.; Foresman, J. B.; Ortiz, J. V.; Cioslowski, J.; Fox, D. J. Gaussian, Inc., Wallingford CT, 2009.

cation-anion cooperative effects.[29] All geometry optimizations and frequency calculations were performed with the Hay-Wadt small core ECP and associated basis sets LANL2TZ (Cu atom) and LANL08 (K atom)[30] and additional polarization functions for Cu (ζ_f = 3.525)[31] and K (ζ_d = 1.000).[32] The full electron Pople's basis set 6-31+G(d,p) was used for all non-metal atoms. Basis sets for copper and potassium and ECPs were obtained from the EMSL basis set exchange.[33] All computed structures were characterized as local stationary points *via* analytical frequency calculations. For saddle points, intrinsic reaction coordinate (IRC) analysis[34] was performed to verify that they connect the right reactants and products on the potential energy surface. The natural bond orbital (NBO)[35] program, as implemented in Gaussian09, was used to obtain atomic charges.

Single-point energies were evaluated with a larger 6-311+G(2d,p) basis set on non-metal elements. BSSE correction was not implemented in this work because it has been shown[23] that the classical counterpoise method[36] usually overestimates the BSSE and that DFT-D calculations with triple-ζ quality basis sets augmented with polarization functions provide reliable results.[23,29a] These single-point energies corrected by the Gibbs free energy correction from unscaled frequency calculations were used to describe the reaction energies throughout the study.

---

[29] (a) Plumley, J. A.; Dannenberg, J. J. *J. Comput. Chem.* **2011**, *32*, 1519. (b) Thanthiriwatte, K. S.; Hohenstein, E. G.; Burns, L. A.; Sherrill, C. D. *J. Chem. Theory Comput*. **2011**, *7*, 88. (c) Nagy, P. I. *J. Phys. Chem. A* **2012**, *116*, 7726. (d) Nagy, P. I. *J. Phys. Chem. A* **2013**, *117*, 2812. (e) Abramson, R. A.; Baldridge, K. K. *J. Chem. Theory Comput*. **2013**, *9*, 1027. (f) Otsuka, T.; Ishii, A; Dub, P. A.; Ikariya, T.; *Am. Chem. Soc*. **2013**, *135*, 9600.
[30] Roy, L. E.; Hay, P. J.; Martin, R. L. *J. Chem. Theory Comput*. **2008**, *4*, 1029.
[31] Ehlers, A. W.; Bohme, M.; Dapprich, S.; Gobbi, A.; Hollwarth, A.; Jonas, V.; Kohler, K. F.; Stegmann, R.; Veldkamp, A.; Frenking, G. *Chem. Phys. Lett.* **1993**, *208*, 111.
[32] Hollwarth, A.; Bohme, M.; Dapprich, S.; Ehlers, A. W.; Gobbi, A.; Jonas, V.; Kohler, K. F.; Stegmann, R.; Veldkamp, A.; Frenking, G. *Chem. Phys. Lett.* **1993**, *208*, 237.
[33] https://bse.pnl.gov/bse/portal
[34] Fukui, K. *Acc. Chem. Res.* **1981**, *14*, 363.
[35] Glendening, E. D.; Read, A. E.; Carpenter, J. E.; Weinhold, F. NBO Version 3.1.
[36] Boys, S. F.; Bernardi, F. *Mol. Phys*. **1970**, *19*, 553.

Crystallographic Studies. Details of crystallographic studies performed by Drs. Jordi Benet-Buchholz and Eddy Martin (ICIQ) can be found in ref. 15. A summary of crystallographic data for **2-5** is presented in Table 1. Crystal data and structure refinement for complex [K(*t*-BuOH)$_4$][(*t*-BuO)$_2$Cu] is presented in Table 2.

Table 1. *Crystallographic data for* ***2-5***

Compound	**2**	**3**	**4**	**5**
Formula	$C_{34}H_{65}Cu_2F_6K_2O_{14}$	$C_{20}H_{42}Cu_1K_1O_8$	$C_{26}H_{54}Cu_2K_1N_2O_8$	$C_{15}H_{37}Cu_1N_2O_3$
Solvents	---	---	---	2 x DMF
Formula weight	1017.14	513.18	625.35	357.01
Crystal size (mm^3)	0.40 x 0.07 x 0.07	0.10 x 0.10 x 0.10	0.25 x 0.15 x 0.15	0.30 x 0.08 x 0.05
Crystal color	colorless	colorless	colorless	colorless
Temp (K)	100	100	100	100
Crystal system	monoclinic	triclinic	triclinic	triclinic
Space group	$P2_1$	P $\bar{1}$	P $\bar{1}$	P $\bar{1}$
A (Å)	14.0312(9)	11.621(2)	8.487(5)	11.7667(12)
B (Å)	11.0236(7)	14.419(5)	13.713(7)	12.5135(13)
C (Å)	29.6611(19)	16.844(4)	14.870(9)	15.4665(16)
α (deg)	90	91.784(12)	79.81(2)	87.893(4)
β (deg)	89.957(2)	92.769(6)	75.34(2)	73.633(4)
γ (deg)	90	111.100(13)	73.641(18)	69.617(3)
V ($Å^3$)	4587.8(5)	2626.6(12)	1596.2(16)	2043.5(4)
Z	4	4	2	4
ρ (g/cm^3)	1.473	1.298	1.301	1.160
μ (mm^{-1})	1.191	1.027	0.860	1.079
θ_{max} (°)	25.40	33.33	25.16	25.00
Reflec. measured	36939	65988	12887	6925
Unique reflections	13159 [R_{int} = 0.0692]	13036 [R_{int} = 0.0612]	4669 [R_{int} = 0.0513]	5973 [R_{int} = 0.0697]
Absorpt. correct.	SADABS	SADABS	SADABS	TWINABS
Trans. min/max	0.6474/0.9213	0.9042/0.9042	0.8138/0.8819	0.0778/0.9480
Parameters	1038	551	672	497
R1/wR2 [I>2σ(I)]	0.0564/0.1303	0.0598/0.1600	0.0912/0.2600	0.0977/0.2320
R1/wR2 [all data]	0.0734/0.1401	0.0965/0.1884	0.1026/0.2713	0.1138/0.2465
Goodness-of-fit (F^2)	1.066	1.021	1.106	1.065
Peak/hole ($e/Å^3$)	1.731/-0.629	1.824/-1.141	2.883/-1.104	0.965/-0.965

***Table 2**. Crystallographic data for [K(t-BuOH)$_4$][(t-BuO)$_2$Cu]*

Empirical formula	$C_{24}H_{58}CuKO_6$	
Formula weight	545.34	
Temperature	100(2) K	
Wavelength	0.71073 Å	
Crystal system	Monoclinic	
Space group	C2/c	
Unit cell dimensions	a = 27.225(4) Å	α= 90.00°
	b = 8.9074(13) Å	β = 129.175(3)°
	c = 17.653(2) Å	γ = 90.00°
Volume	3318.6(8) Å^3	
Z	4	
Density (calculated)	1.092 Mg/m^3	
Absorption coefficient	0.812 mm^{-1}	
F(000)	1192	
Crystal size	0.20 x 0.10 x 0.03 mm^3	
Theta range for data collection	1.93 to 28.32°	
Index ranges	-32 <=h<=36 ,-11 <=k<=10 ,-23 <=l<=22	
Reflections collected	13912	
Independent reflections	4092 [R(int) = 0.0549]	
Completeness to theta =28.32°	98.9%	
Absorption correction	Empirical	
Max. and min. transmission	0.9760 and 0.8544	
Refinement method	Full-matrix least-squares on F^2	
Data / restraints / parameters	4092 / 2 / 162	
Goodness-of-fit on F^2	1.120	
Final R indices [I>2sigma(I)]	R1 = 0.0544 , wR2 = 0.1521	
R indices (all data)	R1 = 0.0748 , wR2 = 0.1618	
Largest diff. peak and hole	1.262 and -0.542 e.Å^{-3}	

REACTION MECHANISMS ON THE WAY FROM CHF3 TO ARCF3. THE NATURE OF THE ORTHO-EFFECT AND ELECTRONIC PROPERTIES OF THE CF3 GROUP.
Andrey I. Konovalov
Dipòsit Legal: T 1587-2015

Chapter 2.

Mechanism of Trifluoromethylation of Haloarenes with $CuCF_3$

Introduction

Since the groundbreaking discovery of the Cu-promoted perfluoroalkylation of aryl iodides by McLoughlin and Thrower [1] in the 1960's (see General Introduction), considerable progress has been made in the area of trifluoromethylation of haloarenes with copper complexes.[2,3,4,5] While most of the reported work targeted the development of new trifluoromethylation methodologies, surprisingly little is known about the mechanism of the copper-mediated Ar-CF_3 bond formation (Scheme 1). The original

[1] (a) McLoughlin, V. C. R.; Thrower, J. U.S. Patent 3408411, 1968. (b) McLoughlin, V. C. R.; Thrower, J. *Tetrahedron* **1969**, *25*, 5921.

[2] For selected monographs, see: (a) Hudlicky, M. *Chemistry of Organic Fluorine Compounds*; Ellis Horwood: New York, 1976. (b) Banks, R. E. *Organofluorine Chemicals and Their Industrial Applications*; Ellis Horwood: West Sussex, U. K., 1979. (c) Filler, R.; Kobayashi, Y. *Biomedicinal Aspects of Fluorine Chemistry*; Kodansha-Elsevier: New York, 1982. (d) Clark, J. H.; Wails, D.; Bastock, T. W. *Aromatic Fluorination*; CRC Press: Boca Raton, FL, 1996. (e) Kirsch, P. *Modern Fluoroorganic Chemistry*; Wiley-VCH: Weinheim, 2004. (f) Uneyama, K. *Organofluorine Chemistry*; Blackwell: Oxford, U. K., 2006. (g) Ojima, I. *Fluorine in Medicinal Chemistry and Chemical Biology*; Wiley-Blackwell: Chichester, U. K., 2009. (h) Petrov, V. A. *Fluorinated Heterocyclic Compounds. Synthesis, Chemistry and Applications*; Wiley: Hoboken, New Jersey, 2009.

[3] For selected reviews, see: (a) Burton, D. J.; Yang, Z. Y. *Tetrahedron* **1992**, *48*, 189. (b) McClinton, M. A.; McClinton, D. A. *Tetrahedron* **1992**, *48*, 6555. (c) Burton, D. J.; Lu, L. *Top. Curr. Chem*. **1997**, *193*, 45. (d) Schlosser, M. *Angew. Chem., Int. Ed.* **2006**, *45*, 5432. (e) Roy, S.; Gregg, B. T.; Gribble, G. W.; Le, V.-D.; Roy, S. *Tetrahedron* **2011**, *67*, 2161. (f) Qing, F.-L.; Zheng, F. *Synlett* **2011**, 1052. (g) Liu, T.; Shen, Q. *Eur. J. Org. Chem.* **2012**, 6679. (h) Lishchynskyi, A.; Novák, P.; Grushin, V. V. In *Science of Synthesis: C-1 Building Blocks in Organic Synthesis 2*; van Leeuwen, P. W. N. M., Ed.; Thieme: Stuttgart, 2013; p. 367.

[4] For a recent comprehensive review of aromatic trifluoromethylation and perfluoroalkylation, see: Tomashenko, O. A.; Grushin, V. V. *Chem. Rev.* **2011**, *111*, 4475.

[5] For most recent reports not covered in the review article cited in ref. 4, see: (a) Zhang, C. P.; Wang, Z. L.; Chen, Q. Y.; Zhang, C. T.; Gu, Y. C.; Xiao, J. C. *Angew. Chem., Int. Ed*. **2011**, *50*, 1896. (b) Popov, I.; Lindeman, S.; Daugulis, O. *J. Am. Chem. Soc*. **2011**, *133*, 9286. (c) Morimoto, H.; Tsubogo, T.; Litvinas, N. D.; Hartwig, J. F. *Angew. Chem., Int. Ed*. **2011**, *50*, 3793. (d) Tomashenko, O. A.; Escudero-Adán, E. C.; Martínez Belmonte, M.; Grushin, V. V. *Angew. Chem., Int. Ed*. **2011**, *50*, 7655. (e) Weng, Z.; Lee, R.; Jia, W.; Yuan, Y.; Wang, W.; Feng, X.; Huang, K.-W. *Organometallics* **2011**, *30*, 3229. (f) Li, Y.; Chen, T.; Wang, H.; Zhang, R.; Jin, K.; Wang, X.; Duan, C. *Synlett* **2011**, 1713. (g) Kondo, H.; Oishi, M.; Fujikawa, K.; Amii, H. *Adv. Synth. Catal.* **2011**, *353*, 1247. (h) Kremlev, M. M.; Mushta, A. I.; Tyrra, W.; Yagupolskii, Y. L.; Naumann, D.; Möller, A. *J. Fluorine Chem*. **2012**, *133*, 67. (i) Sanhueza, I. A.; Nielsen, M. C.; Ottiger, M.; Schoenebeck, F. *Helvetica Chim. Acta* **2012**, *95*, 2231. (j) Chen, M.; Buchwald, S. L. *Angew. Chem., Int. Ed*. **2013**, *52*, 11628. (k) Serizawa, H.; Aikawa, K.; Mikami, K. *Chem. Eur. J*. **2013**, *19*, 17692. (l) Mulder, J. A.; Frutos, R. P.; Patel, N. D.; Qu, B.; Sun, X.; Tampone, T. G.; Gao, J.; Sarvestani, M.; Eriksson, M. C.; Haddad, N.; Shen, S.; Song, J. J.; Senanayake, C. H. *Org. Process Res. Dev*. **2013**, *17*, 940. (m) Nakamura, Y.; Fujiu, M.; Murase, T.; Itoh, Y.; Serizawa, H.; Aikawa, K.; Mikami, K. *Beilstein J. Org. Chem*. **2013**, *9*, 2404. (n) Mormino, M. G.; Fier, P. S.; Hartwig, J. F. *Org. Lett.* **2014**, *16*, 1744. (o) Serizawa, H.; Aikawa, K.; Mikami, K. *Org. Lett*. **2014**, *16*, 3456. (p) Gonda, Z.; Kovács, S.; Wéber, C.; Gáti, T.; Mészáros, A.; Kotschy, A.; Novák, Z. *Org. Lett.* **2014**, *16*, 4268. (q) Alonso, C.; Marigorta, E. M.; Rubiales, G.; Palacios F. *Chem. Rev*. **2015**, *115*, 1847.

studies by McLoughlin and Thrower,1[b] Kumadaki,[6] Yagupolskii,[7] Kondo,[8] Burton,[9] Chen,[10] Tamborski,[11] Fuchikami,[12] and others4,[13] have provided a clear indication that the transformation involves $X/CF_3(R_f)$-exchange (R_f = perfluoroalkyl) on an aryl halide ArX, effected by "$CuCF_3$" or "CuR_f", preformed or generated *in situ* from a variety of CF_3 or R_f sources. In his original seminal work, Burton9 detected three types of $CuCF_3$ species in solution by ^{19}F NMR and monitored their reaction with iodoarenes. Since then, both structurally undefined $CuCF_3$4 and adequately characterized $CF_3Cu(I)$ complexes, such as $[(Ph_3P)(phen)CuCF_3]$,5[d] $[(bathophen)CuCF_3]$5[e] (phen = 1,10-phenanthroline; bathophen = bathophenanthroline), $[(phen)CuCF_3]$,5[c] $[(Ph_3P)_3CuCF_3]$5[d] and $[(NHC)CuCF_3]$ [14] have been shown to trifluoromethylate aryl halides (mostly iodides).

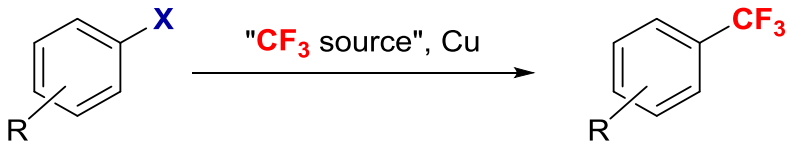

Scheme 1. *Cu-promoted/catalyzed trifluoromethylation of aryl halides*

[6] (a) Kobayashi, Y.; Kumadaki, I. *Tetrahedron Lett*. **1969**, 4095. (b) For a recent account of Kumadaki's work, see: Sato, K.; Tarui, A.; Omote, M.; Ando, A.; Kumadaki, I. *Synthesis* **2010**, 1865.
[7] Kondratenko, N. V.; Vechirko, E. P.; Yagupolskii, L. M. *Synthesis* **1980**, 932.
[8] Matsui, K.; Tobita, E.; Ando, M.; Kondo, K. *Chem. Lett*. **1981**, 1719.
[9] (a) Wiemers, D. M.; Burton, D. J. *J. Am. Chem. Soc.* **1986**, *108*, 832. (b) MacNeil, J. G.; Burton, D. J. *J. Fluorine Chem.* **1991**, *55*, 225.
[10] (a) Chen, Q.-Y.; Wu, S-W. *J. Chem. Soc., Chem. Commun*. **1989**, 705. (b) Chen, Q.-Y.; Wu, S-W. *J. Chem. Soc., Perkin Trans. 1* **1989**, 2385. (c) Chen, Q.-Y.; Duan, J.-X. J. *Chem. Soc., Chem. Commun*. **1993**, 1389. (d) Long, Z.-Y.; Duan, J.-X.; Lin, Y.-B.; Guo, C.-Y.; Chen, Q.-Y. *J. Fluorine Chem*. **1996**, *78*, 177.
[11] Chen, G. J.; Tamborski, C. *J. Fluorine Chem.* **1989**, *43*, 207.
[12] Urata, H.; Fuchikami, T. *Tetrahedron Lett*. **1991**, *32*, 91.
[13] (a) Kuett, A.; Movchun, V.; Rodima, T.; Dansauer, T.; Rusanov, E. B.; Leito, I.; Kaljurand, I.; Koppel, J.; Pihl, V.; Koppel, I.; Ovsjannikov, G.; Toom, L.; Mishima, M.; Medebielle, M.; Lork, E.; Roeschenthaler, G.-V.; Koppel, I. A.; Kolomeitsev, A. A. *J. Org. Chem*. **2008**, *73*, 2607. (b) Kremlev, M. M.; Tyrra, W.; Mushta, A. I.; Naumann, D.; Yagupolskii, Y. L. *J. Fluorine Chem.* **2010**, *131*, 212.
[14] (a) Dubinina, G. G.; Furutachi, H.; Vicic, D. A. *J. Am. Chem. Soc*. **2008**, *130*, 8600. (b) Dubinina, G. G.; Ogikubo, J.; Vicic, D. A. *Organometallics* **2008**, *27*, 6233.

While all of the reports in the area are in agreement on the order of reactivity of haloarenes ArI >> ArBr >> ArCl toward $CuCF_3$ (or CuR_f) and on the importance of amide solvents such as DMF for the reaction, there is less uniformity regarding the mechanism of the CF_3 transfer from Cu to the aromatic substrate. In the vast majority of the reports, reasonably plausible mechanisms are proposed or no mechanistic considerations presented whatsoever. Non-radical reaction pathways are frequently speculated to govern the Ar-CF_3 bond formation. In two instances,[5c,i] radical clock experiments have been performed to observe the lack of formation of cyclized products and, consequently, conclude on the unlikely involvement of free radicals in the reaction. In some other cases, however, signs of single electron processes (SET) have been observed.4 For example, Chen and Wu[10b] have noted the partial suppression of the trifluoromethylation reaction of aryl iodides with FO_2SCF_2I/Cu in the presence of SET scavengers and free radical inhibitors. They have also detected the formation of a free radical addition-elimination product when performing the reaction in the presence of tetramethylethylene.

Apart from the two aforementioned radical clock experiments, the mechanism of trifluoromethylation of aryl halides has been probed by a Hammett correlation study of the decarboxylative reaction of CF_3CO_2Na/CuI with a series of *p*-XC_6H_4I (X = Me, MeO, H, F, Cl, I, CF_3, NO_2) in NMP at 160 ^oC.[15] From the small positive ρ value of +0.46 deduced, a conclusion was drawn on a nucleophilic nature of the reactive species, $[CF_3CuI]^-$ rather than $[CF_3CuI]^{\cdot}$ being proposed as an intermediate. An almost identical study was most recently performed5[j] for the same reaction employing CF_3CO_2K/CuI at 200 ^oC for *p*-IC_6H_4X (X = MeO, *t*-Bu, H, CO_2Et) and *m*-$IC_6H_4CO_2Et$. Essentially the same ρ value of +0.52 was obtained.

[15] Carr, G. E.; Chambers, R. D.; Holmes, T. F. *J. Chem. Soc., Perkin Trans. 1* **1988**, 921.

Objectives

As follows from the above, there have been no reports of detailed mechanistic studies of Cu-mediated trifluoromethylation (or fluoroalkylation) of aryl halides. Considering the importance of such transformations for numerous industrial applications[2,3] and a broad variety of possible reaction pathways for Cu-promoted aromatic coupling reactions,[16,17,18] elucidating the mechanism of the trifluoromethylation of aryl halides with $CuCF_3$ would benefit further developments in the area. Therefore, the objective of our work summarized in this Chapter was to establish the mechanism of trifluoromethylation of haloarenes with the fluoroform-derived $CuCF_3$ reagent recently developed in our laboratory.[19] As in the mechanistic study described in the previous Chapter, in the current project we used the most powerful modern approach to elucidation of reaction mechanisms, involving both experimental and computational studies. The results presented below are believed to contribute to the overall understanding of not only fluoroalkylation reactions but also aromatic substitution with copper compounds in general.

[16] For selected reviews, see: (a) Hassan, J.; Sevignon, M.; Gozzi, C.; Schulz, E.; Lemaire, M. *Chem. Rev*. **2002**, *102*, 1359. (b) Ley, S.; Thomas, A. W. *Angew. Chem., Int. Ed*. **2003**, *42*, 5400. (c) Beletskaya, I. P.; Cheprakov, A. V. *Coord. Chem. Rev*. **2004**, *248*, 2337. (d) Evano, G.; Blanchard, N.; Toumi, M. *Chem. Rev*. **2008**, *108*, 3054. (e) Monnier, F.; Taillefer, M. *Angew. Chem., Int. Ed*. **2009**, *48*, 6954. (f) Rao, H.; Fu, H. *Synlett* **2011**, 745. (g) Evano, G.; Blanchard, N. *Copper-Mediated Cross-Coupling Reactions*; John Wiley & Sons: Hoboken, New Jersey, 2014.

[17] For most recent critical reviews of mechanisms of Cu-mediated/catalyzed coupling reactions of aryl halides, see: (a) Beletskaya, I. P.; Cheprakov, A. V. *Organometallics* **2012**, *31*, 7753. (b) Lefèvre, G.; Franc, G.; Tlili, A.; Adamo, C.; Taillefer, M.; Ciofini, I.; Jutand, A. *Organometallics* **2012**, *31*, 7694. (c) Sperotto, E.; van Klink, G. P. M.; van Koten, G.; de Vries, J. G. *Dalton Trans*. **2010**, *39*, 10338.

[18] (a) Jones, G. O.; Liu, P.; Houk, K. N.; Buchwald, S. L. *J. Am. Chem. Soc.* **2010**, *132*, 6205. (b) Yu, H.-Z.; Jiang, Y.-Y.; Fu, Y.; Liu, L. *J. Am. Chem. Soc.* **2010**, *132*, 18078.

[19] Zanardi, A.; Novikov, M. A.; Martin E.; Benet-Buchholz, J.; Grushin. V. V. *J. Am. Chem. Soc*. **2011**, *133*, 20901.

Results

In 2011, our group reported[4,19] the first reaction of direct cupration of fluoroform furnishing, after stabilization (see Chapter 1), "ligandless" $CuCF_3$. Since then, we have established the mechanism of the cupration reaction[20] and other members of the group have developed a number of trifluoromethylation methods for a variety of organic substrates.[21,22,23,24,25] For the current mechanistic study, we selected fluoroform-derived $CuCF_3$ because of its previously demonstrated[23] ability to smoothly trifluoromethylate a broad variety of aryl halides in high yield and with excellent chemoselectivities under mild conditions (20-80 ^{o}C).

Experimental Studies. The $CuCF_3$ reagent was prepared by the previously developed procedure[19,23] in >90% yield by the reaction of CHF_3 with [K(DMF)][(*t*-BuO)$_2$Cu] (from CuCl and 2 equiv of *t*-BuOK in DMF), and subsequently stabilized with $Et_3N{\cdot}3HF$ (Scheme 2). Strong evidence has been obtained[20,26] (see Chapter 2) for the original product of the cupration reaction being a mixed cuprate [K(DMF)$_n$][(*t*-BuO)Cu(CF_3)] that undergoes acidolysis of the Cu-O bond upon the stabilization with $Et_3N{\cdot}3HF$. As can be seen from the stoichiometry of the overall process (Scheme 2), the reagent solution thus produced contains ca. 1 equiv of "$CuCF_3$", 2 equiv of *t*-BuOH, and 1/3 equiv of Et_3N. The latter two and the DMF solvent stabilize the $CuCF_3$ moiety by coordination through the N and O donor atoms. These interactions are rather weak and

[20] Konovalov, A. I.; Benet-Buchholz, J.; Martin, E.; Grushin, V. V. *Angew. Chem., Int. Ed.* **2013**, *52*, 11637.
[21] Novák, P.; Lishchynskyi, A.; Grushin, V. V. *Angew. Chem., Int. Ed.* **2012**, *51*, 7767.
[22] Novák, P.; Lishchynskyi, A.; Grushin, V. V. *J. Am. Chem. Soc*. **2012**, *134*, 16167.
[23] Lishchynskyi, A.; Novikov, M. A.; Martin, E.; Escudero-Adán, E. C.; Novák, P.; Grushin, V. V. *J. Org. Chem*. **2013**, *78*, 11126.
[24] Lishchynskyi, A.; Berthon, G.; Grushin, V. V. *Chem. Commun.* **2014**, *50*, 10237.
[25] Lishchynskyi, A.; Mazloomi, Z.; Grushin, V. V. *Synlett* **2015**, *26*, 45.
[26] Lishchynskyi, A.; Grushin, V. V. *J. Am. Chem. Soc.* **2013**, *135*, 12584.

consequently the Et_3N, DMF, and *t*-BuOH molecules are easily displaced from the Cu center. This is why we refer to the fluoroform-derived $CuCF_3$ as "ligandless". By no means do we imply that the Cu atom in these species is mono-coordinate, being devoid of any ligands besides CF_3 (see below).

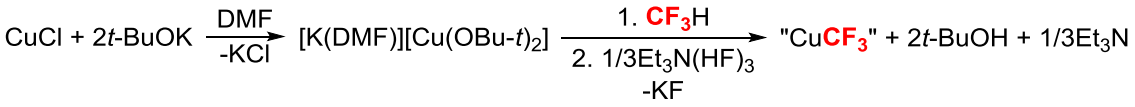

***Scheme 2**. Preparation of "ligandless" $CuCF_3$ from CHF_3, followed by stabilization*

Radical Clock Experiment. It has been previously concluded[23] that radical processes are unlikely involved in the trifluoromethylation of aryl halides with fluoroform-derived $CuCF_3$. In particular, the lack of side-formation of arenes and biaryls in these reactions suggests that aryl radicals are not generated in the transformation. Furthermore, the formation of only small quantities of bis-trifluoromethylated products in the reaction of *p*- and *o*-BrC_6H_4I with $CuCF_3$ is inconsistent with the $S_{RN}1$ mechanism.[27] In the current work, we found that the treatment of 2-allyloxyphenyl iodide, a radical clock substrate (k_c = ca. 10^{10} s^{-1}),[28, 29] with $CuCF_3$ gave rise exclusively to 2-allyloxybenzotrifluoride (Scheme 3). No formation of the cyclized product was observed (^{19}F NMR, GC-MS). This result provides further strong support to the previously drawn conclusion[23] of a non-radical

[27] (a) Bunnett, J. F. *Acc. Chem. Res*. **1978**, *11*, 413. (b) Rossi, R. A.; de Rossi, R. H. *Aromatic Substitution by the $S_{RN}1$ Mechanism;* American Chemical Society: Washington, DC, 1983. (c) Bowman, W. R.; Heaney, H.; Smith, P. H. G. *Tetrahedron Lett*. **1984**, *25*, 5821. (d) van Leeuwen, M.; McKillop, A. *J. Chem. Soc., Perkin 1* **1993**, 2433.
[28] Giese, B.; Kopping, B.; Göbel, T.; Dickhaut, J.; Thoma, G.; Kulicke, K. J.; Trach, F. *Org. Reactions* **1996**, *48*, 301.
[29] (a) Johnston, L. J.; Lusztyk, J.; Wayner, D. D. M.; Abeywickreyma, A. N.; Beckwith, A. L. J.; Scaiano, J. C.; Ingold, K. U. *J. Am. Chem. Soc.* **1985**, *107*, 4594. (b) Abeywickrema, A. N.; Beckwith, A. L. J. *Chem. Commun*. **1986**, 464. (c) Abeywickrema, A. N.; Beckwith, A. L. J.; Gerba, S. *J. Org. Chem.* **1987**, *52*, 4072. (d) Annunziata, A.; Galli, C.; Marinelli, M.; Pau, T. *Eur. J. Org. Chem*. **2001**, 1323.

mechanism of the trifluoromethylation of haloarenes with the $CuCF_3$. It is worth to note that 2-allyloxyphenyl iodide has been widely used to identify radical,[24, 30, 31] and nonradical[31, 32] pathways for a variety of Cu-mediated reactions of aryl halides, including the trifluoromethylation with [(phen)$CuCF_3$].5[c]

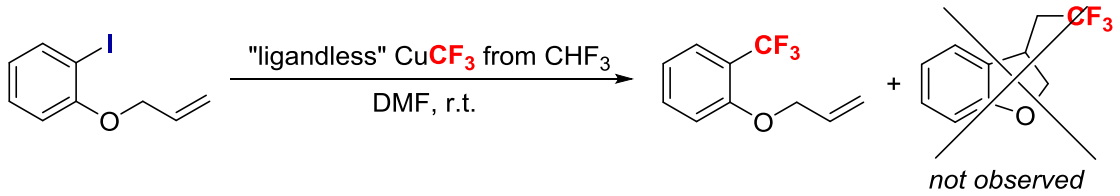

***Scheme 3**. Reaction of fluoroform-derived $CuCF_3$ with 2-allyloxyphenyl iodide*

Determination of Reaction Order. The method of initial rates as measured by ^{19}F NMR was used to determine the order of the reaction of $CuCF_3$ with a broad variety of substrates *p*-RC_6H_4I (R = H, Me, OMe, Cl, CO_2Et, Ac, CN, NO_2), *m*-RC_6H_4I (R = Me, OMe, Cl, CHO, CO_2Et, CN, NO_2), *o*-NCC_6H_4I, and *o*-RC_6H_4Br (R = CO_2Me, CHO, Ac, CN, and NO_2). In the range of concentrations of $CuCF_3$ and ArX 0.095-0.380 M, all but two reactions exhibited clean second order kinetics, first order with respect to each reactant. Deviations from the second order were observed in two cases, for *p*-IC_6H_4CN and *p*-$IC_6H_4NO_2$. With these two aryl iodides, the reaction was ca. 0.5 order with respect to both the substrate and $CuCF_3$. We reasoned that the deviation might deal with the reversible coordination of the CN and NO_2 groups on the substrate

[30] (a) Creutz, S. E.; Lotito, K. J.; Fu, G. C.; Peters, J. C. *Science* **2012**, *338*, 647. (b) Uyeda, C.; Tan, Y.; Fu, G. C.; Peters, J. C. *J. Am. Chem. Soc*. **2013**, *135*, 9548.
[31] Fier, P. S.; Hartwig, J. F. *J. Am. Chem. Soc.* **2012**, *134*, 10795.
[32] (a) Combes, S.; Finet, J.-P. *Tetrahedron* **1999**, *55*, 3377. (b) Tye, J. W.; Weng, Z.; Johns, A. M.; Incarvito, C. D.; Hartwig, J. F. *J. Am. Chem. Soc.* **2008**, *130*, 9971. (c) Tye, J. W.; Weng, Z.; Giri, R.; Hartwig, J. F. *Angew. Chem., Int. Ed*. **2010**, *49*, 2185. (d) Giri, R.; Hartwig, J. F. *J. Am. Chem. Soc.* **2010**, *132*, 15860. (e) Chen, C.; Weng, Z.; Hartwig, J. F. *Organometallics* **2012**, *31*, 8031. (f) Huang, Z.; Hartwig, J. F. *Angew. Chem., Int. Ed*. **2012**, *51*, 1028. (g) Chatterjee, T.; Ranu, B. C. *J. Org. Chem*. **2013**, *78*, 7145. (h) Gurung, S. K.; Thapa, S.; Vangala, A. S.; Giri, R. *Org. Lett*. **2013**, *15*, 5378. (i) Chen, C.; Ouyang, L.; Lin, Q.; Liu, Y.; Hou, C.; Yuan, Y.; Weng, Z. *Chem. Eur. J*. **2014**, *20*, 657. (j) Chen, C.; Hou, C.; Wang, Y.; Hor, T. S. A.; Weng, Z. *Org. Lett*. **2014**, *16*, 524.

to the Cu center, as shown in Scheme 4 for R = CN. The final product would then be formed by four reactions occurring at different rates: (i) the original "ligandless" $CuCF_3$ with the free substrate *p*-IC_6H_4R (R = CN or NO_2), (ii) the original "ligandless" $CuCF_3$ with $[L_m(p\text{-}IC_6H_4R)CuCF_3]$, (iii) the free substrate *p*-IC_6H_4R with $[L_m(p\text{-}IC_6H_4R)CuCF_3]$, and (iv) $[L_m(p\text{-}IC_6H_4R)CuCF_3]$ as a nucleophile ($CuCF_3$) with another molecule of $[L_m(p\text{-}IC_6H_4R)CuCF_3]$ as an electrophile (C-I).

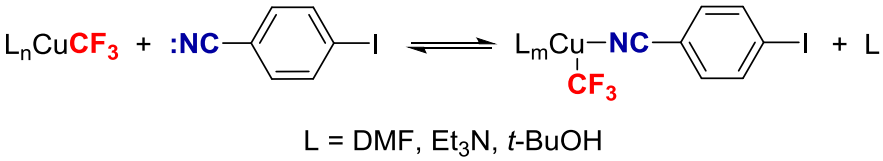

Scheme 4. *Reversible coordination of fluoroform-derived $CuCF_3$ with p-IC_6H_4CN*

To probe this hypothesis (Scheme 4), we repeated the reaction order determination for *p*-IC_6H_4CN and *p*-$IC_6H_4NO_2$ in the presence of MeCN in excess. Being a better ligand for Cu(I) than *p*-IC_6H_4R (R = CN or NO_2), DMF, *t*-BuOH, and Et_3N, acetonitrile was expected to free up the substrate from its Cu complex and drive all ligand exchange equilibria in the system to $[(MeCN)_nCuCF_3]$. Indeed, in the presence of MeCN (50 equiv per Cu), both reactions displayed second order kinetics, first order in Cu and first order in *p*-IC_6H_4R (R = CN or NO_2). The addition of MeCN not only restored the second order of the reaction, but also slowed down the trifluoromethylation by a factor of 4.5. The observed slower rates are consistent with the previously reported[5d,23] inhibition of trifluoromethylation reactions of aryl halides with $CuCF_3$ complexes in the presence of deliberately added ligands with a high affinity for Cu(I). Second order kinetic behavior was invariably observed for the reactions of all of the *o*-RC_6H_4Br and *m*-RC_6H_4I substrates with $CuCF_3$ in DMF in the absence of MeCN.

The lack of deviation from the first order in $CuCF_3$ and in *o*-RC_6H_4X (X = Br, I) or *m*-RC_6H_4I for R = CN and NO_2 may be attributed to an expected[33] weaker binding of the Cu to these groups, as compared with those in the *para*-derivatives *p*-$IC_6H_4NO_2$ and *p*-IC_6H_4CN (Scheme 4).

Hammett Studies. The *Para*-Series. Relative rate constants were determined for the reactions of $CuCF_3$ with 11 iodoarenes *p*-RC_6H_4I (R = H, Me, *t*-Bu, MeO, F, Cl, Br, CO_2Et, Ac, CN, and NO_2) at 298 K. The reactions of $CuCF_3$ in DMF with two or more competing aryl iodides were run under pseudo-first order conditions with [*p*-XC_6H_4I]/[$CuCF_3$] = 10 for each substrate and monitored by ^{19}F NMR. Two sets of experiments were performed. In one, the reactions of all eleven substrates were run in the presence of MeCN (50 equiv per Cu) in order to avoid the above-described deviation from second order kinetics for R = CN and NO_2. The second set of measurements was performed in the absence of MeCN. Within each data set, different runs performed at various concentrations and conversions showed excellent reproducibility and no variation in k_R/k_H within the estimated experimental error of ca. 10%. Notably, the same decrease in the reaction rates by a factor of 4.5 in the presence of 50 equiv of MeCN (see above) was observed for all substrates in the series. Consequently, the k_R/k_H values obtained in the presence and in the absence of MeCN were indistinguishable within the experimental error.

Unexpectedly, plotting the $\lg(k_R/k_H)$ values against the Hammett σ_p constants[34] resulted in no satisfactory linear correlation. Excellent correlations were obtained,

[33] (a) Exner, O.; Böhm, S. *Curr. Org. Chem*. **2006**, *10*, 763. (b) Exner, O.; Böhm, S. *Phys. Chem. Chem. Phys*. **2004**, *6*, 3864. (c) Exner, O.; Böhm, S. *Org. Biomol. Chem*. **2005**, *3*, 1838. (d) Exner, O.; Böhm, S. *Collect. Czech. Chem. Commun.* **2006**, *71*, 1239. (e) Žáček, P.; Dransfeld, A.; Exner, O.; Schraml, J. *Magn. Reson. Chem.* **2006**, *44*, 1073.
[34] Hansch, C.; Leo, A.; Taft, R. W. *Chem. Rev*. **1991**, *91*, 165.

however, for two separate sets within the series (Figure 1, top), one with R = H, Me, *t*-Bu, MeO, Cl, and Br ($\rho = +0.69 \pm 0.1$; $R^2 = 0.99$) and the other with R = F, Cl, Br, CO_2Et, Ac, CN, and NO_2 ($\rho = +1.83 \pm 0.1$; $R^2 = 1.00$).

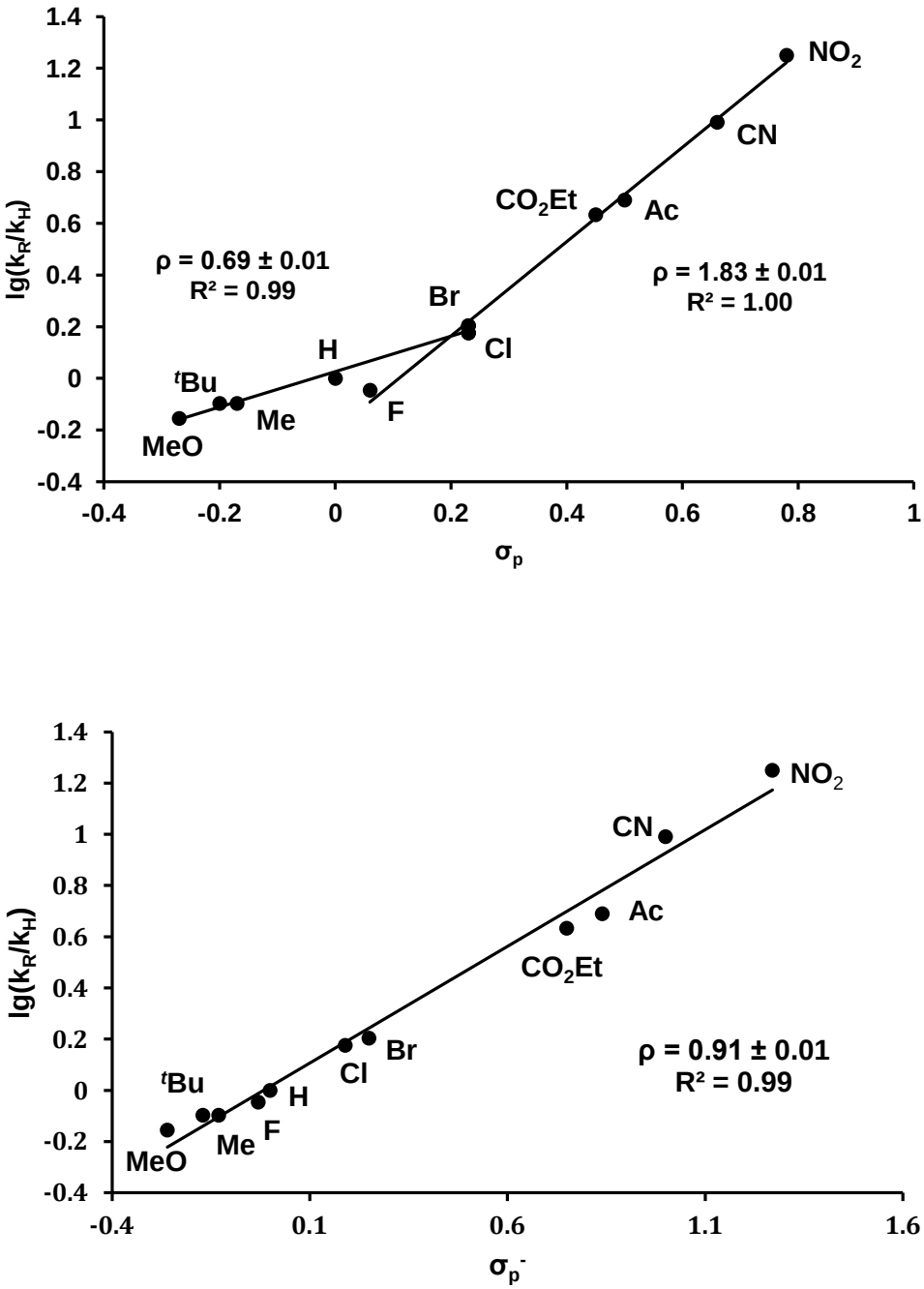

***Figure 1**. Hammett plots for the reactions of p-RC_6H_4I with $CuCF_3$ in the absence of MeCN using σ_p (top) and σ_p^- (bottom)*

We are unaware of similar observations in the chemistry of Cu-catalyzed reactions of aryl halides.[5j,35,36,37,38,39,40,41,42] However, a strikingly similar Hammett pattern with an abrupt line breakage at about the same point, σ_p = +0.23 (Cl), has been reported Foà and Cassar[43] for Ar-Cl oxidative addition to [$(Ph_3P)_3Ni$]. That dual correlation pattern was convincingly interpreted in terms of two different mechanisms governing the transformation. On the other hand, we found that our lg(k_R/k_H) values correlate excellently (ρ = +0.91 ± 0.1; R^2 = 0.99) with σ_p^- (Figure 1, bottom), a parameter that is conventionally used for reactions where considerable resonance interaction takes place between the substituent and the reaction center.[34]

Hammett Studies. **The *Meta*-Series.** An excellent linear correlation of the lg(k_R/k_H) values with the Hammett σ_m constants[34] was obtained for the reactions of $CuCF_3$ with eight iodoarenes *m*-RC_6H_4I (R = H, Me, MeO, CO_2Et, CHO, Cl, CN, and NO_2) at 298 K. Although all of these reactions obeyed second order kinetics in the absence of MeCN (see above), the k_R/k_H determination was repeated in the presence of 50 equiv of MeCN for comparison with the *para*-series. As with the *p*-RC_6H_4I substrates, the addition of MeCN slowed down all of the reactions by the same factor of 4.5. As a result, the Hammett plots for the reactions in the presence of MeCN (ρ = +0.95 ± 0.03; R^2 = 0.99) and in its absence (ρ = +0.97 ± 0.03; R^2 = 0.99) were virtually indistinguishable (Figure 2).

[35] Williams, A. L.; Kinney, R. E.; Bridger, R. F. *J. Org. Chem.* **1967**, *32*, 2501.
[36] Litvak, V. V.; Shein, S. M. *Zh. Org. Khim*. **1974**, *10*, 550.
[37] Litvak, V. V.; Shein, S. M. *Zh. Org. Khim*. **1974**, *10*, 2360.
[38] Aronskaya, N. Yu.; Bezuglyi, V. D. *Zh. Org. Khim*. **1974**, *10*, 268.
[39] Stanko, V. I.; Iroshnikova, N. G. *Zh. Obshch. Khim*. **1979**, *49*, 2076.
[40] (a) Couture, C.; Paine, A. J. *Can. J. Chem*. **1985**, *63*, 111. (b) Paine, A. J. *J. Am. Chem. Soc*. **1987**, *109*, 1496.
[41] Strieter, E. R.; Bhayana, B.; Buchwald, S. L. *J. Am. Chem. Soc*. **2009**, *131*, 78.
[42] Ji, P.; Atherton, J. H.; Page, M. I. *J. Org. Chem*. **2012**, *77*, 7471.
[43] Foà, M.; Cassar, L. *J. Chem. Soc., Dalton Trans.* **1975**, 2572.

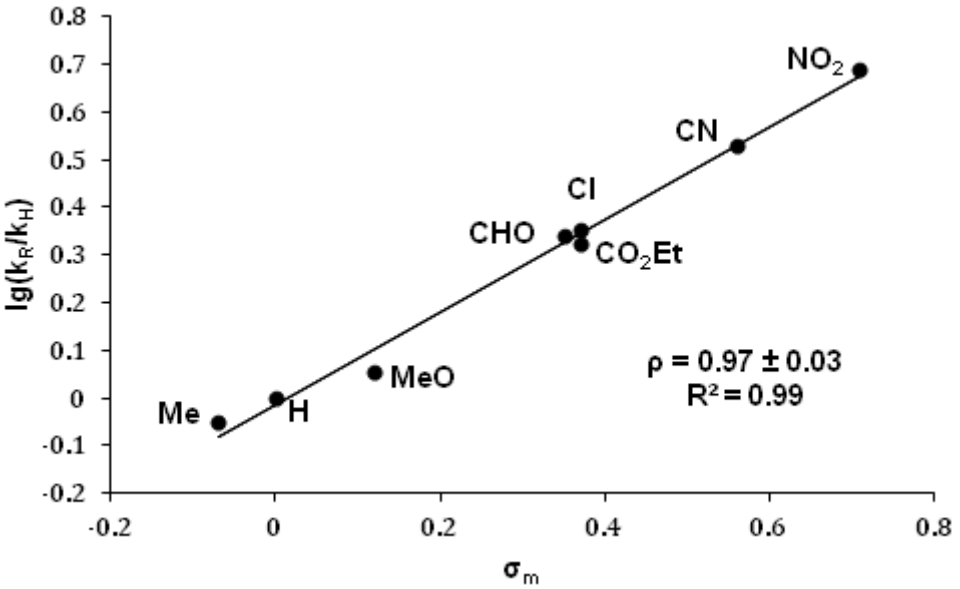

***Figure 2**. Hammett plot for the reactions of m-RC_6H_4I with $CuCF_3$ (without CH_3CN)*

Computational Studies. The "one or two mechanisms" dilemma (Figure 1) could not be solved by experimental methods. We therefore undertook a series of computational studies to gain a deeper insight into the mechanism of the reactions of $CuCF_3$ with aryl halides. DFT calculations based on a mPW2PLYPD(BS2)//B3LYP-D(BS1) protocol (see the Computational Details section) have been used throughout the study. In the following sections, all energies correspond to computed Gibbs free energies in DMF, unless noted otherwise.

Model selection. As discussed above, after the cupration of fluoroform and stabilization of the trifluoromethyl Cu(I) complex produced with $Et_3N{\cdot}3HF$, the resultant reagent solution in DMF comprises of "$CuCF_3$", *t*-BuOH, and Et_3N in a 1:2:0.33 molar ratio (Scheme 2). Given that and the consensus[32b,d,44] that the reactive

[44] See, for example: (a) Strieter, E. R.; Blackmond, D. G.; Buchwald, S. L. *J. Am. Chem. Soc*. **2005**, *127*, 4120. (b) Zhang, S.-L.; Liu, L.; Fu, Y.; Guo, Q.-X. *Organometallics* **2007**, 26, 4546. (c) Kaddouri, H.; Vicente, V.; Quali, A.; Quazzani, F.; Taillefer, M. *Angew. Chem., Int. Ed*. **2009**, *48*, 333. (d) Strieter, E. R.; Bhayana, B.; Buchwald, S. L. *J. Am. Chem. Soc*. **2009**, *131*, 78. (e) Zhang, S.-L.; Ding, Y. *Organometallics* **2011**, 30, 633. (f) Liu, X.; Zhang, S.-L.; Ding, Y. *Dalton Trans*. **2012**, *41*, 5897. (g) Zhang, S.; Zhu, Z.; Ding Y. *Dalton Trans*. **2012**, *41*, 13832.

species in Ullmann-type reactions are complexes of the type [(L)Cu(nucleophile)] we considered [$LCuCF_3$] (L = DMF, *t*-BuOH, Et_3N) as the CF_3-transferring molecules. The computed bond dissociation energies (BDE) showed that Et_3N (modeled as Me_3N) binds to $CuCF_3$ 7.0 kcal/mol more strongly and *t*-BuOH 2.1 kcal/mol less strongly than DMF (Table 1).[45]

Table 1. *L-$CuCF_3$ bond dissociation free energies (BDE)*

Ligand L	L:$CuCF_3$ molar ratio	BDE, kcal/mol
DMF	ca. 28[a]	20.5
t-BuOH	2	18.4
NEt_3[b]	0.33	27.5

[a] Calculated from the actual concentration of $CuCF_3$ solutions used in the experimental studies; [b] Modeled as NMe_3.

In spite of the large DMF to Et_3N molar ratio of ca. 85:1 under the experimental conditions, the computed data indicate that the equilibrium between [(DMF)$CuCF_3$] and [(Me_3N)$CuCF_3$] (eq 1) in the $CuCF_3$ reagent solution is shifted almost entirely to the amino complex. Nevertheless, the species selected for the reactivity computational studies was [(DMF)$CuCF_3$] because the actual reagent solution contains only ca. 0.33 equiv of Et_3N per each equiv of $CuCF_3$, whereas the DMF solvent is abundant (see above and Scheme 2). Furthermore, as the reaction with an aryl iodide occurs, CuI is produced that binds[46] to the tertiary amine more strongly than $CuCF_3$ (eq 2). Finally, as will be shown below, the selected model species [(DMF)$CuCF_3$] is more reactive toward ArX than [(Me_3N)$CuCF_3$]. The complex bearing two DMF ligands on Cu,

[45] As the yield of $CuCF_3$ is slightly below quantitative (Scheme 2), the stabilization with 1/3 mol of $Et_3N{\cdot}3HF$ per 1 mol of CuCl used for the reaction likely results in the presence of small extra quantities of HF in the final reagent solution. Extra $Et_3N{\cdot}3HF$ is often added to the reagent to enhance its reactivity toward haloarenes.[23] HF complexation with $CuCF_3$ can be neglected because of the low computed BDE of 3.5 kcal/mol.
[46] Yoke, J. T., III; Weiss, J. F.; Tollin, G. *Inorg. Chem*. **1963**, *2*, 1210.

[$(DMF)_2CuCF_3$], was computed to lie 6.0 kcal/mol higher in energy than [$(DMF)CuCF_3$] and therefore was disregarded in the DFT study. Consequently, all energies in the DFT study are quoted relative to the combined Gibbs free energies of [$(DMF)CuCF_3$] and the corresponding aryl halide set to zero.

$$[(DMF)Cu\mathbf{CF_3}] + NMe_3 \rightleftharpoons [(Me_3N)Cu\mathbf{CF_3}] + DMF \quad (1)$$

$$\Delta G^o = -7.0 \text{ kcal·mol}^{-1}$$

$$[(Me_3N)Cu\mathbf{CF_3}] + [(DMF)CuI] \rightleftharpoons [(DMF)Cu\mathbf{CF_3}] + [(Me_3N)CuI] \quad (2)$$

$$\Delta G^o = -1.7 \text{ kcal·mol}^{-1}$$

Trifluoromethylation of PhI. Associative and Dissociative Oxidative Addition - Reductive Elimination Pathways. Initially, we studied the reaction of [$(DMF)CuCF_3$] with the simplest iodoarene, PhI, as a model substrate. The reaction of fluoroform-derived $CuCF_3$ with PhI has been experimentally shown[23] to cleanly produce $PhCF_3$ in 95% yield at 99% conversion after 18 h at 50 ^oC. First we probed a mechanism involving Ph-I oxidative addition (OA) to produce a Cu(III) species, followed by Ph-CF_3 reductive elimination (RE). Two alternative computed pathways for this process are shown in Figure 3. One of them (dissociative, shown in blue) involves DMF loss from Cu as the first step, whereas the other one (associative, shown in red) does not.

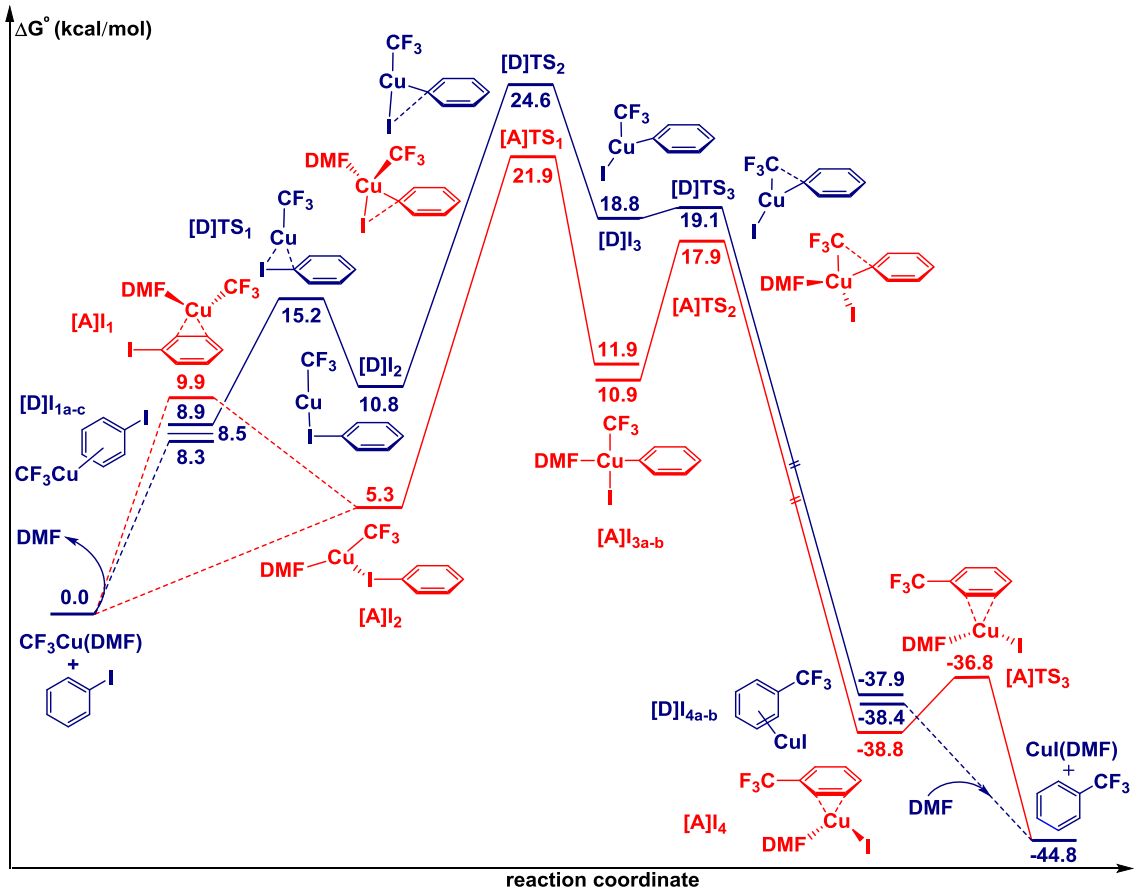

***Figure 3**. Alternative computed reaction profiles for the reaction of [(DMF)CuCF$_3$] with PhI via OA-RE involving (blue, "DOARE") and not involving (red, "AOARE") DMF dissociation*

In the Dissociative OA-RE pathway (DOARE), the [(PhI)CuCF$_3$] adduct in its most stable form **[D]I$_{1a}$** (8.3 kcal/mol) exhibits an η^2-binding mode through one C$_{meta}$-C$_{para}$ bond. Alternative η^2-arene species **[D]I$_{1b}$** and **[D]I$_{1c}$** bound through either a C$_{ortho}$-C$_{meta}$ or a C$_{ipso}$-C$_{ortho}$ bond are only slightly higher in energy, by 0.2 and 0.6 kcal/mol, respectively. The CuCF$_3$ coordination to the C$_{para}$-C$_{meta}$ or C$_{meta}$-C$_{ortho}$ bonds leads to a shortening of the C-I bond by 0.1 Å (C-I = 2.14 Å in free PhI), likely due to electron donation from the π-system of the benzene ring to the Lewis-acidic copper atom. In contrast, in the C$_{ortho}$-C$_{ipso}$ adduct **[D]I$_{1c}$**, the C-I bond is elongated by 0.1 Å and the

iodine atom deviates from the plane of the benzene ring by 10°. This distortion is indicative of predominant binding of Cu to the *ipso*-C atom, the reactive site of the substrate, *i.e.* of Ph-I preactivation. $CuCF_3$ transfer from the π-system in **[D]I$_{1c}$** to the iodine through a low-energy transition state **[D]TS$_1$** (15.2 kcal/mol; Figure 4, left) leads to further elongation of the C-I bond and the formation of a σ-complex with a nearly linear {F_3C-Cu-I} moiety orthogonal to the benzene ring (93°). Characterization of the subsequent C-I activation transition state showed that this I-bound intermediate **[D]I$_2$** is the immediate precursor in this process. The Ph-I OA proceeds *via* a relatively late transition state **[D]TS$_2$** (24.6 kcal/mol; Figure 4, center) with significant C···I elongation (2.73 Å), a short Cu···Ph contact (2.01 Å), and a short Cu-I bond distance (2.44 Å) that is only 0.1 Å longer than in copper iodide. C-I bond cleavage within the near-linear {F_3C-Cu-I} moiety (178°) with the Ph group effectively bridging the Cu-I bond leads to a Cu(III) Y-shaped intermediate, **[D]I$_3$** (18.8 kcal/mol) with an acute Ph-Cu-CF_3 angle of 77° and a Ph···CF_3 contact of 2.4 Å. This geometry facilitates the Ph-CF_3 RE step *via* **[D]TS$_3$** (19.1 kcal/mol; Figure 4, right) with a minimal barrier of 0.3 kcal/mol and results in a dramatic lowering of energy and the formation of a η^2-intermediate (**[D]I$_{4a}$**, -37.9 kcal/mol) with CuI π-bound to C_{ortho}-C_{meta} of the $PhCF_3$ molecule produced. After a rearrangement to the C_{meta}-C_{para} isomer **[D]I$_{4b}$** (-38.4 kcal/mol), DMF coordination to the CuI liberates the $PhCF_3$ molecule.

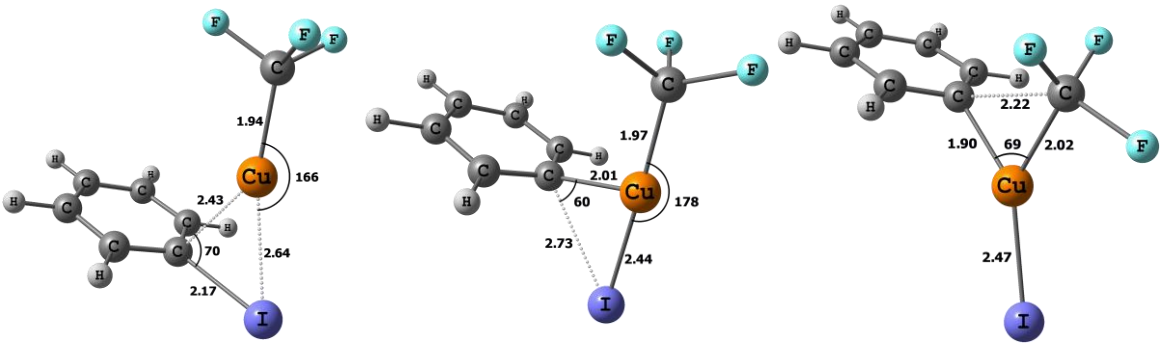

Figure 4. *Computed DOARE transition states for (left) $CuCF_3$ transfer from the π-system to iodine (**[D]TS$_1$**; 15.2 kcal/mol), (center) Ph-I OA to $CuCF_3$ (**[D]TS$_2$**; 24.6 kcal/mol), and (right) Ph-CF_3 RE from Cu (**[D]TS$_3$**; 19.1 kcal/mol)*

In the Associative OA-RE pathway (AOARE; shown in red in Figure 3), PhI can π-coordinate to [(DMF)$CuCF_3$] to produce a η^2-C_{meta}-C_{ortho} complex **[A]I$_1$** at 9.9 kcal/mol or form a more stable iodine-bound σ-complex **[A]I$_2$** (5.3 kcal/mol). The latter displays a nearly linear {(DMF)$CuCF_3$} fragment (179^o), a long Cu···I distance (3.61 Å), and a C-I bond that is almost indistinguishable in length (2.14 Å) from that in free PhI. This weak adduct is connected to an OA transition state **[A]TS$_1$** (21.9 kcal/mol). The C···I (2.42 Å) and Cu···I (2.57 Å) contacts computed for **[A]TS$_1$** (Figure 5, left) are shorter and longer, respectively, than in **[D]TS$_2$** (C···I = 2.73 Å; Cu···I = 2.44 Å), indicating that Ph-I activation *via* AOARE is governed by an earlier transition state than in DOARE. This leads to an energetically lower by 2.7 kcal/mol pathway for the trifluoromethylation with [(DMF)$CuCF_3$] than with [$CuCF_3$]. Descent from **[A]TS$_1$** yields an intermediate **[A]I$_{3a}$** with square-planar Cu(III) (Ph-Cu-I = 90°) at 11.9 kcal/mol that rearranges to a slightly more stable conformer **[A]I$_{3b}$** (10.9 kcal/mol) *via* rotation around the DMF-Cu bond. Involvement of high spin Cu(III) species can be ruled out as optimization of the originally produced d^8 Cu(III) intermediate in a triplet

state produced an energetically prohibited distorted tetrahedral structure at 46.0 kcal/mol.

RE from the Cu(III) intermediate **[A]I_{3b}** that is lower in energy than **[D]I_3** is favored by the formation of a strong Ph-CF_3 bond and occurs with a small barrier of 7.0 kcal/mol *via* **[A]TS_2** (17.9 kcal/mol; Figure 5, left), a transition state that is also lower in energy than its congener **[D]TS_3**. The resultant intermediate **[A]I_4** comprised of a {F_3C-Cu-DMF} moiety η^2-bound to a C_{ortho}-C_{meta} bond of $PhCF_3$ loses the latter *via* **[A]TS_3**. This dissociation process characterized by a very low barrier of only 2 kcal/mol completes the transformation. The calculated overall free energy effect of -44.8 kcal/mol shows that the trifluoromethylation process is highly exergonic.

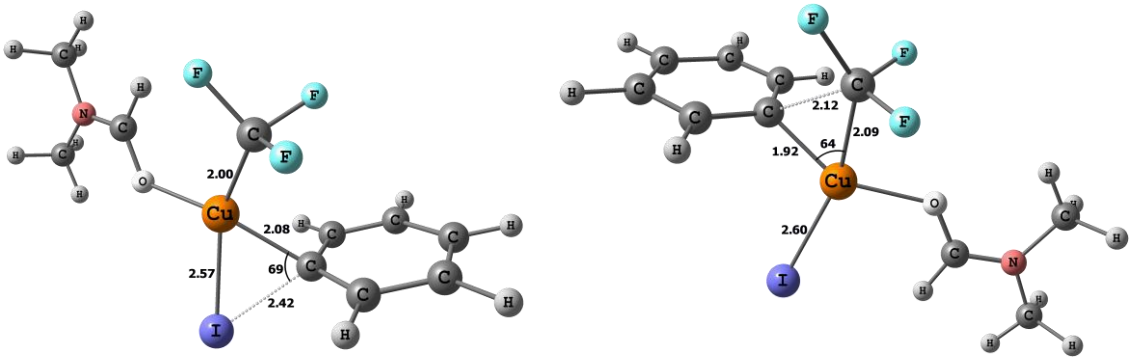

***Figure 5**. Computed AOARE transition states (left) for Ph-I OA to [(DMF)$CuCF_3$] (**[A]TS_1**; 21.9 kcal/mol) and (right) Ph-CF_3 RE from Cu (**[A]TS_2**; 17.9 kcal/mol)*

Alternative mechanisms. A recent computational study[18a] of Ph-I activation with [(L-L)Cu(ZMe)] (L-L = diketone or phen; Z = O, NH) showed that single electron transfer (SET) and halogen atom transfer (HAT) processes can be competitive with concerted oxidative addition. Therefore, these alternatives to the OA-RE mechanism as well as σ-bond metathesis (SBM) and S_NAr were also considered, focusing on the Ph-I activation step. For SBM, the computed barrier was 64.5 kcal/mol (Figure 6).

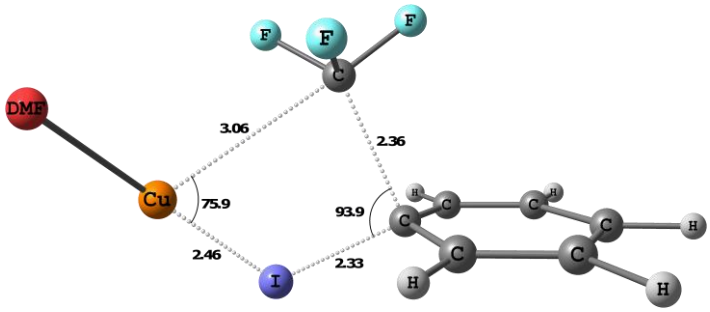

***Figure 6**. Computed transition state for Ph-I SMB to [(DMF)CuCF$_3$]; DMF ligand is omitted ($\Delta G^{\neq}$ = 64.5 kcal/mol)*

The other alternatives were assessed by computing the standard free Gibbs energy change for the following Ph-I activation steps:

SET (outer-sphere):$[(DMF)CuCF_3] + PhI \rightarrow [(DMF)Cu(CF_3)]^+ + PhI^{\bullet-}$ ΔG^o = +82.1 kcal/mol

SET (inner-sphere): $[(DMF)(PhI)CuCF_3] \rightarrow [(DMF)(PhI^{\bullet-})Cu^+CF_3]$ ΔG^o = +51.5 kcal/mol

HAT: $[(DMF)CuCF_3] + PhI \rightarrow [(DMF)(I)CuCF_3] + Ph^{\bullet}$ ΔG^o = +45.9 kcal/mol

S_NAr: $[(DMF)CuCF_3] + PhI \rightarrow [(DMF)(Ph)CuCF_3]^+ + I^-$ ΔG^o = +29.5 kcal/mol

The high computed Gibbs free energy ΔG^o values suggest that these mechanisms are not relevant in the present system.

***Para*-substituted Aryl Iodides**. The above-described OA-RE model (Figure 3) was then applied to a range of *p*-RC_6H_4I substrates, for which relative rates were determined experimentally (see above). Both the DOARE and AOARE pathways were studied for the entire series. The key transition states **[D]TS$_2$** and **[A]TS$_1$** computed for the substituted aryl iodides displayed geometries that were similar to those found for iodobenzene. The energy values presented below correspond to the most stable conformers in all cases.

For DOARE, the computed barriers (in kcal/mol in parentheses) produced the following order of reactivity: NO_2 (25.8) < CO_2Et (25.6) < CN (25.5) < Ac (25.4) < Cl (25.2) < MeO (25.1) < Br (25.0) < F (24.9) < Me (24.6) ≈ H (24.6) < *t*-Bu (24.3). This sequence suggests that electron-withdrawing substituents in the *para*-position would produce slower reaction, which is the opposite of the experimentally observed trend. Attempted correlation of σ_p^- with the $\lg(k_R/k_H)$ numbers derived from computed data produced an unrealistic negative ρ value of -0.56 (Figure 7). We are aware of only one study[40b] reporting a negative ρ value (-0.25) for Cu-mediated reactions of aryl halides.

In sharp contrast, the order of reactivity predicted by the theory for the AOARE pathway (computed barriers in kcal/mol in parentheses), Me (22.8) < MeO (22.6) < F (22.4) < *t*-Bu (22.0) ≈ Cl (22.0) ≈ Br (22.0) < H (21.9) < Ac (22.5) < CO_2Et (21.4) < CN (21.1) < NO_2 (20.3), accords with the experimental data. In spite of a few minor deviations from the computed and experimental data, a much better correlation of the DFT-derived $\lg(k_R/k_H)$ values with σ_p^- is observed, producing ρ = +0.92 (Figure 8) that is in excellent agreement with the experimental value of +0.91 (Figure 1, bottom). The DFT data-derived correlation coefficient R^2 = 0.87 that would be considered unsatisfactory for an experimental Hammett plot, is believed to be acceptable for the computational data, especially considering the fact that the barriers calculated for the 11 different *p*-RC_6H_4I substrates span a very narrow range of 2.5 kcal/mol.

The entire set of computational results described above indicate that the DOARE pathway is not only energetically more demanding than AOARE, but also inconsistent with the experimental Hammett data, whereas AOARE is. This applies to correlations of the DOARE and AOARE $\lg(k_R/k_H)$ values not only with the resonance constant σ_p^- but also with the Hammett σ_p parameter. Therefore, only the AOARE mechanism was considered for the computational Hammett modeling of the *meta*-series.

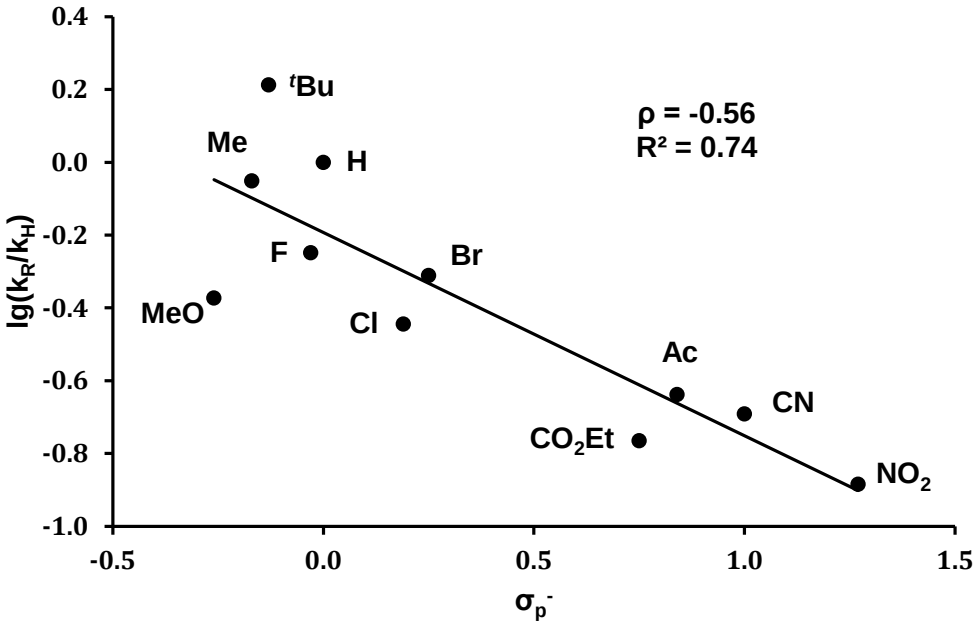

***Figure 7**. Hammett plot of DFT computation-derived $lg(k_R/k_H)$ vs. σ_p^- for the reactions of p-RC_6H_4I with $CuCF_3$ via DOARE*

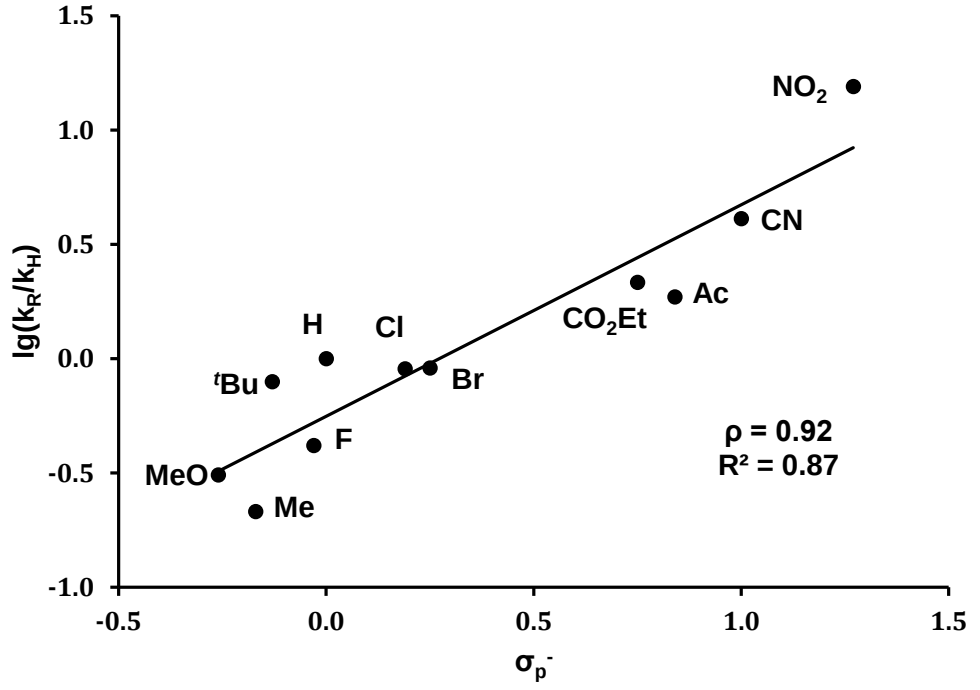

***Figure 8.** Hammett plot of DFT computation-derived $lg(k_R/k_H)$ vs. σ_p^- for the reactions of p-RC_6H_4I with $CuCF_3$ via AOARE*

***Meta*-substituted Aryl Iodides**. The experimentally established susceptibility of the trifluoromethylation of *m*-RC_6H_4I to R (σ_m) is particularly low, as illustrated by the most rapid reaction (R = NO_2) being only 5.5 times faster than the slowest (R = Me). The Arrhenius equation translates this rate constant ratio to ~1.0 kcal/mol for the entire range of $\Delta G^{\neq}$ in the reactions of the *meta*-series. Given this very small value, it was hard to expect DFT calculations to reproduce the experimentally obtained Hammett plot (Figure 2). To our delight, however, the computed barriers (kcal/mol in parentheses) for the AOARE pathway, Me (22.7) < CHO (22.2) ≈ CN (22.2) < Cl (22.1) < H (21.9) ≈ MeO (21.9) ≈ CO_2Et (21.9) < NO_2 (21.8), appeared to be in good agreement with the experimental order of reactivity. While the difference of 0.1 kcal/mol or less for the neighboring members of the series is computationally insignificant, the DFT method identified correctly the most and the least reactive substrates and modeled well the small 0.9 kcal/mol difference in the Gibbs free energies of activation for the two.

Additional calculations related to the AOARE mechanism. We have also computed barriers to OA of PhBr and PhCl to [(DMF)$CuCF_3$]. The values obtained, 25.1 kcal/mol (PhBr) and 28.8 kcal/mol (PhCl) accord with the experimentally observed order of reactivity PhI > PhBr > PhCl. These data confirm that the rate-limiting step of the trifluoromethylation of ArX with $CuCF_3$ is activation of the carbon-halogen bond.

The replacement of DMF in [(DMF)$CuCF_3$] with NMe_3 in the calculations with PhI as the substrate raises the activation barrier by 2.4 kcal/mol. Using the Arrhenius equation, this figure translates to [(Me_3N)$CuCF_3$] being ca. 60 times less reactive toward PhI than [(DMF)$CuCF_3$]. These data are consistent with the experimentally observed[23] inhibiting effect of triethylamine on the trifluoromethylation of aryl halides with fluoroform-derived $CuCF_3$.

It has been well-established4 that under certain conditions $CuCF_3$ can exist in equilibrium with $[Cu(CF_3)_2]^-$ that is less reactive toward haloarenes.[14b] Computing the barrier to the OA-RE pathway for PhI and $[Cu(CF_3)_2]^-$ as the trifluoromethylating agent produced a high value of 28.1 kcal/mol, in full accord with the experimental data.[14b] One can imagine that $[Cu(CF_3)_2]^-$ might react with CuI co-produced in the reaction to give rise to $[(CF_3)CuI]^-$ that might also react with the aromatic iodide. In fact, $[(CF_3)CuI]^-$ has been proposed[15] as the reactive species in the decarboxylative trifluoromethylation of iodoarenes. However, the computed AOARE barrier for Ph-I OA to $[(CF_3)CuI]^-$ (25.3 kcal/mol) is 3.4 kcal/mol higher than to $[(DMF)CuCF_3]$ (21.9 kcal/mol).

Discussion. The combined experimental and computational study shows that the trifluoromethylation of aryl halides with fluoroform-derived $CuCF_3$ is governed by a non-radical mechanism involving Ar-X activation with Cu(I) as the rate-determining step. The most intriguing mechanistic feature of the reaction of the *para*-substituted substrates is the abrupt change in the gradient on the Hammett plot of $\lg(k_R/k_H)$ *vs.* σ_p (Figure 1, top). The two excellent linear correlations, one for R = H, Me, *t*-Bu, MeO, Cl, and Br ($\rho = +0.69$) and the other for R = Cl, Br, CO_2Et, Ac, CN, and NO_2 ($\rho = +1.83$) within the same series might be an indication of two different mechanisms operating in the reaction. A similar Hammett pattern has been previously observed by Foà and Cassar[43] for the oxidative addition of chloroarenes ArCl to $[(Ph_3P)_3Ni]$ and interpreted in terms of two distinct reaction pathways. It was proposed[43] that for electron-donating and weak electron-withdrawing substituents ($\sigma \leq +0.23$), a three-center concerted oxidative addition ($\rho \approx 0$) was operational, whereas for the stronger electron-

withdrawing groups with $\sigma \geq +0.23$, S_NAr ($\rho = +8.8$) governed the transformation. Is this also the case with the reactions in the current study?[47]

The ρ values reported in the literature[5j,15,35-42] for various Cu-mediated aromatic substitution reactions span a narrow range of +0.1 to +1.1. The lower ρ value of +0.69 shown in Figure 1, top, is within this range. In contrast, the higher ρ of +1.83 is unprecedented for this type of transformations. On the other hand, $\rho = +1.83$ is too low a value for a transformation proceeding *via* a Meisenheimer intermediate.[48] For instance, $\rho = +7.55$ and +8.68 at 50 °C have been reported[49] for the methanolysis of *para*-substituted fluoro- and chlorobenzenes. Furthermore, vastly different ρ values of +6.6 and +0.61 have been obtained[36] for the phenoxylation reaction of a series of substituted bromoarenes with PhOK in PhOH-pyridine at 170 °C in the absence and in the presence of a Cu(I) catalyst, respectively.

In contrast with Hammett's σ_p, the resonance parameter σ_p^- correlates linearly with the entire set of $\lg(k_R/k_H)$ obtained for all of the *p*-RC_6H_4I used in the study (Figure 1, bottom). The ρ value of +0.91 derived from the plot falls in the aforementioned range of +0.1 to +1.1 that is characteristic of Cu-mediated coupling reactions of aryl halides. This linear correlation with the resonance parameter σ_p^- is excellent ($R^2 = 0.99$), suggesting that the transformation is governed by only one rather than two mechanisms and that there is substantial mesomeric interaction between an -M substituent on the ring and the reaction center in the transition state for the rate-determining step.[34]

---

[47] There is no mentioning of two correlations in the previously reported[5j,15] Hammett studies of the reaction of aryl iodides with $CuCF_3$ generated in situ from CF_3CO_2M (M = Na, K) with CuI. The limited number of substrates and the high temperatures (160-200 °C) employed in those studies may have made the effect insufficiently noticeable. It is also conceivable that under such vastly different conditions, the effect is poorly pronounced or absent altogether because of a different nature of the reactive $CuCF_3$ species involved.

[48] (a) Miller, J. *Aromatic Nucleophilic Substitution*; Elsevier: London, 1968. (b) Terrier, F. *Nucleophilic Aromatic Displacement: The Influence of the Nitro Group*; VCH: New York, 1991.

[49] (a) Miller, J. *Aust. J. Chem*. **1956**, *9*, 61. (b) Miller, J.; Wan, K.-Y. *J. Chem. Soc*. **1963**, 3492.

Given the above, the question remains whether one or two mechanisms are operational in the trifluoromethylation reaction of haloarenes with the $CuCF_3$ depending on the nature of the substrate. While without additional information this point would be moot, our computational results provide a fairly straightforward answer to this question. The computational data suggest that S_NAr as well as SBM, SET (both outer- and inner-sphere), and HAT mechanisms are prohibitively high in energy. For PhI, both OA-RE mechanisms, dissociative (DOARE, $\Delta G^{\neq}$ = 24.6 kcal/mol) and associative (AOARE, $\Delta G^{\neq}$ = 21.9 kcal/mol), display computed barriers that are in good agreement with the estimated experimental value $\Delta G^{\neq}$ = 24 kcal/mol at 298 K (see the Experimental Section). However, DOARE predicts that electron-enriched iodoarenes should undergo the trifluoromethylation faster than more electron-deficient ones, which is in contradiction with the experimentally observed trend. On the contrary, the AOARE pathway is delightfully consistent with the experimental data obtained in all of the Hammett and ortho-effect studies (see Chapter 3 for the details).

The AOARE mechanism (Figure 3) shows no signs of a Meisenheimer-type intermediate involved in the reaction. Highly informative intimate details of the AOARE process are revealed by the structure of the OA transition state **[A]TS_1**. Although care should be exercised when comparing intermediates and transition states, it might be useful, in this particular case, to juxtapose **[A]TS_1** with structurally

characterized Meisenheimer complexes.[50] The benzene ring in Meisenheimer intermediates conventionally adopts a sofa conformation and a roughly tetrahedral geometry is observed at the sp^3-hybridized *ipso*-carbon. In contrast, for all of the substrates studied in the current work, the benzene ring in **[A]TS$_1$** (Figure 5) shows virtually no deviation from planarity, with the C-C-C *ipso*-angle varying in a narrow range of 121-122^o. The nitro group in the *p*-$NO_2C_6H_4I$-derived **[A]TS$_1$** is coplanar with the benzene ring, showing a noticeable contraction of the C-N bond (1.45 Å) as compared to the experimentally determined (1.472(3) Å)[51] and computed (1.47 Å) values for the reactant. This is a clear indication that in the transition state, the NO_2 group is involved in an enhanced conjugative interaction with the π-system of the benzene ring. A crude yet informative estimate of the magnitude of π-conjugation in **[A]TS$_1$** can be obtained from some reported structural data. The C-N bond distance of 1.45 Å in **[A]TS$_1$** for *p*-$NO_2C_6H_4I$ is longer than in the Meisenheimer complexes[51] and

[50] (a) Ueda, H.; Sakabe, N.; Tanaka, J.; Furusaki, A. *Nature* **1967**, *215*, 956. (b) Ueda, H.; Sakabe, N.; Tanaka, J.; Furusaki, A. *Bull. Chem. Soc. Jpn.* **1968**, *41*, 2866. (c) Destro, R.; Gramaccioli, C. M.; Simonetta, M. *Acta Cryst*. **1968**, *B24*, 1369. (d) Messmer, G. G.; Palenik, G. J. *Acta Crystallogr*. **1971**, *B27*, 314. (e) Gitis, S. S.; Kaminskaya, E. G.; Ivanova, A. I.; Grigor'eva, N. V.; Margolis, N. V.; Kaminskii, A. Ya. *J. Struct. Chem*. **1976**, *17*, 578. (f) Kaminskaya, E. G.; Gitis, S. S.; Ivanova, A. I.; Margolis, N. V.; Kaminskii, A. Ya.; Grigor'eva N. V. *J. Struct. Chem*. **1977**, *18*, 309. (g) Destro, R.; Pilati, T.; Simonetta, M. *Acta Crystallogr*. **1979**, *B35*, 733. (h) Lowe-Ma, C. K. *Acta Cryst*. **1986**, *C27*, 38. (i) Niclas, H. J.; Kind, J.; Ramm, M. *J. Prakt. Chem.* **1991**, *333*, 909. (j) Terrier, F.; Lelievre, J.; Chatrousse, A. P.; Boubaker, T.; Bachet, B.; Cousson, A. *J. Chem., Soc. Perkin Trans. 2* **1992**, 361. (k) Borbulevych, O. Y.; Kovalevsky, A. Y.; Shishkin, O. V.; Atroschenko, Y. M.; Alifanova, E. N.; Gitis, S. S.; Kaminsky, A. Y.; Tarasova, E. Y. *Monatsh. Chem.* **1998**, *129*, 467. (l) Alifanova, E. N.; Kaminskii, A. Ya.; Bel'skii, V. K.; Kalnin'sh, K. K.; Tarasova, E. Yu.; Gitis, S. S. *Russ. J. Gen. Chem*. **1998**, *68*, 1621. (m) Borbulevych, O. Ya.; Antipin, M. Yu.; Olekhnovich, L. P. *Acta Crystallogr.* **1999**, *C55*, 2177. (n) Borbulevych, O. Ya.; Shishkin, O. V.; Budarina, Z. N.; Antipin, M. Yu.; Olekhnovich, L. P. *Acta Crystallogr*. **1999**, *C55*, 1915. (o) Borbulevych, O. Ya.; Shishkin, O. V.; Knyazev, V. N. *Acta Crystallogr*. **1999**, *C55*, 1704. (p) Borbulevych, O. Ya.; Shishkin, O. V.; Knyazev, V. N. *Acta Crystallogr*. **1999**, *C55*, 1918. (q) Borbulevych, O. Y.; Antipin, M. Y.; Shishkin, O. V.; Knyazev, V. N. *J. Mol. Struct*. **2000**, *520*, 141. (r) Borbulevych, O. Ya.; Antipin, M. Yu.; Shishkin, O. V.; Knyazev, V. N. *Russ. Chem. Bull*. **2000**, *49*, 452. (s) Borbulevych, O. Ya.; Shishkin, O. V.; Antipin, M. Yu. *J. Phys. Chem. A* **2002**, *106*, 8109. (t) Borbulevych, O. Ya. *J. Chem. Cryst*. **2005**, *35*, 777. (u) Galkina, I. V.; Takhautdinova, G. L.; Tudrii, E. V.; Yusupova, L. M.; Krivolapov, D. B.; Litvinov, I. A.; Cherkasov, R. A.; Galkin, V. I. *Russ. J. Org. Chem*. **2013**, *49*, 598.

[51] Thalladi, V. R.; Goud, B. S.; Hoy, V. J.; Allen, F. H.; Howard, J. A. K.; Desiraju, G. R. *Chem. Commun*. **1996**, 401.

Domenicano's classical quinoid-like structure of *p*-nitroaniline (1.434(2) Å),[52,53] yet comparable to that in *p*-nitroanisole (1.450(6) Å)[54] with substantial cross-conjugation of the MeO (+M) and NO_2 (-M) groups. The reaction center in **[A]TS$_1$** is therefore undoubtedly influenced by resonance effects of substituents R on the ring, *i.e.* exactly the case where σ_p^- rather than σ_p should be used for Hammett-type correlations.[34] As there cannot be resonance interactions between the *ipso*-carbon and R in the *meta*-position, the excellent linear correlation with σ_m for the *m*-RC_6H_4I series (Figure 2) observed experimentally and supported computationally provides additional evidence for the AOARE pathway with **[A]TS$_1$** as the key transition state.

All of the above points to the trifluoromethylation of aryl halides with $CuCF_3$ being governed by a mechanism involving OA of the Ar-X bond to the Cu(I) center as the rate-determining step, followed by Ar-CF_3 reductive elimination from the resultant Cu(III) intermediate. Since the original work of Cohen[55] in the mid-1970's, the Cu(I)/Cu(III) mechanism for Cu-mediated/catalyzed reactions of haloarenes has received substantial support, especially in recent years.[32b-f,56,57,58,59] For all 18 *para*- and *meta*-substituted iodobenzenes used in the current work, the found **[A]TS$_1$** structures are all very much alike, displaying no signs of variation in the reaction mechanism.

---

[52] (a) Colapietro, M.; Domenicano, A.; Marciante, C.; Portalone, G. *Z. Naturforsch. B* **1982**, *37*, 1309; (b) Colapietro, M.; Domenicano, A.; Marciante, C.; Portalone, G. *Acta Crystallogr. A* **1981**, *37*, C199.
[53] A considerable contribution of the quinoid form (C-NO_2 = 1.437(4) and 1.429(5) Å for two independent molecules) has also been observed for the less accurate structure of *N*,*N*-diethyl-*p*-nitroaniline: Maurin, J.; Krygowski, T. M. *J. Mol. Struct.* **1988**, *172*, 413.
[54] Talberg, H. J. *Acta Chem. Scand. A* **1978**, *32*, 373.
[55] (a) Cohen, T.; Wood, J.; Dietz, A. G., Jr. *Tetrahedron Lett*. **1974**, 3555. (b) Cohen, T.; Cristea, I. *J. Org. Chem*. **1975**, *40*, 3649. (c) Cohen, T.; Cristea, I. *J. Am. Chem. Soc*. **1976**, *98*, 748.
[56] Ouali, A.; Spindler, J.-F.; Jutand, A.; Taillefer, M. *Adv. Synth. Catal*. **2007**, *349*, 1906.
[57] Zhang, Y.; Ding, Y. *Organometallics* **2011**, *30*, 633.
[58] (a) Casitas, A.; King, A. E.; Parella, T.; Costas, M.; Stahl, S. S.; Ribas, X. *Chem. Sci*. **2010**, *1*, 326. (b) Casitas, A.; Canta, M.; Costas, M.; Solà, M.; Ribas, X. *J. Am. Chem. Soc*. **2011**, *133*, 19386. (c) Font, M.; Parella, T.; Costas, M.; Ribas, X. *Organometallics* **2012**, *31*, 7976.
[59] For a recent detailed review of Cu(III) complexes in Cu-mediated coupling reactions, see: Casitas, A.; Ribas, X. *Chem. Sci*. **2013**, *4*, 2301.

Conclusions

The objectives of this project have been successfully met. The trifluoromethylation reaction of a variety of aryl halides with fluoroform-derived $CuCF_3$ has been studied by experimental (radical clock, kinetic, Hammett correlation) and computational (DFT) means. The combined data set points to a bimolecular process involving Ar-X oxidative addition to DMF-stabilized $CuCF_3$ as the rate-determining step, followed by Ar-CF_3 reductive elimination from a Cu(III) intermediate. The computed barrier for the trifluoromethylation of iodobenzene ($\Delta G^{\neq}$ = 21.9 kcal/mol at 298 K) is in good agreement with the experimental value of $\Delta G^{\neq}$ = 24 kcal/mol at 298 K. A radical mechanism has been ruled out on the basis of both experimental and computational data. The latter have also shown prohibitively high barriers to SET (both outer- and inner-sphere) as well as classical S_NAr, SBM, and HAT processes previously proposed in the literature for some other Cu-mediated coupling reactions of aryl halides. Most remarkably, the DFT calculations have successfully reproduced the striking results of the experimental Hammett studies.

The Ar-CF_3 bond forming reaction of ArX with $CuCF_3$ is weakly sensitive to substituents in the *para*- and *meta*-positions of the aromatic ring. The Hammett study of a series of eight *meta*-substituted iodoarenes *m*-RC_6H_4I (R = H, Me, MeO, CO_2Et, CHO, Cl, CN, and NO_2) has produced an excellent linear correlation between $\lg(k_R/k_H)$ and σ_m (ρ = +0.97). Most unexpectedly, however, a sharp change in the gradient has been observed on the Hammett plot of $\lg(k_R/k_H)$ *vs.* σ_p for a series of 11 *para*-substituted iodoarenes. Two linear correlations with σ_p, one for R = H, Me, *t*-Bu, MeO, Cl, and Br (ρ = +0.69) and the other for R = F, Cl, Br, CO_2Et, Ac, CN, and NO_2 (ρ = +1.83) could be generated within the same series (Figure 1, top). While we are unaware of such Hammett dualism reported for Cu-catalyzed/promoted coupling reactions, a strikingly

similar effect has been observed by Foà and Cassar for the oxidative addition of substituted chlorobenzenes to $[(Ph_3P)_3Ni]$.[43] In that report, the two linear Hammett plots within the same series of substrates were convincingly interpreted in terms of two distinct reaction mechanisms, a three-center concerted oxidative addition ($\rho \approx 0$) for electron-donating and weak electron-withdrawing substituents, and S_NAr ($\rho = +8.8$) for stronger electron-acceptors with $\sigma > +0.23$. As tempting as it could be to rationalize the current results in a similar way, an in-depth analysis of the data suggests that regardless of the nature and position of a substituent on the ring, there is only one reaction pathway for the transformation. For solving the mysterious "one or two mechanisms" dilemma, it was critical to find a single linear correlation ($\rho = +0.91$; $R^2 = 0.99$) of the entire set of $\lg(k_R/k_H)$ with the resonance parameter σ_p^- in place of σ_p (Figure 1, bottom). Indicative of only one mechanism with considerable resonance interaction between the reaction center and the substituent, this interpretation has received strong support from (i) comparative analysis of the experimental ρ values; (ii) unambiguous signs of the enhanced -M effects of the substituent in the transition state for the Ar-I oxidative addition; (iii) close similarity of the transition states regardless of substituents in the *meta*- or *para*-positions; and (iv) remarkably faithful reproduction of the Hammett plot by the DFT data. The experimental and computational results obtained on this project shed light on the mechanism of the highly important trifluoromethylation reactions of aryl halides with $CuCF_3$. It is believed that the deeper mechanistic insights stemming from the current study will be useful for further advances in both basic and applied research.

Experimental Section

All chemicals, solvents, and deuterated solvents were purchased from Aldrich, Alfa Aesar, Apollo Scientific, TCI, Deutero, and Acros chemical companies. Anhydrous DMF (Alfa Aesar or from an MBraun SPS) and acetonitrile (distilled from P_2O_5 under argon) were stored over freshly calcined 4 Å molecular sieves in a glove-box. Fluoroform-derived $CuCF_3$ was prepared in DMF and stabilized with $Et_3N{\cdot}3HF$ (1/3 mol per mol $CuCF_3$), as reported previously.[19] A literature procedure[60] was used to synthesize 1-(allyloxy)-2-iodobenzene. NMR spectra were recorded on Bruker Avance 400 Ultrashield and Bruker Avance 500 Ultrashield NMR spectrometers at 25 ^{o}C. Quantitative ^{19}F NMR analyses were carried out with D1 = 5 s. An Agilent Technologies 7890A chromatograph equipped with a 5975C MSD unit was used for GC-MS analysis.

Reaction of $CuCF_3$ with 1-(allyloxy)-2-iodobenzene. In a glove box, the $CuCF_3$ reagent in DMF (0.38 M; 0.6 mL; 0.23 mmol) was added to a mixture of 4,4′-difluorobiphenyl (internal standard; 16 mg; 0.08 mmol) and 1-(allyloxy)-2-iodobenzene (296 mg; 1.14 mmol). The resultant solution was sealed in an NMR tube, brought out, and kept at room temperature for 1 day. Quantitative ^{19}F NMR analysis indicated the formation of 1-(allyloxy)-2-(trifluoromethyl)benzene in 60% yield (δ = -61.4 ppm, singlet) at 70% conversion of the $CuCF_3$. No cyclized product was detected in the reaction solution (^{19}F NMR, GC-MS).

Determination of Reaction Orders by the Method of Initial Rates. All reactions were run to 10-20% conversion. For specifics, see Table 2. **Liquid aryl**

[60] Dahlén, A.; Petersson, A.; Hilmersson, G. *Org. Biomol. Chem*. **2003**, *1*, 2423.

halides. 4,4′-difluorobiphenyl (internal standard; 16 mg; 0.08 mmol) was weighed into a 5-mm glass NMR tube in air. The NMR tube was brought to an argon-filled glove-box and charged with $CuCF_3$ in DMF (0.38 M) or with $CuCF_3$ in DMF (0.38 M) and DMF or MeCN or both for dilution. The total volume of the solution was 0.6 mL in all cases. The tube was sealed with a rubber septum and brought out. A liquid haloarene was added *via* microsyringe (Table 2) and kinetic measurements on the sample by ^{19}F NMR were started immediately. **Solid aryl halides**. A haloarene and the internal standard, 4,4′-difluorobiphenyl (16 mg; 0.08 mmol), were weighed into a 5-mm glass NMR tube in air. The tube was brought to an argon-filled glove-box and either sealed with a rubber septum and brought out, or first charged with DMF, or MeCN, or both (Table 2) and then sealed and brought out. ^{19}F NMR quantitative measurements on the sample were commenced immediately after a solution of $CuCF_3$ in DMF (0.38 M) was syringed in.

Determination of k_R/k_H for *para*- and *meta*-Substituted Aryl Iodides. In an argon-filled glove-box, the $CuCF_3$ reagent in DMF (0.38 M; 0.1 mL; 0.038 mmol) was added to a 5-mm glass NMR tube containing a solution of PhI (43 µL, 0.38 mmol) and an aryl iodide (0.38 mmol; see Table 3 for specifics) in DMF (0.5 mL). The tube was sealed with a rubber septum and its content was thoroughly shaken. Quantitative ^{19}F NMR analysis of the sample was performed ca. 30 min after mixing the reagents. The experiments were repeated with a mixture of MeCN (0.3 mL) and DMF (0.2 mL) in place of 0.5 mL of pure DMF. No significant difference in the relative reactivity was noticed. As *m*-$CF_3C_6H_4OMe$ and $PhCF_3$ exhibit very similar ^{19}F NMR chemical shifts, the relative reactivity of *m*-IC_6H_4OMe was determined in a similar experiment using *m*-IC_6H_4CHO (48 µL; 0.38 mmol) in place of PhI. The *m*-$CF_3C_6H_4OMe$ to *m*-$CF_3C_6H_4CHO$ ratio determined in this experiment was 1:2.

Determination of $\Delta G^{\neq}$ for the Reaction of CHF_3-derived $CuCF_3$ with PhI. The Gibbs free energy of activation for the reaction of the $CuCF_3$ with PhI at 298 K was determined from the data obtained in the kinetic experiments (Table 2). Based on the estimated $k = 4.0 \times 10^{-5}$ mol^{-1} s^{-1} and the initial concentrations of the reagents 0.19 M, $\Delta G^{\neq}$ = 24 kcal/mol (298 K) was calculated using the Eyring equation for second order reactions (Figure 9).[61]

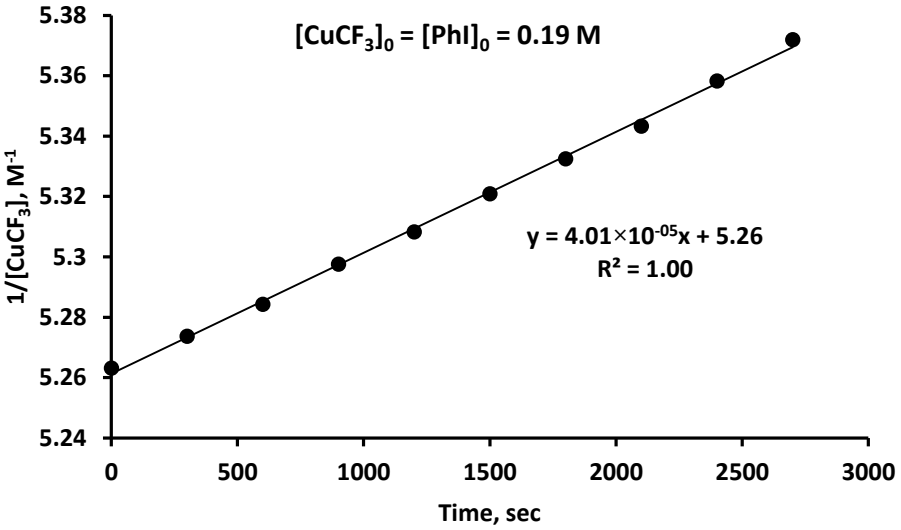

Figure 9. *Plot of 1/[$CuCF_3$] vs. time for the trifluoromethylation reaction of PhI with $CuCF_3$ at 298 K*

[61] (a) http://www.cup.uni-muenchen.de/oc/zipse/arrhenius-and-eyring-equations.html. (b) Miloserdov, F. M.; McMullin, C. L.; Martínez Belmonte, M.; Benet-Buchholz, J.; Bakhmutov, V. I.; Macgregor, S. A.; Grushin, V. V. *Organometallics* **2014**, *33*, 736.

Computational Details. All DFT calculations were carried out using the Gaussian09 suite of programs.[62] The geometries were fully optimized without any constraints with dispersion-corrected B3LYP-D functional[63] and ultrafine integration grid. Solvent effects were taken into account by means of the implicit polarizable continuum model (PCM) and DMF as a solvent ($\varepsilon = 37.219$).[64] Copper and all halogen atoms except fluorine were described with Stuttgart relativistic ECPs and associated basis sets[65] augmented with additional polarization functions on Cl, Br, and I centers (ζ_d = 0.640, 0.428, and 0.289 respectively).[66] Standard full electron Pople's basis set 6-31+G(d) was used for all other atoms.[67] This basis set combination is denoted as BS1. All computed structures were characterized as local stationary points *via* analytical frequency calculations at the standard state (298.15 K, 1 atm). For saddle points, intrinsic reaction coordinate (IRC) analysis [68] with the subsequent geometry optimization was performed to verify that they are linked by the corresponding minima on the potential energy surface.

Additional single-point calculations based on B3LYP-D/BS1 optimized geometries were performed with a double hybrid mPW2PLYPD functional[69] and a larger basis set combination denoted as BS2. This includes the same ECP and basis set

[62] Gaussian09, Revision D.01, Frisch, M. J.; Trucks, G. W.; Schlegel, H. B.; Scuseria, G. E.; Robb, M. A.; Cheeseman, J. R.; Scalmani, G.; Barone, V.; Mennucci, B.; Petersson, G. A.; Nakatsuji, H.; Caricato, M.; Li, X.; Hratchian, H. P.; Izmaylov, A. F.; Bloino, J.; Zheng, G.; Sonnenberg, J. L.; Hada, M.; Ehara, M.; Toyota, K.; Fukuda, R.; Hasegawa, J.; Ishida, M.; Nakajima, T.; Honda, Y.; Kitao, O.; Nakai, H.; Vreven, T.; Montgomery, J. A., Jr.; Peralta, J. E.; Ogliaro, F.; Bearpark, M.; Heyd, J. J.; Brothers, E.; Kudin, K. N.; Staroverov, V. N.; Kobayashi, R.; Normand, J.; Raghavachari, K.; Rendell, A.; Burant, J. C.; Iyengar, S. S.; Tomasi, J.; Cossi, M.; Rega, N.; Millam, N. J.; Klene, M.; Knox, J. E.; Cross, J. B.; Bakken, V.; Adamo, C.; Jaramillo, J.; Gomperts, R.; Stratmann, R. E.; Yazyev, O.; Austin, A. J.; Cammi, R.; Pomelli, C.; Ochterski, J. W.; Martin, R. L.; Morokuma, K.; Zakrzewski, V. G.; Voth, G. A.; Salvador, P.; Dannenberg, J. J.; Dapprich, S.; Daniels, A. D.; Farkas, Ö.; Foresman, J. B.; Ortiz, J. V.; Cioslowski, J.; Fox, D. J. Gaussian, Inc., Wallingford CT, 2009.
[63] (a) Grimme, S. *J. Comp. Chem.* **2004**, *25*, 1463. (b) Grimme, S. *J. Comp. Chem.* **2006**, *27*, 1787.
[64] Cancès, M. T.; Mennucci, B. B.; Tomasi, J. *J. Chem. Phys.* **1997**, *107*, 3032.
[65] Andrae, D.; Haussermann, U.; Dolg, M.; Stoll, H.; Preuss, H. *Theor. Chim. Acta* **1990**, *77*, 123.
[66] Höllwarth, A.; Böhme, M.; Dapprich, S.; Ehlers, A. W.; Gobbi, A.; Jonas, V.; Köhler, K. F.; Stegmann, R.; Veldkamp, A.; Frenking, G. *Chem. Phys. Lett.* **1993**, *208*, 237.
[67] Hariharan, P. C.; Pople, J. A. *Theor. Chim. Acta* **1973**, *28*, 213.
[68] Fukui, K. *Acc. Chem. Res.* **1981**, *14*, 363.
[69] Schwabe, T.; Grimme, S. *Phys. Chem. Chem. Phys.* **2006**, *8*, 4398.

for Cu, Cl, Br, and I with added f-orbital polarization on Cu (ζ_f = 3.525).[70] For the first and second row elements, the all-electron 6-311++G(2d,p) basis set was employed.[71] These mPW2PLYPD/BS2 energies modified by the Gibbs free energy correction from B3LYP-D/BS1 calculations were used to describe the reaction energies throughout the study.[72] Molecular modeling and geometry visualization were performed with the ChemCraft program.[73]

[70] Ehlers, A.W.; Böhme, M.; Dapprich, S.; Gobbi, A.; Höllwarth, A.; Jonas, V.; Köhler, K. F.; Stegmann, R.; Veldkamp, A.; Frenking, G. *Chem. Phys. Lett.* **1993**, *208*, 111.
[71] Frisch, M. J.; Pople, J.A.; Binkley, J. S. *J. Chem. Phys.* **1984**, *80*, 3265.
[72] The mPW2PLYPD(BS2)//B3LYP-D(BS1) combination provides a slightly better agreement with the experimental data for the *para*-series than B3LYP-D(BS2)//B3LYP-D(BS1) (AOARE $\Delta G^{\neq}$ for PhI = 22.9 kcal/mol; ρ = 1.07, R^2 = 0.86) and B2PLYPD(BS2)//B3LYP-D(BS1) (AOARE $\Delta G^{\neq}$ for PhI = 20.3 kcal/mol; ρ = 0.89, R^2 = 0.86).
[73] Zhurko, G.A. *ChemCraft 1.6*, http://www.chemcraftprog.com.

***Table 2**. Determination of reaction orders by the method of initial rates*

Substrate (purity, %)	ArX amount, μL/mg (mmol)	$CuCF_3$ solution, mL (mmol)	Extra solvent (mL)	$[CuCF_3]_0$, M	$[ArX]_0$, M	Initial rate, $M \cdot s^{-1}$	Reaction order, $ArX/CuCF_3$
PhI (> 99)	13 μL (0.114)	0.3 (0.114)	DMF (0.3)	0.19	0.19	$1.4 \cdot 10^{-6}$	1.0/1.0
	13 μL (0.114)	0.6 (0.228)	-	0.38	0.19	$2.8 \cdot 10^{-6}$	
	26 μL (0.228)	0.3 (0.114)	DMF (0.3)	0.19	0.38	$2.8 \cdot 10^{-6}$	
Para-substituted aryl iodides							
$IC_6H_4CO_2Et$ (> 97)	19 μL (0.114)	0.3 (0.114)	DMF (0.3)	0.19	0.19	$6.3 \cdot 10^{-6}$	1.0/1.0
	19 μL (0.114)	0.6 (0.228)	-	0.38	0.19	$1.3 \cdot 10^{-5}$	
	38 μL (0.228)	0.3 (0.114)	DMF (0.3)	0.19	0.38	$1.2 \cdot 10^{-5}$	
IC_6H_4Me (99)	25 mg (0.114)	0.3 (0.114)	DMF (0.3)	0.19	0.19	$1.4 \cdot 10^{-6}$	1.0/1.0
	25 mg (0.114)	0.6 (0.228)	-	0.38	0.19	$2.8 \cdot 10^{-6}$	
	50 mg (0.228)	0.3 (0.114)	DMF (0.3)	0.19	0.38	$2.9 \cdot 10^{-6}$	
IC_6H_4OMe (98)	27 mg (0.114)	0.3 (0.114)	DMF (0.3)	0.19	0.19	$1.3 \cdot 10^{-6}$	1.0/1.0
	27 mg (0.114)	0.6 (0.228)	-	0.38	0.19	$2.5 \cdot 10^{-6}$	
	54 mg (0.228)	0.3 (0.114)	DMF (0.3)	0.19	0.38	$2.6 \cdot 10^{-6}$	
IC_6H_4Cl (99)	27 mg (0.114)	0.3 (0.114)	DMF (0.3)	0.19	0.19	$2.3 \cdot 10^{-6}$	1.0/1.0
	27 mg (0.114)	0.6 (0.228)	-	0.38	0.19	$4.5 \cdot 10^{-6}$	
	54 mg (0.228)	0.3 (0.114)	DMF (0.3)	0.19	0.38	$4.6 \cdot 10^{-6}$	
IC_6H_4Ac (98)	28 mg (0.114)	0.3 (0.114)	DMF (0.3)	0.19	0.19	$6.5 \cdot 10^{-6}$	1.0/1.0
	28 mg (0.114)	0.6 (0.228)	-	0.38	0.19	$1.3 \cdot 10^{-5}$	
	56 mg (0.228)	0.3 (0.114)	DMF (0.3)	0.19	0.38	$1.3 \cdot 10^{-5}$	
IC_6H_4CN (99)	26 mg (0.114)	0.3 (0.114)	DMF (0.3)	0.19	0.19	$1.2 \cdot 10^{-5}$	0.5/0.5
	26 mg (0.114)	0.6 (0.228)	-	0.38	0.19	$1.7 \cdot 10^{-5}$	
	52 mg (0.228)	0.3 (0.114)	DMF (0.3)	0.19	0.38	$1.7 \cdot 10^{-5}$	
	26 mg (0.114)	0.3 (0.114)	MeCN (0.3)	0.19	0.19	$2.7 \cdot 10^{-6}$	1.0/1.0
	26 mg (0.114)	0.15 (0.057)	MeCN (0.3), DMF (0.15)	0.10	0.19	$1.3 \cdot 10^{-6}$	
	52 mg (0.228)	0.3 (0.114)	MeCN (0.3)	0.19	0.38	$5.4 \cdot 10^{-6}$	

$IC_6H_4NO_2$ (98)	28 mg (0.114)	0.3 (0.114)	0.3 (DMF)	0.19	0.19	$2.0 \cdot 10^{-5}$	0.5/0.5
	28 mg (0.114)	0.15 (0.057)	0.45 (DMF)	0.10	0.19	$1.4 \cdot 10^{-5}$	
	14 mg (0.057)	0.3 (0.114)	0.3 (DMF)	0.19	0.10	$1.4 \cdot 10^{-5}$	
	14 mg (0.057)	0.3 (0.114)	0.3 (ACN)	0.19	0.10	$4.4 \cdot 10^{-6}$	1.0/1.0
	28 mg (0.114)	0.3 (0.114)	0.3 (ACN)	0.19	0.19	$8.9 \cdot 10^{-6}$	
	28 mg (0.114)	0.15 (0.057)	0.3 (ACN), 0.15 (DMF)	0.10	0.19	$4.5 \cdot 10^{-6}$	
***Meta*-substituted aryl iodides**							
IC_6H_4Me (99)	15 µL (0.114)	0.3 (0.114)	DMF (0.3)	0.19	0.19	$1.6 \cdot 10^{-6}$	1.0/1.0
	15 µL (0.114)	0.6 (0.228)	-	0.38	0.19	$3.1 \cdot 10^{-6}$	
	30 µL (0.228)	0.3 (0.114)	DMF (0.3)	0.19	0.38	$3.2 \cdot 10^{-6}$	
IC_6H_4OMe (> 98)	15 µL (0.114)	0.3 (0.114)	DMF (0.3)	0.19	0.19	$1.9 \cdot 10^{-6}$	1.0/1.0
	15 µL (0.114)	0.6 (0.228)	-	0.38	0.19	$3.6 \cdot 10^{-6}$	
	30 µL (0.228)	0.3 (0.114)	DMF (0.3)	0.19	0.38	$3.7 \cdot 10^{-6}$	
IC_6H_4Cl (98)	14 µL (0.114)	0.3 (0.114)	DMF (0.3)	0.19	0.19	$4.3 \cdot 10^{-6}$	1.0/1.0
	14 µL (0.114)	0.6 (0.228)	-	0.38	0.19	$8.5 \cdot 10^{-6}$	
	28 µL (0.228)	0.3 (0.114)	DMF (0.3)	0.19	0.38	$8.4 \cdot 10^{-6}$	
IC_6H_4CHO (> 95)	27 mg (0.114)	0.3 (0.114)	DMF (0.3)	0.19	0.19	$3.3 \cdot 10^{-6}$	1.0/1.0
	27 mg (0.114)	0.6 (0.228)	-	0.38	0.19	$6.5 \cdot 10^{-6}$	
	54 mg (0.228)	0.3 (0.114)	DMF (0.3)	0.19	0.38	$6.5 \cdot 10^{-6}$	
$IC_6H_4CO_2Et$ (98)	19 µL (0.114)	0.3 (0.114)	DMF (0.3)	0.19	0.19	$3.9 \cdot 10^{-6}$	1.0/1.0
	19 µL (0.114)	0.6 (0.228)	-	0.38	0.19	$7.7 \cdot 10^{-6}$	
	38 µL (0.228)	0.3 (0.114)	DMF (0.3)	0.19	0.38	$7.8 \cdot 10^{-6}$	
IC_6H_4CN (99)	26 mg (0.114)	0.3 (0.114)	DMF (0.3)	0.19	0.19	$5.4 \cdot 10^{-6}$	1.0/1.0
	26 mg (0.114)	0.6 (0.228)	-	0.38	0.19	$1.0 \cdot 10^{-5}$	
	52 mg (0.228)	0.3 (0.114)	DMF (0.3)	0.19	0.38	$1.1 \cdot 10^{-5}$	
$IC_6H_4NO_2$ (> 99)	28 mg (0.114)	0.3 (0.114)	DMF (0.3)	0.19	0.19	$8.3 \cdot 10^{-6}$	1.0/1.0
	28 mg (0.114)	0.6 (0.228)	-	0.38	0.19	$1.6 \cdot 10^{-5}$	
	56 mg (0.228)	0.3 (0.114)	DMF (0.3)	0.19	0.38	$1.5 \cdot 10^{-5}$	

Table 3. *Determination of k_R/k_H for para- and meta-substituted aryl iodides RC_6H_4I*

R	ArI amount, μL/mg (0.38 mmol)	^{19}F NMR, δ, ppm	k_R/k_H in DMF	k_R/k_H in MeCN
		***para*-substituted aryl iodides**		
H	43 μL	-61.7	1.0	1.0
t-Bu	68 μL	-61.3	0.7	0.7
OMe	89 mg	-60.4	0.7	0.7
Me	83 mg	-61.3	0.8	0.7
F	44 μL	-61.0	0.9	-
Cl	91 mg	-61.6	1.5	1.5
Br	108 mg	-61.8	1.6	1.6
CO_2Et	63 μL	-62.1	4.3	4.8
Ac	94 mg	-62.3	4.9	4.5
CN	87 mg	-62.5	9.8	8.3
NO_2	95 mg	-62.1	17.8	17.7
		***meta*-substituted aryl iodides**		
Me	46 μL	-61.6	0.9	0.9
OMe	48 μL	-61.7	1.1	1.1
Cl	47 μL	-61.9	2.1	2.3
CHO	84 mg	-61.9	2.2	2.2
CO_2Et	64 μL	-61.9	2.1	2.1
CN	87 mg	-62.1	3.3	3.4
NO_2	90 mg	-61.9	4.9	4.5

Chapter 3.

Ortho-Effect in Trifluoromethylation of Haloarenes

Introduction

Over 110 years ago, Ullmann[1] reported that *o*-chlorobenzoic acid and its potassium salt underwent Cu-promoted amination with aniline and phenoxylation with phenol to give the corresponding coupling products (Scheme 1). Importantly, the *meta*- and *para*-isomers as well as chlorobenzene and its many derivatives remain unreactive under similar conditions. Since the original work of Ullmann,[1] the remarkable promoting effect of certain *ortho*-substituents such as COOH and NO_2 on Cu-catalyzed/mediated coupling reactions of aryl halides has been broadly recognized[2,3] and used in synthesis.[4]

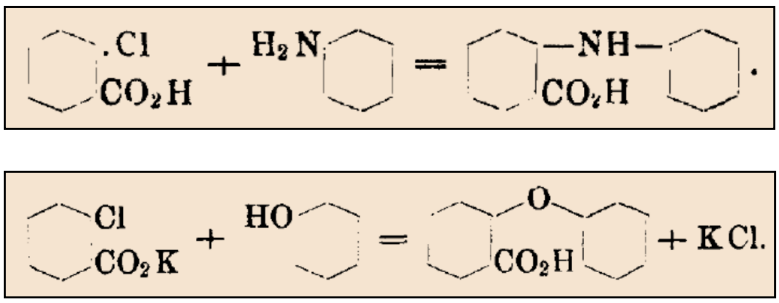

Scheme 1. *Chemical equations of the amination (top) and phenoxylation (bottom) of o-chlorobenzoic acid and its potassium salt, exactly as they appear in the original Ullmann's publications*1

[1] (a) Ullmann, F. *Ber. Dtsch. Chem. Ges.* **1903**, *36*, 2382. (b) Ullmann, F. *Ber. Dtsch. Chem. Ges.* **1904**, *37*, 853.
[2] See, for example: (a) Vorozhtsov, N. N., Jr.; Kobelev, V. A. *Zh. Obshch. Khim*. **1939**, *9*, 1043. (b) Goldberg, A. A. *J. Chem. Soc.* **1952**, 4368. (c) Mayer, W.; Fikentscher, R. *Chem. Ber*. **1958**, *91*, 1536. (d) Vainshtein, F. M.; Tomilenko, E. I.; Shilov, E. A. *Doklady Akad. Nauk SSSR* **1966**, *170*, 1077. (e) Vainshtein, F. M.; Tomilenko, E. I.; Shilov, E. A. *Kinetika i Kataliz* **1969**, *10*, 777. (f) Lisitsyn, V. N.; Shestakov, V. A.; Sycheva, E. D. *Zh. Vses. Khim. Ova im. D. I. Mendeleeva* **1969**, *14*, 117. (g) Castro, C. E.; Havlin, R.; Honwad, V. K.; Malte, A.; Moje, S. *J. Am. Chem. Soc*. **1969**, *91*, 6464.
[3] For reviews, see: (a) Bunnett, J. F.; Zahler, R. E. *Chem. Rev*. **1951**, *49*, 273. (b) Fanta, P. E. *Chem. Rev.* **1964**, *64*, 613. (c) Shein, S. M.; Litvak, V. V. *Zh. Vses. Khim. Ova im. D. I. Mendeleeva* **1976**, *21*, 274. (d) Lindley, J. *Tetrahedron* **1984**, *40*, 1433.
[4] (a) Evano, G.; Blanchard, N. *Copper-Mediated Cross-Coupling Reactions*; John Wiley & Sons: Hoboken, New Jersey, 2014. (b) Rao, H.; Fu, H. *Synlett* **2011**, 745. (c) Monnier, F.; Taillefer, M. *Angew. Chem., Int. Ed*. **2009**, *48*, 6954. (d) Evano, G.; Blanchard, N.; Toumi, M. *Chem. Rev*. **2008**, *108*, 3054. (e) Ma, D.; Cai, Q. *Acc. Chem. Res*. **2008**, *41*, 1450. (f) Beletskaya, I. P.; Cheprakov, A. V. *Coord. Chem. Rev*. **2004**, *248*, 2337. (g) Ley, S.; Thomas, A. W. *Angew. Chem., Int. Ed*. **2003**, *42*, 5400.

Clark and co-workers[5,6] have observed the ortho-effect of a nitro group on the trifluoromethylation of aryl chlorides with $CuCF_3$ generated from Cu and CF_2Br_2 in DMAC. A much weaker reaction rate enhancement was detected for carbonyl *ortho*-substituents CHO, Ac, and CO_2Me, whereas the cyano and amino groups in the *ortho*-position did not alter the reactivity of the C-Cl bond. Following the previously reported explanations,[3] Clark rationalized the lack of ortho-effect of the cyano group in terms of the unattainability of "*the correct transition state geometry*" as shown in Figure 1.5

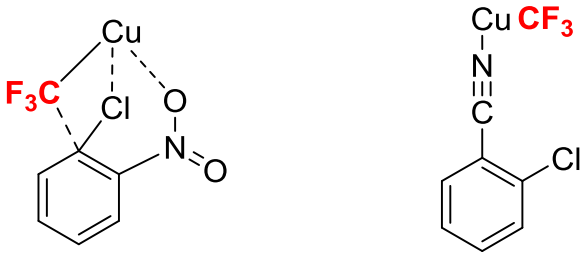

Figure 1*. The proposed*5 *"correct" (o-NO_2) and "incorrect" (o-CN) geometries of the transitions states in the Cu-promoted trifluoromethylation of ortho-substituted ArCl*

In Clark's studies, the ortho-effect could not be explored for aryl iodides and bromides as those produced biaryls rather than trifluoromethylated products under the conditions employed.5 The ortho-effect in the trifluoromethylation reactions of both aryl iodides and bromides with fluoroform-derived $CuCF_3$ was recently observed in our group for a considerable number of substrates.[7] Unexpectedly, it was also found that a methyl group in an *ortho*-position of bromobenzene exhibited the ortho-effect, *i.e. o*-bromotoluene underwent trifluoromethylation with the $CuCF_3$ reagent ca. 3.5 faster than

[5] (a) Clark, J. H.; McClinton, M. A.; Blade, R. J. *J. Chem. Soc., Chem. Commun*. **1988**, 638. (b) Clark, J. H.; Denness, J. E.; McClinton, M. A.; Wynd, A. J. *J. Fluorine Chem*. **1990**, *50*, 411.
[6] For a review of Clark's work, see: Roy, S.; Gregg, B. T.; Gribble, G. W.; Le, V.-D.; Roy, S. *Tetrahedron* **2011**, *67*, 2161.
[7] Lishchynskyi, A.; Novikov, M. A.; Martin, E.; Escudero-Adán, E. C.; Novák, P.; Grushin, V. V. *J. Org. Chem*. **2013**, *78*, 11126.

bromobenzene. It was appropriately remarked that *"it is hard to see how this mechanism can account for the activating effect of the methyl group that is neither an electron-acceptor nor a lone electron pair donor."*7

Objectives

As is clearly seen from the Introduction, the nature of the over-a-century-old, widely recognized phenomenon of the ortho-effect in Cu-mediated coupling reactions of aryl halides still remains uncomprehended. Considering the importance of the ortho-effect for basic chemical knowledge and for numerous synthetic methods employing Cu-mediated coupling reactions of aryl halides, the objective of this project was to understand the causes for the rate enhancement by *ortho*-substituents in this type of transformations.

The model reaction selected for the studies toward meeting the objective was the trifluoromethylation of aryl halides with fluoroform-derived $CuCF_3$. This choice was determined by the following reasons:

- these reactions are efficient and highly selective, while being of considerable importance;
- the ortho-effect has been observed in these transformations, albeit not studied; and
- as described in Chapter 2, the mechanism of these reactions has been studied in considerable detail and established in our previous work.

To meet the objective, we used, again, a combination of experimental and computational methods, which is currently viewed as the most productive approach to elucidation of reaction mechanisms and that has proved to be successful in our mechanistic investigations of the cupration reaction of fluoroform (Chapter 1) and aromatic trifluoromethylation (Chapter 2). The results presented and discussed below reveal, for the first time, the nature of the ortho-effect.

Results

Experimental Studies. First of all, it was critical to experimentally quantify the ortho-effect for a large enough variety of substituents and functional groups. The method of competition kinetics was chosen for the determination, by ^{19}F NMR, of relative rate constants of various *ortho*-substituted haloarenes with the fluoroform-derived $CuCF_3$ reagent previously developed in our laboratory[8] (Chapters 1 and 2). Preliminary experiments indicated that some *o*-RC_6H_4I (*e.g.* R = CO_2H, Ac, CO_2R, NO_2) were too reactive toward the $CuCF_3$ (relative to PhI) for accurate k_R/k_H determination. Therefore, relative rate constants were determined for the trifluoromethylation of a series of less reactive *ortho*-substituted bromoarenes.

In the competition experiments, 1 equiv of $CuCF_3$ was allowed to react with a mixture of various *o*-RC_6H_4Br (10 equiv of each) under pseudo-first-order conditions. Monitoring the reactions by ^{19}F NMR and integration of the peaks from the *o*-$RC_6H_4CF_3$ products yielded the following order of reactivity with relative rate constants shown in parentheses: H (1) < Me (3.5) < MeO (4) < CN (20) < CHO (250) < CO_2Me (850) < NO_2 (4300) < Ac (7300) < CO_2H (150000). This order of reactivity displays a number of peculiar features. In particular, there is no correlation of the relative rate constants with the electronic effects of R.[9] The carboxyl group displaying by far the strongest ortho-effect is a weaker electron acceptor than Ac, CN, and NO_2. The cyano group is a more powerful electron-acceptor than any of the carbonyl substituents that nonetheless make the substrate more reactive. While the nitro group is more electron-withdrawing than acetyl, *o*-bromoacetophenone reacts with $CuCF_3$ faster than *o*-bromonitrobenzene.

[8] Zanardi, A.; Novikov, M. A.; Martin E.; Benet-Buchholz, J.; Grushin, V. V. *J. Am. Chem. Soc*. **2011**, *133*, 20901.
[9] Hansch, C.; Leo, A.; Taft, R. W. *Chem. Rev*. **1991**, *91*, 165.

In contrast with Clark's observations,[5] the acetyl group is a noticeably stronger *ortho*-activator than the nitro group. Even a methyl group *ortho* to the C-Br bond promotes the reaction, as can be seen from 2-bromotoluene being 3.5 times more reactive toward the $CuCF_3$ than bromobenzene. As mentioned above, this is particularly unexpected as the CH_3 substituent is neither an electron-acceptor to activate the carbon-halogen bond on the ring, nor a lone electron pair donor to bind to the Cu atom, thereby bringing it in closer proximity to the reaction site (Figure 1). A similar weak yet recognizable effect of the methyl group has been recently observed for the 3-bromopyridine series.7 Furthermore, bromomesitylene bearing two methyl groups *ortho* to the C-Br bond appeared 1.3 and 4.5 times more reactive than 2-bromotoluene and bromobenzene, respectively.

As followed from the above, the ortho-effect could not be rationalized neither only in terms of relative electron deficiency of the aromatic substrates, nor solely in terms of chelation as previously proposed (Figure 1). Therefore, with the solid experimental data in hand, we proceeded to study the ortho-effect by computational means.

Computational Studies. In this work, we used the computational methods that have proven efficient in the elucidation of the mechanism of the closely related reactions of *para*- and *meta*-substituted haloarenes with fluoroform-derived $CuCF_3$ (Chapter 2).[10] According to the results described in Chapter 2, these reactions involve [(DMF)$CuCF_3$] as the reactive species and are governed by the Associative Oxidative Addition – Reductive Elimination (AOARE) mechanism. Therefore, first we computed the oxidative addition transition states for the reactions of the entire series of *ortho*-

[10] Konovalov, A. I.; Lishchynskyi, A.; Grushin, V. V. *J. Am. Chem. Soc.* **2014**, *136*, 13410.

substituted bromoarenes used in the experimental studies with [(DMF)$CuCF_3$] *via* the AOARE pathway. As can be seen from Table 1, the DFT values for the difference in the Gibbs free energies for the transition states involving PhBr $\Delta G^{\neq}_{H}$ and *o*-RC_6H_4Br $\Delta G^{\neq}_{R}$ are in good agreement with those calculated from the experimental kinetic data. The overall trend is reproduced remarkably well by the computation with only one minor exception (R = CN) that, considering the accuracy of the DFT method, may not be viewed as significant. The consonant experimental and computational data show that the introduction of a substituent into an *ortho*-position of PhBr enhances the reactivity of the bromoarene toward $CuCF_3$. The magnitude of the effect strongly depends on the nature of R and, as mentioned above, does not correlate with its electronic effects.

To gain insight into the origin of the ortho-effect, we calculated AOARE transition states for the oxidative addition of *o*-RC_6H_4I to [(DMF)$CuCF_3$], the highest energy point on the reaction coordinate, and compared them with those previously computed for the corresponding *para*-isomers. As the overall reaction barrier for a transformation is determined by the difference in energies of the reactants and the transition state, we also computed and compared ΔG^{o} for each *o*-RC_6H_4I/*p*-RC_6H_4I pair. Results of these studies are summarized in Table 2. Similar to the *ortho*-substituted aryl bromide series (Table 1), the ortho-effect is observed in all cases, *i.e.* $\Delta G^{\neq}_{H}$-$\Delta G^{\neq}_{o}$ is always a positive value, except for the smallest substituent, F, where it is essentially zero. The computed AOARE barriers are also always lower for the *ortho*-substituted substrates than for their *para*-isomers.

***Table 1**. Experimental and DFT data ortho-effect in reactions of o-RC_6H_4Br with $CuCF_3$*

R	k_R/k_H (experiment)	$\Delta G^{\neq}_H - \Delta G^{\neq}_R$ (kcal/mol)	
		(experiment)	(DFT)
H	1	0.0	0.0
Me	3.5	0.7	0.6
MeO	4	0.8	1.2
CN	20	1.7	1.1
CHO	250	3.2	3.2
CO_2Me	850	3.9	5.4
NO_2	4300	4.9	5.6
Ac	7300	5.2	6.1
CO_2H[a]	150000	6.9	7.0

[a] Computed for the ionized form.

As can be seen from Table 2 and in accord with the literature data,[11] all of the *ortho*-isomers studied lie invariably higher in energy than the *para*-isomers. The G^o_o-G^o_p values for the series vary in a significant range of 0.5-0.6 kcal/mol (F, MeO) to 5.1-5.4 kcal/mol (Ac, NO_2). This difference in the ground state energies between the *ortho*- and *para*-isomers is one of the two intrinsic contributors to the ortho-effect. The other parameter determining the barrier is the difference in the energies of the transitions states, $G^{\neq}_o$-$G^{\neq}_p$ reflecting the degree of stabilization or destabilization upon moving R from the *para*- to the *ortho*-position. As can be seen from Table 2, this *para*-*ortho* "isomerization" of the AOARE transitions state after full optimization can be stabilizing (R = Me, MeO, Ac, CO_2^-), destabilizing (R = Cl, CO_2Et, CN, NO_2, Br, CHO), or energy-neutral (R = F). Importantly, however, the difference G^o_o-G^o_p is always larger than $G^{\neq}_o$-$G^{\neq}_p$, making the corresponding $\Delta G^{\neq}_p$-$\Delta G^{\neq}_o$ value positive and thereby guaranteeing the ortho-effect.

[11] See, for example: (a) Cioslowski, J.; Liu, G.; Moncrieff, D. *J. Phys. Chem. A* **1997**, *101*, 957. (b) Taskinen, E. *Struct. Chem*. **2000**, *11*, 293. (c) Al-Muhtaseb, A. H.; Altarawneh, M. *Comp. Theor. Chem.* **2011**, *966*, 38. (d) Altarawneh, I.; Altarawneh, M.; Rawadieh, S. *Can. J. Chem.* **2013**, *91*, 999.

Table 2. *Computed energy parameters (kcal/mol) for ortho- and para-RC_6H_4I and their reactions with [(DMF)$CuCF_3$]*

R	G^o_o-G^o_p	$\Delta G^{\neq}_o$	$\Delta G^{\neq}_p$	$\Delta G^{\neq}_p$-$\Delta G^{\neq}_o$	$\Delta G^{\neq}_H$-$\Delta G^{\neq}_o$	$G^{\neq}_o$-$G^{\neq}_p$
H	0.0	21.9	21.9	0.0	0.0	0.0
F	0.5	21.9	22.4	0.5	0.0	0.0
CN	0.8	20.5	21.1	0.6	1.4	0.3
Br	2.1	20.9	21.9	1.0	1.0	1.0
Cl	1.9	20.6	21.9	1.3	1.3	0.5
MeO	0.6	20.8	22.6	1.8	1.1	-1.1
Me	1.1	20.9	22.8	1.9	1.0	-0.8
CHO	2.8	19.2	21.9	2.7	2.7	0.1
NO_2	5.4	17.4	20.3	2.9	4.5	2.5
CO_2Et	4.5	17.8	21.4	3.6	4.1	0.9
Ac	5.1	15.8	21.5	5.7	6.1	-0.6
CO_2H[a]	2.5	15.1	22.7	7.6	6.8	-5.1

[a] Computed for the ionized form.

Of the total of eleven *ortho*-substituted iodobenzenes *o*-RC_6H_4I studied (Table 2), six (R = F, CN, Br, Cl, MeO, Me) produce OA transition states **[A]TS$_1$** that are similar in geometry to their *para*-isomeric congeners. In five other cases, however (R = NO_2, CO_2Et, CHO, Ac, CO_2^-), the O atoms of the substituents interact with the Cu center, forming chelate-like structures, as shown in Figures 2 and 3. The Cu-O bond lengths in the transition states, 2.48 Å (CO_2Et), 2.44 Å (NO_2), 2.32 Å (Ac), and 2.14 Å (CO_2^-) vary inversely with the corresponding $\Delta G^{\neq}_H$-$\Delta G^{\neq}_o$ values (Table 2), *i.e.* with the ortho-effect. Even a much weaker Cu···O interaction (3.04 Å > the sum of the van der Waals radii of Cu and O) found in the *o*-formyl-bearing transition state lowers its energy by 0.8 kcal/mol in comparison with the other conformer (Figure 3).

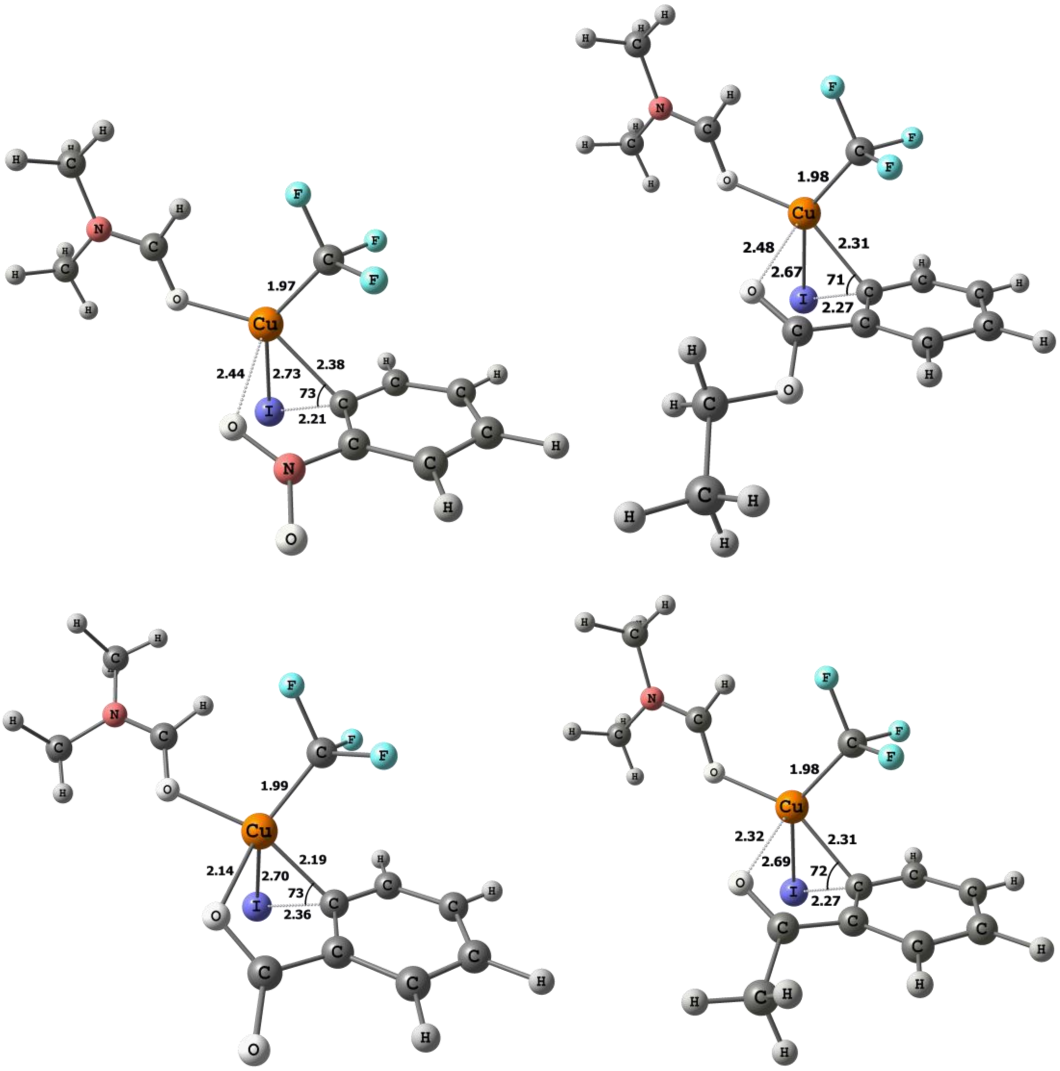

Figure 2. *Computed AOARE transition states of o-*RC_6H_4I *OA to* [(DMF)$CuCF_3$] *for R = NO_2, CO_2Et, Ac, and CO_2^- (clockwise from upper left)*

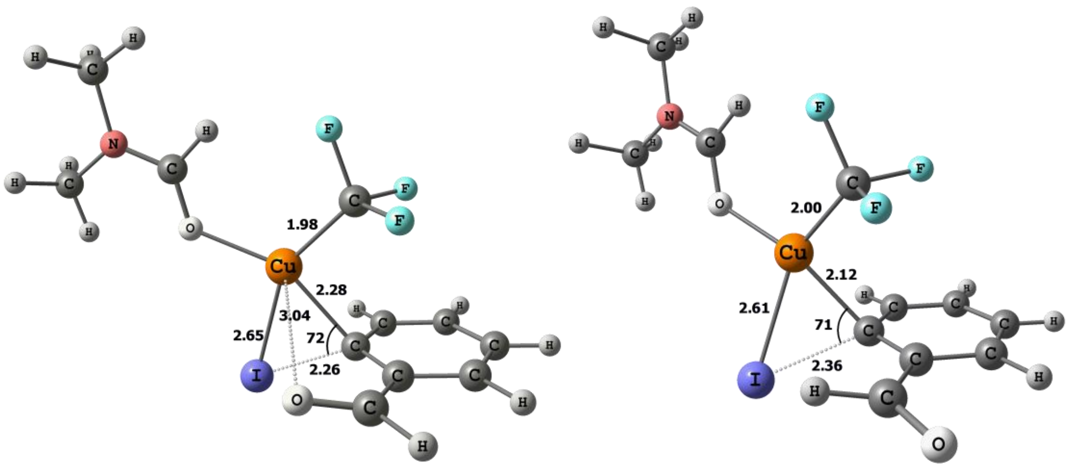

Figure 3. *Computed AOARE transition states of o-*IC_6H_4CHO *OA to* [(DMF)$CuCF_3$] *with (left) and without (right) chelation*

There are two ways to define the ortho-effect. One definition is the enhanced reactivity of an *ortho*-substituted haloarene in comparison with its unsubstituted phenyl halide analogue, *i.e.* $\Delta G^{\neq}_{H}$-$\Delta G^{\neq}_{o}$ (Tables 1 and 2). In this case, the contributions from the steric and electronic factors to the ortho-effect would be particularly difficult to compare as the electronic effects of the substituent R may appear vastly different from those of the hydrogen atom. Alternatively, reaction rates of the *ortho- vs*. *meta*- or *para*-isomers could be compared to quantify the ortho-effect as the difference in the activation barriers $\Delta G^{\neq}_{m}$-$\Delta G^{\neq}_{o}$ or $\Delta G^{\neq}_{p}$-$\Delta G^{\neq}_{o}$ (Table 2), respectively. In these cases, the same substituent possessing certain electronic properties is present on the benzene ring of both substrates, albeit in different positions. Use of $\Delta G^{\neq}_{m}$-$\Delta G^{\neq}_{o}$ is less preferred because resonance effects of the substituent are not transmitted from the *meta*-position. Moving the group from the *para*- to the *ortho*-position within the ring, however, might also result in a partial or full loss of the conjugation from the sterics forcing the substituent out of the plane. In addition, inductive effects are more efficiently transmitted from the more proximal *ortho*- rather than from the *meta*- or *para*-positions. Clearly, separating and quantifying steric and electronic contributions to the overall ortho-effect is nontrivial, especially by solely experimental means. However, the reactions under study are very weakly sensitive to electronic effects of the substituents in general, as follows from the low ρ values determined both experimentally and confirmed computationally. Furthermore, steric factors have a much greater impact on the rate, as follows from a number of experimental observations. For instance, the introduction of a weakly electron-donating methyl group into an *ortho*-position of bromobenzene results in a 3.5-fold increase in the reaction rate of the nucleophilic trifluoromethylation. In line with this, iodobenzene is only ca. 20 times less reactive toward $CuCF_3$ than *p*-nitroiodobenzene, whereas *o*-nitrobromobenzene reacts 4300

faster than bromobenzene. It is therefore justified to focus mainly on steric and coordination factors contributing to the ortho-effect.

In terms of $\Delta G^{\neq}_{p}$-$\Delta G^{\neq}_{o}$, the ortho-effect is a sum of two additives, the difference in the ground free energies of the *ortho*- and *para*-isomers of the substrate G^{o}_{o}-G^{o}_{p} and the energy difference between the corresponding transition states $G^{\neq}_{o}$-$G^{\neq}_{p}$. As established previously[11] and confirmed in the current work, a 1,2-disubstituted benzene always lies higher in energy than its 1,4-isomer. To gain insight into the factors contributing to the lower stability of *ortho*-isomers, we performed molecular mechanics (MM) calculations using the UFF method for the *ortho*- and *para*-isomeric substrates studied in the current work. As can be seen from Table 3, the trend observed in the DFT studies is well reproduced in the MM-derived E^{o}_{o}-E^{o}_{p} values. Depending on the size and the structure of the *ortho*-substituent, the strain imposed on the molecule varies in both the magnitude and contributions from such interactions as van der Waals (VdW) repulsions, stretching, bending, and twisting about the C-R single bond (torsional effects). For the monoatomic (F, Cl, Br) and smaller groups (CN, Me, MeO, CHO), the VdW repulsion is the main source of the strain (ca. 60-85%) with the stretching (ca. 12-21%) and bending (-4-23%) contributing less, albeit noticeably. These effects raise the energy of the *ortho*- *vs.* *para*-isomer (E^{o}_{o}-E^{o}_{p}) by 0.3 kcal/mol (F) to 2.5 kcal/mol (CHO), ultimately resulting in the weak to moderate ortho-effect. The bulkiest groups, Ac, CO_2Et, and NO_2 that are coplanar with the benzene ring when in the *para*-position, are twisted in the *ortho*-isomers (Table 4; see also Figures 2 and 3) to alleviate the repulsion from the neighboring halogen atom. Accordingly, the torsion effect becomes the largest contributor (ca. 50-80%) to the overall strain, with the biggest E^{o}_{o}-E^{o}_{p} difference observed (4.4-4.9 kcal/mol). Note that the smaller formyl group is coplanar with the aromatic ring for both orientations toward the iodine atom.

***Table 3**. Computed (DFT and MM) energy parameters for ortho- and para-RC_6H_4I*

R	G^o_o-G^o_p, kcal/mol (DFT)	E^o_o-E^o_p, kcal/mol (MM)	contributions to strain, %			
			VdW	stretching	bending	torsion
Me	1.1	1.4	64	18	18	
CN	0.8	1.2	70	13	17	
MeO	0.6	0.7	83	21	-4	
F	0.5	0.3	82	12	6	
Cl	1.9	1.4	70	12	18	
Br	2.1	1.7	67	12	21	
CHO	2.8	2.5	60	17	23	
Ac	5.1	4.9	10	5	12	73
CO_2Et	4.5	4.7	21	8	22	49
NO_2	5.4	4.4	5	4	11	80
CO_2H[a]	2.5	4.8	29	10	24	37

[a] Computed for the ionized form.

The strain accumulated in the ground state of the aryl halide results in the weakening of the carbon-halogen bond, as follows from Figure 4 showing correlation between $\Delta G°_p$-$\Delta G°_o$ and the difference in C-I bond dissociation free energy ΔBDE_{p-o} computed for the same series of the *ortho*- and *para*-isomers of RC_6H_4I. The factors causing the molecular strain in the ground state (Table 3) are likely preserved, with a certain degree of fidelity, in the OA transition state since the latter does not exhibit significant additional distortions within the aromatic moiety. This hypothesis receives support from the plot in Figure 5 showing that $\Delta G^{\neq}_p$-$\Delta G^{\neq}_o$ (ortho-effect) vary directly with C-I ΔBDE_{p-o}.

***Table 4**. Dihedral angles between the planes of the benzene ring and R in RC_6H_4I*

R	DFT	MM
ortho-CO_2Et	40	29
para-CO_2Et	0	0
ortho-NO_2	42	41
para-NO_2	0	0
ortho-Ac	31	36
para-Ac	0	0
ortho-CO_2^-	82	25
para-CO_2^-	2	0

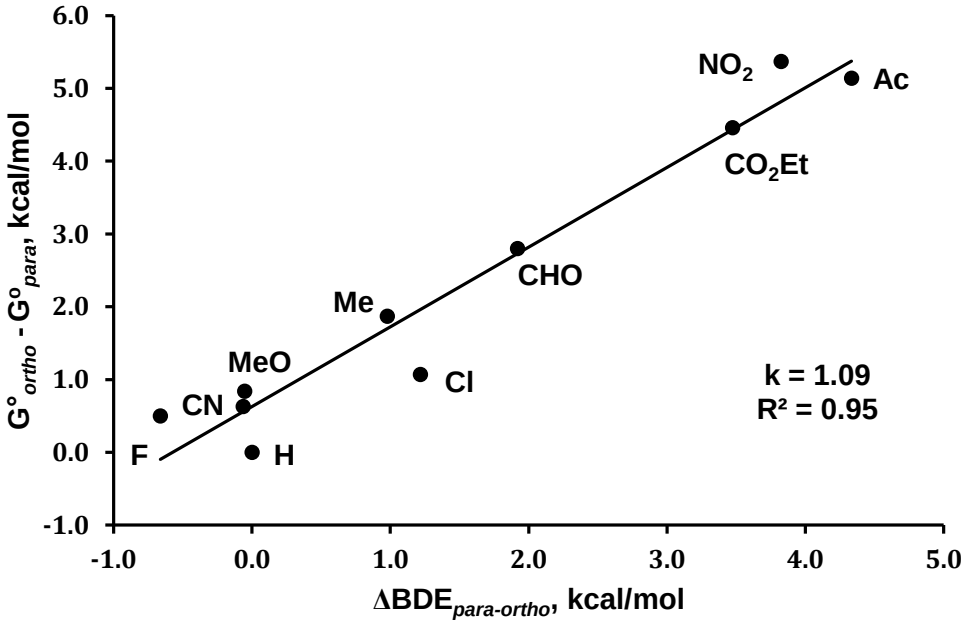

***Figure 4**. Plot of $G°_o$-$G°_p$ with C-I $\Delta BDE_{para\text{-}ortho}$ computed for ortho- and para-isomers of RC_6H_4I*

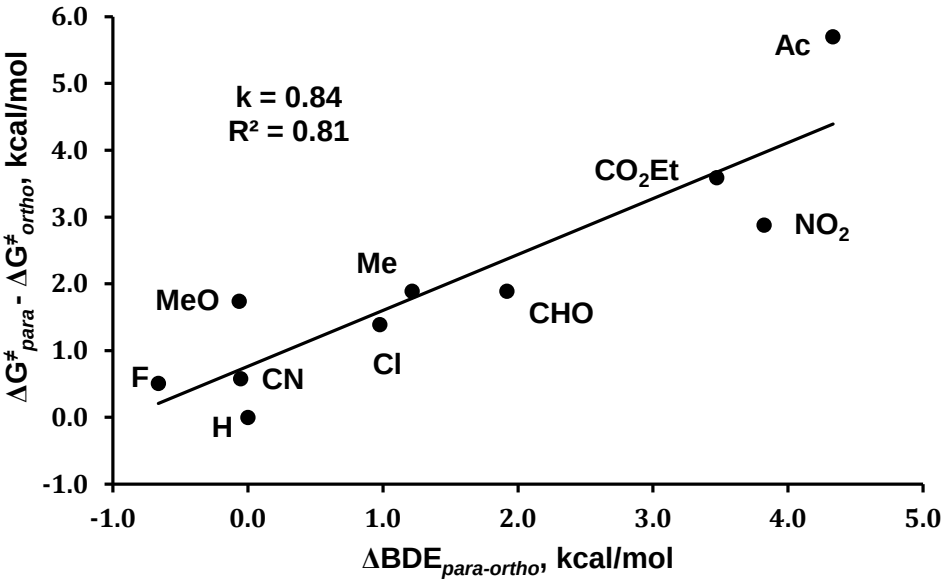

Figure 5. *Plot of $\Delta G^{\neq}_{p}$-$\Delta G^{\neq}_{o}$ (ortho-effect) vs. C-I $\Delta BDE_{para\text{-}ortho}$ computed for the activation barriers of OA of o-RC_6H_4I and p-RC_6H_4I to [(DMF)$CuCF_3$]*

The above shows that apart from the evidently minor contributions of electronic factors, the ortho-effect is largely determined by two parameters. One is the effective steric bulk of the *ortho*-substituent that raises the innate free energy of the substrate by introducing molecular strain and, as a result, weakening the bond to be broken in the rate-determining step of the reaction. The other factor deals with the ability of the functional group in the *ortho*-position to interact with the metal center in the transition state, thereby stabilizing it and lowering the overall barrier to the transformation. The strength of this coordination for R = CHO, CO_2Et, NO_2, Ac, and CO_2^- ultimately translating into the ortho-effect varies in a broad range and may be quantified by the Cu-O distance in the transition state. As discussed above, the magnitude of the ortho-effect in terms of the $\Delta G^{\neq}_{H}$-$\Delta G^{\neq}_{o}$ or $\Delta G^{\neq}_{p}$-$\Delta G^{\neq}_{o}$ values (Table 2) correlates with the strength of the Cu···O interaction, *i.e.* inversely with the distance between the two atoms: CHO (3.04 Å) < CO_2Et (2.48 Å) < NO_2 (2.44 Å) < Ac (2.32 Å) < CO_2^- (2.14 Å).

In the discussion above, the carboxyl group prompting by far the strongest ortho-effect is somewhat set aside from, and not as frequently included in the quantitative comparisons as, CHO, CO_2Et, NO_2, and Ac. This was done intentionally because, unlike in the case of all other *ortho*-substituents in the current study, efficient coordination of the carboxyl to the Cu center involves O-H ionization. Consequently, the *ortho*-halobenzoic acid substrates were modeled in the current work as the corresponding carboxylate anions. Proton transfer from the carboxyl is not expected to be energetically demanding under the experimentally used conditions, particularly, in the presence of Et_3N (see above). However, for the sake of consistency of the data, the acid-base equilibria involved in the trifluoromethylation of *o*-halobenzoic acids were excluded from consideration in the computational studies. This simplification neither influences any of the conclusions nor alters the new level of understanding of the ortho-effect reached in the current study.

Conclusions

We have performed the first detailed study of the ortho-effect, a long-known and broadly used in synthesis, yet poorly understood phenomenon of the enhanced reactivity of *ortho*-substituted aryl halides in Cu-mediated/catalyzed coupling reactions. In the current work, the ortho-effect has been quantified, for the first time, for the reaction of $CuCF_3$ with a series of *o*-RC_6H_4Br using the competition kinetics method to produce the following relative rate constants k_R/k_H: H (1) < Me (3.5) < MeO (4) < CN (20) < CHO (250) < CO_2Me (850) < NO_2 (4300) < Ac (7300) < CO_2H (150000). This order of reactivity determined experimentally and reproduced by DFT calculations cannot be rationalized solely in terms of chelation as has been proposed previously. The positive ρ values obtained by us[10] and reported by others for a variety of Cu-mediated reactions of haloarenes (see Chapter 2) suggest that electron donation from the methyl and methoxy groups in the *ortho*-position should slow down the reaction. In fact, the opposite is observed experimentally, pointing to the minor role of electronic factors in the ortho-effect. Similarly, *p*-nitroiodobenzene is only ca. 20 times more reactive than iodobenzene, whereas *o*-nitrobromobenzene reacts 4300 faster than bromobenzene.

The ortho-effect is largely determined by two parameters. One is the chelation proposed in some previous reports, albeit without any evidence. Coordination of an *ortho*-substituent to the Cu center stabilizes the transition state for the Ar-X oxidative addition, thus lowering the overall barrier for the transformation. The efficacy of the Cu···O interaction measured as the computed distance between the two atoms for CHO (3.04 Å) > CO_2Et (2.48 Å) > NO_2 (2.44 Å) > Ac (2.32 Å) > CO_2^- (2.14 Å) determines the magnitude of the ortho-effect in terms of the $\Delta G^{\neq}_H$-$\Delta G^{\neq}_o$ or $\Delta G^{\neq}_p$-$\Delta G^{\neq}_o$ values. There is, however, another key contributor to the ortho-effect. The steric bulk of the

ortho-substituent raises the ground state free energy of the haloarene (G^o_o-G^o_p or G^o_o-G^o_H) by introducing molecular strain and consequently weakening the Ar-X bond to be broken in the rate-determining step. Apart from the rather insignificant electronic effects, this ground state energy factor is apparently the only one bringing about the ortho-effect in the case of non-chelating groups, such as Me, MeO, CN, Cl, Br, etc. The deeper insights stemming from the current study are expected to find use in the important area of Cu-mediated cross-coupling reactions.

Experimental Section

All chemicals, solvents, and deuterated solvents were purchased from Aldrich, Alfa Aesar, Apollo Scientific, TCI, Deutero, and Acros chemical companies. Anhydrous DMF (Alfa Aesar or from an MBraun SPS) was stored over freshly activated 4 Å molecular sieves in a glove-box. Fluoroform-derived $CuCF_3$ was prepared in DMF and stabilized with $Et_3N{\cdot}3HF$ (1/3 mol per mol $CuCF_3$), as reported previously.8 NMR spectra were recorded on Bruker Avance 400 Ultrashield and Bruker Avance 500 Ultrashield NMR spectrometers at 25 ^oC. Quantitative ^{19}F NMR analyses were carried out with D1 = 5 s.

Determination of k_R/k_H for *ortho*-substituted aryl bromides. PhBr *vs*. *o*-BrC_6H_4R (R = Me, MeO, CN). In a glove-box, to a solution of *o*-BrC_6H_4Me (purity 99%; 0.23 mL; 1.85 mmol) and PhBr (purity 99%; 0.2 mL; 1.85 mmol) in DMF (0.2 mL) placed in a 5-mm glass NMR tube, was added the $CuCF_3$ reagent in DMF (0.37 M; 0.5 mL; 0.19 mmol). The tube was sealed with a rubber septum and its content was thoroughly shaken. Quantitative ^{19}F NMR analysis of the sample was performed 24 h after mixing the reagents. The reaction mixture was diluted with ether (2 mL), washed with water (5 mL), and analyzed by ^{19}F NMR. The $PhCF_3$ (-61.7 ppm) to *o*-$MeC_6H_4CF_3$ (-60.6 ppm) ratio was 1:3.5. This procedure was repeated first with *o*-BrC_6H_4OMe (purity 98%; 0.24 mL; 1.85 mmol) in place of *o*-BrC_6H_4Me and then with *o*-BrC_6H_4CN (purity 99%; 340 mg; 1.85 mmol) in place of *o*-BrC_6H_4Me. The $PhCF_3$ to *o*-$MeOC_6H_4CF_3$ (-61.3 ppm) and to *o*-$NCC_6H_4CF_3$ (-60.9 ppm) ratios were 1:4 and 1:20, respectively.

***o*-BrC_6H_4CHO *vs.* *o*-BrC_6H_4R (R = CN, CO_2Me).** In a glove-box, to a solution of *o*-BrC_6H_4CHO (purity 98%; 0.09 mL; 0.74 mmol) and *o*-BrC_6H_4CN (136 mg; 0.74 mmol) in DMF (0.5 mL) placed in a 5-mm NMR tube, was added the $CuCF_3$ reagent (0.37 M; 0.2 mL; 0.07 mmol). The tube was sealed with a rubber septum and its content was thoroughly shaken. Quantitative ^{19}F NMR analysis of the sample was performed 1 h after mixing the reagents. The reaction mixture was diluted with ether (2 mL), washed with saturated aqueous solution of Na_2CO_3 (5 mL), and analyzed by ^{19}F NMR. The *o*-$CF_3C_6H_4CN$ (-60.9 ppm) to *o*-$CF_3C_6H_4CHO$ (-54.7 ppm) ratio was 1:12. This procedure was repeated with *o*-$BrC_6H_4CO_2Me$ (purity 98%; 0.11 mL; 0.74 mmol) in place of *o*-BrC_6H_4CN. The *o*-$CF_3C_6H_4CHO$ to *o*-$CF_3C_6H_4CO_2Me$ (-58.7 ppm) ratio was 1:3.5.

***o*-$BrC_6H_4CO_2Me$ *vs.* *o*-$BrC_6H_4NO_2$**. In a glove-box, to a solution of *o*-$BrC_6H_4NO_2$ (purity 98%; 76 mg; 0.37 mmol) and *o*-$BrC_6H_4CO_2Me$ (53 µL; 0.37 mmol) in DMF (0.5 mL) placed in a 5-mm NMR tube, was added the $CuCF_3$ reagent (0.37 M; 0.1 mL; 0.04 mmol). The tube was sealed with a rubber septum and its content was thoroughly shaken. Quantitative ^{19}F NMR analysis of the sample performed 30 min after mixing the reagents indicated the *o*-$CF_3C_6H_4CO_2Me$ (-58.7 ppm) to *o*-$CF_3C_6H_4NO_2$ (-59.1 ppm) ratio of 1:5.

***o*-$BrC_6H_4NO_2$ *vs.* *o*-BrC_6H_4Ac**. In a glove-box, to a solution of *o*-BrC_6H_4Ac (purity 99%; 0.1 mL; 0.74 mmol) and *o*-$BrC_6H_4NO_2$ (153 mg; 0.74 mmol) in DMF (0.5 mL) placed in a 5-mm NMR tube, was added the $CuCF_3$ reagent (0.37 M; 0.2 mL; 0.074 mmol). The tube was sealed with a rubber septum and its content was thoroughly shaken. Quantitative ^{19}F NMR analysis of the sample performed 30 min after mixing

the reagents indicated the *o*-$CF_3C_6H_4NO_2$ (-59.1 ppm) to *o*-$CF_3C_6H_4Ac$ (-57.3 ppm) ratio of 1:1.7.

***o*-BrC_6H_4Ac *vs.* *o*-BrC_6H_4R (R = CO_2H and NO_2).** In a glove-box, to a solution of *o*-$BrC_6H_4CO_2H$ (purity 97%; 77 mg; 0.37 mmol), *o*-BrC_6H_4Ac (0.05 mL; 0.37 mmol), and *o*-$BrC_6H_4NO_2$ (76 mg; 0.37 mmol) in DMF (0.5 mL) placed in a 5-mm NMR tube, was added the $CuCF_3$ reagent (0.37 M; 0.1 mL; 0.04 mmol). The tube was sealed with a rubber septum and its content was thoroughly shaken. ^{19}F NMR analysis of the sample performed 10 min after mixing the reagents indicated the *o*-$CF_3C_6H_4NO_2$ (-59.1 ppm) to *o*-$CF_3C_6H_4Ac$ (-57.3 ppm) to *o*-$CF_3C_6H_4CO_2H$ (-58.3 ppm) ratio of 1:2.5:52. Note that the *o*-$CF_3C_6H_4NO_2$ (-59.1 ppm) to *o*-$CF_3C_6H_4Ac$ (-57.3 ppm) ratio of 1:2.5 differs slightly from that (1:1.7) determined in the experiment described above. This minor difference deals with the integration error being considerably larger than the standard value of ca. 10% for weak signals. Therefore, the more accurate 1:1.7 ratio obtained in the previous experiment (*o*-$BrC_6H_4NO_2$ vs. *o*-BrC_6H_4Ac) was used for the order of reactivity.

Computational Details. All DFT calculations were carried out using the Gaussian09 suite of programs.[12] The geometries were fully optimized without any

[12] Gaussian09, Revision D.01, Frisch, M. J.; Trucks, G. W.; Schlegel, H. B.; Scuseria, G. E.; Robb, M. A.; Cheeseman, J. R.; Scalmani, G.; Barone, V.; Mennucci, B.; Petersson, G. A.; Nakatsuji, H.; Caricato, M.; Li, X.; Hratchian, H. P.; Izmaylov, A. F.; Bloino, J.; Zheng, G.; Sonnenberg, J. L.; Hada, M.; Ehara, M.; Toyota, K.; Fukuda, R.; Hasegawa, J.; Ishida, M.; Nakajima, T.; Honda, Y.; Kitao, O.; Nakai, H.; Vreven, T.; Montgomery, J. A., Jr.; Peralta, J. E.; Ogliaro, F.; Bearpark, M.; Heyd, J. J.; Brothers, E.; Kudin, K. N.; Staroverov, V. N.; Kobayashi, R.; Normand, J.; Raghavachari, K.; Rendell, A.; Burant, J. C.; Iyengar, S. S.; Tomasi, J.; Cossi, M.; Rega, N.; Millam, N. J.; Klene, M.; Knox, J. E.; Cross, J. B.; Bakken, V.; Adamo, C.; Jaramillo, J.; Gomperts, R.; Stratmann, R. E.; Yazyev, O.; Austin, A. J.; Cammi, R.; Pomelli, C.; Ochterski, J. W.; Martin, R. L.; Morokuma, K.; Zakrzewski, V. G.; Voth, G. A.; Salvador, P.; Dannenberg, J. J.; Dapprich, S.; Daniels, A. D.; Farkas, Ö.; Foresman, J. B.; Ortiz, J. V.; Cioslowski, J.; Fox, D. J. Gaussian, Inc., Wallingford CT, 2009.

constraints with dispersion-corrected B3LYP-D functional[13] and ultrafine integration grid. Solvent effects were taken into account by means of the implicit polarizable continuum model (PCM) and DMF as a solvent (ε = 37.219).[14] Copper and all halogen atoms except fluorine were described with Stuttgart relativistic ECPs and associated basis sets[15] augmented with additional polarization functions on Cl, Br, and I centers (ζ_d = 0.640, 0.428, and 0.289 respectively).[16] Standard full electron Pople's basis set 6-31+G(d) was used for all other atoms.[17] This basis set combination is denoted as BS1. All computed structures were characterized as local stationary points *via* analytical frequency calculations at the standard state (298.15 K, 1 atm). For saddle points, intrinsic reaction coordinate (IRC) analysis [18] with the subsequent geometry optimization was performed to verify that they are linked by the corresponding minima on the potential energy surface.

Additional single-point calculations based on B3LYP-D/BS1 optimized geometries were performed with a double hybrid mPW2PLYPD functional[19] and a larger basis set combination denoted as BS2. This includes the same ECP and basis set for Cu, Cl, Br, and I with added f-orbital polarization on Cu (ζ_f = 3.525).[20] For the first and second row elements, the all-electron 6-311++G(2d,p) basis set was employed.[21] These mPW2PLYPD/BS2 energies modified by the Gibbs free energy correction from B3LYP-D/BS1 calculations were used to describe the reaction energies throughout the study. The UFF method as implemented in Gaussian09 was used to perform the MM

[13] (a) Grimme, S. *J. Comp. Chem.* **2004**, *25*, 1463. (b) Grimme, S. *J. Comp. Chem.* **2006**, *27*, 1787.
[14] Cancès, M. T.; Mennucci, B. B.; Tomasi, J. *J. Chem. Phys.* **1997**, *107*, 3032.
[15] Andrae, D.; Haussermann, U.; Dolg, M.; Stoll, H.; Preuss, H. *Theor. Chim. Acta* **1990**, *77*, 123.
[16] Höllwarth, A.; Böhme, M.; Dapprich, S.; Ehlers, A. W.; Gobbi, A.; Jonas, V.; Köhler, K. F.; Stegmann, R.; Veldkamp, A.; Frenking, G. *Chem. Phys. Lett.* **1993**, *208*, 237.
[17] Hariharan, P. C.; Pople, J. A. *Theor. Chim. Acta* **1973**, *28*, 213.
[18] Fukui, K. *Acc. Chem. Res.* **1981**, *14*, 363.
[19] Schwabe, T.; Grimme, S. *Phys. Chem. Chem. Phys.* **2006**, *8*, 4398.
[20] Ehlers, A.W.; Böhme, M.; Dapprich, S.; Gobbi, A.; Höllwarth, A.; Jonas, V.; Köhler, K. F.; Stegmann, R.; Veldkamp, A.; Frenking, G. *Chem. Phys. Lett.* **1993**, *208*, 111.
[21] Frisch, M. J.; Pople, J.A.; Binkley, J. S. *J. Chem. Phys.* **1984**, *80*, 3265.

calculations.[22] Molecular modeling and geometry visualization were performed with the ChemCraft program.[23]

[22] Rappé, A. K.; Casewit, C. J.; Colwell, K. S.; Goddard, W. A.; Skiff, W. M. *J. Am. Chem. Soc.* **1992**, *114*, 10024.
[23] Zhurko, G.A. *ChemCraft 1.6*, http://www.chemcraftprog.com.

Chapter 4.

Electronic Properties of the CF_3 Group

Introduction

The trifluoromethyl group (CF_3) that is ubiquitous in this Thesis, plays a prominent role in the design of bioactive compounds and specialty materials.[1,2] Owing to the highest electronegativity of fluorine atom, the CF_3 group is uniformly viewed as an electron acceptor. For instance, Uneyama in his monograph writes *"All of trifluoromethyl and polyfluoroalkyl groups are net electron-withdrawing substituents irrespective of the fluoro substituents being connected with the reaction center through either σ-bond or π-bond, and no electron-donating effect arises from them."*1[c] This opinion is echoed by the Kirk-Othmer Encyclopedia of Chemical Technology: *"Benzotrifluoride undergoes electrophilic substitution reactions, e.g. halogenation, nitration, typical of an aromatic containing a strong electron-withdrawing group. The trifluoromethyl group (sometimes referred to as a pseudohalogen) is meta-directing."*[3] Indeed, the *meta*-directing effect of the CF_3 group in S_EAr reactions has been widely recognized and confirmed in countless studies since the original Swarts report of the nitration of $PhCF_3$ as early as 1898.[4] Furthermore, the deactivation of the aromatic ring bearing a CF_3 substituent toward electrophilic attack is in harmony with the opposite trend observed for S_NAr reactions.[5] Numerous other facts provide strong support for electron-withdrawing properties of the CF_3 group, including the increased acidity of trifluoromethylated acids and alcohols and the diminished basicity of CF_3-substituted amines.1 A striking example is 1,2,3,4,5-pentakis(trifluoromethyl)cyclopentadiene that is more acidic than nitric acid HNO_3.[6]

[1] (a) Kirsch, P. *Modern Fluoroorganic Chemistry*; Wiley-VCH: Weinheim, 2004. (b) Chambers, R. D. *Fluorine in Organic Chemistry*; Wiley-Blackwell: FL, USA, 2004. (c) Uneyama, K. *Organofluorine Chemistry*; Blackwell: Oxford, U. K., 2006.
[2] Tomashenko, O. A.; Grushin, V. V. *Chem. Rev.* **2011**, *111*, 4475.
[3] Boudakian, M. M. In: *Kirk-Othmer Encyclopedia of Chemical Technology*; Wiley: Weinheim, 2000.
[4] Swarts, F. *Bull. Sci. Acad. Roy. Belg*. **1898**, *35*, 375.
[5] DePasquale, R. J.; Tamborski, C. *J. Org. Chem.* **1967**, *32*, 3163.
[6] Laganis, E. D.; Lemal, D. M. *J. Am. Chem. Soc*. **1980**, *102*, 6633.

The quantification of electronic effects of the CF_3 group leaves even less room for doubt about its electron-withdrawing nature. The group electronegativity values of 2.28 and 3.49 on the Pauling scale assigned to CH_3 and CF_3, respectively, show that the triple fluorination of the methyl produces a substituent that is more electronegative than the Cl atom (χ_{Cl} = 3.16).[7] The Hammett, Taft and modified Swain-Lupton constants conventionally used to quantify electronic properties of a group also clearly suggest that CF_3 is an electron acceptor.[8] In accordance with these data, the reported[9] redox potentials indicate that $PhCF_3$ is more electron-deficient than $PhCH_3$ and C_6H_6.

Table 1. *Hammett, Taft, and Modified Swain-Lupton Substituent Constants*8

R	σ_m	σ_p	σ_I	σ_R	*F*	*R*
F	0.34	0.06	0.57	-0.33	0.45	-0.39
CH_3	-0.07	-0.17	-0.01	-0.13	0.01	-0.18
CH_2F	0.12	0.11	0.20	0	0.15	-0.04
CHF_2	0.29	0.32	0.36	0.06	0.29	0.03
CF_3	0.43	0.54	0.46	0.09	0.38	0.16

Given the above, one might wonder as to why electronic properties of the trifluoromethyl group should be analyzed and studied any further. However, things are not always as simple as they seem: a closer look at the CF_3 substituent might take by surprise even a highly educated and experienced chemist.

In 1967, at the dawn of the age of computational chemistry, Pople and Gordon[10] reported unexpected results of their CNDO/2 calculations performed on a series of simple hydrocarbons and their fluorinated derivatives. In their article, they wrote that

[7] Huheey, J. E. *J. Phys. Chem.* **1965**, *69*, 3284.
[8] Hansch, C.; Leo, A.; Taft, R. W. *Chem. Rev*. **1991**, *91*, 165.
[9] Loutfy, R. O.; Loutfy, R. O. *Can. J. Chem*. **1976**, *54*, 1454.
[10] Pople, J. A.; Gordon, M. *J. Am. Chem. Soc*. **1967**, *89*, 4253.

their results *"challenge the common interpretation of fluorine as an inductive-type substituent leading to positive character in a saturated hydrocarbon which diminishes steadily with the distance down the chain*

$$F^{\delta-}\leftarrow C^{\delta+}\leftarrow C^{\delta\delta+}\leftarrow C^{\delta\delta\delta+}\ \ldots$$

The calculations rather suggest that the induced charges alternate in a decaying manner, so that the β position is normally negative

$$F^{\delta-}\leftarrow C^{\delta+}\leftarrow C^{\delta\delta-}\leftarrow C^{\delta\delta+}\ \ldots"$$

In CF_3-containing molecules, this polarization $[F_3C]\leftarrow C^{\delta\delta-}\leftarrow C^{\delta\delta+}$ should reinforce the primary dipole moment from the C-F bond, which is consistent with the experimental data. Soon after it was published, the Pople-Gordon model received both significant support[11] as well as some disapproval[12] from other studies. In 1975, a particularly important report was published by Holmes and Thomas,[13] who probed the electron density distribution in mono- and di-trifluoromethylated benzenes by X-ray photoelectron spectroscopy (ESCA). While the aromatic ring in the trifluoromethylated derivatives was found to be more electron-deficient than in benzene, the point-charge analysis suggested a large negative charge on the *ipso*-carbon (Scheme 1), in accord with the Pople-Gordon "β-effect". All other carbon atoms appeared positively charged, in spite of being more distal from the CF_3 substituent.

[11] (a) Brownlee, R. T. C.; Taft, R. W. *J. Am. Chem. Soc*. **1970**, *92*, 7007. (b) Williamson, K. L.; Mosser, S.; Stedman, D. E. *J. Am. Chem. Soc.* **1971**, *93*, 7208. (c) Morishima, I.; Yoshikawa, K.; Okada, K.; Yonezawa, T.; Goto, K. *J. Am. Chem. Soc.* **1973**, *95*, 165. (d) Davis, D. W.; Banna, M. S.; Shirley, D. A. *J. Chem. Phys.* **1974**, *60*, 237. (e) Ernstbrunner, E. E.; Hudec, J. *J. Am. Chem. Soc.* **1974**, *96*, 7106. (f) Eliel, E. L.; Rao, V. S.; Vierhapper, F. W.; Juaristi, G. Z. *Tetrahedron Lett.* **1975**, 4339. (g) Eliel, E. L.; Vierhapper, F. W. *J. Org. Chem.* **1976**, *41*, 199. (h) Lambert, J. B.; Netzel, D. A.; Sun, H.; Lilianstrom, K. K. *J. Am. Chem. Soc.* **1976**, *98*, 3778.

[12] (a) Sardella, D. J. *J. Am. Chem. Soc*. **1972**, *94*, 5206. (b) Stolow, R. D.; Samal, P. W.; Giants, T. W. *J. Am. Chem. Soc*. **1981**, *103*, 197.

[13] Holmes, S. A.; Thomas, T. D. *J. Am. Chem. Soc.* **1975**, *97*, 2337.

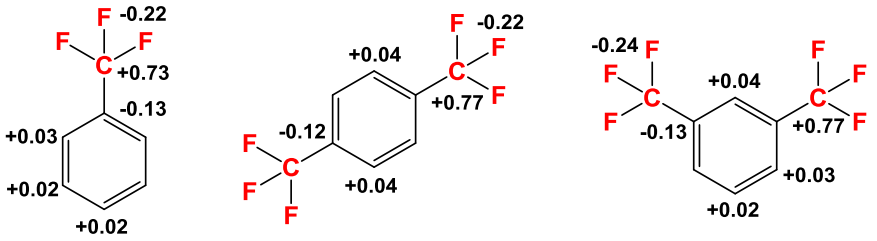

Scheme 1. *ESCA-derived charge distribution in trifluoromethylated benzenes*[13]

The Holmes-Thomas ESCA results suggested that atomic-charge-wise, the CF_3 group on the ring is formally *an electron donor* to an adjacent atom. This was emphasized in the article title "Electron Distribution in Trifluoromethylbenzenes. Electron Donation by the Trifluoromethyl Group".[13]

Similar charge distribution patterns have been observed in other studies of a variety of trifluoromethylated aliphatic and aromatic compounds,[11,14] although no firm support for charge alternation beyond the β-carbon has been found.[12b,15] Importantly, more advanced calculations[15] show the β-effect for NPA but not for AIM charges.

The origin of the β-effect of the CF_3 group has been a subject of various interpretations. In the original Pople-Gordon work,[10] it was attributed to weak π-electron donation from the fluorine lone electron pairs to the β-atom. A similar hyperconjugative mechanism was also proposed by Holmes and Thomas to account for their results.[13]

For trifluoromethylated aromatics, back-donation from the fluorine lone pairs to the π-system was proposed as early as 1965.[16] Although such interactions might exist in certain systems, their contribution is rather minor.[13] Another rationale is based on the

[14] (a) Nelson, G. L.; Levy, G. C.; Cargioli, J. D. *J. Am. Chem. Soc*. **1972**, *94*, 3089. (b) Jullien, J.; Martin-Christol, A. L.; Stahl-Lariviere, H. *Tetrahedron* **1976**, *32*, 1117. (c) Levy, J. B. *Struct. Chem.* **1999**, *10*, 121. (d) Palmer, M. H. *J. Mol. Struct*. **2000**, *500*, 225. (e) Nolan, E. M.; Linck, R. G. *J. Phys. Chem. A* **2002**, *106*, 533.
[15] Nolan, E. M.; Linck, R. G. *J. Am. Chem. Soc*. **2000**, *122*, 11497.
[16] Sheppard, W. A. *J. Am. Chem. Soc*. **1965**, *87*, 2410.

so-called $+I_\pi$ effect that causes polarization of the π-system toward the positive dipole of the CF_3.[17] Levy[14c] has explained the β-effect in terms of electrostatic interactions between the CF_3 group and an adjacent atom lowering the total energies of the molecules.

As can be seen from the above, electronic effects of the CF_3 group are not without contradiction, and the notion of this substituent being invariably an electron acceptor does not appear to be always entirely correct. A new wave of questions and doubts about electronic properties of the trifluoromethyl group has recently been spurred by an abrupt increase in studies of CF_3-ligated transition metal complexes over the last decade. Prompted by the need for new trifluoromethylation methods, these investigations have produced interesting and intriguing results. A separate section entitled "Electronic Effects of CF_3: Is It an Electron Acceptor or Donor?" can be found in a comprehensive review on aromatic trifluoromethylation reactions with transition metal.2 This section analyzes the complexity of electronic effects of the CF_3 group not only as a substituent in organic compounds but also as a ligand in metal complexes.

In 2006, an article appeared reporting X-ray structures of $[CF_3Pd(dppe)Cl]$ and its non-fluorinated analogue $[CH_3Pd(dppe)Cl]$.[18] In spite of the vastly different electronic parameters of CF_3 and CH_3 (see above), these two molecules were found to be virtually superimposable (Figure 1). The Pd-P bonds trans to the carbon, 2.345(1) Å (CF_3) and 2.339(1) Å (CH_3) were nearly identical in length, suggesting similar structural trans influence of the CF_3 and CH_3 ligands. As the trans influence of a ligand is often associated with its electron donation to the metal, the structures of $[CX_3Pd(dppe)Cl]$ (X = F or H) suggested that the Pd atom receives similar amounts of electron density from the σ-bonded carbon regardless of whether it is fluorinated or not.

[17] Bromilow, J.; Brownlee, R. T. C.; Topsom, R. D.; Taft, R. W. *J. Am. Chem. Soc.* **1976**, *98*, 2020.
[18] Grushin, V. V.; Marshall, W. J. *J. Am. Chem. Soc.* **2006**, *128*, 4632.

This conclusion is rather striking, given (i) the fact that CH_3 is one of the strongest trans-influencing ligands in organometallic chemistry and (ii) the vastly different electronic parameters of the methyl and trifluoromethyl groups (Table 1). Although the significant trans influence[19] and trans-effect[20] of CF_3 have been reported before, it is the $[CF_3Pd(dppe)Cl]/[CH_3Pd(dppe)Cl]$ pair of structures that provided a particularly clear illustration of the issue and prompted further studies of the CF_3 group as a ligand.

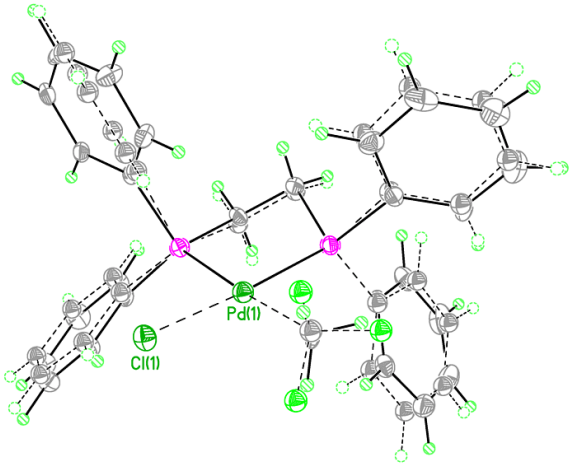

Figure 1. *Superimposed molecules of $[CF_3Pd(dppe)Cl]$ and $[CH_3Pd(dppe)Cl]$ displaying nearly identical coordination geometry around Pd*[18]

Similar observations have been made for other square-planar complexes. The Rh-P bond trans to CF_3 in $[CF_3Rh(PPh_3)_3]$ (2.313(1) Å)[21] is one of the very longest Rh-P bonds ever reported for a large number of crystallographically characterized

[19] (a) Appleton, T. G.; Chisholm, M. H.; Clark, H. C.; Manzer, L. E. *Inorg. Chem.* **1972**, *11*, 1786. (b) Appleton, T. G.; Clark, H. C.; Manzer, L. E. *Coord. Chem. Rev.* **1973**, *10*, 335. (c) Bennett, M. A.; Chee, H.-K.; Robertson, G. B. *Inorg. Chem.* **1979**, *18*, 1061. (d) Bennett, M. A.; Chee, H.-K.; Jeffery, J. C.; Robertson, G. B. *Inorg. Chem.* **1979**, *18*, 1071. (e) Hughes, R. P.; Meyer, M. A.; Tawa, M. D.; Ward, A. J.; Williamson, A.; Rheingold, A. L.; Zakharov, L. N. *Inorg. Chem.* **2004**, *43*, 747.
[20] (a) Blake, D. M.; Shields, S.; Wyman, L. *Inorg. Chem*. **1974**, *13*, 1595. (b) Michelin, R. A.; Belluco, U.; Ros, R. *Inorg. Chim. Acta* **1977**, *24*, L33. (c) Greene, T. R.; Roper, W. R. *J. Organomet. Chem.* **1986**, *299*, 245. (d) Hughes, R. P.; Overby, J. S.; Williamson, A.; Lam, K.-C.; Concolino, T. E.; Rheingold, A. L. *Organometallics* **2000**, *19*, 5190.
[21] (a) Goodman, J.; Grushin, V. V.; Larichev, R. B.; Macgregor, S. A.; Marshall, W. J.; Roe, D. C. *J. Am. Chem. Soc*. **2009**, *131*, 4236. (b) Goodman, J.; Grushin, V. V.; Larichev, R. B.; Macgregor, S. A.; Marshall, W. J.; Roe, D. C. *J. Am. Chem. Soc*. **2010**, *132*, 12013.

Wilkinson's catalyst-type complexes [$XRh(PPh_3)_3$]. Not only is this bond longer than the one trans to CH_3 (2.282(4) Å), but is as long as those trans to H and CN, the strongest trans-influencing ligands in coordination chemistry. A few years after the [$CF_3Pd(dppe)Cl$]/[$CH_3Pd(dppe)Cl$] report,[18] Vicic *et al.*[22] published X-ray structures of three complexes [XNi(BOXAM)] (X = Ph, CH_3, CF_3) displaying crystallographically indistinguishable Ni-N bond distances for the N trans to the carbon (Scheme 2). Surprisingly, no comment was made on these similar trans influences of the CF_3, CH_3, and Ph ligands in the original publication.[22] While the concept of trans influence is obviously inapplicable to tetrahedral complexes, the close similarity of coordination geometry parameters in [$CF_3Cu(PPh_3)_3$][23] and [$CH_3Cu(PPh_3)_3$][24] might be indicative of comparable electron donation to Cu from the CF_3 and CH_3 ligands.

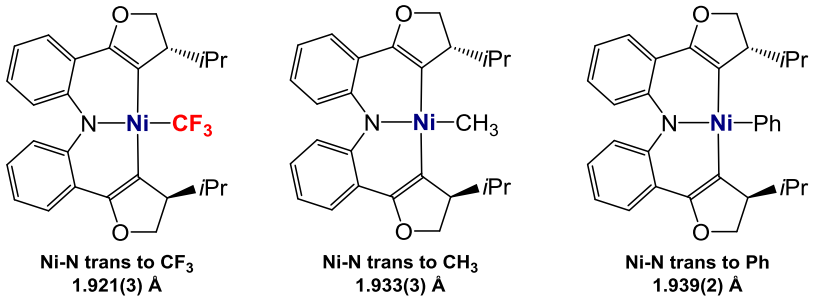

Scheme 2. *Structurally characterized Ni(BOXAM) complexes*[22]

A combined experimental and computational study of a series of Wilkinson's catalyst-type complexes suggested that the extreme fluxionality of [$CF_3Rh(PPh_3)_3$] in solution (k = 12.1 s^{-1} at -100 ^oC) was likely due to strong *electron-donation* from the CF_3 ligand to the metal.[21] This counterintuitive conclusion was corroborated by the

[22] Kieltsch, I.; Dubinina, G. G.; Hamacher, C.; Kaiser, A.; Torres-Nieto, J.; Hutchison, J. M.; Klein, A.; Budnikova, Yu.; Vicic, D. A. *Organometallics* **2010**, *29*, 1451.
[23] Tomashenko, O. A.; Escudero-Adán, E. C.; Martínez Belmonte, M.; Grushin, V. V. *Angew. Chem., Int. Ed.* **2011**, *50*, 7655.
[24] Coan, P. S.; Folting, K.; Huffman, J. C.; Caulton, K. G. *Organometallics* **1989**, *8*, 2724.

computed natural atomic charges for the simplified $[CX_3Rh(PH_3)_3]$ models, of which two sets, for X = H and F, are shown in Scheme 3. While the NPA charges on the atoms comprising the CH_3 and CF_3 ligands are as expected, the CF_3-ligated Rh bears a *larger negative* charge than its CH_3 counterpart, in spite of the opposite, high positive charge on the adjacent fluorinated carbon.

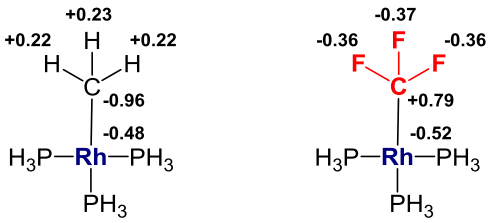

Scheme 3. *NPA charge distribution in $[CH_3Rh(PH_3)_3]$ and $[CF_3Rh(PH_3)_3]$*[21]

The charge distribution pattern shown in Scheme 3 brings about the question as to whether this is just an artefact, or characteristic of other $[CF_3ML_n]$/$[CH_3ML_n]$ pairs. A more recent targeted computational study[25] along with other reports[26,27,28,29] on a variety of metal complexes indicate that in some cases the charge on the metal atom is similar for the CF_3 and CH_3 species. In most instances, however, the metal in $[CF_3ML_n]$ compounds bears a larger negative (or a smaller positive) charge relative to that in $[CH_3ML_n]$. These data challenge the previously reported[30] explanation of the widely recognized[31] enhanced stability of trifluoromethyl metal complexes, based on the proposed induction of a positive charge on the metal by the CF_3 ligand: a compression

[25] Algarra, A. G.; Crushin, V. V.; Macgregor, S. A. *Organometallics* **2012**, *31*, 1467.
[26] Huang, H.; Rheingold, A. L.; Hughes, R. P. *Organometallics* **2010**, *29*, 3672.
[27] Taw, F. L.; Clark, A. E.; Mueller, A. H.; Janicke, M. T.; Cantat, T.; Scott, B. L.; Hay, P. J.; Hughes, R. P.; Kiplinger, J. L. *Organometallics* **2012**, *31*, 1484.
[28] Yamaguchi, Y.; Ichioka, H.; Klein, A.; Brennessel, W. W.; Vicic, D. A. *Organometallics* **2012**, *31*, 1477.
[29] Romine, A. M.; Nebra, N.; Konovalov, A. I.; Martin, E.; Benet-Buchholz, J.; Grushin, V. V. *Angew. Chem., Int. Ed.* **2015**, *54*, 2745.
[30] Brockway, D. J.; West, B. O.; Bond, A. M. *J. Chem. Soc., Dalton Trans.* **1979**, 1891.
[31] Hughes, R. P. *Adv. Organomet. Chem*. **1990**, *31*, 183.

of the metal atom and, as a consequence, increased orbital overlap would yield a shorter, stronger bond. In contrast, the bizarre charge distribution exemplified in Scheme 3 is consistent not only with the strong trans influence of the CF_3 group but also with the β-effect in fluorinated organic compounds (see above).

Crystal Field Theory considerations suggest that the positive charge on the carbon atom of the CF_3 ligand should stabilize d orbitals on the metal, both filled and empty. This has indeed been established in earlier experimental and computational studies[32,33] and reconfirmed more recently.[21,25] In $[CX_3Rh(PH_3)_3]$ (Scheme 3), similar d orbitals on Rh are 9-15 kcal/mol more stable for X = F than for X = H. In other words, the metal atom in a CF_3 complex has a more stable set of orbitals while being more electron-rich (in terms of a computed charge). This combination brings about interesting and often unexpected reactivity patterns.

At the same time, like organic CF_3 derivatives reviewed earlier in this section, trifluoromethyl metal complex molecules, *as a whole*, are more electron-deficient than their CH_3 analogues. This follows from electrochemical studies[22,28,30, 34] and, conceivably, from the diminished reactivity of $[CF_3ML_n]$ species toward oxidative addition.[35,36]

[32] Hall, M. B.; Fenske, R. F. *Inorg. Chem.* **1972**, *11*, 768.
[33] Yang, D. S.; Bancroft, G. M.; Puddephatt, R. J.; Tse, J. S. *Inorg. Chem.* **1990**, *29*, 2496.
[34] Klein, A.; Vicic, D. A.; Biewer, C.; Kieltsch, I.; Stirnat, K.; Hamacher, C. *Organometallics* **2012**, *31*, 5334.
[35] (a) Appleton, T. G.; Clark, H. C.; Manzer, L. E. *J. Organomet. Chem.* **1974**, *65*, 275. (b) Appleton, T. G.; Hall, J. R.; Neale, D. W.; Williams, M. A. *J. Organomet. Chem.* **1984**, *276*, C73. (c) Appleton, T. G.; Berry, R. D.; Hall, J. R.; Neale, D. W. *J. Organomet. Chem.* **1988**, *342*, 399.
[36] As reactivity is a kinetic parameter, the large size of the CF_3 group may contribute to slower reaction rates.

Objectives

As is clear from the Introduction above, electronic properties of the CF_3 group in both organic and organometallic compounds are a subject of controversy. Considerable progress has recently been made in our understanding of the influence of this important substituent and ligand on a variety of molecular systems. Nonetheless, much deeper insight is needed into the factors governing electron density distribution in trifluoromethylated molecules and their CH_3 counterparts.

Experimental methods are not always available for obtaining answers to certain scientific questions. In the context of the current topic, for example, it is hard to experimentally probe and quantify the accumulation of a negative charge on the aromatic carbon bearing a CF_3 group: benzotrifluorides just do not undergo electrophilic *ipso*-substitutions. Another example is the strong trans influence of the trifluoromethyl ligand that has been established beyond any doubt by experimental means, but still remains poorly understood. When dealing with such problems, the scientist has to rely on theoretical methods. The objective of the current project was therefore to perform a systematic comparative analysis of stereoelectronic effects of the trifluoromethyl and methyl groups in organic and organometallic molecules using most advanced powerful computational tools.

Results

To gain insight into the origin of the stereoelectronic properties of the CF_3 group, a comparative analysis was performed for a series of trifluoromethylated molecules and their non-fluorinated counterparts. Scheme 4 displays the set of model compounds **1**-**7** selected for our initial studies to examine the general character of changes prompted by the replacement of the methyl group with CF_3. To obtain a clearer picture, models containing sterically crowded and highly polar moieties were excluded from the study. Nonetheless, the selected set is representative of a broad range of organic species bearing the CX_3 (X = H or F) group on a hydrogen atom (**1**), an sp^3- (**2**), sp^2- (**3**, **4**), and sp- (**5**) carbon, and a heteroatom having a vacant orbital (**6**) or a lone electron pair (**7**).

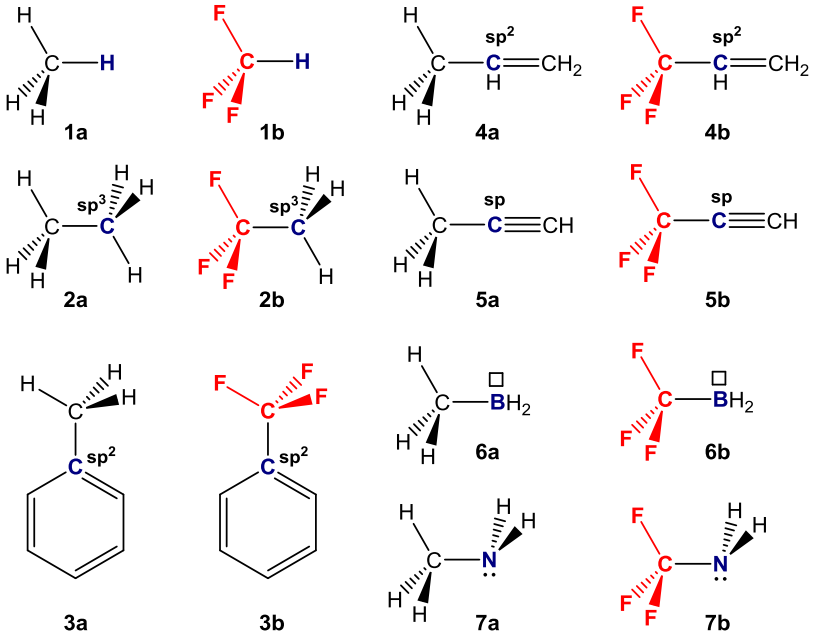

Scheme 4*. Organic compounds **1-7** selected for analysis*

Partial atomic charges are often used in discussions of structural and reactivity differences between similar compounds.[37] Therefore, we first analyzed charge distribution in the selected molecules.

Charge Distribution Analysis. As atomic charges cannot be directly observed by any experimental or theoretical means, the concept of partitioning of the electron density between individual atoms in a molecule is somewhat ill-defined. Consequently, many methodologies based on various approximations have been developed. In research, different atomic charges are used for different purposes, as there is no optimal charge model that is suitable for every task. Therefore, to ensure that calculated charge distribution patterns and conclusions drawn from them are not an artifact emerging from a particular method of analysis, we employed different population schemes in our work: Minimum Basis Set (MBS) Mulliken, Hirshfeld, Bader (AIM), NPA, and GAPT.[38]

The computed partial charges for the CX_3 groups and atoms A they are attached to in molecules **1-7** are summarized in Table 7 (see the Computational Data section below). Table 2 lists the differences in the atomic $\Delta A = q_{CH_3}(A) - q_{CF_3}(A)$ and group $\Delta CX_3 = q(CH_3) - q(CF_3)$ charges for each pair, with positive values corresponding to a larger positive (or smaller negative) charge in the CH_3 species. Note that $|\Delta A|$ and $|\Delta CX_3|$ for a particular pair are not necessarily equal because ΔA refers only to the adjacent atom, not the entire CX_3-derivatized moiety whose other atomic charges are also affected, although only slightly, by changing X = H to X = F.

[37] Bachrach, S. M. *Rev. Comp. Chem*. **1994**, *5*, 171.
[38] For the difference between these methods see: (a) Cramer, C. J. *Essentials of Computational Chemistry*; Wiley-VCH, 2004. (b) Jensen, F. *Introduction to Computational Chemistry*; Wiley-VCH, 2007.

Table 2**. Pairwise comparison of partial charges in **1-7

No	Mulliken		NPA		AIM		Hirshfeld		GAPT	
	ΔA	ΔCX_3	ΔA	ΔCX_3	ΔA	ΔCX_3	ΔA	ΔCX_3	ΔA	ΔCX_3
1	-0.04	+0.04	+0.07	-0.07	-0.09	+0.09	-0.03	+0.03	+0.06	-0.06
2	+0.03	+0.09	+0.10	-0.01	-0.03	+0.18	0.00	+0.07	+0.18	+0.00
3	+0.03	+0.11	+0.14	0.00	-0.02	+0.21	+0.03	+0.08	+0.24	-0.04
4	+0.03	+0.10	+0.14	0.00	-0.04	+0.20	+0.01	+0.09	+0.23	-0.02
5	+0.01	+0.11	+0.14	0.00	-0.14	+0.21	0.00	+0.10	+0.32	-0.12
6	-0.02	+0.11	+0.07	-0.02	+0.03	+0.05	-0.03	+0.08	+0.09	+0.02
7	-0.01	+0.10	+0.04	+0.03	+0.01	+0.12	-0.03	+0.09	+0.19	-0.02

The Mulliken, AIM, and Hirshfeld population analyses produced positive ΔCX_3 values, indicating that the total charge on the CF_3 moiety is less positive or more negative than on the CH_3. In other words, the CF_3 group makes the rest of the molecule more electron-deficient, which is consistent with the CF_3 group being more electronegative than the methyl. In contrast, the NPA and GAPT methods suggest stronger electron donation to A from CF_3 than from CH_3, as manifested by invariably positive ΔA values. The NPA- and GAPT-derived ΔCX_3 values vary in sign yet only slightly in magnitude.

The Mulliken population analysis[39] suggests that atom A bears a larger negative charge for fluorinated than non-fluorinated **2-5**. For **1**, **6**, and **7**, the opposite trend is observed. For all seven systems, however, |ΔA| is small (≤ 0.04). Although the original Mulliken methodology[40] has a number of widely recognized drawbacks that challenge reliability of the results, a nearly identical charge distribution pattern was observed using the totally different Hirshfeld approach.[41] More consistent with chemical

[39] Montgomery, J. A.; Frisch, M. J.; Ochterski, J. W.; Petersson, G. A. *J. Chem. Phys.* **2000**, *112*, 6532.
[40] Mulliken, R. S. *J. Chem. Phys*. **1962**, *36*, 3428.
[41] Hirshfeld, F. L. *Theor. Chim. Acta* **1977**, *44*, 129.

intuition, the Hirshfeld method also suggests that the charges on A are weakly sensitive to the nature of the CX_3 substituent. Apart from small nuances, these results are consistent with the AIM[42] data.

The dipole moment-based GAPT analysis[43] shows that atom A bearing the CX_3 group is much more negatively charged for X = F than for X = H. A similar trend was observed using the NPA scheme[44] that is believed to be the most reliable method for computing atomic charges in molecules.[45] The previously observed[15] (see above) inconsistency of the AIM and NPA charge distribution patterns is disturbing, as both methods are expected[46] to give similar results.

The above results do not allow us to draw a definite conclusion regarding the donor/acceptor ability of the CF_3 group relative to methyl. The fact that the AIM and NPA schemes give opposite trends suggests that at least one of them is likely wrong. To gain insight into the key factors prompting the observed difference and shed more light on electronic effects of the CF_3 group, we then performed a more detailed population analysis.

NBO Analysis. The concept of the Natural Bond Orbital (NBO) analysis[45] is based on the transformation of a given wave function into a localized form that is as close as possible to a classical Lewis structure for a molecule. The NPA data above (part of the more general NBO approach) predict that (i) the CF_3 and CH_3 groups bear very similar charges in analogous compounds and (ii) the charge on atom A bonded to CX_3 is more negative for X = F than for X = H, usually by 0.07-0.14e. Perhaps the most

[42] (a) Bader, R. F. W. *Atoms in Molecules, a Quantum Theory*; Clarendon Press: Oxford, 1990. (b) Carroll, M. T.; Chang, C.; Bader, M. F. W. *Mol. Phys.* **1988**, *63*, 387.
[43] Cioslowski, J. *J. Am. Chem. Soc.* **1989**, *111*, 8333.
[44] Reed, A. E.; Weinstock, R. B.; Weinhold, F. *J. Chem. Phys*. **1985**, *83*, 735.
[45] Weinhold, F.; Landis, C. R. *Valency and Bonding: A Natural Bond Order Donor-Acceptor Perspective*; Cambridge University Press: Cambridge, U. K., 2005.
[46] Weinhold, F.; Landis, C. R. *Discovering Chemistry with Natural Bond Orbitals*; Wiley, 2012.

striking example is the charge distribution in **1a** *vs.* **1b**. In all other cases (**2-7**) the more negative or less positive charge on the adjacent atom A might be somehow rationalized in terms of some unconventional field effect tricks, re-polarizing the electron density toward the CF_3 group. However, the charge distribution in the **1a**/**1b** pair states unambiguously that CF_3 is a stronger electron-donor than CH_3 by 0.07e. We therefore performed NBO analysis for this simplest yet apparently most enigmatic pair comprising **1a** (methane, H-CH_3) and **1b** (fluoroform, H-CF_3).

In **1a**, the C-H bonding orbital $\sigma_{C\text{-}H} = 0.7853(sp^3)_C + 0.6191(s)_H$ results from the combination of the sp^3 hybrid on C (61.7%) and the s orbital on H (38.3%). The larger coefficient for the atomic orbital coming from C reflects its higher electronegativity. The analogous C-H bonding orbital in **1b**, $\sigma_{C\text{-}H} = 0.7722(sp^{1.85})_C + 0.6354(s)_H$, has higher s character and a smaller contribution from the carbon (59.6%). When translated to the NPA population, this difference explains a higher donating ability of the CF_3 group.

A comment is due on the carbon hybridization. The greater s character of the orbital on carbon of the CF_3 group is, intuitively, consistent with Bent's rule stating that *"atomic s character concentrates in orbitals directed toward electropositive substituents"*.[47] This also means that a carbon atom directs orbitals of greater p character toward more electronegative substituents, *i.e.* fluorine atoms in our case. The formal rationale for Bent's rule is based on the fact that for the main group elements, the valence s orbital is always lower in energy than the p valence orbitals. On the other hand, the different hybridization of the carbon is at the root of the discrepancy between the NPA and AIM charges. As a result of the larger s character of its hybrid orbital, the carbon claims to itself electrons that are further away in space, and possibly outside its

[47] Bent, H. A. *Chem. Rev.* **1961**, *61*, 275.

basin in the AIM calculation. This is yet another indication that computed atomic charges might not be an appropriate tool for comparison of bonding abilities of the CF_3 and CH_3 groups.

Additional important information that could be extracted from the NBO analysis was the natural bond C-H ionicities of 23.3% and 19.2% for **1a** and **1b**, respectively, using the equation below:

$$AB\ bond\ ionicity = \left|\frac{c_A^2 - c_B^2}{c_A^2 + c_B^2}\right|.$$

These ionicity values suggest that the C-H bond in fluoroform is 4% more covalent than in methane, *i.e.* the electron pair shared by the C and H atoms is shifted slightly more toward the latter in CHF_3 relative to CH_4. The resultant increase in electron density on the H atom might suggest that CF_3 is a stronger σ-donor than CH_3. This view, however, is nuanced by another NBO tool, the Natural Steric (NST)[48] analysis, showing that the fluorine lone pairs strongly repel the electrons of the coplanar C-H bond. Originating from the Pauli repulsion, this steric pressure raises the energy of the molecule by 24.1 kcal/mol and "pushes" the C-H bond electron density toward the proton to alleviate the destabilizing effect. As a consequence, this distortion increases the electron density on the H atom by 0.04e (57.1% of the overall ΔA value). Interestingly, a similar p-π effect was proposed by Sheppard[16] for unsaturated systems 50 years ago, albeit without firm evidence.

Second-order perturbative analysis suggested that the fluorine lone pairs are involved in hyperconjugative coupling with the antibonding $\sigma^*_{C\text{-}H} = 0.6354(sp^{1.85})_C - 0.7722(s)_H$ orbital. Figure 2 exhibits a graphical representation of the overlap between the lone pairs and the back lobe of the $\sigma^*_{C\text{-}H}$ orbital polarized toward the proton. This

[48] (a) Badenhoop, J. K.; Weinhold, F. *J. Chem. Phys.***1997**, *107*, 5406. (b) Badenhoop, J. K.; Weinhold, F. *Int. J. Quantum Chem.* **1999**, *72*, 269.

$n_F \rightarrow \sigma^*_{C\text{-}H}$ hyperconjugation lowers the energy of **1b** by 21.1 kcal/mol, largely reducing the destabilizing effect of the steric repulsion. An increase in the population of the $\sigma^*_{C\text{-}H}$ explains the noticeably lower C-H bond order in fluoroform (0.915) than in methane (0.945), even though the corresponding bonds in **1a** and **1b** are almost of the same length (1.092 and 1.094 Å, respectively). According to Natural Coulomb Electrostatics (NCE)[49] analysis, this delocalization also makes the H atom in fluoroform more negative than in methane by 0.03e (42.9% of the ΔA value). A large natural bond-bond polarizability index[50] $NBBP(n_F,\sigma_{C\text{-}H}) = 0.036$, which shows how the distortion of one bond affects the strength of another bond through delocalization effects, provides another evidence for strong interaction of the F lone pairs with $\sigma^*_{C\text{-}H}$ of CHF_3.

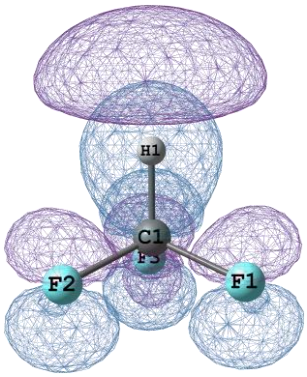

Figure 2. *$n_F \rightarrow \sigma^*_{C\text{-}H}$ hyperconjugation in **1b**, isovalue 0.05*

More complex yet consistent patterns were produced by NBO analysis of the rest of the compounds (**2-7**) in the series (Table 8, Computational Data section). In all cases the atom that is attached to the CF_3 group directs orbitals of higher p character toward the latter that, unlike the methyl, creates steric strain (19-25 kcal/mol). Consequently, the electron pair of the CF_3-A bond is slightly polarized away from the

[49] Glendening, E. D.; Landis, C. R.; Weinhold, F. *WIREs Comput. Mol. Sci.* **2012**, *2*, 1.
[50] Zimmerman, H. E.; Weinhold, F. *J. Am. Chem. Soc.* **1994**, *116*, 1579.

CF_3 group. The $n_F \rightarrow \sigma^*_{C-A}$ hyperconjugation stabilizes the trifluoromethylated molecules by 12-25 kcal/mol, while weakening the CF_3-A bonds, as manifested by their generally lower computed bond orders.

In conclusion, the detailed NBO analysis of **1**-**7** shows that the difference in the donor/acceptor behavior of the CF_3 and CH_3 groups depends on a number of stereoelectronic factors whose overall effect may not always be obvious. The NBO method suggests that CF_3 is a weaker donor than CH_3. This is not reflected, however, by the raw NPA charges, which may not be properly compared for the CF_3 derivatives and their CH_3 analogues because of the difference in hybridization of the carbon orbitals contributing to the A-CX_3 σ-bond.

AIM Analysis. Bader's Atom in Molecules (AIM) topological analysis represents an orbital-free approach to atomic charge evaluation. In the AIM scheme, the partial charges are defined by integration of the electron density within the so-called "atomic basins" separated by zero-flux surfaces.[42] Apart from charges on atoms, this method provides means to calculate other useful parameters, including atomic shapes, volumes, and multiple electric moments.

The AIM data presented in Table 2 above suggest that for most of the model pairs in the series, CX_3-bonded atom A bears a larger positive (or a smaller negative) charge for X = F than for X = H. This difference stems from the lower total number of electrons assigned to the atomic basin of A for the trifluoromethylated derivatives (see Table 9 in the Computational Data section below). Although these atoms are smaller in size, their local electron density calculated per volume is usually higher.

The AIM analysis shows that electron density at the bond critical point (BCP) between the CX_3 group and an adjacent atom ranges from 0.187 to 0.329 e/Bohr^3. In

addition, the Laplacian of the electron density $\nabla^2\rho_B(r)$ is negative, whereas the total electronic energy H(r) is positive. Together, these characteristic parameters indicate that the CX_3-A bond can be identified as covalent with the dominance of the stabilizing potential energy G(r). The delocalization indices DI, *i.e.* bond orders, are considerably lower for the CF_3-A bonds, which is consistent with the NBO data above. Apart from **6**, which exhibits strong hyperconjugation between $\sigma_{C\text{-}X}$ and the vacant p orbital on the boron, π-binding or any other lateral interactions perturbing the σ-bond symmetry are virtually negligible, as manifested by the very low bond ellipticities $\varepsilon(r)$.

In comparison with the non-fluorinated systems, the CF_3-A BCP is more shifted toward A by 1-4%. As BCP marks the border between two connected atoms, this shift provides additional evidence for the compression of A in the trifluoromethylated molecules. Given the fact that the position of BCP is a measure of relative electronegativities of two connected atoms, one may argue that the CF_3 group is more electron-withdrawing or less electron-donating than methyl.

The discrepancy between the computed AIM and NPA charges (Table 2) is apparently due to different methodologies these two methods are based upon. While AIM employs the idea of atomic basins, NBO analyzes hybrid atomic orbitals contributing to the covalent bonds. AIM and NBO should produce similar charge distribution patterns if the atoms involved have similar hybridizations. This, however, is not the case for the CF_3 and CH_3 groups.

Transition Metal Compounds. We expanded our analysis to a set of organometallic compounds of the d-block elements **8**-**13** (Scheme 5). The selected complexes cover transition metals from periods 4 through 6 and various ligands and geometries, including octahedral (**8**, **9**), trigonal bipyramidal (**10**, **11**), and square planar

(**12**, **13**). The manganese complexes **8** have been previously studied by means of Hückel[32] and NBO[25] analyses and were included in the series for comparative purposes. In all cases the M-CF_3 bond was computed to be clearly shorter (0.04-0.12 Å) than the corresponding M-CH_3 bond. At the same time, the M-L bond in the trans position to the CF_3 is longer, although the elongation is in general smaller (0.01-0.04 Å).

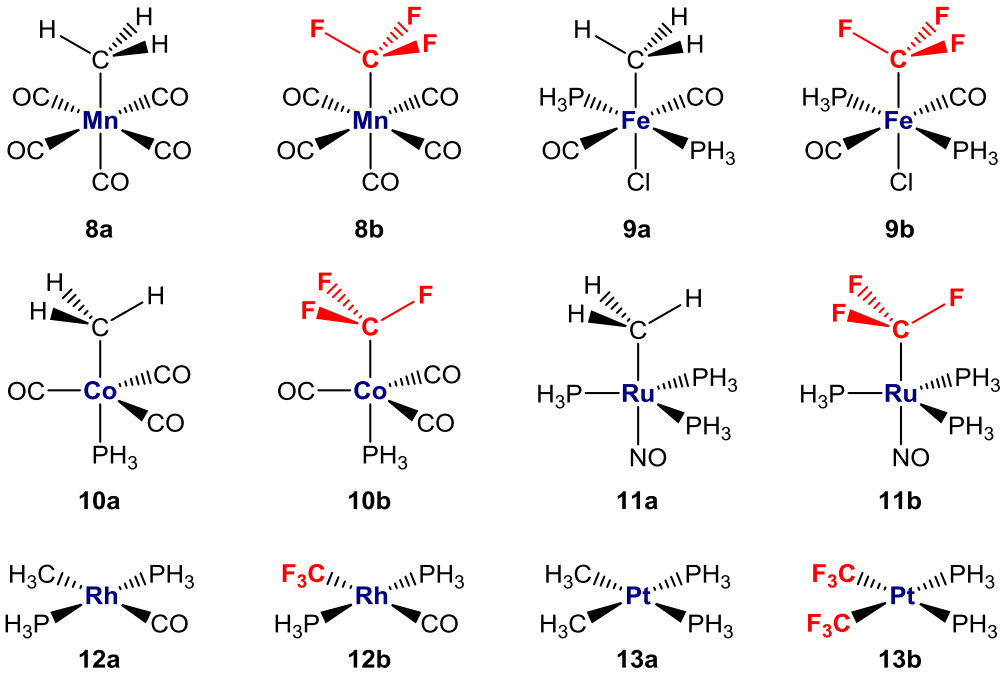

Scheme 5. *Organometallic compounds* ***8-13*** *selected for analysis*

Charge Distribution Analysis. The calculated metal (M) and group charges (CX_3) are presented in Table 10 in the Computational Data section. The pairwise differences in metal (ΔM) and group (ΔCX_3) charges between the CH_3- and CF_3-bearing complexes are listed below in Table 3. Mulliken charges were not calculated for this set because the MBS scheme is inapplicable to transition metals, and results with large basis sets are often physically unreasonable.[38]

The data in Table 3 indicate that for all population analyses, there is more charge transfer from CH_3 than from CF_3 (all ΔCX_3 values are positive). This is in contrast with the result reported in Table 2 for organic molecules. It further suggests that population analysis is not a proper tool to analyze this topic, as one expects the trends to be conserved when going from organic to organometallic molecules. The computed absolute ΔM values for **8**-**13** (Table 3) are generally lower than for **1**-**7** studied earlier (Table 2), yet the method-dependent variations in sign of ΔM follow the same trend for both series.

Table 3*. Pairwise comparison of partial charges for* ***8-13***

No	NPA		AIM		Hirshfeld		GAPT	
	ΔM	ΔCX_3	ΔM	ΔCX_3	ΔM	ΔCX_3	ΔM	ΔCX_3
8	+0.06	+0.07	-0.01	+0.22	+0.02	+0.12	-0.06	+0.12
9	+0.09	+0.03	-0.01	+0.20	+0.03	+0.10	-0.08	+0.14
10	+0.05	+0.07	-0.03	+0.19	+0.02	+0.11	-0.10	+0.13
11	+0.04	+0.07	-0.03	+0.22	+0.01	+0.08	-0.04	+0.09
12	+0.04	+0.04	-0.05	+0.18	+0.01	+0.08	-0.06	+0.10
13	+0.06	+0.02	-0.14	+0.15	-0.01	+0.06	-0.11	+0.10

NBO Analysis. Care should be exercised when performing NBO analysis for transition metal compounds. According to the prevalent analysis the outer p orbitals of the metal participate in the bonding very weakly and, therefore, they are excluded from the valence shell and treated as Rydberg orbitals. As a consequence, the NBO scheme employs the so-called duodectet (12) rule[51] that determines exceptions from the 18e rule (such as square-planar 16e and linear 14e species) by invoking hypervalent 3-center 4e-

[51] (a) Maseras, F.; Morokuma, K. *Chem. Phys. Lett.* **1992**, *195*, 500. (b) Landis, C. R.; Weinhold, F. *J. Comp. Chem.* **2007**, *28*, 198.

bonds. For most of the complexes studied here, the default analysis leads to poor Lewis structures that cannot be analyzed to evaluate the role of electronic effects of specific substituents. A solution to this problem is to use the CHOOSE procedure that enables the user to specify a reliable reference structure.

The NBO analysis gave a pattern that is similar to the one observed for the organic molecules (Table 11, Computational Data section below). The M-CF_3 bond is ca. 0.04-0.11 Å shorter and has a higher bond order than the corresponding M-CH_3 bond. The hyperconjugation $n_F \rightarrow \sigma^*_{C\text{-}M}$ (8-24 kcal/mol) is weaker than in the organic molecules. Examination of the Fock matrix suggests that F_{ij} elements related to this donor-acceptor interaction are significantly smaller in **8-13** as compared to **1-7**. All these features point to a less pronounced charge transfer from the CF_3 group to the adjacent metal-based moiety.

Interestingly, both the carbon of the CF_3 and the metal center have higher s character hybrids directed toward each other. This observation can be rationalized in terms of the extended Bent's rule, which states that *"the energetically lower lying valence orbital concentrates in bonds directed toward electropositive substituents"*.[52] As the valence s orbital in transition metals is always above the valence d orbitals, the CF_3 group is more electronegative than CH_3 by this rule and in accordance with the literature7 and our own data for **1-7** above. In contrast with the A-CF_3 bond of **1-7**, the M-CF_3 bond in **8-13** is more polarized toward the CF_3 (by 2-4%), probably due to more ionic character. The change in hybridization of the atomic orbitals contributing to the bond pair, however, is not sufficient to invert the charge transfer, as was the case for the organic fragments, because of the higher ionicity. The qualitative description of the bonding is nevertheless the same. The NBO analysis of the M-CX_3 bond in **8-13**

[52] Jonas, V.; Boehme, C.; Frenking, G. *Inorg.Chem*. **1996**, *35*, 2097.

suggests that the CF_3 ligand behaves as a weaker σ-donor and stronger π-acceptor than the CH_3 ligand.

AIM Analysis. The topological analysis of **8-13** (Table 12, the Computational Data section below) shows that the bond between the CX_3 group and the metal is more ionic that the corresponding bond in **1-7**. Typical values of the electron density $\rho_b(r)$ in BCP for **8-13** are 0.073-0.139 e/Bohr^3, whereas for the organic species the range is 0.187-0.329 e/Bohr^3. In addition, the positive Laplacian $\nabla^2\rho_b(r)$ indicates that electron density is depleted from the bonding area. This is consistent with the very low positive H(r) parameter, which reflects the greater contribution of the destabilizing kinetic energy V(r) to the M-CX_3 bond energy. In AIM terms, this means that the type of bonding between the CX_3 group and the metal is intermediate between the shared (covalent) and closed-shell (ionic and van der Waals) categories. Like in the organic systems, the CH_3/CF_3 replacement results in significant contraction of the adjacent atom, in this case the metal. In addition, the M-CF_3 BCP is slightly shifted (ca. 1%) toward the metal center, an effect that is less pronounced than in **1-7**.

The extremely low bond ellipticies ε(r) for both M-CH_3 and M-CF_3 suggest that electron delocalization effects play an almost negligible role in the M-CX_3 bonding. The generally smaller delocalization indices (DI) serving as a numerical measure of the electron sharing ability also support this conclusion and provide another evidence for the more ionic M-CX_3 bond character. In summary, the AIM analysis clearly points to a lower electron donating ability of CF_3 *vs.* CH_3.

Trans influence in [Mn(CO)$_5$R] Compounds. As described above, the experimentally observed structural trans influence of CF_3 in metal complexes is similar

to that of CH_3. This is certainly counterintuitive if the CF_3 group is a weaker donor. We therefore decided to further investigate the origin of this behavior. We started off by calculating Mn-CO bond dissociation energies (BDE) in a series of $[Mn(CO)_5R]$ compounds (Table 4),[53] including **8a** and **8b** from the set under investigation (Scheme 5). The Mn complexes were selected because they were studied previously.[25,32]

Table 4. *Trans influence in $[Mn(CO)_5R]$*

R	Mn-R, Å	Mn-CO_{trans}, Å	Mn-CO_{eq}, Å	BDE (Mn-CO_{trans}), kcal/mol
CH_3	2.206	1.824	1.843	38.2
CF_3	2.109	1.842	1.854	32.3
H	1.573	1.841	1.841	36.3
F	1.953	1.815	1.865	40.9
Cl	2.401	1.806	1.864	41.9
Br	2.545	1.806	1.863	41.9
I	2.744	1.804	1.861	42.0
CN	1.995	1.837	1.860	36.5
SiH_3	2.471	1.828	1.842	37.6
SiF_3	2.362	1.840	1.848	35.5

The data in Table 4 suggest that CF_3 has the strongest trans influence of all considered ligands, exceeding even those of H and SiF_3, although only slightly. The optimized geometries show that depending on the ligand R, the Mn-CO_{trans} bond distances vary in a range of 1.804-1.842 Å. The spread of the Mn-CO_{eq} bond lengths is narrower, 1.841-1.865 Å, indicating that the *cis*-CO are less sensitive to the nature of R.

The stretching of the Mn-CO_{trans} bond results in lower bond dissociation energies. An excellent linear correlation is observed between the Mn-CO_{trans} bond

[53] These calculations were performed at DFT/BP86 level of theory.

length and the corresponding BDE (R^2 = 0.98, Figure 3) for all of the ligands but CF_3. Although the Mn-CO_{trans} bond distance in $[Mn(CO)_5H]$ is virtually as long as in **8b**, the BDE of this bond in the latter is lower by 4.0 kcal/mol. This indicates that the CF_3 has not only a strong structural but also a significant energetic trans influence.

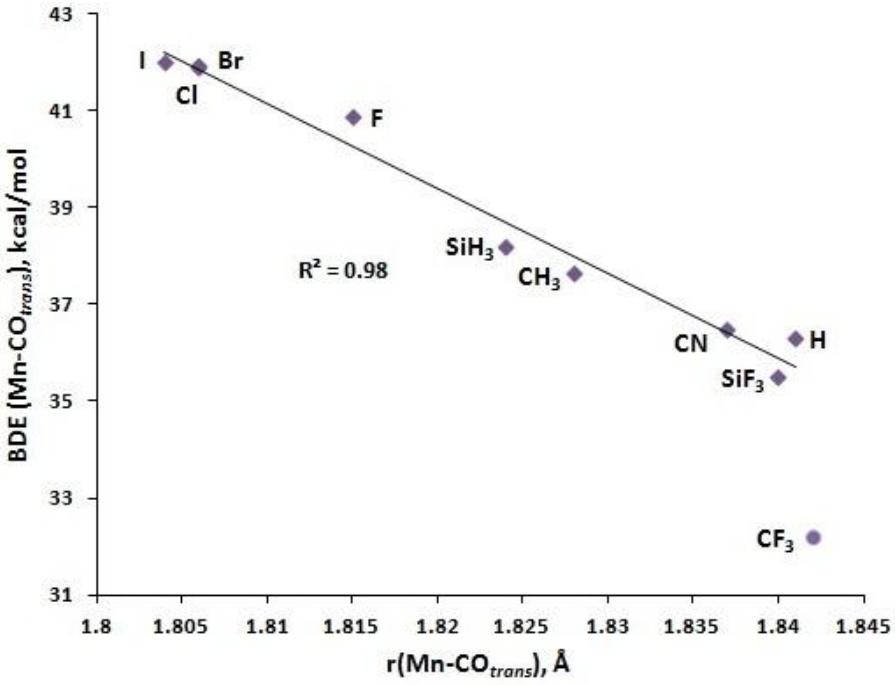

***Figure 3**. Mn-CO_{trans} bond distance - BDE correlation for $[Mn(CO)_5R]$ with R = CF_3 omitted from the linear regression*

As the strong trans influence of the CF_3 ligand in **8b** has been known for a long time,[54] there have been several attempts to rationalize it in terms of various orbital interactions. Experimental IR studies have found no signs of $d_{Mn} \rightarrow \sigma^*_{Mn\text{-}CF_3}$ back-bonding interaction.[55] Negative hyperconjugation $d_{Mn} \rightarrow \sigma^*_{C\text{-}F}$ has been proposed,[32] but more recent calculations suggest that it does not exceed the σ-bond interaction $\sigma_{CF_3} \rightarrow$ Mn.[25] Being rather weak, $d_{Mn} \rightarrow \sigma^*_{C\text{-}F}$ in **8b** is nonetheless considerably stronger than

[54] Beagley, B.; Young, G. G. *J. Mol. Struct.* **1977**, *40*, 295.
[55] Graham, W. A. G. *Inorg. Chem*. **1968**, *7*, 315.

electron donation from Mn to σ^*_{C-H}, σ^*_{Si-H}, and σ^*_{Si-F} in the CH_3, SiH_3, and SiF_3 complexes.[56] It is generally accepted that the trans influence and the closely related trans effect of a particular ligand are determined by its σ-donation and π-acidity.[57,58] Previous experimental and computational work did not shed light on the origin of the higher trans influence of CF_3 relative to CH_3. Being consistent with the literature data, our calculations described above cannot rationalize this puzzling phenomenon, either. Further investigations, however, have allowed us to gain insight into the nature of the strong trans influence of the CF_3 ligand.

Comparative Analysis of 13a and 13b. Analysis of the frontier molecular orbitals in **13** indicated that the HOMO is predominantly metal-based, whereas the LUMO is largely ligand-centered, although with a considerable contribution from the metal d orbitals (Figure 4). In addition, the HOMO, LUMO, and all valence d orbitals in **13b** are by 0.7-1.4 eV lower in energy than in **13a**. In orbital-controlled reactions, this should lead to lower reactivity of **13b** toward electrophiles and higher reactivity toward nucleophiles. The substantial dissimilarity in the shape of the frontier orbitals on **13a** and **13b** suggested different electronic hardness of the Pt atoms in these complexes, defined as the resistance to deformation of the electron density. Indeed, the Pt center in **13b** (η = 2.74 eV) is considerably harder than that in **13a** (η = 2.60 eV).[59] This is consistent with smaller atomic volumes and larger positive charges of the metal atoms in trifluoromethylated compounds, as predicted by the topological analysis (see above).

[56] Leyssens, T.; Peeters, D.; Orpen, A. G.; Harvey, J. N. *Organometallics* **2007**, *26*, 2637.
[57] (a) Cotton, F. A.; Wilkinson, G. *Advanced Inorganic Chemistry, 4th ed.*; Wiley: New York, 1980. (b) Crabtree, R. H. *The Organometallic Chemistry of the Transition Metals 4th ed.*; Wiley: New Jersey, 2005.
[58] (a) Although the less studied steric trans influence is expected to be weak, it is worth keeping in mind that CF_3 has a much larger effective steric bulk than methyl. The van der Waals radii (hemisphere volumes) of CF_3 and CH_3 are 2.7 Å (42.5 $Å^3$) and 2.0 Å (16.8 $Å^3$), respectively.[58b] (b) Seebach, D. *Angew. Chem., Int. Ed.* **1990**, *29*, 1320.
[59] Calculated as $\eta = (E_{LUMO}-E_{HOMO})/2$. According to this equation, a harder molecule has a larger HOMO-LUMO gap, whereas a softer molecule has a smaller HOMO-LUMO gap.

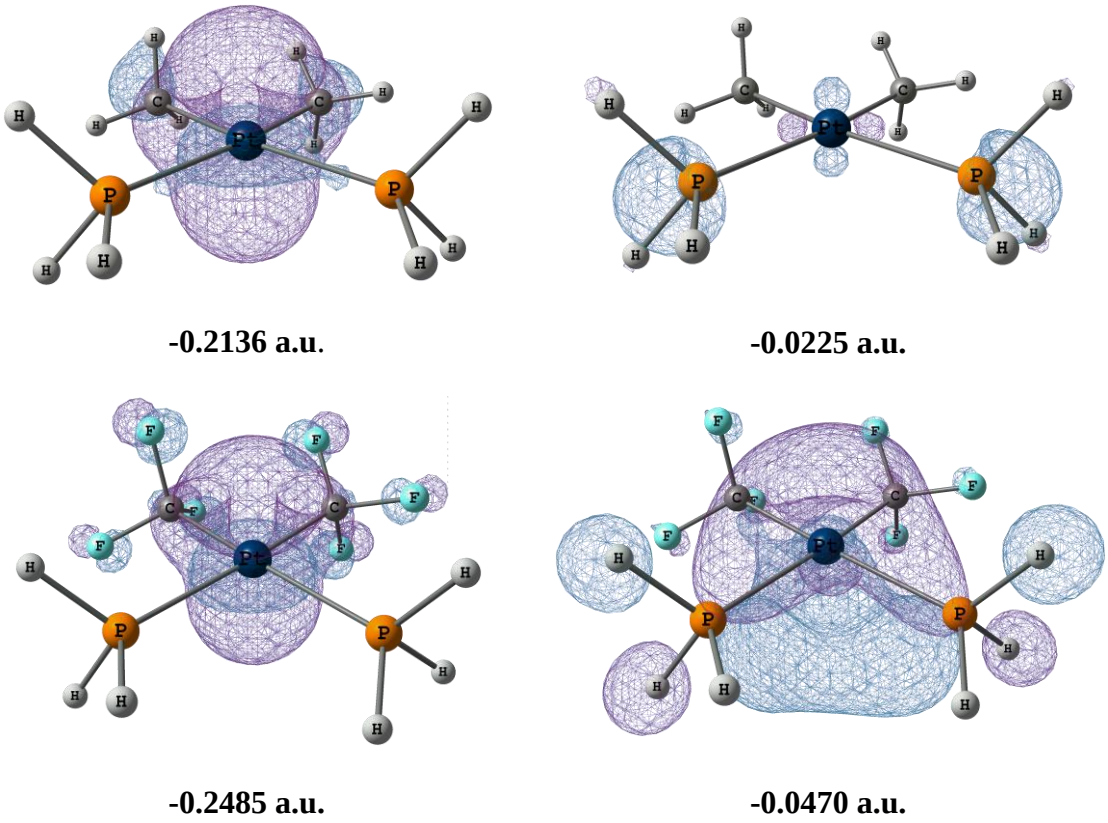

-0.2136 a.u. **-0.0225 a.u.**

-0.2485 a.u. **-0.0470 a.u.**

***Figure 4**. HOMO (left) and LUMO (right) of **13a** (top) and **13b** (bottom), with corresponding energies, isovalue 0.04*

Additional support for the harder Pt atom in **13b** was obtained from the molecular electrostatic potential (MESP) maps that enable to visualize the size and shape of molecules as well as charge distribution within them (Figure 5). The comparative analysis of the electrostatic potentials mapped onto the iso-electron density surface clearly shows more electron density around the Pt center in **13a**. Furthermore, the less negative MESP value of Pt in **13b** (-14.63 eV) relative to that in **13a** (-14.67 eV) points to less pronounced charge delocalization, yet another sign of a harder atom. These results also attest to the weaker electron-donating nature of the CF_3 ligand with respect to the CH_3.

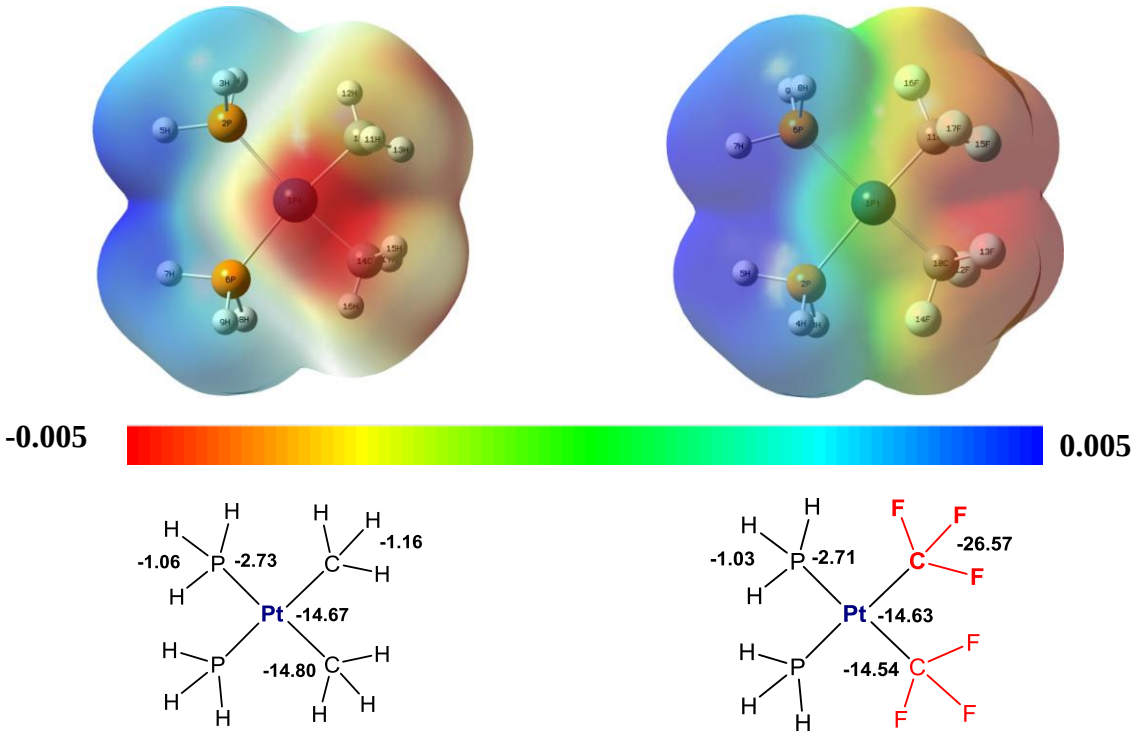

***Figure 5**. Top: electrostatic surface potentials of complexes **13a** (left) and **13b** (right) with regions of negative charge in red and positive charge in blue: isovalue 0.02; density 0.005. Bottom: calculated electrostatic potentials in eV*

In the light of these results, it seems possible to rationalize why upon replacement of hydrogens with fluorines on the carbon in a closely related amino phosphine complex, *cis*-[$(CX_3)_2Pt(NH_3)(PH_3)$] (Scheme 6), the Pt-P bond *elongates* (by 0.037 Å), whereas the Pt-N bond *contracts* by nearly the same value (0.030 Å).

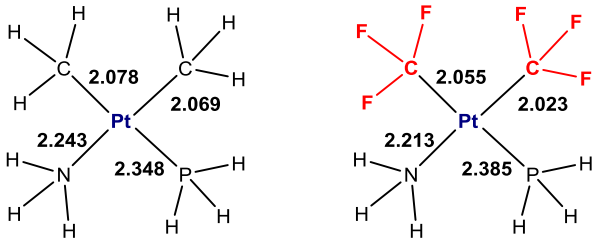

***Scheme 6**. Trans influence in [$(CX_3)_2Pt(NH_3)(PH_3)$]*

Evidently, NH_3, a hard Lewis base, prefers to bind to the harder Pt atom in **13b**, whereas soft PH_3 favors the softer Pt center in **13a**. The CF_3 making the metal harder should also affect the bonding not only to the trans ligand but also to other ligands in the coordination sphere of the metal. Indeed, we observed a considerable cis influence in $[CF_3Pt(PH_3)_2F]$, which is consistent with the higher hardness of the CF_3-ligated Pt atom (Scheme 7).

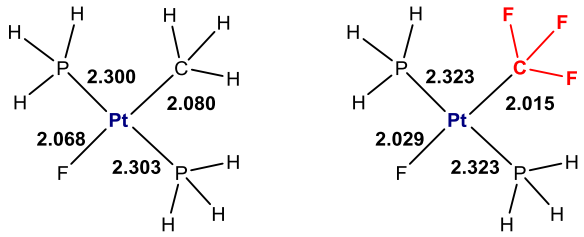

***Scheme 7**. Cis influence in $[CX_3Pt(PH_3)_2F]$*

The Hard and Soft Acids and Bases (HSAB) principle[60] states that soft acids form stronger bonds with soft bases, whereas hard acids form stronger bonds with hard bases. As a soft Lewis acid, Pt^{2+} has a high affinity for PH_3, a soft base. Upon binding to a CF_3 ligand, however, the metal center becomes harder, which weakens its bonds to soft ligands in the coordination sphere. A closer examination of Scheme 5 shows that besides CH_3 and CF_3, all other ligands on the metals in the selected models **8-13** are soft (CO, NO, PH_3) or borderline (Cl). We therefore concluded that the analysis of **13** above should be applicable to the entire series. However, there was clearly a need for a detailed comparative study of CF_3 and CH_3 complexes bearing a hard ligand.

Bonding in CF_3 and CH_3 Complexes Bearing a Hard Ligand. To further probe the hard-soft idea described above, we studied four square-planar 16e Rh

[60] Pearson, R. G. *J. Chem. Sci.* **2005**, *117*, 369.

complexes with a hard (NH_3) or soft (PH_3) ligand trans to the CX_3 group: $[CH_3Rh(PH_3)_2(NH_3)]$ (**14a**), $[CF_3Rh(PH_3)_2(NH_3)]$ (**14b**), $[CH_3Rh(PH_3)_3]$ (**14c**), and $[CF_3Rh(PH_3)_3]$ (**14d**). The computed coordination bond distances for **14a-d** are presented in Scheme 8.

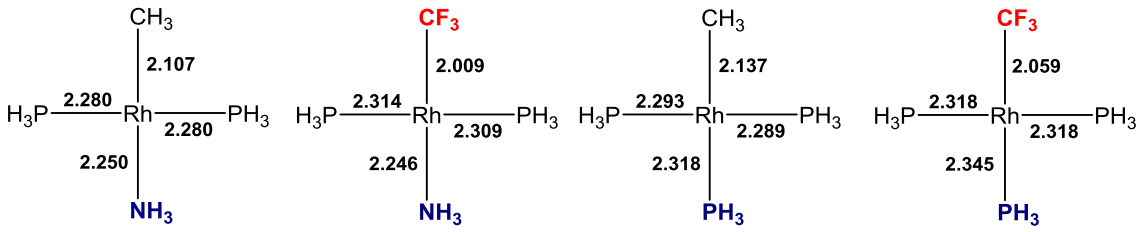

Scheme 8**. Computed bond distances (Å) in **14a-d

In agreement with reported[21,25] computational studies, the trans Rh-PH_3 bond in **14d** was computed to be longer than in **14c**. This effect has been previously observed in the X-ray structures of the PPh_3 analogues of these complexes, $[CH_3Rh(PPh_3)_3]$ and $[CF_3Rh(PPh_3)_3]$.[21] The Rh-PH_3 bonds in **14b** and **14d** cis to the CF_3 group are longer than in the CH_3 complexes **14a** and **14c**, possibly due (at least, in part) to the larger size of the CF_3 group. The Rh-NH_3 bond in **14b**, however, is slightly shorter than in **14a**. Therefore, the bonding pattern in **14a-d** is consistent with the HSAB principle.[60]

To deepen our understanding of the nature of the metal-ligand bonding in **14a-d**, we performed Energy Decomposition Analysis (EDA) [61] as implemented in the ADF program.[62] Within this scheme, the total bonding energy (ΔE_{int}) between the structural moieties is partitioned into two physically meaningful components, $\Delta E_{int} = \Delta E_{steric} + \Delta E_{orb}$, where ΔE_{steric} is the steric energy term and ΔE_{orb} is the orbital contribution. The

[61] (a) Kitaura, K.; Morokuma, K. *Int. J. Quantum Chem.* **1976**, *10*, 325. (b) Ziegler, T.; Rauk, A. *Inorg. Chem.* **1979**, *18*, 1558.
[62] (a) te Velde, G.; Bickelhaupt, F. M.; Baerends, E. J.; Fonseca, G. C.; van Gisbergen, S. J. A.; Snijders, J. G.; Ziegler, T. *J. Comput. Chem.* **2001**, *22*, 931. (b) Scientific Computing & Modelling (SCM) Corporation http://www.scm.com is gratefully acknowledged for the trial licence.

former is not directly related to steric interactions and can, in turn, be decomposed into the destabilizing Pauli repulsion term ΔE_{Pauli} and the stabilizing electrostatic ΔE_{elstat} energy: $\Delta E_{steric} = \Delta E_{Pauli} + \Delta E_{elstat}$. The ΔE_{Pauli} term corresponds to the four-electron repulsion, whereas ΔE_{elstat} refers to attractive Coulomb interaction between the fragments. The ΔE_{orb} term accounts for charge transfer *via* orbital mixing of both inter- and intra-fragments and can be split up into σ-, π-, and δ-contributions according to the molecular symmetry to estimate the strength of orbital interactions. The results of the EDA analysis of **14a-d** are presented in Table 5. For the sake of comparison, we also performed additional calculations for a reoptimized system, **14d*** where the Rh-PH_3 bond was frozen at the same distance as in **14c**. This allowed us to exclude the distance dependence of the interaction energy between the $[CX_3Rh(PH_3)_2]$ and PH_3 moieties.

As expected, the metal-ligand bond stretching in **14a** *vs.* **14b** and **14d** *vs.* **14c** results in smaller energies of interaction between the metal-containing fragment and the ligand. It is noteworthy that although the Rh-NH_3 bonds in **14a** and **14b** are very close in length, their interaction energies are quite different. The lower ΔE_{int} value for **14b**, nevertheless, accords well with the enhanced hardness of the CF_3-ligated metal center.

Table 5**. EDA analysis of **14a-d** and **14d*

	14a	**14b**	**14c**	**14d**	**14d***
$r_{Rh\text{-}Ltrans}$	2.250	2.246	2.318	2.345	2.318
ΔE_{int}	-16.9	-18.8	-29.2	-26.8	-27.0
ΔE_{orb}	-21.4 (27.2%)	-22.9 (27.7%)	-50.2 (33.3%)	-47.8 (33.8%)	-50.7 (33.6%)
ΔE_{elstat}	-57.3 (72.8%)	-59.8 (72.3%)	-100.3 (66.7%)	-93.8 (66.2%)	-100.4 (66.4%)
ΔE_{Pauli}	61.8	63.9	121.3	114.8	124.1
ΔE_{ster}	4.5	4.1	21.0	21.0	23.7

Bond lengths in Å. Energy values in kcal/mol. The values in parentheses are percentage contributions to the total attractive interaction *i.e.* $\Delta E_{orb}+ \Delta E_{elstat}$.

Essentially the same trend was observed for the orbital component of the total interaction energy, even though the ΔE_{orb} values for **14c** and **14d** are more than twice as large as those for **14a** and **14b**. This is probably due to the weaker σ-donating and π-accepting ability of NH_3 *vs.* PH_3.[63] Unfortunately, this hypothesis cannot be verified by standard EDA because **14a-d** are unsymmetrical and, therefore, ΔE_{orb} cannot be symmetry-decomposed to individual orbital contributions. However, the Extended Transition State (ETS) method combined with the Natural Orbitals for Chemical Valence (NOCV) theory make it possible to quantify energies of particular orbital interactions even for non-symmetric molecules. [64] The ETS-NOCV energy decomposition scheme operates with an auxiliary function called "deformation density", Δρ, which can be partitioned into specific orbital interactions between the fragments. The latter is defined as the difference between the molecular electron density and the sum of atomic densities placed at the nuclear geometry of the molecule. Positive and negative Δρ values describe regions of charge accumulation and depletion, respectively.

One might reason that during the formation of a molecule from individual atoms, the electron density flows from negative to positive areas. The ETS-NOCV method enables to estimate not only the orbital interaction energy but also the amount of electrons transferred, which is expressed in NOCV eigenvalues ν assigned to each interacting orbital pair. The combined results of the ETS-NOCV energy and charge decomposition analysis for **14a-d** and **14d*** are presented in Table 6.

[63] (a) Marynick, D. S. *J. Am. Chem. Soc.* **1984**, *106*, 4064. (b) Orpen, A. G.; Connelly, N. G. *Organometallics* **1990**, *9*, 1206. (c) Mitoraj, M. P.; Michalak, A. *Inorg. Chem.* **2010**, *49*, 578.
[64] (a) Mitoraj, M.; Michalak, A. *J. Mol. Model.* **2007**, *13*, 347. (b) Mitoraj, M.; Michalak, A; Ziegler, T. *J. Chem. Theory Comput.* **2009**, *5*, 962.

Table 6**. ETS-NOCV decomposition analysis for **14a-d** and **14d*

	14a	**14b**	**14c**	**14d**	**14d***
ΔE_{orb}	-21.4	-22.9	-50.2	-47.8	-50.7
$\Delta\rho_\sigma$	-14.8 (69.2%)	-16.1 (70.3%)	-21.7 (43.2%)	-23.5 (49.2%)	-24.5 (48.3%)
	[0.367]	[0.374]	[0.503]	[0.511]	[0.521]
$\Delta\rho_{\pi\perp}$	-1.4 (6.5%)	-1.4 (6.1%)	-12.1 (24.1%)	-10.0 (20.9%)	-10.7 (21.1%)
	[0.105]	[0.107]	[0.378]	[0.345]	[0.353]
$\Delta\rho_{\pi\parallel}$	-1.4 (6.5%)	-1.4 (6.1%)	-10.1 (20.1%)	-8.9 (18.6%)	-9.6 (18.9%)
	[0.105]	[0.107]	[0.307]	[0.288]	[0.296]
$\Delta\rho_{pol}$	-1.5 (7.0%)	-1.5 (6.6%)	-4.3 (8.6%)	-3.4 (7.1%)	-3.7 (7.3%)
	[0.117]	[0.109]	[0.159]	[0.139]	[0.144]
$\Delta\rho_{rest}$	-2.3 (10.8%)	-2.5 (10.9%)	-2.0 (4.0%)	-2.0 (4.2%)	-2.2 (4.3%)

Energy values in kcal/mol. Values in parentheses are percentage contributions to the total orbital interaction ΔE_{orb}. Values in square brackets are NOCV eigenvalues ν.

The data in Table 6 suggest that 89-96% of the deformation density related to the bonding between the metal-containing fragment and ligand trans to CH_3 or CF_3 can be approximated by four pairs of complementary NOCVs. Each of them is responsible for a particular type of interactions: (i) σ-donation from the ligand lone pair to the metal, (ii) $\pi_\perp$-back-donation from an occupied d orbital of the metal to the ligand virtual orbital orthogonal to the molecular plane, (iii) similar, although slightly weaker $\pi_\parallel$-back-donation within the molecular plane, and (iv) σ-back-donation supported by inter-fragment polarization. The relevant NOCVs contours for **14c** are presented in Figure 6.

The $\Delta\rho_\sigma$ term describes the formation of the σ-component of the Rh-PH_3 bond. The charge depletion on the P atom results in charge accumulation not only in between the Rh and PH_3 but also on the opposite side, trans to the ligand. Such a pattern has been observed in other transition metal complexes[65] and appears to be general. As follows from the ν eigenvalue, this interaction accounts for 0.503e charge transfer

[65] Mitoraj, M.; Michalak, A. *Organometallics* **2007**, *26*, 6576.

toward the metal. The $\Delta\rho_{\pi_\perp}$ and $\Delta\rho_{\pi_\parallel}$ ν values of 0.378e and 0.307e, respectively, are indicative of strong π-character of the Rh-PH_3 bond. The fourth (and last) contribution, from $\Delta\rho_{pol}$ (ν = 0.159e), is rather small, portraying Rh-CH_3 polarization toward *trans*-PH_3 due to σ-back-donation from the CH_3 group to the $\sigma^*_{Rh\text{-}P}$ orbital.

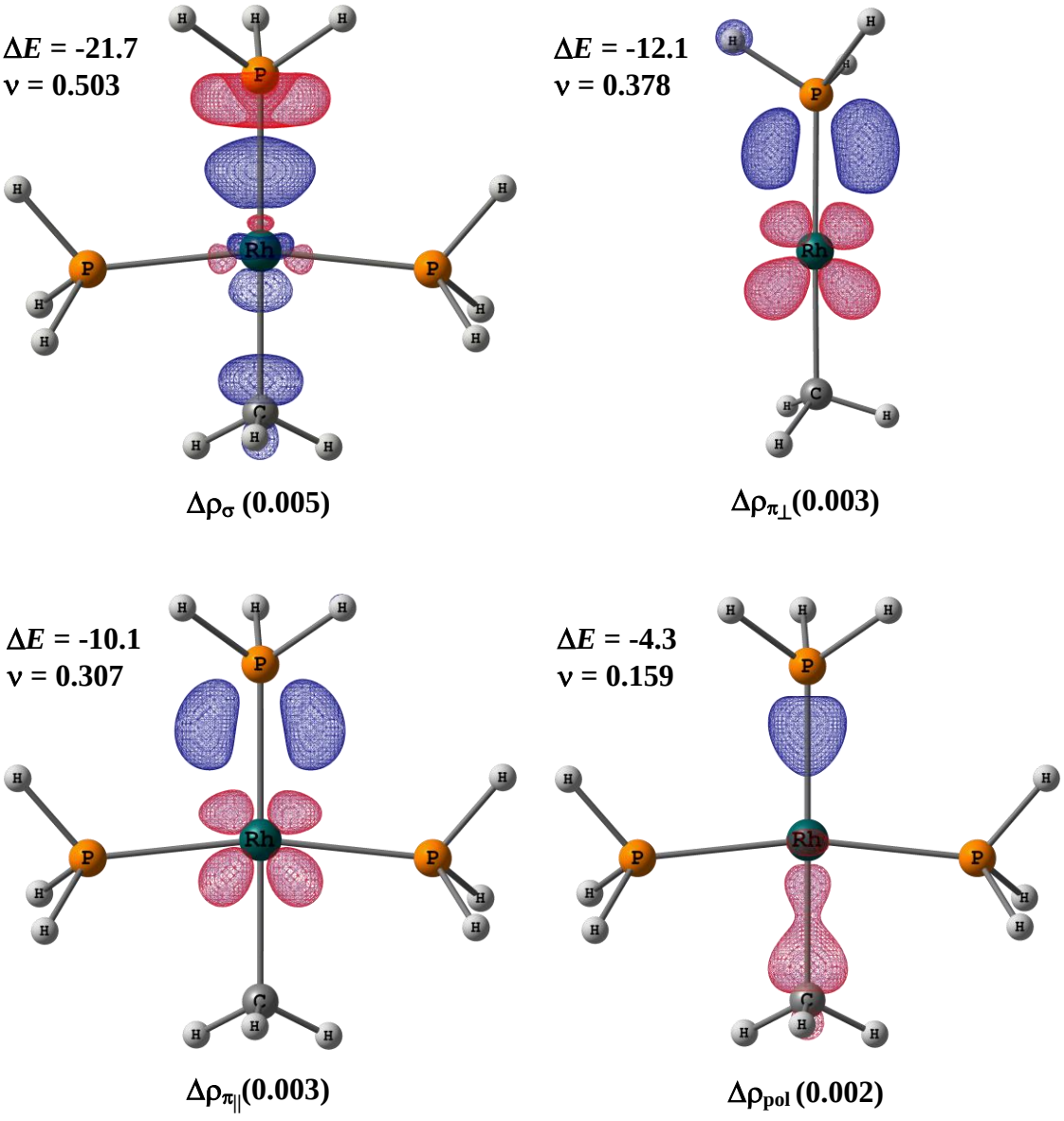

Figure 6*.Contours of deformation density distribution in* ***14c*** *with regions of charge accumulation in blue and charge depletion in red, displaying energy values ΔE in kcal/mol, NOCV eigenvalues ν, and contour isovalues in parentheses. In the top right plot PH_3 ligands cis to the CH_3 group are omitted for clarity*

Although similar deformation density distribution was observed for all other models **14**, the data in Table 6 indicate that the π-back-donation in **14a-b** is much weaker than in **14c-d**, its magnitude being comparable to that of $\Delta\rho_{pol}$. The latter varies almost insignificantly within the series, which points to its minor role in the metal-ligand bonding. As manifested by the NOCVs eigenvalues (Table 6), the CH_3/CF_3 replacement entails an increase in the ligand-to-metal electron donation and a decrease in the metal-to-ligand back-donation. This is fully consistent with the harder character of the CF_3-ligated metal center due to the electron density depletion, as predicted by the topological analysis above and supported by the MESP maps. Our results confirm that CF_3 as a group is more electronegative than CH_3: the metal bearing a CF_3 ligand withdraws electrons from the other ligands more strongly and is less prone to share its d electrons.

Looking back at the EDA analysis, it is worth to note, however, that the ΔE_{orb} term is of secondary importance for the total attractive energy. The major role is played by the ΔE_{elstat} term, which ranges from 66-67% for **14c-d** to 72-73% for **14a-b** (Table 5). The significantly higher contribution of Coulomb interaction to the Rh-NH_3 bonding also accords with the harder nature of the NH_3 ligand and more ionic bond character. The main contribution, however, comes from the Pauli repulsion. Considering that the lone pair of PH_3 is more diffuse than that of NH_3, it seems reasonable that ΔE_{Pauli}, which is responsible for the steric repulsion between the moieties, is much larger for **14c-d** even despite the longer metal-ligand bond distances. Somewhat surprising, however, is the considerably higher ΔE_{Pauli} value for **14b** (63.9 kcal/mol) *vs.* **14a** (61.8 kcal/mol) that, upon initial consideration, contradicts the compression of the CF_3-ligated atom, as predicted by the AIM analysis. A similar difference is also observed for **14c** and **14d*** with equally long Rh-PH_3 bond distances. This fact is more puzzling,

given the nearly identical ΔE_{orb} and ΔE_{elstat} values computed for each of the two. At the same time, ΔE_{Pauli} in **14d** is significantly lower than in **14c** and **14d***, which correlates with the longer Rh-PH_3 bond distance. These observations suggest that it is the Pauli repulsion that is the driving force that pushes the ligand away from the metal in order to minimize the destabilizing steric effects. This, however, does not guarantee an observable manifestation of the trans influence. As follows from the comparative analysis of the ΔE_{ster} term, the enhanced electrostatic interaction between the NH_3 ligand and the CF_3-ligated metal fragment efficiently offsets the growing repulsion. As a result, the combination of ΔE_{elstat} + ΔE_{Pauli} for **14b** (4.1 kcal/mol) is slightly lower than for **14a** (4.5 kcal/mol).

Conversely, Coulomb interaction is less important for the bonding between soft Rh(I) and PH_3, and therefore cannot compensate for the larger Pauli repulsion in **14d***. As a consequence, the Rh-PH_3 bond elongates until ΔE_{ster} for **14d** equals that for **14c** (21.0 kcal/mol). As one can expect, metal-ligand bond stretching also results in losses in orbital interaction. However, the EDA analysis demonstrates that the contribution from ΔE_{orb} is less sensitive to variations in the distance than ΔE_{elstat}. This possibly deals with the fact that the inverse dependence on the interatomic distance for ΔE_{orb} is *linear*, but for ΔE_{elstat} it is *square*. As a result, the latter changes more significantly than the former upon elongation of the bond. Therefore, it might be fair to say that the magnitude of the trans influence in trifluoromethylated complexes is mainly determined by the ΔE_{ster} term.

While the stronger Coulomb interaction between the CF_3-containig fragment and the ligand can be attributed to the lower electron density on the metal, the nature of the increase in the Pauli repulsion seems unclear. The ETS-NOCV analysis suggests that the metal-ligand bonding leads to partial electron density accumulation in the opposite

site on the metal, which, in principle, could enhance the repulsion between the metal and the CX_3 group. This also implies that a better σ-donating ligand should increase the repulsion. With respect to the ligand itself, however, this explanation is not applicable because CF_3 is more electron-accepting than CH_3. To understand why the CH_3/CF_3 replacement results in the larger ΔE_{Pauli} term we performed NST analysis[48] which enables to decompose destabilizing steric interaction into specific orbital contributions.

Total steric energies calculated for the NH_3 ligand and the rest of the Rh complex (60.7 and 64.0 kcal/mol for **14a** and **14b**, respectively) reproduce well the corresponding ΔE_{Pauli} values (61.8 and 63.9 kcal/mol, see Table 5). Pairwise comparison of equivalent four-electron interactions in **14a** *vs.* **14b** shows that only three groups of orbitals contribute to the overall ΔE_{Pauli} difference: (i) core 3s and 3p orbitals of the Rh atom (15% contribution), (ii) orbitals related to the PH_3 ligands (20% contribution), and (iii) $\sigma_{Rh\text{-}C}$ orbital that provides the rest 65% of the difference. Interestingly, the metal d orbitals in **14b** create a slightly lower steric pressure as compared to **14a**, which is consistent with the smaller size of the CF_3-ligated Rh atom. As follows from the detailed NBO analysis, the first two terms come from the higher polarization of the orbitals toward the NH_3 ligand. The origin of the third term, however, seems obscure even after examination of the NBO metrics for the Rh-CX_3 bond. Likewise, the Rh-CF_3 bond in **7-13** is more polarized toward the CF_3 group (Figure 7). The higher electronegativity of the latter also results in larger s character of the metal hybrid, which is consistent with the extended Bent's rule (see above).

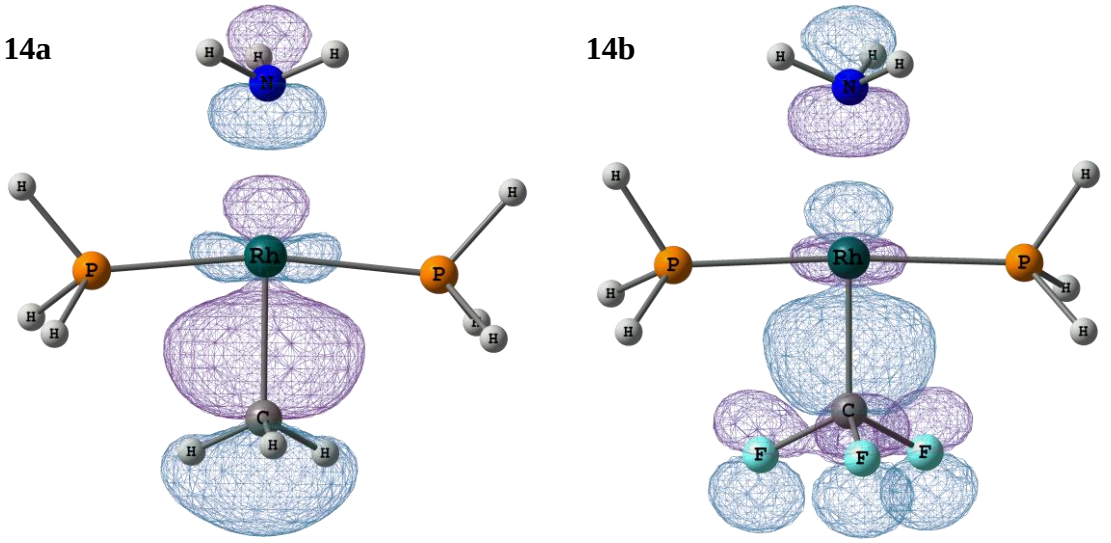

$\sigma_{Rh\text{-}C} = 0.6222(sd^{1.76})_{Rh} + 0.7828(sp^{3.65})_C$ $\sigma_{Rh\text{-}C} = 0.5953(sd^{1.63})_{Rh} + 0.8035(sp^{1.43})_C$

Rh (38.7%), C (61.3%) Rh (35.4%), C (64.6%)

Figure 7. *n_N and $\sigma_{Rh\text{-}C}$ orbitals in **14a** and **14b** with NBO metrics for the Rh-CX_3 bond, isovalue 0.04*

Figure 7 displays the charge accumulation from the Rh-CX_3 bond in the trans position due to the involvement of the metal d orbital in the Rh-C σ-bond formation. In addition, it clearly shows the antibonding combination of the $\sigma_{Rh\text{-}C}$ orbital and the lone pair on the N atom, which accounts for the Pauli repulsion between the metal-containing fragment and the NH_3 ligand trans to the CX_3. Higher polarization of the Rh-CF_3 bond should reduce the steric pressure. Keeping in mind however, that 5s atomic orbital is bigger than 4d orbitals, the higher s character of the metal hybrid in **14b** ($sd^{1.63}$) suggests that the Rh-NH_3 repulsion should be stronger in this complex, as compared with **14a** ($sd^{1.76}$). Furthermore, the Rh-CF_3 bond is shorter than the Rh-CH_3 bond (see Scheme 8), suggesting that in the CF_3 complex the electron cloud is closer to the trans ligand, which therefore should experience stronger Pauli repulsion. Evidently, there is a competition between these factors determining the way how the electron density of the Rh-CX_3 bond is distributed along the bond axis. To figure out which

contribution is more significant, we scanned the electron density along the Rh-CX_3 bond in the metal-containing fragments of **14a** and **14b** from the trans side (Figure 8).

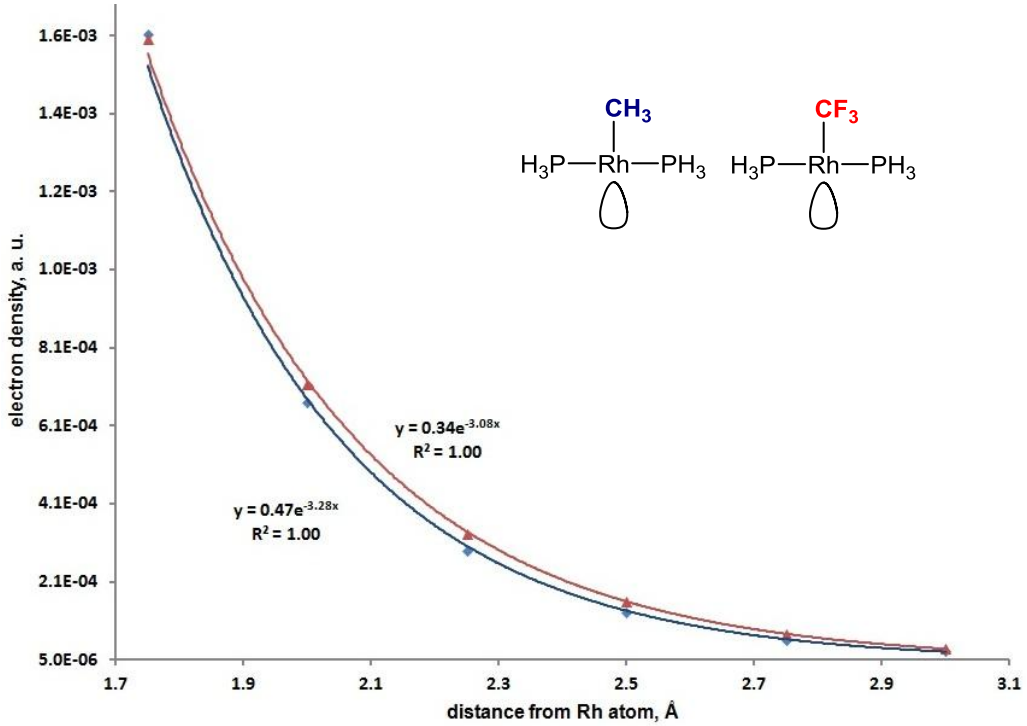

Figure 8**. Electron density scan plots for Rh-containing fragments of **14a** and **14b

The curves on the plot in Figure 8 show that within the range of 1.7-3.0 Å from the metal atom, the total electron density is slightly higher in the CF_3-containing fragment. (Outside this range the trend is actually opposite.) The axial electron density in both species can be perfectly approximated by an exponential distribution. The maximum difference is observed at ca. 2.15 Å, close to the Rh-NH_3 bond distance in **14a** (2.250 Å) and **14b** (2.246 Å). Almost the same profiles were obtained for the $\sigma_{Rh\text{-}C}$ orbital isovalues pointing to the electron density in this area being mainly determined by the $\sigma_{Rh\text{-}C}$ orbital contribution. Assuming that an increase in electron density should simultaneously raise steric pressure, we can conclude that it is the re-hybridization of the metal atom in the CF_3 complex that accounts for the higher Pauli repulsion.

Thus, the trans influence in the EDA scheme appears as Pauli repulsion in the region where the bonding pair is located. This Pauli repulsion strongly depends not only on the donating ability of the trans ligand, but also on hybridization of the orbitals involved in this donation. It so happens that the CF_3 donates less than the CH_3 in absolute terms, but its donation targets the metal s orbital that plays a more important role in the trans influence.

In the light of these observations, it is now possible to explain why the counterintuitive strong trans influence of the CF_3 group is not observed in linear d^{10} complexes. For example, as follows from NBO analysis of $[CH_3Cu(PH_3)]$ (**15a**) and $[CF_3Cu(PH_3)]$ (**15b**), the metal hybrid in the $\sigma_{Cu\text{-}C}$ molecular orbital is nearly of pure s character (Figure 9). As the occupied d orbitals participate in the bonding very weakly, the factor that accounts for an increase in the electron density in between the metal atom and the ligand is eliminated. As a consequence, the higher polarization of the Cu-CF_3 bond toward the CF_3 group leads to a lower steric pressure between the CF_3Cu and PH_3 (58.8 and 54.9 kcal/mol for **15a** and **15b**, respectively) even despite the shorter Cu-PH_3 bond distance in **15b** (2.253 Å) *vs.* **15a** (2.262 Å).

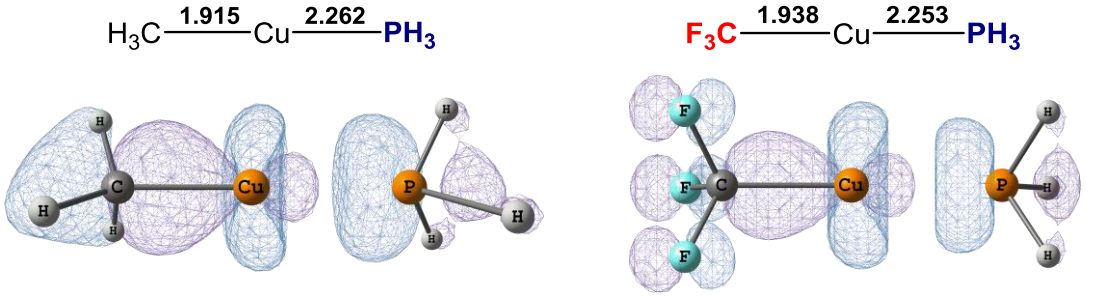

$\sigma_{Cu\text{-}C} = 0.5170(sd^{0.08})_{Cu} + 0.8560(sp^{4.16})_C$ Cu (26.7%), C (73.3%)

$\sigma_{Cu\text{-}C} = 0.4818(sd^{0.08})_{Cu} + 0.8763(sp^{1.43})_C$ Cu (23.2%), C (76.8%)

Figure 9. *n_P and $\sigma_{Cu\text{-}C}$ orbitals in **15a** and **15b** with the corresponding NBO metrics for the $\sigma_{Cu\text{-}C}$ orbital, isovalue 0.04*

To summarize our work, it has been shown that hybridization of the metal has a pivotal role in the occurrence of the trans influence. Originally introduced by Pidcock, Richards, and Venanzi in 1966,[66,67] the trans influence and the closely related trans effect have been the subject of numerous experimental[68] and theoretical[69] studies.[70] The generally accepted explanation of both phenomena is based on the idea of competition between mutually trans ligands to share their electron density with the metal center.[69f,j] Consequently, stronger electron-donating ligands weaken the bond trans to them to a greater extent. More recent calculations demonstrate that, in EDA terms, Pauli repulsion plays the key role in the labilization of trans-ligands.[69l] This more modern view maintains the link between the trans influence/effect and the σ-donating ability of the ligand, which suggests that as a weaker donor CF_3 should have a smaller trans influence than CH_3. However, this is evidently not the case, and we believe that we have found an explanation for this counterintuitive behavior.

The electron density of the M-CX_3 bond is accumulated not only in the interatomic region but also on the opposite side of the metal due to the involvement of the d orbitals. Accordingly, a ligand trans to the CX_3 group becomes a subject to Pauli

[66] Pidcock, A.; Richards, R. E.; Venanzi, L. M. *J. Chem. Soc. A* **1966**, 1707.
[67] The trans influence, a *thermodynamic* parameter, takes its roots in the *kinetic* phenomenon of trans effect, discovered in the seminal pioneering work of Il'ya I. Chernyaev as early as the mid-1920s. For the original Chernyaev's reports of the trans effect, see: Chernyaev, I. I. *Izv. Inst. Izucheniyu Platiny* **1926**, *4*, 243 and **1927**, *5*, 118.
[68] For selected examples, see: (a) Basolo, F.; Gray, H. B.; Pearson, R. G. *J. Am. Chem. Soc.* **1960**, *82*, 4200. (b) Belluco, U.; Cattalini, L.; Turco, A. *J. Am. Chem. Soc.* **1964**, *86*, 226. (c) Belluco, U.; Cattalini, L.; Turco, A. *J. Am. Chem. Soc.* **1964**, *86*, 3257. (d) Gosling, R.; Tobe, M. L. *Inorg. Chem.* **1983**, *22*, 1235. (e) Wendt, O. F.; Elding, L. I. *J. Chem. Soc., Dalton Trans.* **1997**, 4725. (f) Wendt, O. F.; Elding, L. I. *Inorg. Chem.* **1997**, *36*, 6028. (g) Otto, S. Elding, L. I. *J. Chem. Soc., Dalton Trans.* **2002**, 2354. (h) Kuznik, N.; Wendt, O. F. *J. Chem. Soc., Dalton Trans.* **2002**, 3074.
[69] For selected examples, see: (a) Chatt, J.; Duncanson, L. A.; Venanzi, L. M. *J. Chem. Soc.* **1955**, 4456. (b) Orgel, L. E. *J. Inorg. Nucl. Chem.* **1956**, *2*, 137. (c) Randic, M. *J. Chem. Phys.* **1962**, *36*, 3278. (d) Zumdahl, S. S.; Drago, R. S. *J. Am. Chem. Soc.* **1968**, *90*, 6669. (e) Vanquickenborne, L. G.; Vranckx, J.; Goeller-Walrand, C. *J. Am. Chem. Soc.* **1974**, *96*, 4121. (f) Burdett, J. K.; Albright, T. A. *Inorg. Chem.* **1979**, *18*, 2112. (g) Lin, Z.; Hall, M. B. *Inorg. Chem.* **1991**, *30*, 646. (h) Anderson, K. M.; Orpen, A. G. *Chem. Commun.* **2001**, 2682. (i) Lau, J. K.-C.; Deubel, D. V. *Chem.-Eur. J.* **2005**, *11*, 2849. (j) Chval, Z.; Sip, M.; Burda, J. V. *J. Comput. Chem.* **2008**, *29*, 2370. (k) Mitoraj, M. P.; Zhu, H.; Michalak, A.; Ziegler, T. *Int. J. Quantum Chem.* **2009**, *109*, 3379. (l) Pinter, B.; Van Speybroeck, V.; Waroquier, M.; Geerlings, P.; De Proft, F. *Phys. Chem. Chem. Phys.* **2013**, *15*, 17354.
[70] For a review of the trans influence, see ref. 19b.

repulsion from the M-CX_3 bond. Our NBO analysis indicates that the CH_3/CF_3 replacement results in re-hybridization of the metal center in such a way that it enhances s character of the metal hybrid. As valence s orbitals in the transition metals have a larger extension than the corresponding d orbitals, this leads to an increase in electron density on the opposite coordination site and, consequently, to a larger steric pressure on the trans ligand. While the magnitude of this effect depends on the contribution from the s orbital, it is in fact the d orbitals that transmit the pressure from the metallofragment to the ligand.

At the same time, the higher polarization of the M-CF_3 bond toward the CF_3 group leads to an overall electron density depletion of the system, which accounts for stronger electrostatic interaction ΔE_{elstat} between the metal and the trans-ligand. In this way, the sum ΔE_{Pauli} + ΔE_{elstat} determines which contribution will be dominant in the overall interaction energy change. For smaller and harder ligands, the stabilizing term ΔE_{elstat} will make up for the destabilizing term ΔE_{Pauli}, ultimately resulting in shorter metal-ligand bonds trans to the CF_3. On the contrary, for larger and softer ligands the Coulomb attraction is diminished, consequently being unable to compete with the Pauli repulsion that forces the metal-ligand bond to elongate until a new optimum distance is found.

Our computational studies above shed new light on the peculiar stereoelectronic properties of the CF_3 group, remove the contradiction between its weak donation and the strong trans influence, and link the trans influence/effect to orbital hybridization of the metal atom.

Conclusions

The objective of the work has been met. DFT calculations have been performed in order to understand how the CH_3/CF_3 replacement in a series of simple organic and organometallic compounds can affect their electronic structures. Different population analysis methods have been found to produce substantially different trends in the donation ability of the CF_3 group. These results demonstrate that computed raw atomic charges are not necessarily the correct technique to compare electronic properties of CH_3 and CF_3 as substituents and ligands.

More elaborate studies using NBO and AIM analyses have demonstrated that CF_3 is a weaker electron donor (or stronger acceptor) than CH_3. On replacement of a methyl group on an atom with a trifluoromethyl group, that atom becomes smaller in size and less polarizable. In organometallic compounds, CF_3-ligation of a metal raises its hardness.

Our calculations show that CF_3 is a strong trans-influencing ligand. This is in agreement with previously reported experimental and computational data but in contradiction with the widely accepted correlation of the trans influence of a ligand with its σ-donation. Through our detailed studies, we provide the first rationale for this counterintuitive behavior, based on s/d re-hybridization of the metal atom upon replacement of its methyl ligand with CF_3.

Computational Data

All DFT calculations were carried out using the Gaussian09 suite of programs.[71] The geometries were fully optimized in the gas phase using the B3LYP functional and ultrafine integration grid. Transition metals, P, Cl, Br, and I atoms were described with Stuttgart relativistic ECPs and associated basis sets[72] augmented with additional polarization functions on P, Cl, Br, and I centers (ζ_d= 0.387, 0.640, 0.428 and 0.289 respectively).[73] Standard full electron Pople's basis set 6-31G(d,p) was used for all other atoms.[74] All computed structures were characterized as local stationary points *via* analytical frequency calculations at the standard state (298.15 K, 1 atm). Natural bond orbital analysis was performed with NBO 6.0 program.[75] The topological analysis was carried out using AIM methodology as implemented in the AIMALL package.[76]

EDA-NOCV analysis was carried out using ADF program (version 2014.01)[62] at BP86/TZVP level of theory with the geometries optimized by Gaussian09 program. Relativistic effects for the Rh atom were accounted using the zeroth-order regular approximation (ZORA).[77]

---

[71] Gaussian09, Revision D.01, Frisch, M. J.; Trucks, G. W.; Schlegel, H. B.; Scuseria, G. E.; Robb, M. A.; Cheeseman, J. R.; Scalmani, G.; Barone, V.; Mennucci, B.; Petersson, G. A.; Nakatsuji, H.; Caricato, M.; Li, X.; Hratchian, H. P.; Izmaylov, A. F.; Bloino, J.; Zheng, G.; Sonnenberg, J. L.; Hada, M.; Ehara, M.; Toyota, K.; Fukuda, R.; Hasegawa, J.; Ishida, M.; Nakajima, T.; Honda, Y.; Kitao, O.; Nakai, H.; Vreven, T.; Montgomery, J. A., Jr.; Peralta, J. E.; Ogliaro, F.; Bearpark, M.; Heyd, J. J.; Brothers, E.; Kudin, K. N.; Staroverov, V. N.; Kobayashi, R.; Normand, J.; Raghavachari, K.; Rendell, A.; Burant, J. C.; Iyengar, S. S.; Tomasi, J.; Cossi, M.; Rega, N.; Millam, N. J.; Klene, M.; Knox, J. E.; Cross, J. B.; Bakken, V.; Adamo, C.; Jaramillo, J.; Gomperts, R.; Stratmann, R. E.; Yazyev, O.; Austin, A. J.; Cammi, R.; Pomelli, C.; Ochterski, J. W.; Martin, R. L.; Morokuma, K.; Zakrzewski, V. G.; Voth, G. A.; Salvador, P.; Dannenberg, J. J.; Dapprich, S.; Daniels, A. D.; Farkas, Ö.; Foresman, J. B.; Ortiz, J. V.; Cioslowski, J.; Fox, D. J. Gaussian, Inc., Wallingford CT, 2009.
[72] Andrae, D.; Haussermann, U.; Dolg, M.; Stoll, H.; Preuss, H. *Theor. Chim. Acta* **1990**, *77*, 123.
[73] Höllwarth, A.; Böhme, M.; Dapprich, S.; Ehlers, A.; Gobbi, A.; Jonas, V.; Köhler, K. F.; Stegmann, R.; Veldkamp, A.; Frenking, G. *Chem. Phys. Lett.* **1993**, *208*, 237.
[74] Hariharan, P. C.; Pople, J. A. *Theor. Chim. Acta* **1973**, *28*, 213.
[75] NBO 6.0. Glendening, E. D.; Badenhoop, J. K.; Reed, A. E.; Carpenter, J. E.; Bohmann, J. A.; Morales, C. M.; Landis, C. R.; Weinhold, F. Theoretical Chemistry Institute, University of Wisconsin, Madison, 2013.
[76] AIMAll (Version 10.05.04), Keith, T. A. TK Gristmill Software, Overland Park KS, USA, 2010
[77] van Lenthe, E.; van Leeuwen, R.; Baerends, E. J.; Snijders, J. G. *Int. J. Quantum Chem.* **1996**, *57*, 281.

Molecular modelling and geometry visualization were performed with the ChemCraft program.[78] Partial charges, NBO and AIM data obtained for organic and transition metal compounds are presented below in Tables 7-12.

[78] Zhurko, G. A. *ChemCraft 1.6*, http://www.chemcraftprog.com

UNIVERSITAT ROVIRA I VIRGILI
REACTION MECHANISMS ON THE WAY FROM CHF3 TO ARCF3. THE NATURE OF THE ORTHO-EFFECT AND ELECTRONIC PROPERTIES
OF THE CF3 GROUP.
Andrey I. Konovalov
Dipòsit Legal: T 1587-2015

Table 7**. Computed partial charges for the CX_3 group (X = H or F) and the adjacent atom (A) in **1-7

No	Mulliken		NPA		AIM		Hirshfeld		APT	
	q(A)	q(CX_3)	q(A)	q(CX_3)	q(A)	q(CX_3)	q(A)	q(CX_3)	q(A)	q(CX_3)
1a	+0.090	-0.090	+0.233	-0.233	-0.016	+0.016	+0.038	-0.038	-0.001	+0.001
1b	+0.132	-0.132	+0.162	-0.162	+0.074	-0.074	+0.069	-0.069	-0.057	+0.057
2a	-0.239	0	-0.688	0	+0.090	0	-0.102	0	+0.106	0
2b	-0.265	-0.086	-0.790	+0.009	+0.119	-0.177	-0.101	-0.072	-0.073	-0.003
3a	+0.014	+0.024	-0.034	+0.035	+0.009	+0.034	0	+0.029	+0.084	+0.011
3b	-0.019	-0.084	-0.174	+0.039	+0.032	-0.178	-0.025	-0.054	-0.158	+0.050
4a	-0.078	+0.023	-0.217	+0.010	+0.002	+0.038	-0.045	+0.027	+0.087	-0.002
4b	-0.110	-0.079	-0.352	+0.014	+0.038	-0.165	-0.058	-0.058	-0.141	+0.016
5a*	-0.055	+0.104	-0.027	+0.042	-0.197	+0.185	-0.056	+0.099	+0.026	+0.108
5b*	-0.065	-0.006	-0.162	+0.046	-0.057	-0.025	-0.055	-0.005	-0.295	+0.229
6a	+0.222	-0.092	+0.475	-0.299	+2.009	-0.684	+0.199	-0.043	+0.606	-0.211
6b	+0.243	-0.200	+0.406	-0.275	+1.979	-0.733	+0.233	-0.127	+0.518	-0.226
7a	-0.550	+0.110	-0.903	+0.153	-1.008	+0.332	-0.267	+0.050	-0.421	+0.187
7b	-0.543	+0.015	-0.946	+0.120	-1.019	+0.214	-0.234	-0.044	-0.607	+0.210

* For this pair the AIM charges were recalculated using a bigger basis set 6-311G(d,p) because the standard 6-31G(d,p) basis produces significant numerical errors.

UNIVERSITAT ROVIRA I VIRGILI
REACTION MECHANISMS ON THE WAY FROM CHF3 TO ARCF3. THE NATURE OF THE ORTHO-EFFECT AND ELECTRONIC PROPERTIES
OF THE CF3 GROUP.
Andrey I. Konovalov
Dipòsit Legal: T 1587-2015

Table 8**. NBO data for the CX_3-A bonds in **1-7

No	distance, Å	Wiberg bond order	X_3C-A hybrids		bond ionicity, %	$CX_3 \rightarrow \sigma^*_{C\text{-}A}$ hyperconjugation, kcal/mol	$CX_3 \rightarrow \sigma_{C\text{-}A}$ polarizability index	$CX_3 \rightarrow \sigma_{C\text{-}A}$ steric repulsion, kcal/mol
			$\underline{C}X_3$	A				
1a	1.092	0.945	$sp^{3.00}$ (61.7)	s (38.3)	23.3	0	0	0
1b	1.094	0.915	$sp^{1.85}$ (59.6)	s (40.4)	19.2	21.1	0.036	24.1
2a	1.530	1.040	$sp^{2.52}$(50.0)	$sp^{2.52}$ (50.0)	0	0	0	0
2b	1.505	1.019	$sp^{1.71}$ (49.0)	$sp^{2.80}$ (51.0)	2.0	20.9	0.038	23.8
3a	1.511	1.028	$sp^{2.43}$ (49.2)	$sp^{2.19}$ (50.8)	1.6	0	0	0
3b	1.505	0.986	$sp^{1.71}$ (48.1)	$sp^{2.49}$ (51.9)	3.8	19.8	0.037	22.8
4a	1.501	1.048	$sp^{2.45}$ (50.4)	$sp^{2.04}$ (49.6)	0.8	0	0	0
4b	1.496	1.002	$sp^{1.73}$ (49.2)	$sp^{2.36}$ (50.8)	1.6	12.8	0.034-0.042	23.1
5a	1.459	1.078	$sp^{2.58}$ (49.7)	$sp^{1.10}$(50.3)	0.6	0	0	0
5b	1.463	1.012	$sp^{1.89}$ (47.7)	$sp^{1.24}$ (52.3)	4.6	21.6	0.043	21.4
6a	1.558	0.967	$sp^{2.17}$ (67.8)	$sp^{1.98}$ (32.2)	35.6	12.3	0	0
6b	1.592	0.898	$sp^{1.52}$ (66.0)	$sp^{2.33}$ (34.0)	32.0	13.3[a]	0.015	24.5
7a	1.464	1.023	$sp^{2.98}$ (40.7)	$sp^{2.04}$ (59.3)	18.6	0[b]	0	0[c]
7b	1.403	1.079	$sp^{2.01}$ (39.3)	$sp^{2.14}$ (60.7)	21.4	24.9[d]	0.049-0.059	19.1[e]

[a] Hyperconjugation between CF_3 and the vacant orbital on B gives 8.3 kcal/mol. [b] $n_N \rightarrow \sigma^*_{C\text{-}H}$ hyperconjugation gives 10.3 kcal/mol. [c] $n_N \rightarrow CH_3$ repulsion is 15.1 kcal/mol. [d] $n_N \rightarrow \sigma^*_{C\text{-}F}$ hyperconjugation gives 25.7 kcal/mol. [e] $n_N \rightarrow CF_3$ repulsion is 14.4 kcal/mol.

UNIVERSITAT ROVIRA I VIRGILI
REACTION MECHANISMS ON THE WAY FROM CHF3 TO ARCF3. THE NATURE OF THE ORTHO-EFFECT AND ELECTRONIC PROPERTIES OF THE CF3 GROUP.
Andrey I. Konovalov
Dipòsit Legal: T 1587-2015

Table 9**. AIM data for **1-7

No	V_A, Bohr^3	N(e) in V_A	$\rho_A(r)$, e/Bohr^3	$\rho_B(r)$, e/Bohr^3	$\nabla^2\rho_B(r)$, a. u.	V(r), a. u.	G(r), a. u.	H(r), a. u.	L(r), a. u.	ε(r)	DI	BCP-A, %
1a	50.23	0.992	0.020	0.276	-0.948	-0.329	0.046	0.283	0.237	0.000	0.984	37.7
1b	45.24	0.903	0.020	0.305	-1.239	-0.363	0.026	0.336	0.310	0.000	0.839	34.5
2a	68.90	5.901	0.086	0.243	-0.556	-0.248	0.055	0.193	0.139	0.000	1.013	50.0
2b	65.52	5.872	0.090	0.272	-0.719	-0.305	0.063	0.242	0.180	0.000	0.898	46.3
3a	68.32	5.982	0.088	0.253	-0.600	-0.265	0.058	0.208	0.150	0.031	1.011	50.4
3b	66.25	5.961	0.090	0.273	-0.727	-0.303	0.061	0.242	0.182	0.042	0.892	46.5
4a	80.20	5.984	0.075	0.257	-0.621	-0.274	0.060	0.215	0.155	0.036	1.035	50.4
4b	78.08	5.949	0.076	0.277	-0.752	-0.311	0.062	0.250	0.188	0.037	0.902	46.7
5a*	111.32	6.169	0.055	0.264	-0.675	-0.313	0.072	0.241	0.169	0.000	1.090	52.9
5b*	104.29	6.031	0.058	0.282	-0.773	-0.321	0.064	0.257	0.193	0.000	0.941	49.0
6a	26.88	2.988	0.115	0.188	-0.147	-0.349	0.156	0.193	0.037	0.275	0.526	32.5
6b	26.77	3.018	0.113	0.187	-0.141	-0.350	0.157	0.193	0.035	0.399	0.455	31.7
7a	111.75	7.983	0.071	0.268	-0.755	-0.402	0.106	0.295	0.189	0.041	1.020	59.1
7b	106.93	7.996	0.075	0.329	-1.093	-0.503	0.115	0.388	0.273	0.106	0.920	56.8

V_A = atomic volume (0.001 isovalue); N(e) in V_A = number of electrons belonging to the atom; $\rho_A(r)$ = electron density in the atomic basin; $\rho_B(r)$ = electron density in the X_3C-A bond critical point (BCP); $\nabla^2\rho_B(r)$ = Laplacian of the electron density in BCP; V(r) = potential energy density in BCP; G(r) = Lagrangian form of kinetic energy density in BCP; H(r) = Hamiltonian form of kinetic energy density in BCP = -(V(r) + G(r)); L(r) = Lagrangian density in BCP = H(r) – G(r); ε(r) = bond elipticity; DI = delocalization index; BCP-A, % = BCP – α-atom bond distance to bond length ratio.

* For this pair, the wave functions were obtained with a larger basis set 6-311G(d,p) as the standard 6-31G(d,p) basis produces significant numerical errors.

Table 10**. Computed partial charges on the metal (M) and the CX_3 groups (X = H or F) in **8-13

No	NPA		AIM		Hirshfeld		APT	
	q(M)	q(CX_3)	q(M)	q(CX_3)	q(M)	q(CX_3)	q(M)	q(CX_3)
8a	-0.828	-0.224	+1.009	-0.261	-0.037	-0.114	-2.253	-0.006
8b	-0.888	-0.291	+1.017	-0.484	-0.057	-0.235	-2.193	-0.125
9a	-0.226	-0.301	+0.868	-0.324	+0.008	-0.148	-1.066	-0.104
9b	-0.313	-0.333	+0.877	-0.526	-0.026	-0.243	-0.987	-0.240
10a	-0.008	-0.180	+0.627	-0.188	-0.073	-0.070	-1.389	+0.010
10b	-0.061	-0.247	+0.655	-0.381	-0.089	-0.178	-1.290	-0.116
11a	-0.236	-0.314	+0.446	-0.355	-0.310	-0.109	-1.247	-0.057
11b	-0.274	-0.384	+0.474	-0.570	-0.319	-0.192	-1.205	-0.149
12a	-0.288	-0.369	+0.208	-0.359	-0.087	-0.184	-0.951	-0.132
12b	-0.326	-0.406	+0.253	-0.541	-0.094	-0.265	-0.891	-0.228
13a	+0.135	-0.304	+0.099	-0.238	-0.288	-0.082	-0.442	-0.085
13b	+0.077	-0.322	+0.243	-0.389	-0.282	-0.139	-0.329	-0.180

Table 11**. NBO data for the CX_3-M bond in **8-13

No	distance, Å	Wiberg bond order	X_3C–M hybrids		bond ionicity, %	$CX_3 \rightarrow \sigma^*_{C\text{-}M}$ hyperconjugation, kcal/mol	$CX_3 \rightarrow \sigma_{C\text{-}M}$ polarizability index[a]	$CX_3 \rightarrow \sigma_{C\text{-}M}$ steric repulsion, kcal/mol
			$\underline{C}X_3$	M				
8a	2.200	0.428	$sp^{3.75}$ (59.4)	$sd^{3.47}$ (40.6)	18.8	0	0	0
8b	2.094	0.472	$sp^{1.54}$ (63.4)	$sd^{2.96}$ (36.6)	26.8	13.5	0.027(F), 0.007(v)	23.1
9a	2.084	0.590	$sp^{3.22}$ (63.2)	$sd^{3.46}$ (36.9)	26.3	0	0	0
9b	1.980	0.612	$sp^{1.41}$ (65.4)	$sd^{3.02}$ (34.6)	30.8	18.2	0.015-0.026(F)	26.4
10a	2.058	0.560	$sp^{4.36}$ (47.9)	$sd^{17.99}$ (52.1)	4.2	2.9	0	0
10b	1.961	0.567	$sp^{1.75}$ (59.0)	$sd^{2.09}$ (41.0)	18.0	24.4	0.054(F), 0.008(v)	22.6
11a	2.241	0.511	$sp^{3.65}$ (55.2)	$sd^{92.22}$ (44.8)	10.4	1.5	0	0
11b	2.166	0.528	$sp^{1.40}$ (60.5)	$sd^{32.66}$ (39.5)	21.0	9.1	0.010(F), 0.008(v)	22.6
12a	2.152	0.480	$sp^{3.65}$ (63.7)	$sd^{2.01}$ (36.3)	27.4	0	0	0
12b	2.101	0.494	$sp^{1.43}$ (67.2)	$sd^{1.76}$(32.8)	34.4	8.2	0.014(F), 0.008(v)	24.5
13a	2.104	0.569	$sp^{4.06}$ (59.0)	$sd^{1.11}$(41.0)	18.0	0	0	0
13b	2.063	0.579	$sp^{1.68}$ (61.4)	$sd^{1.07}$(38.6)	22.8	17.6	0.012-0.034(F)	25.7

[a] F: fluorine lone pairs, v: vicinal C-X bond.

Table 12**. AIM data for **8-13

No	V_M, Bohr^3	N(e) in V_M	$\rho_M(r)$, e/Bohr^3	$\rho_B(r)$, e/Bohr^3	$\nabla^2\rho_B(r)$, a. u.	V(r), a. u.	G(r), a. u.	H(r), a. u.	L (r), a. u.	ε(r)	DI	BCP-M, %
8a	56.78	23.990	0.423	0.073	0.126	-0.065	0.048	0.016	-0.032	0.001	0.586	48.7
8b	55.93	23.982	0.429	0.094	0.199	-0.107	0.079	0.029	-0.050	0.002	0.596	47.9
9a	60.66	25.132	0.414	0.091	0.151	-0.087	0.063	0.025	-0.038	0.045	0.753	48.9
9b	59.88	25.123	0.420	0.116	0.254	-0.144	0.104	0.040	-0.064	0.045	0.746	48.2
10a	78.02	26.368	0.338	0.094	0.127	-0.081	0.057	0.025	-0.032	0.000	0.760	49.7
10b	75.96	26.341	0.347	0.120	0.212	-0.132	0.093	0.040	-0.053	0.000	0.731	48.9
11a	140.43	43.542	0.310	0.088	0.116	-0.083	0.056	0.027	-0.029	0.000	0.732	51.1
11b	138.16	43.515	0.315	0.103	0.213	-0.118	0.086	0.033	-0.053	0.000	0.686	50.2
12a	174.89	44.751	0.256	0.101	0.151	-0.108	0.073	0.035	-0.038	0.051	0.822	51.8
12b	170.76	44.708	0.262	0.116	0.251	-0.147	0.105	0.042	-0.063	0.063	0.747	50.7
13a	192.49	77.862	0.404	0.123	0.099	-0.134	0.079	0.055	-0.025	0.008	0.919	53.9
13b	181.37	77.723	0.429	0.139	0.197	-0.175	0.112	0.063	-0.049	0.017	0.833	52.5

V_M = atomic volume (0.001 isovalue); N(e) in V_M = number of electrons belonging to the metal; $\rho_A(r)$ = electron density in the metal basin; $\rho_B(r)$ = electron density in the X_3C-M bond critical point (BCP); $\nabla^2\rho_B(r)$ = Laplacian of the electron density in BCP; V(r) – potential energy density in BCP; G(r) = Lagrangian form of kinetic energy density in BCP; H(r) = Hamiltonian form of kinetic energy density in BCP = -(V(r) + G(r)); L(r) = Lagrangian density in BCP = H(r) – G(r); ε(r) = bond elipticity; DI = delocalization index; BCP-M, % = BCP – α-atom bond distance to bond length ratio.

REACTION MECHANISMS ON THE WAY FROM CHF3 TO ARCF3. THE NATURE OF THE ORTHO-EFFECT AND ELECTRONIC PROPERTIES OF THE CF3 GROUP.
Andrey I. Konovalov
Dipòsit Legal: T 1587-2015

REACTION MECHANISMS ON THE WAY FROM CHF3 TO ARCF3. THE NATURE OF THE ORTHO-EFFECT AND ELECTRONIC PROPERTIES OF THE CF3 GROUP.
Andrey I. Konovalov
Dipòsit Legal: T 1587-2015

REACTION MECHANISMS ON THE WAY FROM CHF3 TO ARCF3. THE NATURE OF THE ORTHO-EFFECT AND ELECTRONIC PROPERTIES OF THE CF3 GROUP.
Andrey I. Konovalov
Dipòsit Legal: T 1587-2015

UNIVERSITAT ROVIRA I VIRGILI

Tarragona

2015